**Universidad del ROSARIO**

**VNiVERSiDAD Ð SALAMANCA**

# ESTUDIO DE INTERACCIONES HOSPEDERO-PATÓGENO Y PROTEÍNA-PROTEÍNA EN *Plasmodium vivax*: EVALUACIÓN DE LAS PROTEÍNAS DEL CUELLO DE ROPTRIAS -2, -4 Y -5 Y DEL ANTÍGENO APICAL DE MEMBRANA-1

**Gabriela Arévalo Pinzón M.Sc.**

Trabajo de grado presentado como requisito para optar al título de Doctor en Ciencias Biomédicas de la Universidad del Rosario y Doctor de la Universidad de Salamanca dentro del Programa de Salud y Desarrollo en los Trópicos

**BOGOTÁ D.C., 2018**

**ESTUDIO DE INTERACCIONES HOSPEDERO-PATÓGENO Y PROTEÍNA-PROTEÍNA EN *Plasmodium vivax*: EVALUACIÓN DE LAS PROTEÍNAS DEL CUELLO DE ROPTRIAS -2, -4 Y -5 Y DEL ANTÍGENO APICAL DE MEMBRANA-1**

**Gabriela Arévalo Pinzón M.Sc.**

Directores

**Manuel Alfonso Patarroyo Gutiérrez M.D., Dr.Sc.**

Fundación Instituto de Inmunología de Colombia (FIDIC) - Universidad del Rosario

**Manuel Fuentes García M.D., PhD**

Centro de Investigación del Cáncer - Universidad de Salamanca

Tutor

**Pedro Fernández-Soto PhD**

Universidad de Salamanca

DOCTORADO EN CIENCIAS BIOMÉDICAS

UNIVERSIDAD DEL ROSARIO

DOCTORADO EN SALUD Y DESARROLLO EN LOS TRÓPICOS

UNIVERSIDAD DE SALAMANCA

BOGOTÁ D.C., 2018

Aprobado por el tribunal evaluador en cumplimiento de los requisitos exigidos para otorgar al título de **Doctor en Ciencias Biomédicas de la Universidad del Rosario y Doctor de la Universidad de Salamanca.**

_____

Dr. Paul Laissue Hormaza M.D., M.Sc., PhD

Jurado Universidad del Rosario

_____

Dra. Concepción Judith Puerta Bula PhD

Jurado Pontificia Universidad Javeriana

_____

Dr. Julio López Abán PhD

Jurado Universidad de Salamanca

*A lo más preciado de mi mundo: mi familia:*

*Marlén, Juan Manuel, William y Elena*

# AGRADECIMIENTOS

A mi director, **Manuel Alfonso Patarroyo**, quien considero ha sido mi maestro y me ha guiado por este mundo de la ciencia y a quien admiro por su perseverancia en seguir formándonos…gracias por creer en mí, incluso más de lo que yo confío en mí.

A mi jefe, **Manuel Elkin Patarroyo**, por permitir formarme en uno de los mejores institutos de investigación...que sepa que, en tanto pueda, seguiré allí.

A mi amigo, compañero y jefe de grupo, **Hernando Curtidor**….por escucharme, tenerme paciencia, pero lo más importante, apoyarme en cada paso en esta formación doctoral.

Al **Dr Manuel Fuentes** por recibirme en su laboratorio y por ser parte de este proyecto de investigación.

A **Julio López Abán**, quien me acompaño en una de las experiencias más enriquecedoras para mi investigación, y quien, con su insistencia, permitió hacer realidad el vínculo Rosario-Salamanca.

A todas aquellas personas que pertenecen y a las que pasaron por el grupo de **Receptor-Ligando**, e hicieron parte de este proyecto.

Al grupo funcional de **Biología Molecular e Inmunología**, por enseñarme parte de sus conocimientos y acogerme en su grupo durante mucho tiempo.

A mis amigas, compañeras y estudiantes, **Maritza Bermúdez** y **Diana Hernández**, …¡qué satisfactorio ha sido conocer y trabajar con personas como ustedes!

A **Andrés Moreno**, un compañero excepcional, con quien comparto y disfruto de la investigación en malaria.

A todos mis estudiantes de **pregrado** de la **Universidad Colegio Mayor de Cundinamarca**, a quienes tuve el privilegio de dirigir su tesis.

A mi más sincera amiga **Giovanna Fernanda**….amiga, que sean muchos años más…que sigas ahí, …siempre.

A mi amiga y profesora **Ruth Sánchez**, quién sino ella, para creer en mi talento.

A mi **Tía Martha** por hacer mi vida sencilla…por cuidar de lo que más amo.

A la **Universidad del Rosario** y en especial a la Escuela de Medicina y Ciencias de la Salud y a la Facultad de Ciencias Naturales y Matemáticas, por abrirme la puerta hacia mi formación doctoral y brindarme los medios para culminar satisfactoriamente mis estudios.

A los **Doctores Luisa Matheus** y **Paul Laissue**, por su ayuda en este proceso de formación doctoral. Gracias por sus enseñanzas.

A la **Universidad de Salamanca** y, en especial, a los **Doctores Antonio Muro** y **Esther del Olmo**, por su ayuda y colaboración en este proceso de doble titulación.

A **COLCIENCIAS**, por su apoyo en la financiación de mis estudios doctorales.

# LISTA DE FIGURAS

# LISTA DE ANEXOS

# LISTA DE ABREVIATURAS

| Abreviatura | Término |
|---|---|
| ADNc | ADN complementario |
| AMA1 | Apical Merozoite Antigen-1 |
| ARP | Asparagine Rich Protein |
| AVEXIS | Avidity-based Extracellular Interaction Screen |
| CME | Células Madre Embriónicas |
| CMH | Complejo Mayor de Histocompatibilidad |
| CMHem | Células Madre Hematopoyéticas |
| CSP | Circumsporozoite Protein |
| CyRPA | Cysteine-Rich Protective Antigen |
| cHABPs | Conserved High-Activity Binding Peptides |
| DAPA | protein arrays from DNA |
| DARC | Duffy Antigen Receptor for Chemokines |
| DBL | Duffy Binding Ligand |
| DBP | Duffy Binding Protein |
| EBA | Erythrocyte Binding Antigen |
| EBL | Erythrocyte Binding-Like |
| EBP | Erythrocyte Binding Protein |
| FIDIC | Fundación Instituto de Inmunología de Colombia |
| GAMA | GPI-Anchored Micronemal Antigen |
| GPI | Glycosylphosphatidylinositol |
| GST | Glutathione S-Transferase |
| INS | Instituto Nacional de Salud |
| IMPIPS | Immune Protection-Inducing Protein Structures |
| IPP | Interacciones Proteína-Proteína |
| kD | Dissociation equilibrium constant |
| $K_{on}$ | Velocidades de asociación |
| $K_{off}$ | Velocidades de disociación |
| MSPs | Merozoite Surface Proteins |
| MTI | Mosquiteros Tratados con Insecticidas |
| mHABPs | Modified HABPs |
| NAPPA | Nucleic Acids Programmable Protein Arrays |
| OMS | Organización Mundial de la Salud |
| PISA | Protein *in situ* arrays |
| *Pv*AMA-DI-II | Dominio I y II de *Pv*AMA1 |
| *Pv*AMA-DII-III | Dominio II y III de *Pv*AMA1 |
| *Pv*RON2-RI | Región central de *Pv*RON2 |
| *Pv*RON2-RII | Región carboxi-terminal de *Pv*RON2 |
| RAP | Rhoptry-Associated Proteins |
| RRL | Rabbit Reticulocyte Lysate |
| RONs | Rhoptry Neck Proteins |
| RBP | Reticulocyte Binding Protein |
| Rh | Reticulocyte-binding protein homologues |
| RCT | Receptor de Células T |
| SCU | Sangre de Cordón Umbilical |
| SIVIGILA | Sistema de Vigilancia en Salud Pública |
| TRAMP | Thrombospondin-Related Apical Merozoite Protein |
| VCG-1 | Vivax Colombia Guaviare 1 |
| WGE | Wheat Germ Extract |

# TABLA DE CONTENIDO

# RESUMEN

La malaria es una de las enfermedades tropicales transmitidas por vectores más importantes a nivel mundial, donde *Plasmodium vivax* representa una de las especies más ampliamente distribuidas, afectando ~13.8 millones de personas por año. Pese a ello, el progreso aparentemente lento de la infección y los niveles bajos de parasitemia en el humano, comparados a lo reportado en *Plasmodium falciparum*, han llevado a clasificar a la infección por *P. vivax* erróneamente como benigna. Esto, sumado a los retos experimentales que trae consigo el cultivo de este parásito, obstaculizan en gran medida el conocimiento a nivel biológico, celular y molecular, necesario para el desarrollo de métodos de control efectivos contra *P. vivax*.

Hoy en día, se conoce que un inadecuado diagnóstico, el mal manejo terapéutico y/o el retraso en el tratamiento, pueden llevar a recaídas y estados de enfermedad grave, similares a los reportados para la malaria producida por *P. falciparum*, lo que impone retos en la búsqueda de nuevas alternativas específicas contra esta especie. Teniendo en cuenta la necesidad de identificar posibles blancos terapéuticos contra *P. vivax*, este trabajo se enfocó en estudiar interacciones del tipo receptor-ligando y proteína-proteína de moléculas de *P. vivax* localizadas en los organelos apicales de esquizontes intraeritrocíticos.

Basados en estudios previos en *P. falciparum* y *Toxoplasma gondii*, donde se describe la importancia funcional de las proteínas localizadas en el cuello de las roptrias (RONs) -2, -4 y 5 y del antígeno apical de membrana 1 (AMA1), se caracterizó en *P. vivax* la unión de cada una de estas proteínas con reticulocitos humanos y se evaluó la capacidad de *Pv*RON2 para establecer interacciones con las proteínas *Pv*RON4, *Pv*RON5 y *Pv*AMA1. Para esto, inicialmente se caracterizó mediante herramientas bioinformáticas y experimentales la presencia de los genes

*pvron4* y *pvron5* en el genoma y transcriptoma de esquizontes de la cepa Vivax Colombia Guaviare 1 (VCG-1) de *P. vivax*. Estos dos genes codifican proteínas de alto peso molecular que se expresan en el polo apical de esquizontes y co-localizan con proteínas presentes en las roptrias. Para evaluar la capacidad de interacción de las proteínas *Pv*RON2, *Pv*RON4, *Pv*RON5 y *Pv*AMA1 con receptores sobre la membrana de reticulocitos humanos, todas ellas fueron producidas de forma recombinante y purificadas mediante cromatografía de afinidad.

Se encontró que la proteína recombinante *Pv*RON5 se unió tanto a normocitos como a reticulocitos CD71$^+$, con una marcada preferencia por reticulocitos humanos. Por su parte, las proteínas recombinantes que incluyen los dominios I y II de *Pv*AMA-1 (*Pv*AMA-DI-DII), la región central de la proteína *Pv*RON2 (*Pv*RON2-RI) y la región carboxi-terminal de *Pv*RON4, interactúan específicamente con reticulocitos CD71$^+$CD45$^-$. Los estudios de competencia de unión con péptidos sintéticos que cubren las secuencias de las proteínas recombinantes mostraron que los péptidos 21270 (derivado del DI de *Pv*AMA1), 40305 (de *Pv*RON4) y 40595 (de *Pv*RON2-RI) fueron capaces de inhibir la unión de las proteínas recombinantes a reticulocitos CD71$^+$CD45$^-$, lo que sugiere que estas secuencias peptídicas contienen parte de las propiedades de unión de cada una de las proteínas de las que derivan. Los tres péptidos se unen específicamente y con alta afinidad a eritrocitos con porcentajes de unión mayores al 2% (obtenidas de las curvas de unión específica), permitiendo catalogarlos como péptidos con alta capacidad de unión a eritrocitos (HABPs, del inglés High Activity Binding Peptides). La unión de las proteínas *Pv*AMA1 y *Pv*RON4 a eritrocitos humanos fue sensible al tratamiento de los eritrocitos con diferentes enzimas (tripsina, quimotripsina y/o neuraminidasa), sugiriendo que la naturaleza de los receptores para estas proteínas es de tipo proteico. Estos resultados destacan la función de adhesina de las proteínas evaluadas y revelan las regiones mínimas de interacción con la célula hospedera, que sumado a la

expresión de estas proteínas en esquizontes intraeritrocíticos y su localización en organelos apicales, sugieren una fuerte participación de estas moléculas durante el proceso de invasión de los merozoitos de *P. vivax* a reticulocitos humanos.

Finalmente, mediante resonancia de plasmones de superficie, se caracterizaron las interacciones entre la proteína *Pv*RON2 con las proteínas *Pv*RON4, *Pv*RON5 y *Pv*AMA1. Los análisis revelaron que la región carboxi-terminal de la proteína *Pv*RON2 (*Pv*RON2-RII) y *Pv*RON2-RI interactúan específicamente y con alta afinidad con el dominio II y III de *Pv*AMA1 (*Pv*AMA-DII-DIII) y con una menor afinidad con las proteínas *Pv*AMA-DI-DII, *Pv*RON4 y *Pv*RON5. Al modificar algunos residuos de la proteína *Pv*AMA1, reportados en *P. falciparum* como críticos en la interacción RON2-AMA1, no se encontraron diferencias importantes en los valores de las velocidades de asociación ($K_{on}$), disociación ($K_{off}$) y en la constante de disociación de la interacción (*kD*). Esto sugiere que, si bien existen interacciones proteína-proteína (IPP) conservadas entre estos parásitos (*Pv-Pf*), cada parásito utiliza distintas regiones de las proteínas para interactuar, lo que resalta su capacidad para especializarse o restringirse para invadir un tipo de célula específica y pone de manifiesto aún más la necesidad de diseñar medidas de control específicas contra *P. vivax*.

# SUMMARY

Malaria is one of the most important tropical diseases transmitted by vectors worldwide; *Plasmodium vivax* represents one of the most widely distributed species (affecting ~ 13.8 million people worldwide per year). Despite this, the apparently slow progress of infection and low parasitaemia levels in humans compared to those reported in *Plasmodium falciparum* have erroneously led to *P. vivax* infection being classified as benign. Added to this, the experimental challenges involved in culturing this parasite greatly hinder accumulating the biological, cellular and molecular knowledge necessary for developing effective control methods against *P. vivax*.

It is known nowadays that unsuitable diagnosis, poor therapeutic management and/or delayed treatment can lead to relapses and severe disease states similar to those reported for *P. falciparum* malaria, thereby imposing challenges regarding the search for new, specific, alternative approaches to tackling this species. The present work has been focused on studying receptor-ligand and protein-protein interactions of *P. vivax* molecules located in intra-erythrocyte schizonts' apical organelles regarding the need for identifying therapeutic targets against *P. vivax*.

Protein interaction with human reticulocytes was characterised in *P. vivax* and *Pv*RON2 ability to establish interactions with *Pv*RON4, *Pv*RON5 and *Pv*AMA1 was evaluated, based on previous *P. falciparum* and *Toxoplasma gondii* studies, describing the functional importance of rhoptry neck proteins. Work began by using bioinformatics and experimental tools for predicting *pvron4* and *pvron5* genes in the *P. vivax* VCG-1 (*Vivax* Colombia Guaviare 1) strain's genome and schizonts transcriptome. These two genes encode high molecular weight proteins which are expressed at schizonts' apical poles and co-localise with proteins in the rhoptries. Such proteins were produced recombinantly and purified by affinity chromatography for evaluating *Pv*RON2, *Pv*RON4, *Pv*RON5 and *Pv*AMA1 ability to interact with receptors on human reticulocyte membrane.

Recombinant $Pv$RON5 bound to both CD71$^+$ normocytes and reticulocytes, having a marked preference for human reticulocytes. $Pv$AMA1 domains I and II ($Pv$AMA-DI-DII), $Pv$RON2 central region ($Pv$RON2-RI) and $Pv$RON4 carboxy-terminal region specifically interacted with CD71$^+$CD45$^-$ reticulocytes. Competition studies with synthetic peptides covering recombinant protein sequences showed that $Pv$AMA1-derived peptide 21270, $Pv$RON4-derived 40305 and $Pv$RON2-RI-derived 40595, were capable of inhibiting recombinant protein binding to CD71$^+$CD45$^-$ reticulocytes, suggesting that these peptide sequences contained some of the evaluated proteins' binding properties.

The three peptides bound specifically and with high affinity to erythrocytes having higher (2%) binding percentages (obtained from specific binding curves), thereby allowing their classification as high erythrocyte binding capacity peptides (HABPs). $Pv$AMA1 and $Pv$RON4 binding to human erythrocytes was sensitive to erythrocytes treatment with different enzymes (trypsin, chymotrypsin and/or neuraminidase), suggesting the receptors' protein type nature. These results highlighted the adhesin function of the proteins evaluated and revealed minimum host cell interaction regions suggesting these molecules' active participation during *P. vivax* merozoite invasion of human reticulocytes (along with these proteins' expression in intra-erythrocytic schizonts and location in apical organelles).

Surface plasmon resonance was used for characterising $Pv$RON2 interactions with $Pv$RON4, $Pv$RON5 and $Pv$AMA1. This revealed that $Pv$RON2-RI and carboxy-terminal regions ($Pv$RON2-RII) specifically interacted and with great affinity with $Pv$AMA1 domain II and III ($Pv$AMA-DII-DIII) but with less affinity with $Pv$AMA-DI-DII, $Pv$RON4 and $Pv$RON5. No significant differences were found in interaction association ($K_{on}$) or dissociation ($K_{off}$) rates or dissociation constant (kD) values when modifying some $Pv$AMA1 residues reported as being critical in the *P.*

*falciparum* RON2-AMA-1 interaction, suggesting that although conserved interactions between these parasites (*Pv-Pf*) have been observed, each parasite uses different regions to interact, thereby highlighting their ability to specialise or restrict themselves to invading a specific cell type and the need for designing specific control measures against *P. vivax*.

# 1. Introducción General

La malaria es un problema de salud pública global, causada por parásitos del género *Plasmodium* y transmitida a través de la picadura del mosquito *Anopheles* hembra. Aunque en los últimos años se ha reportado una disminución del 41% en la incidencia global de malaria y un 62% en la mortalidad [1], la Organización Mundial de la Salud (OMS) reportó que en 2016 se presentaron cerca de 216 millones de casos por malaria con un total de muertes a nivel global de ~445.000 [2]. Estas cifras que indican disminución en el número de casos anuales, reflejan los esfuerzos focalizados en contra de la especie de *Plasmodium* más prevalente y mortal en África Subsahariana: *P. falciparum*. Sin embargo, no se ha prestado igual atención a controlar la malaria causada por *P. vivax*, que es la segunda especie con mayor distribución a nivel mundial y la causante de la enfermedad tropical más importante en las Américas (responsable del 64% de las infecciones) y en algunas regiones del sureste asiático y del Mediterráneo oriental [2]. Durante el 2016, la transmisión de malaria se intensificó de manera significativa en algunos países de la región de las américas como Colombia, Ecuador y Venezuela [3] (Figura 1). En Colombia, la malaria representa un grave problema de salud pública, debido a las condiciones climáticas y geográficas que lo hacen apto para la transmisión de enfermedades tropicales. En el país durante el 2016, se notificaron al Sistema de Vigilancia en Salud Pública (SIVIGILA) del Instituto Nacional de Salud (INS) 83.356 casos de malaria, siendo las especies más prevalentes *P. falciparum* y *P. vivax* [3].
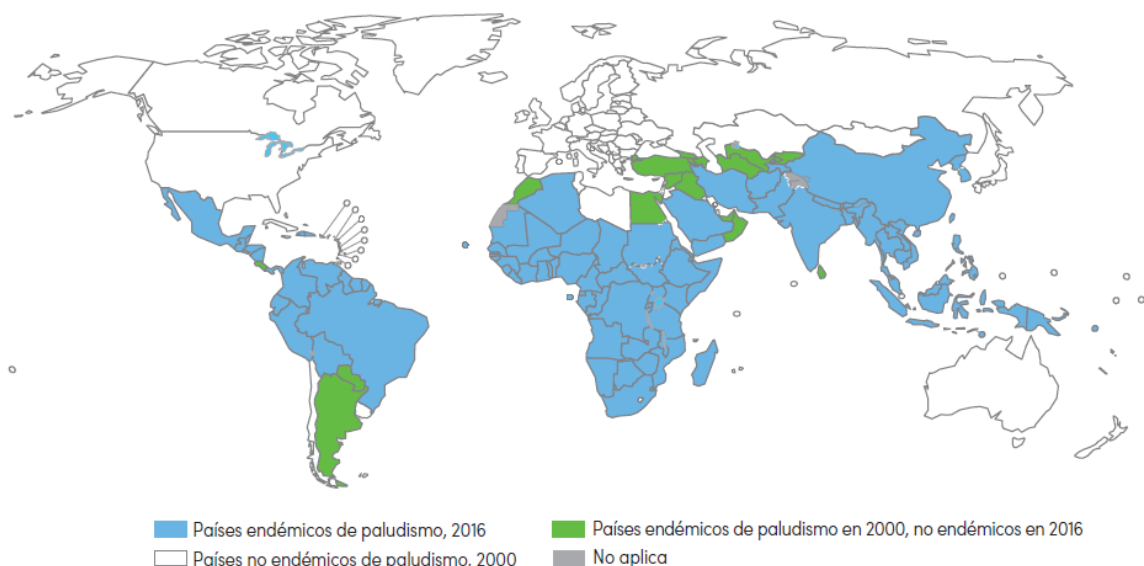
**Figura 1. Países endémicos de paludismo en 2000 y 2016.**
*Fuente: Figura tomada de la base de datos del Reporte Mundial de Malaria del 2016 [1].*

Es de resaltar que, aunque por mucho tiempo la infección por *P. vivax* ha sido considerada benigna, alrededor del 35% de la población mundial (2.500 millones de personas) se encuentra en riesgo de infección [1, 4] y actualmente existen reportes que muestran un incremento en el número de casos de enfermedad severa y muerte atribuidos exclusivamente a esta especie parasitaria [5-7]. Por otra parte, las características biológicas y epidemiológicas de *P. vivax,* como su capacidad de invadir selectivamente reticulocitos, de permanecer latente en forma de hipnozoito durante el estadio hepático (que conduce a recaídas y ataques clínicos repetidos) [8], de formar gametocitos infecciosos en las fases tempranas de la infección, incluso antes de la aparición de los síntomas, y de la capacidad del vector transmisor de sobrevivir en zonas templadas, imponen retos importantes, no sólo en el tratamiento y eliminación de la malaria por *P. vivax*, sino en abordar el estudio a nivel biológico de este parásito [9-11].

Teniendo en cuenta que el conocimiento de la biología de *P. vivax* puede aumentar los blancos de acción sobre este patógeno, una de las alternativas es identificar antígenos de *P. vivax* presentes

en las formas invasivas del parásito y caracterizar, además, la capacidad de estos nuevos antígenos para formar complejos macromoleculares y/o interactuar con receptores sobre reticulocitos humanos durante el proceso de invasión. Hoy en día, se conoce que en muchos procesos celulares de los microorganismos, las proteínas median, a través de la formación de complejos reversibles o irreversibles con otras macromoléculas (tales como proteínas o ácidos nucleicos), una red de estructuras y respuestas biológicas claves para la patogenicidad, invasión a la célula hospedera y supervivencia [12-14].

Sin embargo, existen diferentes retos metodológicos a la hora de abordar el estudio a nivel molecular de *P. vivax*, principalmente porque no se cuenta con una fuente estable y continua de material genético y proteínas de esta especie, sumado a la dificultad de obtener altas cantidades de muestras enriquecidas en reticulocitos humanos para los estudios funcionales [15, 16]. Estos dos inconvenientes, se traducen en la falta de un cultivo continuo *in vitro*, lo que impide además, el uso de aproximaciones genéticas para estudiar el rol de las proteínas durante el ciclo de invasión a los reticulocitos [16]. Estudios utilizando cepas de *P. vivax* adaptadas a primates no-humanos [17, 18] o el uso de sangre de pacientes infectados [19], han permitido el desarrollo de aproximaciones comparativas con otras especies de *Plasmodium* [20] y han proporcionado una fuente importante de material parasitario para el desarrollo reciente de ciencias ómicas con este parásito [19, 21-24].

En este contexto, la Fundación Instituto de Inmunología de Colombia (FIDIC), ha desarrollado una aproximación comparativa para caracterizar e identificar en *P. vivax*, antígenos involucrados en la invasión, previamente descritos en *P. falciparum*, como potenciales candidatos a vacuna [25-27]. Con esta metodología, hasta el 2013 se habían caracterizado cerca de 16 proteínas a nivel mundial en *P. vivax* [20], en comparación con las ~60 proteínas identificadas en *P. falciparum*, de

las cuales, la mayoría ya han sido caracterizadas en detalle y se conocen sus receptores sobre la membrana de los eritrocitos [28, 29].

El ciclo de invasión de *Plasmodium* es bastante complejo e involucra dos organelos presentes en los esporozoitos (invaden células hepáticas) y merozoitos (invaden eritrocitos), denominados micronemas y roptrias [30]. Ambos organelos contienen un gran número de proteínas que son liberadas secuencialmente justo en el momento de invasión, siendo las responsables, junto al motor actina-miosina, de la reorientación del parásito sobre su célula hospedera y la formación de un enlace fuerte con la membrana del eritrocito que le permite invadir eficientemente [29]. En *P. falciparum*, la formación del enlace fuerte e irreversible está a cargo de un complejo macromolecular formado entre proteínas del cuello de las roptrias (RONs, del inglés Rhoptry Neck Proteins) -2, -4 y -5 [31-33] y del antígeno apical de membrana 1 (AMA1, del inglés Apical Membrane Antigen-1) [34]. Se ha propuesto que este complejo actúa a través de la interacción independiente de receptores de la célula hospedera, donde los parásitos secretan las proteínas RONs dentro de la célula diana y RON2 es utilizado por el parásito como receptor para la proteína AMA1, lo que le permite al parásito culminar exitosamente su proceso de invasión [35] (Figura 2).

El uso de anticuerpos monoclonales, péptidos o moléculas químicas orientadas al bloqueo de la formación del complejo AMA1-RON2, ha sido una estrategia utilizada por algunos investigadores para inhibir la entrada de merozoitos de *P. falciparum* a los eritrocitos [34, 36]. Por otro parte, estudios de interacciones receptor-ligando han mostrado que la proteína *Pf*AMA-1 (dominio III) se une a un receptor denominado *Kx* en la superficie del eritrocito [37], mientras que la proteína *Pf*RON2 utiliza la región carboxi-terminal para interactuar con la membrana del eritrocito [38]. Péptidos de 20 residuos derivados de la proteína *Pf*RON5 interactúan específicamente con

receptores sobre la superficie del eritrocito, que son capaces de inhibir *in vitro* la invasión de los merozoitos a la célula hospedera [39]. Lo anterior destaca la importancia de estas proteínas y sus interacciones, en el proceso de invasión al eritrocito de *P. falciparum*.
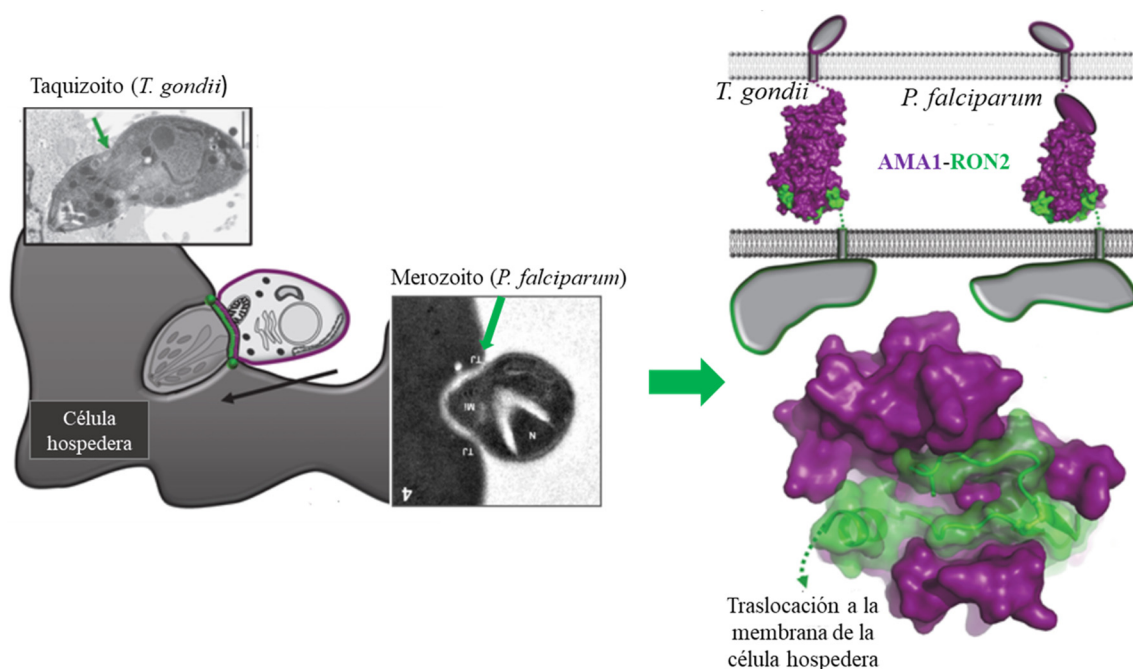


**Figura 2. Modelo de formación del enlace fuerte propuesto para los parásitos Apicomplexa T. gondii y P. falciparum**.
*La proteína RON2 (verde) es anclada sobre la membrana de la célula hospedera mientras la proteína AMA1 (morado) interactúa con la región extracelular de RON2. De esta forma, el parásito se une irreversiblemente a la célula hospedera. El enlace fuerte se mueve progresivamente hacia la parte posterior del parásito, impulsándolo dentro de la vacuola parasitófora. Figura modificada a partir de [40, 41].*

Basados en la importancia de las proteínas RONs en *P. falciparum* y en otros parásitos *Apicomplexa* como *T. gondii*, se caracterizó el primer miembro del cuello de las roptrias de *P. vivax*, denominado RON2, el cual es ortólogo a *Pf*RON2 [42]. Este hallazgo nos permite sugerir que, en *P. vivax*, la formación del enlace fuerte puede contener las mismas proteínas encontradas en *P. falciparum* y pueden estar participando en interacciones del tipo receptor-ligando e interacciones proteína-proteína del parásito. Este trabajo estuvo orientado, en primera instancia, a la identificación y caracterización a nivel bioinformático y experimental de los genes *pvron4* y

*pvron5*, así como a la localización sub-celular de las proteínas codificadas por estos genes. Una vez caracterizadas estas nuevas proteínas, se estableció una metodología para evaluar la capacidad de unión de las proteínas *Pv*AMA1, *Pv*RON2, *Pv*RON4 y *Pv*RON5 a reticulocitos humanos. Finalmente, se midieron las interacciones binarias proteína-proteína de *Pv*RON2 con *Pv*AMA1, *Pv*RON4 y *Pv*RON5.

La caracterización de estas interacciones, permitió definir las regiones conservadas mínimas de interacción de las proteínas *Pv*RON2, *Pv*RON4, *Pv*RON5 y *Pv*AMA1, con receptores sobre la membrana de reticulocitos humanos. Igualmente, se determinaron las regiones de interacción de las proteínas *Pv*RON4, *Pv*RON5 y *Pv*AMA1 con *Pv*RON2, lo que contribuirá a definir nuevos blancos moleculares para el desarrollo de vacunas contra esta especie parasitaria. Es de resaltar que las regiones de interacción identificadas en este trabajo, particularmente las de unión a la célula hospedera, interactúan específica y selectivamente con reticulocitos humanos CD71^{+}, lo que lleva a sugerir que, si bien existen proteínas ortólogas entre *P. falciparum* y *P. vivax*, cada parásito se ha especializado en utilizar diferentes regiones de cada proteína para interactuar con los receptores particulares de su célula blanco, enfatizando aún más la necesidad de diseñar intervenciones y estrategias de prevención dirigidas específicamente contra *P. vivax*.

## 2. Hipótesis

1. Los genes *ron4* y *ron5* están presentes en el genoma de *P. vivax*, se transcriben y expresan en esquizontes tardíos de la cepa VCG-1 de *P. vivax*.

2. Regiones de las proteínas *Pv*RON2, *Pv*RON4, *Pv*RON5 y *Pv*AMA1 interactúan con receptores sobre la membrana de reticulocitos humanos.

3. Diferentes regiones de *Pv*RON2 interactúan con *Pv*RON4, *Pv*RON5 o *Pv*AMA1.

## 3. Objetivos

Para dar respuestas a las hipótesis planteadas, se establecieron los siguientes objetivos:

### 3.1 Objetivo General

Estudiar las interacciones hospedero-patógeno y proteína-proteína de las proteínas del cuello de las roptrias *Pv*RON2, *Pv*RON4, *Pv*RON5 y el antígeno apical de membrana-1 (AMA1) en *P. vivax*.

### 3.2 Objetivos específicos

1. Identificar y caracterizar los genes *pvron4* y *pvron5* en *P. vivax*, así como las proteínas que codifican.
2. Caracterizar la interacción de las proteínas *Pv*RON2, *Pv*RON4, *Pv*RON5 y *Pv*AMA1 con reticulocitos humanos.
3. Evaluar las interacciones binarias entre la proteína *Pv*RON2 con *Pv*RON4, *Pv*RON5 y *Pv*AMA1.

## 4   Identificación de Nuevos Antígenos en *Plasmodium vivax*

La malaria es una enfermedad parasitaria causada por protozoarios del género *Plasmodium*, que se transmite al humano a través de la picadura de un vector artrópodo (mosquito *Anopheles*). En el humano, el parásito sufre una serie de transformaciones morfológicas y cambios a nivel transcripcional y proteico, que le permiten llevar a cabo una invasión eficiente (a dos diferentes células hospederas), y a su vez, escapar del sistema inmune humano. El ciclo del parásito inicia con la inoculación de los esporozoitos dentro del torrente sanguíneo, éstos alcanzan el hígado e invaden a los hepatocitos, donde se dividen y se diferencian para producir miles de merozoitos [43]. Una vez los merozoitos son liberados del esquizonte hepático, se da inicio a la fase sanguínea o intraeritrocítica, donde cada uno de los merozoitos liberados tiene la capacidad de invadir eritrocitos humanos. Durante esta fase, los parásitos desarrollan ciclos repetidos de replicación, egreso y re-invasión de nuevos eritrocitos, donde el parásito pasa de anillo a trofozoito y finalmente a la fase de esquizonte. Este proceso toma entre 48-72 horas, dependiendo de la especie de *Plasmodium* (Figura 3), y da lugar a las manifestaciones clínicas y patológicas de la enfermedad [44, 45]. Entender los mecanismos moleculares responsables del proceso por el cual los merozoitos se unen e invaden eritrocitos [29, 46], ha sido uno de los mayores focos de investigación básica en malaria, cuyo objetivo final es el desarrollo de medicamentos y vacunas contra esta parasitosis.
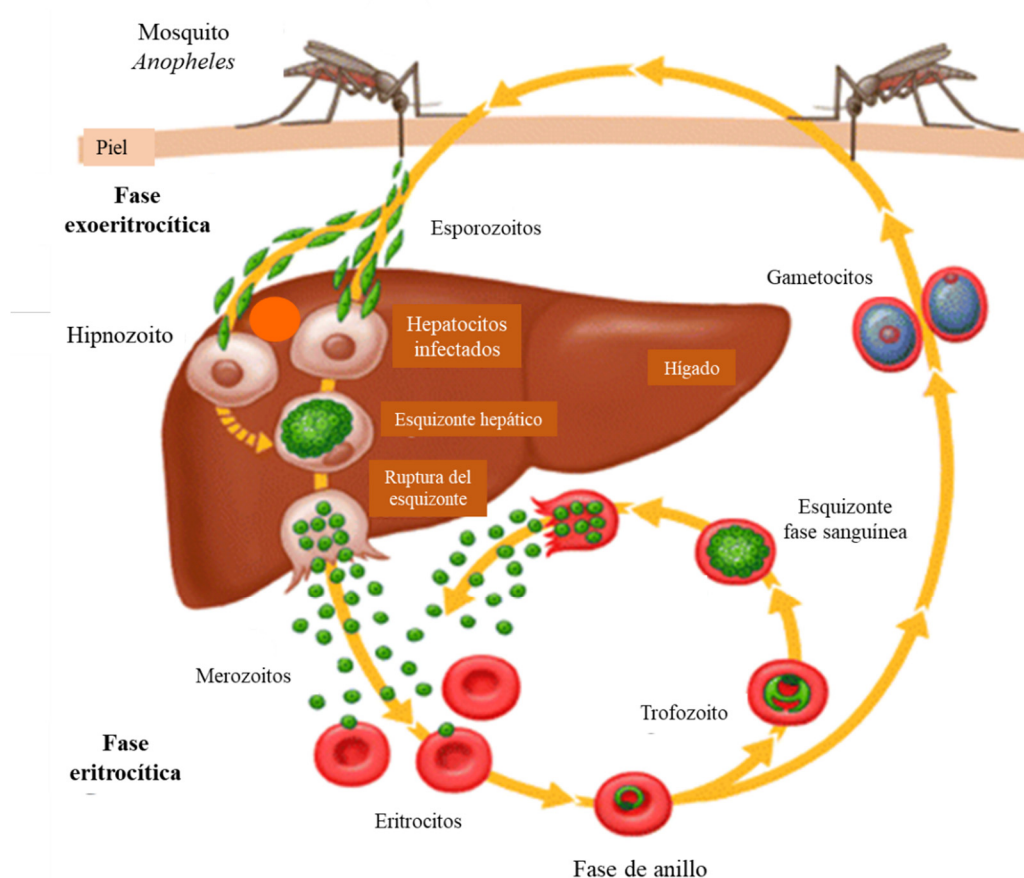
**Figura 3. Ciclo de vida de Plasmodium *en el humano.***
*El parásito de la malaria alterna entre dos formas parasitarias con distinta preferencia celular: el esporozoito invade células hepáticas, mientras que el merozoito invade eritrocitos. Una parte de los merozoitos que ingresan al eritrocito pasan a anillos y luego se diferencian a gametocitos, que son tomados por el mosquito, para perpetuar el ciclo de vida. Tomado y modificado de [47].*

En contraste a los procesos de invasión de virus y bacterias, los merozoitos invaden activamente los eritrocitos, a través de un proceso altamente organizado y orquestado por la interacción secuencial de ligandos del merozoito presentes sobre la membrana del parásito o descargados desde las roptrias y micronemas (organelos especializados de *Plasmodium*), con receptores sobre la célula hospedera [29, 40] (Figura 4). La información respecto a este proceso de invasión, se ha obtenido a partir de los estudios realizados con *Plasmodium knowlesi* y *P. falciparum* [41, 48] y ha sido conceptualmente dividido en cuatro fases: 1) reconocimiento inicial a través de interacciones

débiles y transitorias, que se asocian con ondas de deformación de la membrana del eritrocito, mediadas por la interacción de moléculas del parásito pertenecientes a las proteínas de superficie del merozoito (MSPs, del inglés merozoite surface proteins), entre ellas MSP-1, con la superficie del eritrocito [29, 49]. 2) Después de la unión, el eritrocito presenta una mayor deformación y el parásito reorienta su polo apical para quedar en contacto directo con la membrana de la célula hospedera [29]. Este proceso en *P. falciparum*, denominado reorientación, es mediado por el motor actina-miosina y por la liberación temprana de las proteínas de unión a eritrocitos (EBAs, del inglés Erythrocyte Binding Antigens) desde los micronemas y las proteínas homólogas a las de unión a reticulocito (Rhs, del inglés Reticulocyte-binding protein homologues) a partir de las roptrias, que se unen con alta afinidad a un rango amplio de receptores sobre la célula hospedera [50, 51]. Estas proteínas, además, definen en *P. falciparum* vías de invasión alternas, donde distintas combinaciones receptor-ligando pueden operar independientemente, para mediar la reorientación durante el proceso de invasión [52, 53]. 3) Luego de la reorientación, se da la formación de un pre-enlace fuerte, donde la proteína *Pf*Rh5 (presente solo en *P. falciparum* y *P. reichenowi*) es translocada a la membrana del eritrocito, formando un complejo proteico con otros antígenos del parásito, para unirse al receptor basigina (CD147) presente en el eritrocito, lo que desencadena la liberación de las RONs. Esta liberación favorece la transferencia de las RONs dentro de la membrana del eritrocito [29]. 4) Finalmente, se forma el enlace fuerte caracterizado por la presencia de una estructura similar a un anillo, que inicia desde el polo apical del parásito y se mueve progresivamente hacia la parte posterior, a medida que éste entra en la célula hospedera dentro de la vacuola parasitófora [54]. En *T. gondii* y *P. falciparum* se ha encontrado que este proceso es mediado por la translocación de las proteínas RONs hacia el citosol de la célula hospedera; allí, RON2 es insertada dentro de la membrana de la célula para servir de receptor a la

proteína AMA1, y esta interacción proporciona un punto de anclaje fuerte, que le permite al parásito una invasión exitosa [35, 55].
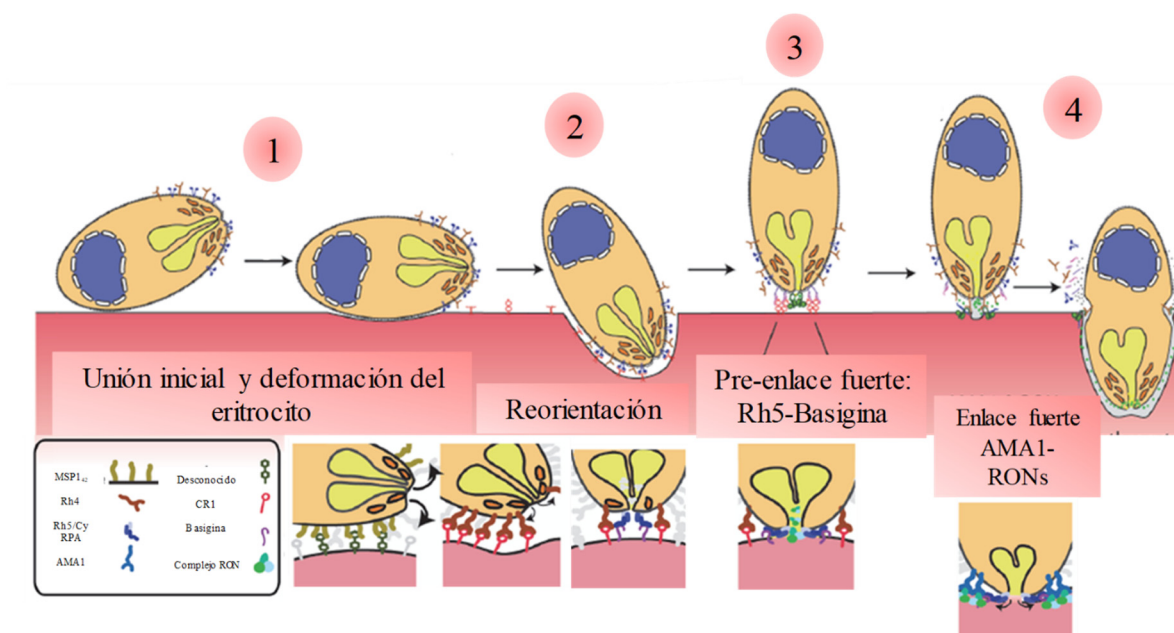


**Figura 4. *Proceso de invasión de los merozoitos de* Plasmodium *a eritrocitos humanos.***
*Se muestran cada una de las cuatro fases previas a la entrada del merozoito a su célula hospedera. En cada una de las fases, se han definido interacciones específicas entre ligandos del merozoito y receptores del eritrocito: CR1 (Complement Receptor 1 ) Modificado a partir de [29].*

Datos relacionados con el transcriptoma de *P. falciparum* involucran cerca de 60 candidatos que presentan picos transcripcionales justo en las horas finales del ciclo intraeritrocítico y que estarían codificando proteínas que participan durante las cuatro fases de invasión al eritrocito descritas previamente [28]. Dentro de estas proteínas, aquellas localizadas en las roptrias, han tomado gran importancia debido a que este organelo contiene diferentes compartimentos que le permiten liberar secuencialmente cada antígeno y participar de forma organizada en los procesos de adhesión, formación del enlace fuerte, sellamiento de la vacuola parasitófora y funciones post-invasión [30, 56]. Entre estos antígenos, las proteínas RONs han sido implicadas en la formación de la estructura central del proceso de invasión, denominada enlace fuerte, junto con la proteína AMA1 liberada de los micronemas [55] (Figura 2). Este complejo es similar en *P. falciparum* y *T.*

*gondii*, lo que lleva a sugerir que este macro-complejo es conservado a través del phylum *Apicomplexa* [35, 56]. Sin embargo, se han encontrado algunas diferencias relacionadas con la composición del complejo, entre las que se incluye la ausencia del ortólogo RON8 en parásitos no-coccidias [57] y la presencia de proteínas parálogas a *Tg*RON2 y *Tg*AMA1 que cooperan en la formación del enlace fuerte, cuando se hace la disrupción condicional de los genes *ama1* y *ron2*; este proceso es distinto en *P. falciparum*, donde no se reportan parálogos para estas proteínas [58]. Estos hallazgos llevan a sugerir que las diferencias encontradas en la formación del enlace fuerte respecto a su composición proteica, podrían reflejar la especificidad de invasión de cada parásito por su respectiva célula hospedera.

Si bien este proceso de invasión es conservado dentro del género *Plasmodium*, aún existen vacíos en el conocimiento respecto a las proteínas involucradas y a las interacciones moleculares que ocurren durante el proceso de invasión en los esporozoitos y merozoitos de *P. vivax*. Es de resaltar, que a diferencia de *P. falciparum* que es capaz de invadir los eritrocitos de cualquier estadio madurativo, *P. vivax* invade preferencialmente reticulocitos que aún expresan el antígeno CD71 sobre su superficie [59]. Esta preferencia celular, es uno los principales factores que ha afectado el desarrollo de un cultivo continuo *in vitro* de *P. vivax* y por tanto, el uso de aproximaciones genéticas y moleculares para estudiar el papel funcional de las proteínas en esta especie de parásito [18, 60].

Hasta hace poco, se creía que la invasión de los merozoitos de *P. vivax* dependía únicamente de la interacción entre la proteína de unión a Duffy (DBP, del inglés Duffy Binding Protein) con su receptor, el antígeno Duffy de unión a quimoquinas (DARC, del inglés Duffy antigen receptor for chemokines) [61] y de la interacción entre las proteínas de unión a reticulocito (RBPs, del

inglés Reticulocyte Binding Proteins) con proteínas expresadas solo en reticulocito [62]. Sin embargo, el antígeno DARC se expresa tanto en normocitos como en reticulocitos y análisis comparativos del proteoma de reticulocitos versus normocitos, muestran que la mayor diferencia entre estas dos células se relaciona con la abundancia de proteínas que hay en cada célula, más que en la exclusividad de alguna proteína en particular, lo cual no explica completamente la selectividad restringida de *P. vivax* por su célula hospedera [63]. Recientemente, se reportó la presencia de *P. vivax* en células negativas para el antígeno Duffy, lo que soporta la existencia de vías alternas de invasión (independiente de Duffy) [64], y pone de manifiesto la necesidad de identificar y caracterizar más antígenos con relevancia funcional, dentro de las diferentes fases del proceso de invasión del merozoito al reticulocito.

Apoyados por los estudios comparativos con otras especies de *Plasmodium*, como *P. falciparum* y *P. knowlesi*, así como los reportes recientes del genoma, transcriptoma y algunos estudios de proteoma con esquizontes de *P. vivax* [19, 22, 23, 65], se ha seguido una metodología a nivel bioinformático y experimental para identificar en *P. vivax* proteínas con posible función en la invasión a los reticulocitos. De esta forma, hasta el 2013, de las 38 proteínas identificadas en *P. vivax*, 16 de ellas fueron identificadas por nuestro grupo usando esta estrategia, entre las que se incluyen la proteína apical del merozoito relacionada con trombospondina (TRAMP, del inglés thrombospondin-related apical merozoite protein) [26], *Pv*RON2 [42], *Pv*RON1 [66], la proteína rica en asparaginas (ARP, del inglés Asparagine-Rich Protein) [67] y la proteína de superficie *Pv*41, entre otros [68]. Dada la relevancia funcional de las proteínas RONs durante el proceso de invasión en parásitos Apicomplexa, en este trabajo se identificaron los genes *pvron4* y *pvron5* en el genoma de la cepa VCG-1 de *P. vivax* y se determinó la transcripción de ellos en esquizontes

tardíos del ciclo intraeritrocítico. Estos genes codifican para proteínas de ~80kDa (*Pv*RON4) y ~133kDa (*Pv*RON5), que experimentan diferentes procesamientos proteolíticos y se expresan en el cuello de las roptrias de esquizontes tardíos de la cepa VCG-1. Toda esta información, fue recopilada en dos artículos que fueron publicados en la revista Malaria Journal [69, 70], los cuales se muestran a continuación.

MALARIA
JOURNAL

RESEARCH

Open Access

# Annotation and characterization of the *Plasmodium vivax* rhoptry neck protein 4 (*Pv*RON4)

Gabriela Arévalo-Pinzón[1,2], Hernando Curtidor[1,2], Jesica Abril[1] and Manuel A Patarroyo[1,2*]

## Abstract

**Background:** The tight junction (TJ) is one of the most important structures established during merozoite invasion of host cells and a large amount of proteins stored in *Toxoplasma* and *Plasmodium* parasites' apical organelles are involved in forming the TJ. *Plasmodium falciparum* and *Toxoplasma gondii* apical membrane antigen 1 (AMA-1) and rhoptry neck proteins (RONs) are the two main TJ components. It has been shown that RON4 plays an essential role during merozoite and sporozoite invasion to target cells. This study has focused on characterizing a novel *Plasmodium vivax* rhoptry protein, RON4, which is homologous to *Pf*RON4 and *Pk*RON4.

**Methods:** The *ron4* gene was re-annotated in the *P. vivax* genome using various bioinformatics tools and taking *Pf*RON4 and *Pk*RON4 amino acid sequences as templates. Gene synteny, as well as identity and similarity values between open reading frames (ORFs) belonging to the three species were assessed. The gene transcription of *pvron4*, and the expression and localization of the encoded protein were also determined in the VCG-1 strain by molecular and immunological studies. Nucleotide and amino acid sequences obtained for *pvron4* in VCG-1 were compared to those from strains coming from different geographical areas.

**Results:** *Pv*RON4 is a 733 amino acid long protein, which is encoded by three exons, having similar transcription and translation patterns to those reported for its homologue, *Pf*RON4. Sequencing *Pv*RON4 from the VCG-1 strain and comparing it to *P. vivax* strains from different geographical locations has shown two conserved regions separated by a low complexity variable region, possibly acting as a "smokescreen". *Pv*RON4 contains a predicted signal sequence, a coiled-coil α-helical motif, two tandem repeats and six conserved cysteines towards the carboxy-terminus and is a soluble protein lacking predicted transmembranal domains or a GPI anchor. Indirect immunofluorescence assays have shown that *Pv*RON4 is expressed at the apical end of schizonts and co-localizes at the rhoptry neck with *Pv*RON2.

**Conclusions:** Genomic, transcriptional and expression data reported for *Pv*RON4, as well as its primary structure characteristics suggest that this protein participates in reticulocyte invasion, as has been shown for its homologue *Pf*RON4.

**Keywords:** Bioinformatics analysis, Invasion, *Plasmodium vivax*, Rhoptry neck protein, Rhoptry, Tight junction

## Background

Malaria is a parasitic disease, primarily affecting pregnant females and children aged less than five years in tropical and subtropical areas around the world, mainly in sub-Saharan Africa [1]. A substantial increase in cases of *Plasmodium vivax* malaria has been reported recently in Asia and Latin America [2]. Such data, added to an increase in the number of severe disease reports, death

and resistance to first-generation anti-malarial drugs attributed to *P. vivax* [3-5], emphasize the need for developing effective control tools and acknowledging this parasite species as an important agent of vector-transmitted tropical diseases.

Basic research around the world into *P. vivax* has lagged behind compared to *Plasmodium falciparum* mainly due to a lack of *in vitro* continuous culturing as this requires a large amount of reticulocytes for maintaining and propagating this parasite species [6]. Among the various strategies being used to overcome this problem, comparative

* Correspondence: mapatarr.fidic@gmail.com
[1]Fundación Instituto de Inmunología de Colombia FIDIC, Carrera 50 # 26-20, Bogotá, Colombia
[2]Universidad del Rosario, Carrera 24 # 63C-69, Bogotá, Colombia

analysis with other species, such as *P. falciparum* and adapting *P. vivax* strains to *Aotus* monkeys [7], have allowed the identification during the last few years of several antigens in *P. vivax* which could be participating in invasion [8-11].

The merozoite's rapid and coordinated invasion of red blood cells (RBC) is mediated by initial contact with the host cell, re-orientation of the parasite's apical pole and active internalization into the host cell involving many sub-compartmentalized proteins localized in secretory organelles, such as micronemes and rhoptries [12]. The rhoptries are pear-shaped structures having two compartments called neck and bulb; despite being present in all parasites belonging to the phylum *Apicomplexa*, their size and number varies according to the target cell being invaded [13]. Transmission electron microscopy studies of *P. falciparum* and *Toxoplasma gondii* have revealed that some antigens are site-specifically distributed in a rhoptry [14,15]; such distribution seems to be the rule concerning important organization facilitating protein function in tight junction (TJ) and/or parasitophorous vacuole (PV) formation. Proteomics analysis of *T. gondii* rhoptries has shown minimum overlapping with *P. falciparum* proteins, except for some proteins localized in the rhoptry neck (RON), which could be involved in functions common to both parasites [16]. RON2 [17], RON4 [18] and RON5 [19] proteins have been identified to date in *P. falciparum*, forming part of a high molecular weight complex interacting with a microneme-derived protein called apical membrane antigen 1 (AMA-1) [20]. The assembly of this macromolecular complex allows TJ formation or irreversible binding which is important since this acts as a foothold for the parasite's motor machinery to propel the parasite into the PV for successful invasion.

Surface plasmon resonance (SPR) studies have determined that the *Pf*RON2 binding region to *Pf*AMA-1 lies within residues 2,020-2,059 and contains two conserved cysteines which are strongly implicated in the peptide's structure [21]. Crystallization of the *Pf*AMA-1/*Pf*RON2 complex has shown that the peptide binds in a U-shape to the AMA-1 ectodomain, inducing a conformational change in AMA-1 domain II (DII) [21], similar to that found for the interaction between *Tg*AMA-1/*Tg*RON2 [21]. Interestingly, different methodological approaches have proposed that blocking the interaction between AMA-1 and RON2 inhibits parasite invasion of its host cell [20,22,23]. Knowledge regarding these interactions has been key in understanding 4G2 antibody's invasion-inhibitory action (binding to AMA-1 DII), thereby impeding displacement in domain II and thus blocking interaction with RON2 [21].

*Pf*RON4 is the second most studied antigen from the aforementioned complex after AMA-1 and RON2. This is one of the most important proteins as it is most likely essential in merozoite and sporozoite invasion of their respective host cells [24]. No evidence has been advanced to date regarding the role played by RON4 in TJ formation and it is not known which proteins interact directly with it within the complex. However, RON4 has been the only protein from the whole complex that has been convincingly localized to junction constriction during invasion [25]. In fact, immunoprecipitation assays with *Plasmodium yoelii* merozoite proteins have supported RON4 (*Py*P140)-AMA1 interaction but *Py*RON2 and *Py*RON5 have not been identified within the complex. Importantly, immunogenicity studies have shown that *Pf*RON4 sequences elicit immunogenic responses in natural human malaria infection, suggesting their exposure to the immune system during host cell invasion as has been proposed for other important antigens, such as merozoite surface proteins (MSP) [26].

The importance of RON proteins in *P. falciparum* and in the model *Apicomplexa* parasite, *T. gondii*, has led to interest in identifying the functional characterization of RON proteins in other genera, such as *Neospora*, *Cryptosporidium*, *Babesia,* and other *Plasmodium* species [8,27]. Recent studies have shown that although most proteins from the complex are conserved within *Apicomplexa*, some are exclusive to certain members [27]. Such divergence regarding the complex's molecular composition suggests differences in TJ formation among *Apicomplexa* members and partly explains host cell specificity among parasites [27].

This study was thus aimed at making a correct annotation for *pvron4* in the *P. vivax* genome and characterizing *Pv*RON4 in late-stage schizonts from the VCG-1 strain. *Pv*RON4 is a 733 amino acid long protein containing typical characteristics concerning antigens involved in invasion, such as having a signal peptide, coiled-coil α-helical motifs, low complexity regions, and long conserved segments. Immunofluorescence studies using rhoptry and membrane markers as reference have shown that *Pv*RON4, just like its homologue in *P. falciparum* (*Pf*RON4), is localized in the rhoptries and could thus be participating in invasion.

## Methods
### Bioinformatics tools
The Basic Local Alignment Search Tool (BLAST), from the National Center for Biotechnology Information (NCBI), was used to find the homologous gene to *pfron4* (PF11_0168) and *pkron4* (PKH_091340) in the *P. vivax* genome. The presence of and boundaries between *pvron4* introns and exons was evaluated using Genscan [28], Spidey [29] and tBlastn. Gene structure, open reading frame (ORF) transcription direction, nucleotide and amino acid level identity, and similarity values between

*P. falciparum-P. vivax* and *Plasmodium knowlesi-P. vivax* were taken into account for synteny analysis.

Bioinformatics tools, such as SignalP [30], were used for evaluating the presence of a signal peptide in *Pv*RON4 sequence; TMHMM, Polyphobius and PredGPI were used to predict transmembranal domains and glycosylphosphatidylinositol (GPI) anchors, since the presence of these motifs and domains is typical of several antigens considered as candidates for an anti-malarial vaccine [31-33]. Sequence tandem repeats extraction and architecture modelling (XSTREAM, variable 'X') was used for finding repeat sequences and the simple modular architecture research tool (SMART) [34] with Globplot for searching for other important motifs and domains.

### DNA, RNA and protein source and cDNA synthesis

A blood sample taken from an *Aotus sp.* monkey infected with the Colombian *P. vivax* Guaviare 1 strain (VCG-1) was used for extracting nucleic acids and proteins. The VCG-1 strain had been cultured via successive passes *in vivo* in *Aotus sp.* monkeys from the primate station in Leticia, Amazonas, as thoroughly described [7]. The monkeys were kept under constant care, supervised by a primatologist, according to the conditions established by Colombian Animal Protection law (law 84/1989) and Corpoamazonía (the Colombian entity regulating environmental matters in the region) (resolution 00066, September 13, 2006).

A schizont-enriched sample was obtained using a discontinuous Percoll gradient (GE Healthcare) and genomic DNA (gDNA) was isolated using a Wizard genomic DNA purification kit (Promega), following the manufacturer's recommendations. RNA was isolated from the parasite using the Trizol method [35], followed by treatment with RQ1 RNase-free DNase (Promega). Purified RNA and gDNA integrity was examined by electrophoresis on agarose gels. Five microlitres of RNA were taken as template for cDNA synthesis, using a one-step RT-PCR SuperScript III kit (Invitrogen).

### Primer design and *pvron4* amplification

Based on bioinformatics analysis, the PVX_091435 gene ID gene was re-annotated (Figure 1) and such information was used to design primers for amplifying *pvron4* from gDNA and cDNA. *pvron4*G1 5'- ATG TCT CGT AAA AGG GTT TT-3' and *pvron4*G2 5'-CAA GTC TTC AAA AAT GAG ATT T-3' primers amplified from predicted ATG until the stop codon. These primers were included in PCR reactions with Gotaq flexi DNA polymerase (Promega) with gDNA or RT-PCR products from samples treated with or without reverse transcriptase (RT$^+$ and RT$^-$ respectively) at 25 μL final volume, according to the manufacturer's instructions. Amplification conditions
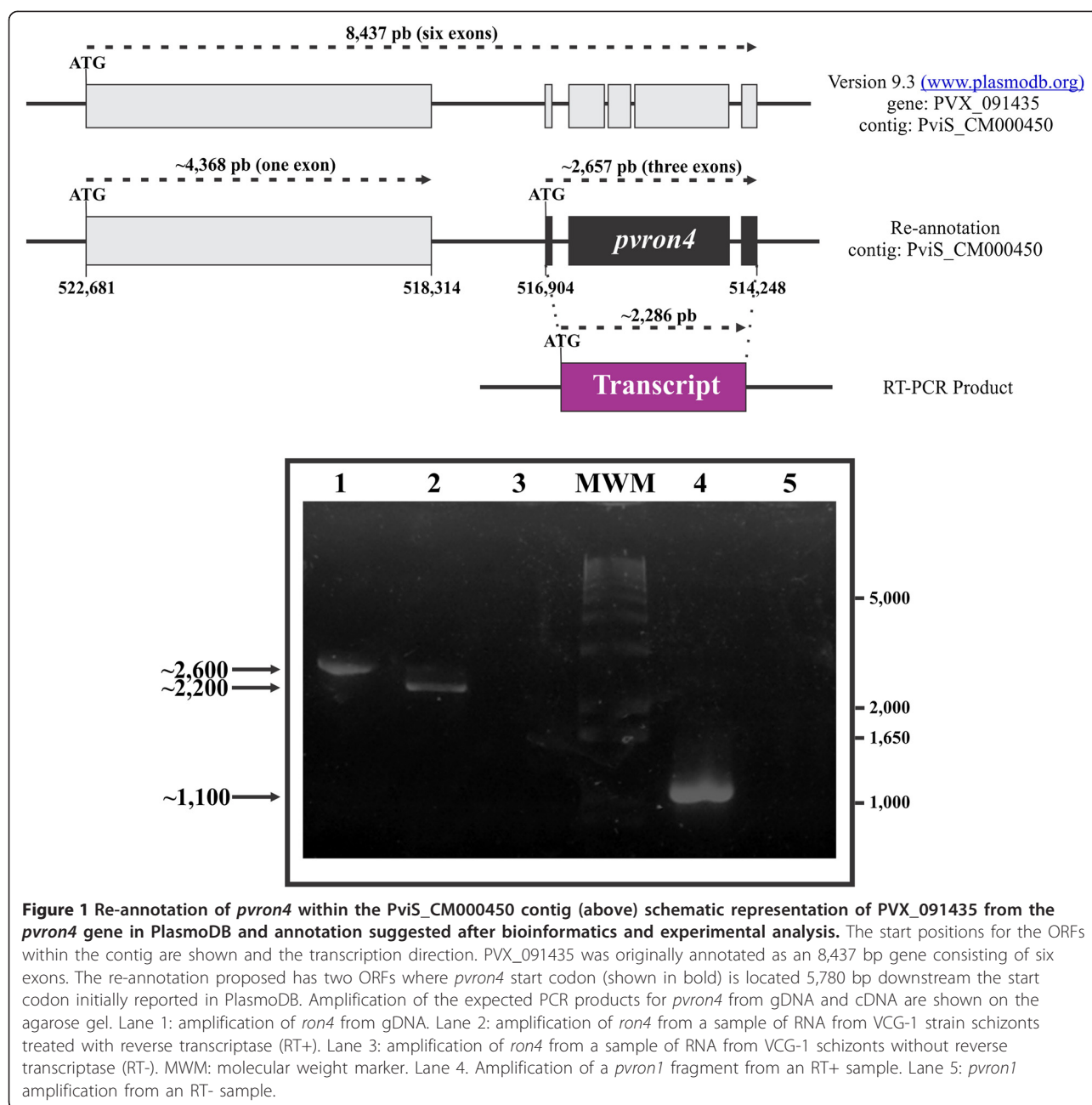
were as follows: a 5-min cycle at 95°C, followed by 35 cycles of 1 min at 56°C, 3 min at 72°C and 1 min at 95°C. A final extension step lasted 10 min at 72°C. A *pvron1* region (~1053 from cDNA) transcribed during the erythrocyte phase was amplified using direct 5′- atg GCG AAG GAG CCC AAG TG-3′ and reverse 5′- ATC CCT AGC AAT GCT TCG -3′ primers for evaluating cDNA contamination by gDNA [36].

Primers called ExtD: 5'-TCC AGA CGT GTC AGA GTG-3' and ExtR: 5'- TAG CTT CGT TCC TTT GGG-3' were also designed; they were localized 72 bp upstream of the start codon and 49 bp downstream the stop codon of the *pvron4* gene, respectively. Amplification conditions from gDNA and cDNA were the same as those used for the *pvron4*G1 and *pvron4*G2 primers. The polymerase chain reaction (PCR) products were visualized on 1% agarose gel and then purified with a Wizard PCR preps kit (Promega). PCR products from gDNA and cDNA were cloned in pGEM-T (Promega) and pEXP5-CT/TOPO vectors (Invitrogen) respectively by TA cloning. Positive clones and PCR products were sequenced in an ABI PRISM 310 Genetic Analyzer. The sequences were analyzed using CLC DNA Workbench (CLC bio) and compared to the Sal-1, Mauritania I and India VII strain sequences [37] using Clustal W [38].

### Obtaining polyclonal antibodies against *Pv*RON4, *Pv*12 and *Pv*RON2

Taking the amino acid sequence predicted for *Pv*RON4 as reference, two 20 residue-long, B-epitope peptides were selected, chemically synthesized in solid phase and cysteine and glycine (CG) were added to amino and carboxy termini for polymerization. Synthetized peptides were numbered 36114 (CG$^{181}$GSASESAAPSEEKASEE NVP$^{200}$GC) and 36115 (CG$^{719}$AAEVEKRGFDEDYIQEEI KN $^{738}$GC). These peptides were selected based on high average values for Parker's antigenicity, hydrophilicity and solvent accessibility using Antheprot software [39] and high values obtained when using Bepipred (0.35 default threshold and 75% specificity) [40]. It was also taken into account that the peptides corresponded to different protein regions, for detecting fragments in case of proteolytic processing occurring in *Pv*RON4.

Seven to eight week-old BAlb/C mice were intraperitoneally (ip) inoculated with 75 μg of each polymeric peptide emulsified in Freund's complete adjuvant (FCA) on day 0 for evaluating *Pv*RON4 expression in VCG-1 strain schizonts. Three boosters were given on days 30, 45 and 60 using the same peptides emulsified in Freund's incomplete adjuvant (FIA). Polyclonal antibodies against *Pv*12 localized on the membrane and *Pv*RON2 localized in the rhoptries were obtained for *Pv*RON4 localization studies. Peptide 35520 (CG$^{1674}$KLQQEQNELNEEKERQ

**Figure 1 Re-annotation of *pvron4* within the PviS_CM000450 contig (above) schematic representation of PVX_091435 from the *pvron4* gene in PlasmoDB and annotation suggested after bioinformatics and experimental analysis.** The start positions for the ORFs within the contig are shown and the transcription direction. PVX_091435 was originally annotated as an 8,437 bp gene consisting of six exons. The re-annotation proposed has two ORFs where *pvron4* start codon (shown in bold) is located 5,780 bp downstream the start codon initially reported in PlasmoDB. Amplification of the expected PCR products for *pvron4* from gDNA and cDNA are shown on the agarose gel. Lane 1: amplification of *ron4* from gDNA. Lane 2: amplification of *ron4* from a sample of RNA from VCG-1 strain schizonts treated with reverse transcriptase (RT+). Lane 3: amplification of *ron4* from a sample of RNA from VCG-1 schizonts without reverse transcriptase (RT-). MWM: molecular weight marker. Lane 4. Amplification of a *pvron1* fragment from an RT+ sample. Lane 5: *pvron1* amplification from an RT- sample.

RQEN[1693]GC) [8] was used for *Pv*RON2 and peptides CG-AKIRVRKRSGEEYDKEIFNL-GC and CG-AHFEFA TTPDDQNSVSEPRA-GC were used for *Pv*12 [10]. These peptides were inoculated into negative New Zealand rabbits for recognizing *P. vivax*-derived proteins by Western blot, as described previously [8,10]. Animal sera was collected and stored at -70°C for later studies. Animal immunization and bleeding was done according to Colombian animal protection recommendations (Law 84/1989) and Resolution 8430/1993 for handling live animals for research or experimentation purposes.

## *Pv*RON4 immunodetection assays
### ELISA
A previously described ELISA test was used for determining inoculated peptide immunogenicity [19]. Briefly, each of the inoculated peptides was sown in 96-well ELISA plates and incubated at 1:100 dilution of each serum. A peroxidase-coupled, anti-mouse antibody was used as secondary antibody (Vector Laboratories), diluted 1:5,000.

### Western blot
The proteins were extracted from a *P. vivax* schizont-enriched sample and separated on an SDS-PAGE gel, as

previously described [8]. Proteins transferred to a nitro-cellulose membrane were incubated with pre-immune or immune serum. In a parallel assay, immune serum was pre-incubated with inoculated polymeric peptides before being incubated with the nitrocellulose membrane. A peroxidase-coupled, anti-mouse IgG antibody was used as secondary antibody (Vector Laboratories).

### Indirect immunofluorescence

A suspension of erythrocytes parasitized by *P. vivax* VCG-1 was washed thrice with PBS (pH 7.2–7.4), then centrifuged at 2,500×g for 4 min and suspended in a 1:1 PBS–fetal bovine serum solution. This solution was seeded on eight-well multitest slides and left to dry at room temperature for 24 hr. Parasites slides were fixed using a 4% formaldehyde solution followed by three washes with PBS. The slides were blocked with 1% skimmed milk in PBS for 30 min and incubated with anti-*Pv*RON4 primary antibody obtained in mice and anti-*Pv*12 or anti-*Pv*RON2 antibodies in 1:40 dilution. Fluorescein-labelled anti-rabbit IgG (FITC) (Vector Laboratories) and rhodamine-labelled anti-mouse IgG (Millipore) were used as secondary antibody for 60 min, followed by three PBS washes. Parasite nuclei were stained with a 2 µg/mL solution of 4′,6-diamidino-2-phenylindole (DAPI) for 20 min at room temperature and fluorescence was visualized in a fluorescence micro-scope (Olympus BX51) using an Olympus DP2 camera and Volocity software (Perkin Elmer).

### Statistical analysis

Differences in antibody production between pre-immune and post-third immunization sera obtained from ELISA were evaluated using non-parametric Wilcoxon signed rank test.

## Results and discussion

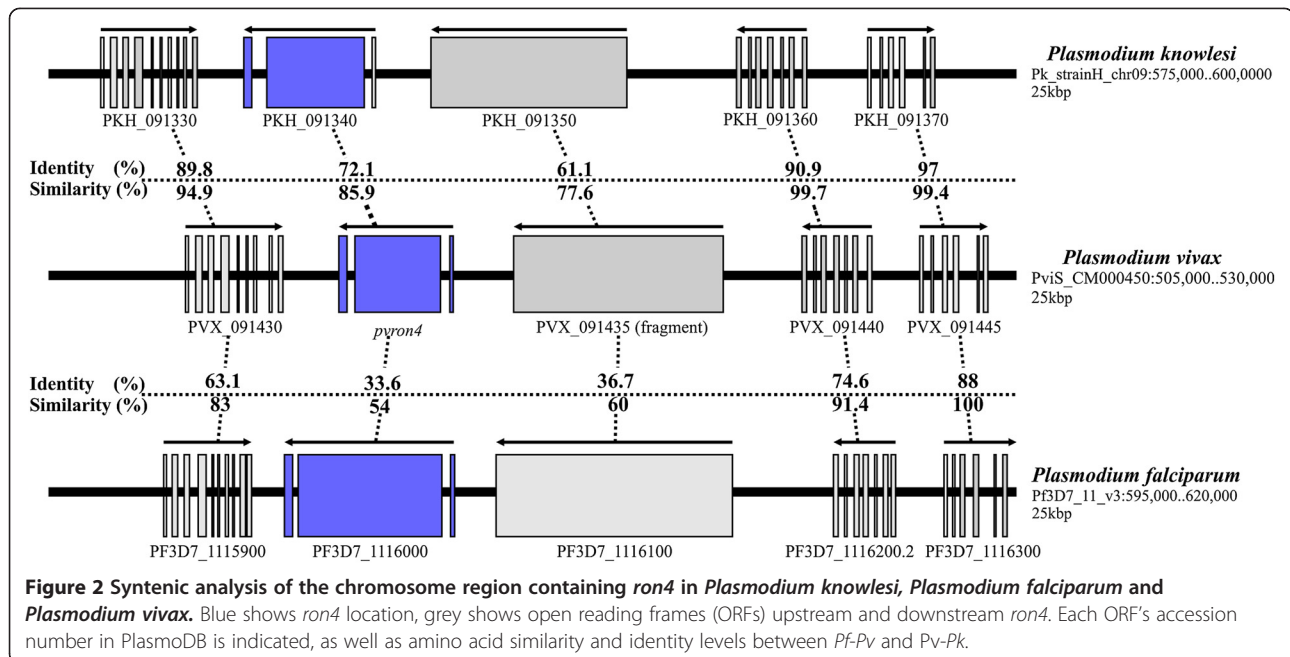### In-silico re-annotation of the ron4 gene in Plasmodium vivax

The search for the *pvron4* gene was initially made using the *Pf*RON4 protein amino acid sequence (PF11_0168) containing 1,201 residues [18]. tBlastn results revealed a nucleotide region having a high probability of containing *pvron4* in the PviS_CM000450 contig localized in chromosome 9. Analysis showed a *pvron4* segment running from nucleotide 516,555 to 514,248 corresponding to residues 484 to 1,201 in *P. falciparum*; however, the beginning of *pvron4* could not be found. The *P. knowlesi* RON4 (PKH_091340) amino acid sequence reported in PlasmoDB was used to overcome this. *Plasmodium knowlesi* is a parasite which infects *Macaca fascicularis* monkeys and shares a close phylogenetic relationship with *P. vivax* as shown in small subunit rRNA analysis and the high identity and similarity values between

orthologous proteins [9,41]. This led to finding that *pvron4* was located between nucleotide 516,904 and 514,248, having a ~2,657 bp length. Interestingly, a putative gene called PVX_091435 (8,437 bp and six exons) was found to be annotated in this nucleotide region which is also found when *Pf*RON4 and *Pk*RON4 amino acid sequences are used as templates for Blastp analysis (Figure 1). However, analyzing the presence of and boundaries for the exons/introns proposed for the PVX_091435 gene indicated that its gene structure had not been correctly annotated (Figure 1). In-silico analysis of this genome locus suggested that there were two ORFs; the first had high similarity (60%) with a *P. falciparum* serine esterase and began at position 522,681 of the PviS_CM000450 contig and ended at nucleotide 518,314 (Figure 1) while the second ORF was found downstream serine esterase in position 516,904 and referred to *pvron4*. The suggested *pvron4* structural region had three exons; a first short one ~78 bp (in ORF -1) having consensus intron splice sites, a second long ~2,019 bp (in ORF -2) having its respective donor site sequence ending with a ~189 bp exon (in ORF -3) (Figure 1).

Once *ron4* structure had been annotated, a syntenic analysis was made for evaluating neighboring genes' structure (number of introns and exons), transcription orientation and determining identity (ID) and similarity (SI) values at protein level. *Pv*RON4 amino acid alignment with *Pf*RON4 and *Pk*RON4 showed that ID and SI values were greater with *Pk*RON4 (Figure 2) thereby agreeing with the close relationship between these two parasite species. This coincided with previous studies showing greater similarity between *P. vivax* and *P. knowlesi* proteins than with other *Plasmodium* species [10,11]. Conservation was also found regarding the structure of genes upstream and downstream *ron4* in *P. falciparum*, *P. vivax* and *P. knowlesi*, having 61.1%-97% and 77.6%-99.7% amino acid ID and SI values for *Pk-Pv* respectively, and 33.6%-88% and 54%-100% for *Pf-Pv*, respectively (Figure 2).

### Transcription and analysis of the VCG-1 strain pvron4 sequence

The *pvron4* gene was amplified from gDNA and cDNA to confirm its presence and re-annotation. Figure 1 shows that a ~2,600 bp gDNA product was obtained and a ~2,200 bp product from cDNA (RT+) thereby confirming the presence of intron regions. No amplification was observed from RT- samples, indicating that the cDNA preparation had no gDNA contamination. PCR amplification of the *pvron4* encoding sequence suggested the presence of this transcript (~2,200 bp) in mature *P. vivax* blood stages, similar to that found for *pvron1* (Figure 1) [36]. The *pvron4* transcription time coincided with that displayed by *pfron4* (42-48 hr of the intra-

**Figure 2 Syntenic analysis of the chromosome region containing *ron4* in *Plasmodium knowlesi*, *Plasmodium falciparum* and *Plasmodium vivax*.** Blue shows *ron4* location, grey shows open reading frames (ORFs) upstream and downstream *ron4*. Each ORF's accession number in PlasmoDB is indicated, as well as amino acid similarity and identity levels between *Pf-Pv* and *Pv-Pk*.

erythrocyte cycle) [42]. Transcriptome and proteome analysis of *P. falciparum* has shown that most ORFs transcribed at the end of the intra-erythrocyte cycle are expressed during and participate in host cell invasion [42,43].

When aligning *pvron4* gDNA and cDNA nucleotide sequences obtained from sequencing three independent clones it was found that the gDNA was 2,573 bp while cDNA was 2,202 bp. The gene consisted of three exons and two intron regions, encoding a 733 residue-long protein (~80 kDa); this genomic organization coincided with that proposed by bioinformatics analysis (Figure 1). When comparing the sequences obtained from VCG-1 to those reported for Sal-1 (PVX_091435), a match was found from nucleotide 516,904 onwards within the contig, coinciding with previous analysis proposed for *pvron4* localization and structure (Figure 1). The alignment showed that exon 2 was shorter in VCG-1 (1,932 bp) compared to Sal-1 (2,019 bp) due to deletions corresponding to a loss of 81 nt (27 amino acid residues) between amino acids 235-262 and a deletion of two triplets (GTG AGG) encoding glycine (G671) and glutamic acid (E672). According to bioinformatics analysis, exon two encoded a low complexity region rich in tandem repeats (TR) (Figure 3). Analysis also revealed a change at nucleotide level involving T for G in position 810 (T810G); this substitution led to a valine (V) being changed for a glycine (G) in position 199 (V199G). A substitution of A for G was found in VCG-1 strain intron 2 compared to Sal-1. VCG-1 gDNA and cDNA consensus sequences were deposited in [GenBank: KF378614 and KF378615].

Comparative analysis between VCG-1 *Pv*RON4 (Colombian), Sal-1 (El Salvador), India VII (southern Asia) and Mauritania I (Africa) amino acid sequences revealed differences regarding protein length (see Additional file 1), mainly due to large deletions between residues 179-305 where the TRs occurred. The first 150 amino acids corresponded to a conserved region followed by a variable zone having repeat regions and a highly conserved carboxy-terminal in the strains evaluated here. Such distribution was similar to that reported for several antigens proposed as candidates for an anti-*P. falciparum* vaccine where proteins' conserved regions are surrounded by variable and low complexity regions acting as immune system distractors, while important functional regions for the parasite remain poorly recognized. The circumsporozoite protein (CSP) consists of a central repeat region, which is diverse across *Plasmodium* species, and flanking the repeats are two conserved domains: region I, at the N-terminus of the repeats, and a known C-terminal cell-adhesive adhesive motif, termed type I thrombospondin repeat (TSR) [44]. Even though the repeat regions' function has not been made clear to date, it has been found that they are species-specific, low complexity and (in many cases) are responsible for the diversity between different parasite isolates [45]. It has been suggested that the presence of polymorphic repeats affects antibody affinity maturation, thus suppressing antibody response to critical epitopes or adjacent regions [46].

## Bioinformatics analysis of *Pv*RON4 primary sequence

The *Pv*RON4 amino acid sequence was scanned for predicting different characteristics. VCG-1 *Pv*RON4 had
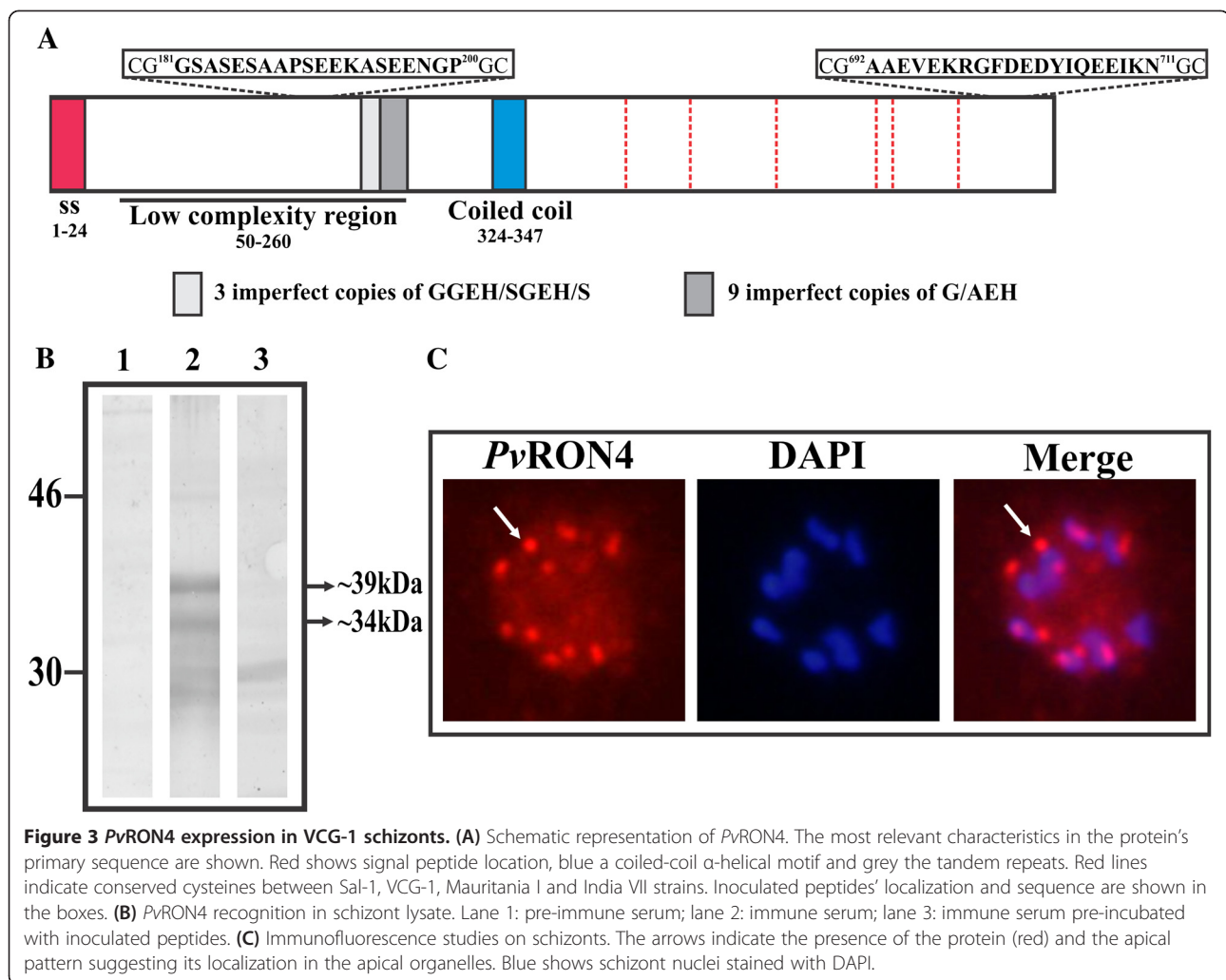
**Figure 3** *Pv*RON4 expression in VCG-1 schizonts. **(A)** Schematic representation of *Pv*RON4. The most relevant characteristics in the protein's primary sequence are shown. Red shows signal peptide location, blue a coiled-coil α-helical motif and grey the tandem repeats. Red lines indicate conserved cysteines between Sal-1, VCG-1, Mauritania I and India VII strains. Inoculated peptides' localization and sequence are shown in the boxes. **(B)** *Pv*RON4 recognition in schizont lysate. Lane 1: pre-immune serum; lane 2: immune serum; lane 3: immune serum pre-incubated with inoculated peptides. **(C)** Immunofluorescence studies on schizonts. The arrows indicate the presence of the protein (red) and the apical pattern suggesting its localization in the apical organelles. Blue shows schizont nuclei stained with DAPI.

a signal peptide within the first 24 amino acids (Figure 3A) and a probable type I peptidase cleavage site between residues S24-F25, suggesting that once the protein has been synthesized, it is transported to be either secreted or inserted into cell membranes. In fact, it has been reported that *Pf*RON4 and *Tg*RON4 homologous proteins are secreted by the parasite towards host cell membrane [47,48]. Bioinformatics analysis detected no potential transmembrane domains or GPI anchors in *Pv*RON4, *Tg*RON4 and *Pf*RON4, thereby classifying them as soluble proteins. It has been shown that some soluble *P. falciparum* merozoite surface proteins, such as MSP 3, 6, 7 and 9, are associated and/or interact with membrane-anchored antigens [49]. Interestingly, *Pv*RON4 contained a coiled-coil α-helical motif in its sequence between residues 324-347 (Figure 3A) suggesting *Pv*RON4 participation in protein-protein interaction and complex formation. A low complexity (Figure 3A), highly variable region was found (see Additional file 1) between residues

50 to 260 containing two TRs. The first repeat consisted of seven amino acids (GGEH/SGEH/S) and the second of three amino acids having nine imperfect copies of G/AEH residues. A conserved region between residues 277 and 733 was found when comparing RON4 from VCG-1 with other *P. vivax* strains, such region being characterized by having six conserved cysteines. Several functionally relevant malarial antigens, such as AMA-1 and RON2, have cysteine-containing regions forming disulphide bridges and/or ordered 3D structures for fulfilling their biological function [21]. However, further structural and functional studies are needed for evaluating this conserved domain's importance in *Pv*RON4 and the influence of repeat regions in an immune response against *Pv*RON4.

## *Pv*RON4 expression and localization in VCG-1 late-stage schizonts

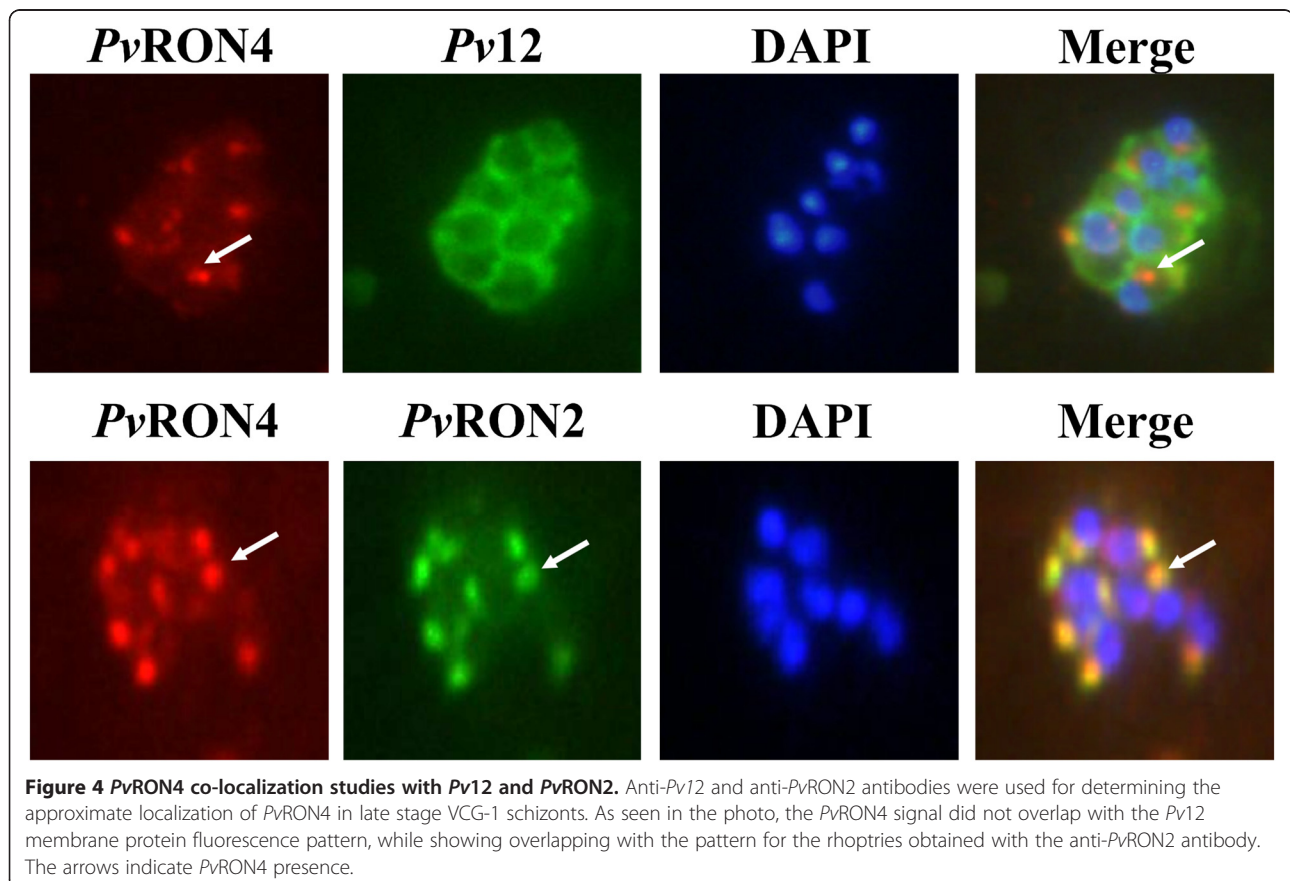Anti-*Pv*RON4 antibodies were induced in mice for evaluating *Pv*RON4 expression and cell localization in *P.*

*vivax* schizonts. ELISA revealed that immune sera showed high reactivity against 35114 and 35115 peptides ($A_{620}$ 0.63 ± 0.22) compared to pre-immune sera ($A_{620}$ 0.03 ± 0.01) (p=0.00). Sera ability to recognize *Pv*RON4 in VCG-1 schizont lysate was then evaluated using Western blot. Figure 3B shows that polyclonal antibodies specifically recognized ~39 kDa and ~34 kDa bands which were not recognized by either the pre-immune sera or hyper-immune sera which had been pre-incubated with the inoculated peptides. Taking a ~80 kDa predicted *Pv*RON4 size, two bands below the expected molecular weight were detected, suggesting that *Pv*RON4 undergoes a similar proteolytic processing to that reported for most proteins localized in the apical organelles, including other RON proteins [47]. It has been suggested that rhoptry proteins' proteolytic cleavage is an essential event for maturation and/or promoting interaction with cell surface receptors or between parasite proteins [47,50].

The anti-*Pv*RON4 antisera also recognized the protein on VCG-1 late-stage schizonts, having the typical apical organelle punctate pattern (Figure 3C) common to other apical proteins [8,18]. Co-localization studies using antibodies against *Pv*RON4 and *Pv*12 showed that while *Pv*12 was expressed on merozoite surface with a bunch of grapes-like pattern, *Pv*RON4 had a punctate pattern, not overlapping *Pv*12 staining (Figure 4). When anti-*Pv*RON4 antibodies were used with anti-*Pv*RON2, the staining overlapped, coinciding with *Tg*RON4 and *Pf*RON4 localization in the rhoptry neck (Figure 4). Previous studies in *T. gondii* and *P. falciparum* have shown that RON4 is the only protein where strong evidence has been produced concerning localization in the TJ [25,51] and has been chosen as a model for studying the dynamics of merozoite invasion of RBC [25].

## Conclusions

Bioinformatics and experimental analyses allowed the identification of a new gene having three exons and encoding the *Pv*RON4 protein. Like *Pf*RON4, its *P. falciparum* homologue, *Pv*RON4 is expressed in late schizonts and is localized in the rhoptries. Strong evidence regarding RON4 association in the TJ and its conservation in the *Plasmodium* genus has highlighted this protein's importance and the need for evaluating its mechanism of action and association within the *P. vivax* AMA1-RON complex.



**Figure 4 *Pv*RON4 co-localization studies with *Pv*12 and *Pv*RON2.** Anti-*Pv*12 and anti-*Pv*RON2 antibodies were used for determining the approximate localization of *Pv*RON4 in late stage VCG-1 schizonts. As seen in the photo, the *Pv*RON4 signal did not overlap with the *Pv*12 membrane protein fluorescence pattern, while showing overlapping with the pattern for the rhoptries obtained with the anti-*Pv*RON2 antibody. The arrows indicate *Pv*RON4 presence.

## Additional file

**Additional file 1:** *Pv*RON4 amino acid alignment between different *Plasmodium vivax* strains. Conserved cysteines between VCG-1 (Colombia), Sal-1 (Salvador), India VII (India) and Mauritania I (Africa) strains are shown in red.

### Competing interests

The authors declare that they have no competing interests.

### Authors' contributions

GAP carried out bioinformatics analyses, molecular biology assays and wrote the initial manuscript. HC synthesized and purified the peptides used for rabbit and mice immunizations and analyzed data. JA carried out immunoassays. MAP evaluated and coordinated assays, and revised the final manuscript. All authors read and approved the final manuscript.

### References

1. WHO: *World malaria report*. Geneva: WHO Press; 2011.
2. Price RN, Tjitra E, Guerra CA, Yeung S, White NJ, Anstey NM: **Vivax malaria: neglected and not benign.** *Am J Trop Med Hyg* 2007, **77**:79–87.
3. Beg MA, Khan R, Baig SM, Gulzar Z, Hussain R, Smego RA Jr: **Cerebral involvement in benign tertian malaria.** *Am J Trop Med Hyg* 2002, **67**:230–232.
4. Anstey NM, Russell B, Yeo TW, Price RN: **The pathophysiology of vivax malaria.** *Trends Parasitol* 2009, **25**:220–227.
5. Baird JK: **Resistance to therapies for infection by *Plasmodium vivax*.** *Clin Microbiol Rev* 2009, **22**:508–534.
6. Noulin F, Borlon C, Van Den Abbeele J, D'Alessandro U, Erhart A: **1912-2012: a century of research on *Plasmodium vivax* in vitro culture.** *Trends Parasitol* 2013, **29**:286–294.
7. Pico De Coana Y, Rodriguez J, Guerrero E, Barrero C, Rodriguez R, Mendoza M, Patarroyo MA: **A highly infective *Plasmodium vivax* strain adapted to *Aotus* monkeys: quantitative haematological and molecular determinations useful for *P. vivax* malaria vaccine development.** *Vaccine* 2003, **21**:3930–3937.
8. Arevalo-Pinzon G, Curtidor H, Patino LC, Patarroyo MA: **PvRON2, a new *Plasmodium vivax* rhoptry neck antigen.** *Malar J* 2011, **10**:60.
9. Mongui A, Perez-Leal O, Rojas-Caraballo J, Angel DI, Cortes J, Patarroyo MA: **Identifying and characterising the *Plasmodium falciparum* RhopH3 *Plasmodium vivax* homologue.** *Biochem Biophys Res Commun* 2007, **358**:861–866.
10. Moreno-Perez DA, Areiza-Rojas R, Florez-Buitrago X, Silva Y, Patarroyo ME, Patarroyo MA: **The GPI-anchored 6-Cys protein Pv12 is present in detergent-resistant microdomains of *Plasmodium vivax* blood stage schizonts.** *Protist* 2013, **164**:37–48.
11. Moreno-Perez DA, Mongui A, Soler LN, Sanchez-Ladino M, Patarroyo MA: **Identifying and characterizing a member of the RhopH1/Clag family in *Plasmodium vivax*.** *Gene* 2011, **481**:17–23.
12. Cowman AF, Berry D, Baum J: **The cellular and molecular basis for malaria parasite invasion of the human red blood cell.** *J Cell Biol* 2012, **198**:961–971.
13. Baum J, Gilberger TW, Frischknecht F, Meissner M: **Host-cell invasion by malaria parasites: insights from *Plasmodium* and *Toxoplasma*.** *Trends Parasitol* 2008, **24**:557–563.
14. Nichols BA, Chiappino ML, O'Connor GR: **Secretion from the rhoptries of Toxoplasma gondii during host-cell invasion.** *J Ultrastruct Res* 1983, **83**:85–98.
15. Stewart MJ, Schulman S, Vanderberg JP: **Rhoptry secretion of membranous whorls by *Plasmodium falciparum* merozoites.** *Am J Trop Med Hyg* 1986, **35**:37–44.
16. Bradley PJ, Ward C, Cheng SJ, Alexander DL, Coller S, Coombs GH, Dunn JD, Ferguson DJ, Sanderson SJ, Wastling JM, Boothroyd JC: **Proteomic analysis of rhoptry organelles reveals many novel constituents for host-parasite interactions in *Toxoplasma gondii*.** *J Biol Chem* 2005, **280**:34245–34258.
17. Cao J, Kaneko O, Thongkukiatkul A, Tachibana M, Otsuki H, Gao Q, Tsuboi T, Torii M: **Rhoptry neck protein RON2 forms a complex with microneme protein AMA1 in *Plasmodium falciparum* merozoites.** *Parasitol Int* 2009, **58**:29–35.
18. Morahan BJ, Sallmann GB, Huestis R, Dubljevic V, Waller KL: *Plasmodium falciparum*: **genetic and immunogenic characterisation of the rhoptry neck protein PfRON4.** *Exp Parasitol* 2009, **122**:280–288.
19. Curtidor H, Patino LC, Arevalo-Pinzon G, Patarroyo ME, Patarroyo MA: **Identification of the *Plasmodium falciparum* rhoptry neck protein 5 (PfRON5).** *Gene* 2011, **474**:22–28.
20. Collins CR, Withers-Martinez C, Hackett F, Blackman MJ: **An inhibitory antibody blocks interactions between components of the malarial invasion machinery.** *PLoS Pathog* 2009, **5**:e1000273.
21. Vulliez-Le Normand B, Tonkin ML, Lamarque MH, Langer S, Hoos S, Roques M, Saul FA, Faber BW, Bentley GA, Boulanger MJ, Lebrun M: **Structural and functional insights into the malaria parasite moving junction complex.** *PLoS Pathog* 2012, **8**:e1002755.
22. Srinivasan P, Beatty WL, Diouf A, Herrera R, Ambroggio X, Moch JK, Tyler JS, Narum DL, Pierce SK, Boothroyd JC, Haynes JD, Miller LH: **Binding of *Plasmodium* merozoite proteins RON2 and AMA1 triggers commitment to invasion.** *Proc Natl Acad Sci USA* 2011, **108**:13275–13280.
23. Lamarque M, Besteiro S, Papoin J, Roques M, Vulliez-Le Normand B, Morlon-Guyot J, Dubremetz JF, Fauquenoy S, Tomavo S, Faber BW, Kocken CH, Thomas AW, Boulanger MJ, Bentley GA, Lebrun M: **The RON2-AMA1 interaction is a critical step in moving junction-dependent invasion by apicomplexan parasites.** *PLoS Pathog* 2011, **7**:e1001276.
24. Giovannini D, Spath S, Lacroix C, Perazzi A, Bargieri D, Lagal V, Lebugle C, Combe A, Thiberge S, Baldacci P, Tardieux I, Menard R: **Independent roles of apical membrane antigen 1 and rhoptry neck proteins during host cell invasion by apicomplexa.** *Cell Host Microbe* 2011, **10**:591–602.
25. Riglar DT, Richard D, Wilson DW, Boyle MJ, Dekiwadia C, Turnbull L, Angrisano F, Marapana DS, Rogers KL, Whitchurch CB, Beeson JG, Cowman AF, Ralph SA, Baum J: **Super-resolution dissection of coordinated events during malaria parasite invasion of the human erythrocyte.** *Cell Host Microbe* 2011, **9**:9–20.
26. McBride JS, Heidrich HG: **Fragments of the polymorphic Mr 185,000 glycoprotein from the surface of isolated *Plasmodium falciparum* merozoites form an antigenic complex.** *Mol Biochem Parasitol* 1987, **23**:71–84.
27. Straub KW, Cheng SJ, Sohn CS, Bradley PJ: **Novel components of the Apicomplexan moving junction reveal conserved and coccidia-restricted elements.** *Cell Microbiol* 2009, **11**:590–603.
28. Burge C, Karlin S: **Prediction of complete gene structures in human genomic DNA.** *J Mol Biol* 1997, **268**:78–94.
29. *Spidey*. http://www.ncbi.nlm.nih.gov/spidey/.
30. Nielsen H, Engelbrecht J, Brunak S, von Heijne G: **Identification of prokaryotic and eukaryotic signal peptides and prediction of their cleavage sites.** *Protein Eng* 1997, **10**:1–6.
31. Kall L, Krogh A, Sonnhammer EL: **An HMM posterior decoder for sequence feature prediction that includes homology information.** *Bioinformatics* 2005, **21**(Suppl 1):i251–257.
32. Krogh A, Larsson B, von Heijne G, Sonnhammer EL: **Predicting transmembrane protein topology with a hidden Markov model: application to complete genomes.** *J Mole Biol* 2001, **305**:567–580.
33. Pierleoni A, Martelli PL, Casadio R: **PredGPI: a GPI-anchor predictor.** *BMC Bioinformatics* 2008, **9**:392.
34. Letunic I, Goodstadt L, Dickens NJ, Doerks T, Schultz J, Mott R, Ciccarelli F, Copley RR, Ponting CP, Bork P: **Recent improvements to the SMART domain-based sequence annotation resource.** *Nucleic Acids Res* 2002, **30**:242–244.
35. Chomczynski P: **A reagent for the single-step simultaneous isolation of RNA, DNA and proteins from cell and tissue samples.** *Biotechniques* 1993, **15**:532–534. 536-537.
36. Moreno-Perez DA, Montenegro M, Patarroyo ME, Patarroyo MA: **Identification, characterization and antigenicity of the *Plasmodium vivax* rhoptry neck protein 1 (PvRON1).** *Malar J* 2011, **10**:314.

37. Neafsey DE, Galinsky K, Jiang RH, Young L, Sykes SM, Saif S, Gujja S, Goldberg JM, Young S, Zeng Q, Chapman SB, Dash AP, Anvikar AR, Sutton PL, Birren BW, Escalante AA, Barnwell JW, Carlton JM: **The malaria parasite** *Plasmodium vivax* **exhibits greater genetic diversity than** *Plasmodium falciparum*. *Nat Genet* 2012, **44**:1046–1050.
38. Thompson JD, Higgins DG, Gibson TJ: **CLUSTAL W: improving the sensitivity of progressive multiple sequence alignment through sequence weighting, position-specific gap penalties and weight matrix choice.** *Nucleic Acids Res* 1994, **22**:4673–4680.
39. Geourjon C, Deleage G, Roux B: **ANTHEPROT: an interactive graphics software for analyzing protein structures from sequences.** *J Mol Graph* 1991, **9**:188–190. 167.
40. Larsen JE, Lund O, Nielsen M: **Improved method for predicting linear B-cell epitopes.** *Immunome Res* 2006, **2**:2.
41. Escalante AA, Ayala FJ: **Phylogeny of the malarial genus** *Plasmodium*, **derived from rRNA gene sequences.** *Proc Natl Acad Sci USA* 1994, **91**:11373–11377.
42. Bozdech Z, Llinas M, Pulliam BL, Wong ED, Zhu J, DeRisi JL: **The transcriptome of the intraerythrocytic developmental cycle of** *Plasmodium falciparum*. *PLoS Biol* 2003, **1**:E5.
43. Florens L, Washburn MP, Raine JD, Anthony RM, Grainger M, Haynes JD, Moch JK, Muster N, Sacci JB, Tabb DL, Witney AA, Wolters D, Wu Y, Gardner MJ, Holder AA, Sinden RE, Yates JR, Carucci DJ: **A proteomic view of the** *Plasmodium falciparum* **life cycle.** *Nature* 2002, **419**:520–526.
44. Dame JB, Williams JL, McCutchan TF, Weber JL, Wirtz RA, Hockmeyer WT, Maloy WL, Haynes JD, Schneider I, Roberts D, Sanders GS, Reddy EP, Diggs CL, Miller LH: **Structure of the gene encoding the immunodominant surface antigen on the sporozoite of the human malaria parasite** *Plasmodium falciparum*. *Science* 1984, **225**:593–599.
45. Fenton B, Walker A, Walliker D: **Protein variation in clones of** *Plasmodium falciparum* **detected by two dimensional electrophoresis.** *Mol Biochem Parasitol* 1985, **16**:173–183.
46. Hisaeda H, Yasutomo K, Himeno K: **Malaria: immune evasion by parasites.** *Int J Biochem Cell Biol* 2005, **37**:700–706.
47. Besteiro S, Michelin A, Poncet J, Dubremetz JF, Lebrun M: **Export of a** *Toxoplasma gondii* **rhoptry neck protein complex at the host cell membrane to form the moving junction during invasion.** *PLoS Pathog* 2009, **5**:e1000309.
48. Proellocks NI, Coppel RL, Waller KL: **Dissecting the apicomplexan rhoptry neck proteins.** *Trends Parasitol* 2010, **26**:297–304.
49. Kauth CW, Woehlbier U, Kern M, Mekonnen Z, Lutz R, Mucke N, Langowski J, Bujard H: **Interactions between merozoite surface proteins 1, 6, and 7 of the malaria parasite** *Plasmodium falciparum*. *J Biol Chem* 2006, **281**:31517–31527.
50. Pachebat JA, Kadekoppala M, Grainger M, Dluzewski AR, Gunaratne RS, Scott-Finnigan TJ, Ogun SA, Ling IT, Bannister LH, Taylor HM, Mitchell GH, Holder AA: **Extensive proteolytic processing of the malaria parasite merozoite surface protein 7 during biosynthesis and parasite release from erythrocytes.** *Mol Biochem Parasitol* 2007, **151**:59–69.
51. Lebrun M, Michelin A, El Hajj H, Poncet J, Bradley PJ, Vial H, Dubremetz JF: **The rhoptry neck protein RON4 re-localizes at the moving junction during** *Toxoplasma gondii* **invasion.** *Cell Microbiol* 2005, **7**:1823–1833.

MALARIA JOURNAL

**RESEARCH**                                                                              **Open Access**

# The *Plasmodium vivax* rhoptry neck protein 5 is expressed in the apical pole of *Plasmodium vivax* VCG-1 strain schizonts and binds to human reticulocytes

Gabriela Arévalo-Pinzón[1,2†], Maritza Bermúdez[1,2†], Hernando Curtidor[1,2] and Manuel A Patarroyo[1,2*]

## Abstract

**Background:** Different proteins derived from the membrane or the apical organelles become involved in malarial parasite invasion of host cells. Among these, the rhoptry neck proteins (RONs) interact with a protein component of the micronemes to enable the formation of a strong bond which is crucial for the parasite's successful invasion. The present study was aimed at identifying and characterizing the RON5 protein in *Plasmodium vivax* and evaluating its ability to bind to reticulocytes.

**Methods:** Taking the *Plasmodium falciparum* and *Plasmodium knowlesi* RON5 amino acid sequences as template, an in-silico search was made in the *P. vivax* genome for identifying the orthologous gene. Different molecular tools were used for experimentally ascertaining *pvron5* gene presence and transcription in *P. vivax* VCG-1 strain schizonts. Polyclonal antibodies against *Pv*RON5 peptides were used for evaluating protein expression (by Western blot) and sub-cellular localization (by immunofluorescence). A 33 kDa *Pv*RON5 fragment was expressed in *Escherichia coli* and used for evaluating the reactivity of sera from patients infected by *P. vivax*. Two assays were made for determining the RON5 recombinant fragment's ability to bind to reticulocyte-enriched human umbilical cord samples.

**Results:** The *pvron5* gene (3,477 bp) was transcribed in VCG-1 strain schizonts and encoded a ~133 kDa protein which was expressed in the rhoptry neck of VCG-1 strain late schizonts, together with *Pv*RON2 and *Pv*RON4. Polyclonal sera against *Pv*RON5 peptides specifically detected ~85 and ~30 kDa fragments in parasite lysate, thereby suggesting proteolytic processing in this protein. Comparative analysis of VCG-1 strain *Pv*RON5 with other *P. vivax* strains having different geographic localizations suggested its low polymorphism regarding other malarial antigens. A recombinant fragment of the *Pv*RON5 protein (r*Pv*RON5) was recognized by sera from *P. vivax*-infected patients and bound to red blood cells, having a marked preference for human reticulocytes.

**Conclusions:** The *pvron5* gene is transcribed in the VCG-1 strain, the encoded protein is expressed at the parasite's apical pole and might be participating in merozoite invasion of host cells, taking into account its marked binding preference for human reticulocytes.

**Keywords:** Malaria, New antigens, *Plasmodium vivax*, *Pv*RON5, Rhoptry neck proteins

* Correspondence: mapatarr.fidic@gmail.com
†Equal contributors
¹Fundación Instituto de Inmunología de Colombia (FIDIC), Carrera 50 # 26-20, Bogotá, Colombia
²Universidad del Rosario, Carrera 24 # 63C-69, Bogotá, Colombia

Arévalo-Pinzón *et al. Malaria Journal* (2015) 14:106

Page 2 of 14

## Background

The rhoptries, together with the micronemes, form the main secretory organelles of most infective forms of parasites from *Apicomplexa* (the phylum to which *Plasmodium* belongs) [1]. The importance of the rhoptries is reflected in the wide range of proteins contained in these organelles, which are involved in invasion of host cells. Some of these proteins are restricted to the apical duct (known as the rhoptry neck) or to the rhoptry bulb, which is characterized by having a high lipid content [2]. Protein spatial localization within the rhoptries in malaria allows the parasite to carry out different functions during the coordinated invasion of its host cell, which has been correlated with each protein's release time [3]. Proteins from the rhoptries are thus implicated in specific recognition of the host cell, in tight or moving junction (TJ-MJ) formation, parasitophorous vacuole formation and host cell remodelling [3,4].

Rhoptry neck proteins (called RONs) have been strongly associated with the formation of the TJ, an electron dense circular structure which is formed between the parasite and the host cell, constituting the central axis where the different invasion events become organized [5]. RON2, RON4 and RON5 proteins have been identified in the TJ formed by *Plasmodium falciparum* (and RON8 in *Toxoplasma gondii*), associated with a micronemal protein called apical membrane antigen 1 (AMA-1) [6-8]. Besteiro *et al.,* described an organizational model of MJ in *T. gondii* for the first time, consisting of a multi-protein rhoptry/microneme complex where it has been suggested that the parasite supplies its own receptors (RON proteins) for gaining access to the host cell [9]. The different interactions between MJ components have been mapped in detail since these first studies. Crystallization studies of the AMA-1 ectodomain in complex with a RON2 extracellular peptide have revealed a conformational change in AMA-1 domain II leading to a perfect fit having high affinity between both proteins [10,11]. The description of this interaction has provided the molecular basis for understanding the invasion inhibition mechanisms displayed by the 4G2 [12] and 1F9 [13] monoclonal antibodies directed against *Pf*AMA-1 and peptides identified from random peptide libraries expressed on phage surface, such as R1 [14]. *Pf*RON2 binding to *Pf*AMA-1 is not affected by *Pf*AMA1's high polymorphism in the parasite's distinct strains; furthermore, the *Pf*RON2 peptide which binds to the hydrophobic groove shows crossed invasion inhibition between strains [11], thereby highlighting its biological importance in developing prophylactic methods. Interestingly, a recent study has shown that immunization with the AMA1-RON2 functional complex, but not with individual antigens, induced complete antibody-mediated protection against homologous experimental challenge with the lethal *Plasmodium yoelii* YM strain [15]. Such protection would seem to be partly mediated by antibodies having specificity for new epitopes surrounding the RON2 binding site [15].

While different studies have established the importance of RON2-AMA-1 interaction, other ones obtaining partial or total AMA-1 knockouts, have led to questioning the role of this protein in the TJ formation [16,17]. It has been shown that the absence of AMA-1 in *T. gondii* is complemented and/or compensated by two homologous genes [18]; however, RON proteins continue to gain importance in spite of such discrepancies. Bearing in mind that it has not been possible to inactivate the *ron4* gene in *Plasmodium berghei*, following various attempts to do so, it has been suggested that the RON4 protein plays an important role in merozoites [17]. A significant reduction in the invasion of hepatic cells has been found following conditional silencing of the *ron4* gene in *P. berghei* sporozoites [17]. It has been found to date that the *T. gondii* RON4 protein carboxyl terminal region, but not that of *P. falciparum,* has been associated with the tubulin β-chain in mammalian cells, thereby suggesting RON4 translocation to host cell cytoskeleton, acting as anchoring site for parasite entry [19] and partly confirming the aforementioned model proposed by Besteiro *et al.* [9].

Few studies have dealt with a functional role for *Pf*RON5 within the TJ, even though some methodological approaches have shown its association with the RON/AMA1 multi-protein complex [9,12]. It has been shown recently that the conditioned absence of RON5 in tachyzoites caused the complete degradation of *Tg*RON2 and incorrect *Tg*RON4 localization in the rhoptries, having significant implications within the parasite's invasion cycle [20]. The functional dissection of each *Tg*RON5 region has led to it becoming established that the *Tg*RON5 prodomain, together with the last portion of the *Tg*RON5 amino region (RON5N), participate in the correct targeting of the rhoptry neck proteins, while the carboxyl terminal region is essential for stabilizing *Tg*RON2 [20]. Interestingly, it has been described that the *P. falciparum* *Pf*RON5 sequence contains peptides, which bind saturably, and having high affinity for binding to receptors on red blood cell (RBC) membrane which are sensitive to enzyme treatment [21]. Such peptides, called high activity binding peptides (HABPs), can inhibit merozoite *in vitro* invasion of their host cells [21], thereby highlighting the role of *Pf*RON5 during parasite invasion. Although most studies have described the possible translocation of some RONs to the host cell membrane, its mechanisms and signals have not been explored in detail. This translocation could be preceded by RON proteins' specific interaction with receptors on RBC membrane, as has been previously reported for *Pf*RON5 [21] and *Pf*RON2 [22]. Such interaction might have functional relevance when designing control methods aimed at blocking RON-AMA1 complex formation.

Arévalo-Pinzón *et al. Malaria Journal* (2015) 14:106

Page 3 of 14

Taking into account the major role that RON proteins display in *T. gondii* and *P. falciparum* parasite invasion cycles, a comparative approach together with an adaptation of a *Plasmodium vivax* strain in *Aotus* monkeys [23] has been used for identifying and characterizing new proteins, such as *Pv*RON2 [24] and *Pv*RON4 proteins [25] in the second-most important species causing malaria around the world: *P. vivax* [26]. Such approach has provided the basis for advances made in identifying *P. vivax* proteins containing important characteristics which are typical of vaccine candidates, such as expression in late schizonts, localization on/in cell membrane or secretory organelles and, in some cases, high antigenic and immunogenic capacity [27]. Some antigens, such as merozoite surface protein-1 (*Pv*MSP-1), reticulocyte binding protein-1 (*Pv*RBP-1) and the Duffy binding protein (*Pv*DBP), have reticulocyte-specific binding sequences and have been considered to date among the most promising vaccine candidate antigens [27].

The gene encoding the *Pv*RON5 protein was identified in the present work; it consisted of a 1,158 residue antigen which was found to be conserved among *P. vivax* strains from different geographical regions and which was found to be expressed at *P. vivax* schizonts' apical pole, together with *Pv*RON4 and *Pv*RON2 proteins. *Pv*RON5 anti-peptide antibodies recognized two bands in *P. vivax* schizont lysate, suggesting that proteolytic processing could be implicated in the protein's functional activation. Analytical and molecular biology techniques led to obtaining the r*Pv*RON5, which was recognized by sera from patients having active *P. vivax* infection. Immunoprecipitation and immunofluorescence studies have shown that r*Pv*RON5 binds to reticulocyte-enriched samples, suggesting that this protein might be involved in merozoite invasion of human reticulocytes.

## Methods
### In-silico search for *pfron5* and *pkron5* homologous gene in *Plasmodium vivax*
The presence of the *pvron5* gene in the *P. vivax* genome was evaluated by using the *P. falciparum* (PF3D7_0817700) and *Plasmodium knowlesi* (PKH_051420) RON5 protein amino acid (aa) sequences deposited in PlasmoDB [28] and the Basic Local Alignment Search Tool (BLAST) [29], from the National Center for Biotechnology Information (NCBI) as template. Genscan [30], Spidey [31] and tBlastn were used for determining the presence and boundaries of the exons and introns present in the *pvron5* gene. The study of synteny considered the presence of open reading frames (ORFs), gene structure, transcription direction, and values regarding identity and similarity between *P. vivax-P. knowlesi* and *P. vivax-P. falciparum* species.

Primers were designed on the ORF having the highest score in bioinformatics' analysis based on the results for

the above. Three sets of primers were designed for the complete amplification of genomic DNA (gDNA) while two primers were designed for complementary DNA (cDNA) covering from the start codon to the stop codon. Different primers were needed for the complete sequencing of cDNA. Table 1 lists the forward and reverse primers used for PCR amplification and sequencing for each amplicon.

Different bioinformatics tools were used for evaluating important motifs and domains in the hypothetical *Pv*RON5 sequence. Signal P software was used for evaluating signal peptide presence [32], Polyphobius for determining the presence of transmembrane domains [33] and PredGPI for GPI anchors [33]. The BaCelLo tool was used for predicting *Pv*RON5 sub-cellular localization [34]. Sequence tandem repeat extraction and architecture modelling (XSTREAM, variable 'X') was used for finding repeat sequences and the simple modular architecture research tool (SMART) for searching for other important motifs and domains [35].

### The source of nucleic acids and cDNA synthesis
Vivax Colombia Guaviare 1 (VCG-1) strain parasites were used as source for DNA, RNA and parasite proteins. These samples had been obtained as described previously [23] and after nucleic acid and protein extraction, stored at –70°C until use. RNA extracted by using the TRIzol method [36] and Superscript III enzyme (Invitrogen), were used for cDNA synthesis following the manufacturer's specifications.

### PCR conditions, cloning and sequencing
KAPA HiFi HotStart DNA polymerase (Kapa Biosystems) was used for amplifying *pvron5* from gDNA in 25 μL final reaction volume containing 12.5 μL 2x KAPA HiFi Ready Mix, 1.5 μL of each primer (Table 1) at 5 μM concentration and 7.5 μL of nuclease-free water. The amplification conditions for the three products amplifying gDNA consisted of one 3-min cycle at 95°C followed by 35 cycles lasting 20 sec at 98°C, 15 sec at 60°C and 3 min 30 sec at 72°C with a final extension cycle lasting 5 min at 72°C. cDNA was amplified with *Pv*RON5-F and *Pv*RON5-R primers and the TAQXpedite high fidelity enzyme (Epicentre Biotechnologies) at final 25 μL volume, according to the manufacturer's recommendations. A denaturing cycle was used which lasted 30 sec at 95°C followed by 35 cycles at 95°C for 10 sec, 58°C for 10 sec and 72°C for 2 min. The same conditions and previously described primers were used for amplifying the *pvrhoph3* gene from cDNA [37].

The amplified products were visualized on 1% agarose gels and their molecular weights calculated based on a molecular weight marker. The product obtained from cDNA was purified by using an Ultra Clean Gel Spin DNA purification kit (MOBIO Laboratories), according

Arévalo-Pinzón et al. Malaria Journal (2015) 14:106

Page 4 of 14

**Table 1 Primers used in amplifying and sequencing PvRON5 from gDNA and cDNA**

| Name | Sequence 5 → 3 | Amplicon | Target |
|------|----------------|----------|--------|
| A1 | CGT CTG TAA GAC CTC CC | 3.404 bp | gDNA |
| A3 | CGA TGA AGC CCT TCT CC | | gDNA |
| A5 | CGG GAC AAG CTG AAT AAC | 1.815 bp | gDNA |
| A7 | TGA CGT CGG CGC AGA TG | | gDNA |
| A9 | AGT GCC TCC ATG GAC AAT A | 3.158 bp | gDNA |
| A11 | GCT GAT CGG TCG GCT GA | | gDNA |
| PvRON5-F | ATG CTG AAG TAC GTG CTA CTC | 3.477 bp | cDNA |
| PvRON5-R | GGG TAT CCT CGT GTG CAC | | cDNA |
| PvRON5-sec-F1 | CGT CTG TAA GAC CTC CC | NA | cDNA sequencing |
| PvRON5-rev-R1 | CGA TGA AGC CCT TCT CC | NA | cDNA sequencing |
| PvRON5-sec-F2 | CGG GAC AAG CTG AAT AAC | NA | cDNA sequencing |
| PvRON5-sec-R2 | TGA CGT CGG CGC AGA TG | NA | cDNA sequencing |
| PvRON5-sec-F3 | AGT GCC TCC ATG GAC AAT A | NA | cDNA sequencing |
| PvRON5-sec-R3 | GCT GAT CGG TCG GCT GA | NA | cDNA sequencing |

NA: Not applicable, gDNA: genomic deoxyribonucleic acid, cDNA: complementary deoxyribonucleic acid.

to the manufacturer's specifications. An additional reaction was needed for adding adenines to the product's 3′ end for its TA cloning into pGEM-T vector (Promega). The construct was used for transforming TOP10 cells and three positive clones were selected which had been obtained from independent PCR reactions which were sent for sequencing on an ABI PRISM 310 Genetic Analyzer. CLC DNA Workbench (CLC bio) software was used for analyzing the sequences; the resulting cDNA sequence was deposited in GenBank. Clustal W software was used for comparing the VCG-1 strain's cDNA sequence to those of the Sal-1, Mauritania I, Brazil I, North Korean and India VII strain sequences [38].

### PvRON5 recombinant fragment cloning, expression and purification

A nucleotide construct encoding 296 aa from PvRON5 (residues 863T to 1158P) was commercially synthesized by GenScript, thereby optimizing a variety of parameters (i.e. Escherichia coli codon bias, GC content and mRNA secondary structure), which are critical for the gene fragment's efficient expression. The synthetic gene was ligated in pQE30 vector (Qiagen) BamHI and HindIII sites and the new construct was named pQE30-rRON5. This plasmid was used for transforming JM109 strain E. coli cells, followed by sequencing with the vector's primers.

Kanamycin-resistant and ampicillin-sensitive M15 cells were transformed with the pQE30-rRON5 plasmid. rPvRON5 expression was obtained by inoculating 200 mL Luria Bertani (LB) medium containing 0.1 mg/mL ampicillin and 25 μg/mL kanamycin with 10 mL culture grown overnight. The culture was grown in conditions involving constant shaking at 37°C until 0.4-0.6 optical density was reached at 620 nm. rPvRON5 expression was induced by adding isopropyl β-D-1-thiogalactopyranoside (IPTG, Invitrogen) at 1 mM final concentration for 4 hr at 37°C with constant shaking. The cell culture was spun at $10,000 \times g$ for 30 min at 4°C and the bacterial pellet containing the protein in inclusion bodies was washed twice with buffer A (20 mM Tris–HCl pH 8.0, 1 mM EDTA, 1 mM iodoacetamide, 1 mM PMSF and 1 μg/mL leupeptin) supplemented with lysozyme, followed by cell disruption using a sonicator (Branson). Following the aforementioned treatment, the inclusion bodies were recovered by spinning at $10,000 \times g$ for 30 min at 4°C and washed once with buffer A supplemented with 2 M urea. The recombinant protein was then solubilized with lysis buffer containing 10 mM Tris–HCl, 100 mM $NaH_2PO_4$, 6 M urea, 10 mM imidazole and 10% glycerol. Protein presence in the supernatant was evaluated by Western blot using an anti-polyhistidine monoclonal antibody (Sigma).

The recombinant protein (rPvRON5) was purified by affinity chromatography using $Ni^{2+}$-NTA agarose (Qiagen), as recommended by the manufacturer. Briefly, the supernatant was placed on a $Ni^{2+}$-NTA column, which had been previously equilibrated in lysis buffer. The column was extensively washed with lysis buffer and then washed with decreasing amounts of urea (6–0 M) in the same lysis buffer. The recombinant protein was then eluted with an imidazole linear gradient (0.03 M-0.5 M) in washing buffer (10 mM Tris–HCl, 100 mM $NaH_2PO_4$ at pH 8.0). The fractions were analyzed using SDS-PAGE and stained with Coomassie blue. The fractions containing a single band at the expected height were pooled and dialyzed against 1X phosphate buffer. Concentration was determined by the bicinchoninic acid method (Bio-Rad) using bovine serum albumin (BSA, Sigma) as standard.

Arévalo-Pinzón et al. Malaria Journal (2015) 14:106

Page 5 of 14

## Producing polyclonal antibodies against PvRON5, PvRON4 and PvRON2 proteins

The hypothetical PvRON5 sequence was used for predicting linear B-cell epitopes. Selected peptides were synthesized for rabbit immunization and producing polyclonal antibodies, as has been described previously [24]. Peptides were chemically synthesized in solid phase and one cysteine and one glycine (CG) were added to the amino and carboxy termini during synthesis. Each peptide was lyophilized and analyzed by reverse phase high performance liquid chromatography (RP-HPLC) and MALDI-TOF mass spectrometry (Auoflex, Bruker Daltonics). Polymer peptides 36927 (CG$^{775}$ATR$T$DHFSRSASMDNNKKSR$^{794}$GC) in which a cysteine (C) had been replaced by threonine (T) in position 778, 36930 (CG$^{351}$NASYDLEEYQNEFKPTNTSQ$^{370}$GC) and 39274 (CG$^{69}$MFDPKDKKFVPSKSKKAHIV$^{88}$GC) were selected for antibody production. Antibodies thus obtained were later used for evaluating protein expression in late schizonts. Synthetic peptide 39276 (CG$^{989}$GIDEDNERFYVLQDKTKVPE$^{1008}$GC) was inoculated for producing antibodies recognizing rPvRON5 in binding assays.

Four New Zealand rabbits (numbered 2, 3, 32, and 60) were then selected after having been evaluated by Western blot as being negative for recognition of P. vivax proteins. Rabbits 2 and 3 were subcutaneously immunized with 500 μg of peptides 39274 and 39276 respectively, emulsified in Freund's complete adjuvant (FCA), while rabbits 32 and 60 were inoculated with a mixture of peptides 36927 (250 μg) and 36930 (250 μg) in FCA. Booster immunizations on days 20 and 40 were administered using the same peptides emulsified in Freund's incomplete adjuvant (FIA). Antibodies directed against PvRON4 and PvRON2 proteins were used for co-localization studies, inoculating the previously described peptides in mice [24,25]. This involved taking two BAlb/C mice which were intraperitoneally immunized (ip) with 75 μg PvRON2 polymer peptides 35519 and 35520 [24] emulsified in FCA, while another two mice were immunized with PvRON4 peptides 36114 and 36115 [25]. Three boosters were given on days 30, 45 and 60 using the same peptides emulsified in FIA. Rabbit and mouse sera was collected on day 60 and 75, respectively, and used for further assays. Animal immunization and bleeding was done according to Colombian animal protection recommendations (Law 84/1989 and Resolution 8430/1993) for handling live animals for research or experimentation purposes. All experimental procedures involving animals had been previously approved by the Fundación Instituto de Inmunología's ethics committee.

## PvRON5 polymer peptide recognition by rabbit sera

Polymer peptides (1 μg) were sown in 96-well ELISA plates, as previously described [39]. The plates were incubated with sera from each rabbit in 1:100 dilution for 1:30 min at 37°C, followed by three washes with 0.05% PBS-Tween. Peroxidase-coupled anti-rabbit (Vector Laboratories) at 1:5,000 dilution was used as secondary antibody. Immunoreactivity was revealed by using a TMB Micro-well Peroxidase Substrate System kit (KPL Laboratories), according to the manufacturer's instructions. Absorbance was read at 620 nm on an ELISA reader (Lab Systems Multiskan MS).

## Evaluating PvRON5 expression in late schizonts

PvRON5 expression was determined by Western blot (WB) and immunofluorescence. Regarding WB, the parasite proteins extracted from the VCG-1 strain were electrophoresed in reducing conditions on 10% polyacrylamide/SDS gels (SDS-PAGE). The proteins were then transferred to polyvinylidene difluoride (PVDF) membranes, which had been previously activated with methanol. Following transfer, the membrane containing the parasite proteins was blocked with a 5% milk solution in 0.05% PBS-Tween and 3-mm wide strips were cut to be incubated with the sera (pre-immune or immune) from rabbits immunized with PvRON5 polymer peptides (1:40 dilution in blocking solution). In another assay, immune serum was pre-incubated with inoculated polymer peptides before being incubated with the PVDF membrane. Each strip was washed thrice with 0.05% PBS-Tween and incubated with anti-rabbit phosphatase-coupled antibodies (Biomedicals) in 1:5,000 dilution. The reaction was revealed by using a BCIP/NBT kit (Promega), according to the manufacturer's instructions.

Indirect immunofluorescence (IFA) involved using a previously described protocol, with some modifications [25]. Briefly, the eight-well chamber slides containing parasitized RBCs were fixed with 4% formaldehyde and then permeabilized for 10 min with 1% v/v Triton X-100. The slides were blocked with 1% PBS/BSA solution at 37°C for 30 min and incubated with primary anti-PvRON5, PvRON2 or PvRON4 antibodies in 1:40 dilution in blocking solution. Fluorescein-labelled anti-rabbit IgG (FITC) (Vector Laboratories) and rhodamine-labelled anti-mouse IgG (Millipore) were used as secondary antibodies. Parasite nuclei were stained with 4′, 6-diamidino-2-phenylindole (DAPI) and fluorescence was visualized by fluorescence microscope (Olympus BX51) using an Olympus DP2 camera and Volocity software (Perkin Elmer).

## Antigenicity studies with rPvRON5

The rPvRON5 recombinant protein was electrophoresed on 12% SDS-PAGE gels and then transferred to PVDF membranes. The membrane was blocked and cut into 3-mm wide strips which were incubated with sera from P. vivax-infected patients (1:100) who were living in different endemic regions in Colombia. Healthy individuals'

Arévalo-Pinzón *et al. Malaria Journal* (2015) 14:106

Page 6 of 14

sera were used as controls. The membranes were then incubated with phosphatase-coupled anti-human antibodies (Biomedicals) in 1:4,000 dilution and the reaction was revealed with a BCIP/NBT kit, according to the manufacturer's instructions.

The r*Pv*RON5 recognition was determined by ELISA. In brief, 96-well plates coated with 2 μg r*Pv*RON5 were incubated with a 1:100 dilution of serum samples from *P. vivax*-infected individuals and 1:5,000 anti-human IgG as secondary antibody.

### Obtaining reticulocyte-enriched fractions

A previously described protocol was followed for reticulocyte enrichment [40], with some modifications. Around 30 ml of umbilical cord blood (n = 5) were obtained from the District Blood Bank in Bogotá, Colombia. The plasma was removed after being washed in PBS several times. The packed RBC were diluted ten times in PBS and passed three times through CF11 columns (Whatman) to eliminate platelets and white cells. A 70% Percoll solution in 0.15 M NaCl was prepared from a Percoll stock in 9:1 Percoll-1.5 M NaCl ratio. The RBC were spun, diluted by half and placed on the 70% Percoll gradient which was spun at $2,500 \times g$ for 25 min. The fine reticulocyte band formed on the Percoll interface was carefully removed and then washed twice with PBS. Reticulocyte viability and count were monitored in each process using cresyl blue supravital stain.

### r*Pv*RON5 binding to reticulocyte-enriched samples

The interaction between r*Pv*RON5 with reticulocyte-enriched samples and RBC passed through CF11 columns was determined in two experiments. The first involved incubating 100 μL r*Pv*RON5 recombinant protein with 100 μL RBC or enriched reticulocytes, taken to 300 μL final volume with PBS at 4°C overnight. The mixture was passed through a 400 μL dibutyl phthalate cushion and spun at $2,500 \times g$ for 5 min. The supernatant was skimmed off and the pellet was washed twice with PBS before eluting the protein with PBS/1 M NaCl. The supernatant was pre-incubated at 4°C for 3 hr with protein G conjugated sepharose beads (GammaBind Plus Sepharose, GE Healthcare) diluted to 50% in NETT buffer (50 mM Tris–HCl, 0.15 M NaCl, 1 mM EDTA, and 0.5% Triton X-100) supplemented with 0.5% BSA. The recovered supernatants were incubated with anti-polyhistidine monoclonal antibody (Sigma) in 1:4,000 dilution with gentle shaking at 4°C for 5 hr and 20 μL 50% protein G-conjugated beads were then added. Following incubation, the mixture was spun at $3,800 \times g$ for 5 min and the beads were washed once with NETT-0.5% BSA. The immune-precipitated recombinant protein was extracted from the beads by incubation with SDS-PAGE reducing loading buffer at 100°C for 3 min. Supernatants were collected for WB

analysis using peroxidase-coupled anti-histidine monoclonal antibody.

The second assay involved 5% reticulocyte-enriched samples in HEPES buffered saline (HBS) solution being incubated with 15 μg r*Pv*RON5 at 4°C overnight. The samples were spun, washed once with HBS buffer and 50 μL bis (sulfosuccinimidyl) suberate (BS$^3$-Pierce) was added at 250 μg/mL final concentration for 1 hr at room temperature (RT) with slow shaking. The samples were then washed twice with HBS buffer and the RBC or reticulocytes were blocked with 1% BSA in HBS buffer for 1 hr at 4°C. Following two washes with HBS, the samples were incubated with primary anti-RON5 antibody (rabbit 3) in 1:40 dilution and anti-CD71 monoclonal antibody (Life Technologies) in 1:100 dilution for 1 hr at 4°C. Antibody which did not bind was removed by two washings with HBS. The samples were then incubated with fluorescein-labelled anti-rabbit IgG (FITC) (Vector Laboratories) and rhodamine-labelled anti-mouse IgG (Millipore). Associated fluorescence was visualized on a fluorescence microscope (Olympus BX51) using an Olympus DP2 camera and Volocity software (Perkin Elmer). The following negative controls were included for evaluating non-specific reactivity between polyclonal antibody (recognizing r*Pv*RON5) and secondary antibody with proteins on target cell membrane: reticulocytes or RBC incubated only with polyclonal antibody against r*Pv*RON5 followed by FITC-coupled secondary antibodies, reticulocytes or RBC incubated with only FITC-coupled secondary antibodies and reticulocytes or RBC incubated with r*Pv*RON5 followed by incubation with FITC-coupled secondary antibody.

### Statistical analysis

Differences in antibody production between pre-immune and post-third immunization rabbit sera obtained by ELISA were evaluated using non-parametric Wilcoxon signed rank test. Ten photos were selected for evaluating the differences between reticulocyte-associated fluorescence compared to RBC-associated in r*Pv*RON5 target cell binding assays; in each photograph, reticulocytes and RBCs were numbered. One reticulocyte and one RBC were randomly chosen in each photo for measuring 256 fluorescence points per cell using ImageJ 1.48 software. The 512 data obtained per photo were loaded into the SPSS software (version 20.0) and the differences evaluated by non-parametric Wilcoxon signed rank test. The images presented in the manuscript are representative of at least 10 individual observations.

## Results

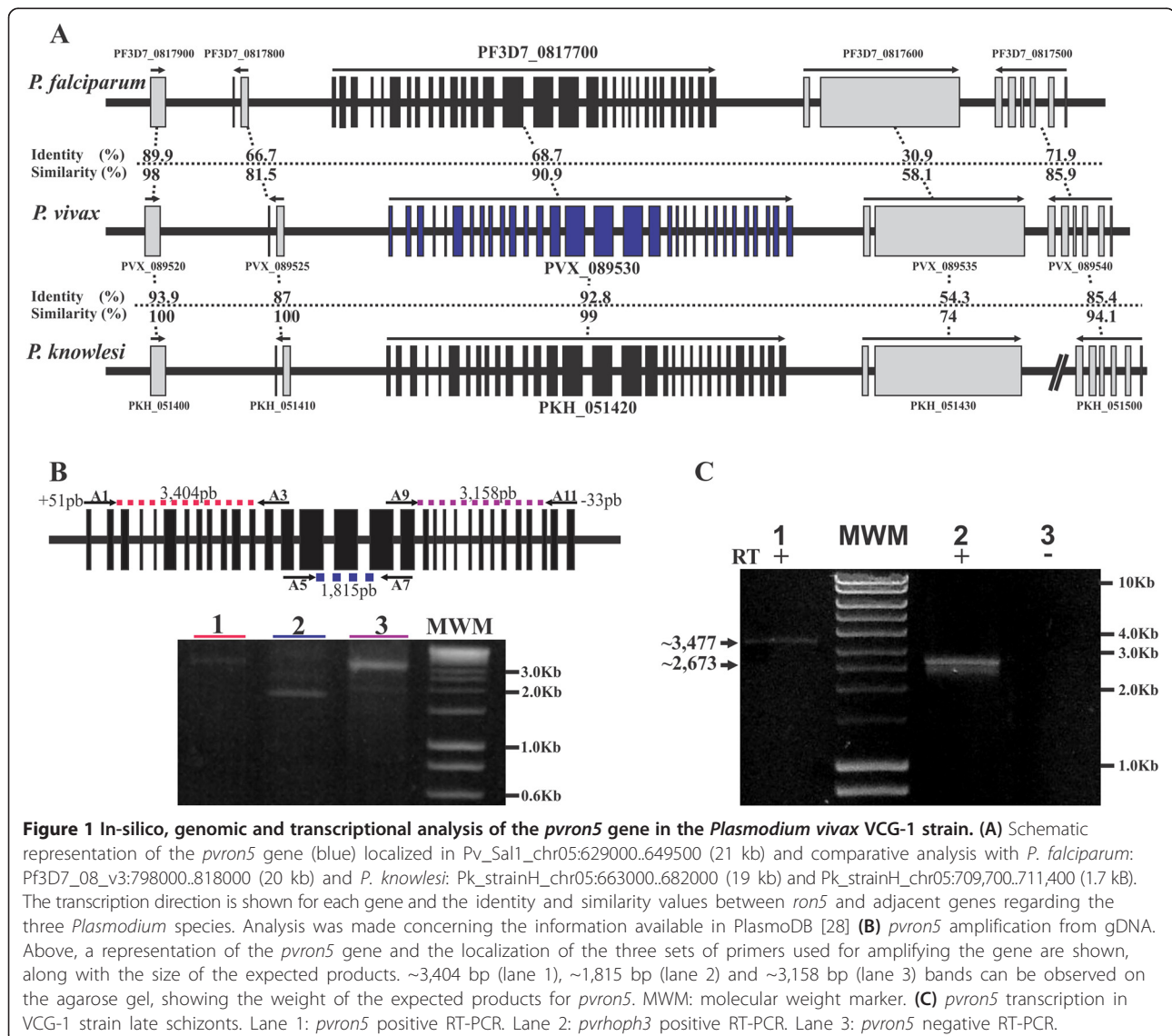### In-silico identification and molecular characterization of the *pvron5* gene

In spite of a lack of an *in vitro P. vivax* continuous culture providing sufficient parasite samples for study, a

Arévalo-Pinzón *et al. Malaria Journal* (2015) 14:106

Page 7 of 14

comparative approach involving other important species such as *P. falciparum* and the use of *Aotus* monkeys for maintaining a *P. vivax*-adapted strain [23] has led to the identification of a significant number of antigens (16 new proteins) which could be participating in invasion [27].

The gene encoding the *Pv*RON5 protein was identified in this study; this antigen is expressed in the schizont phase of the intra-erythrocyte cycle. An initial search was made in tBlastn regarding the *pvron5* gene using the *Pf*RON5 aa sequence (1,156 aa). The analysis revealed a high probability that the target gene would be localized in chromosome 5 (Pv_sal1_chr05) of the *P. vivax* genome between base pairs 635,954 to 642,743 (i.e., *Pf*RON5 aa 105 to 1,156). The *P. knowlesi* RON5 aa sequence was used for searching for the start codon, as this parasite was phylogenetically closest to *P. vivax*. This analysis revealed that the *pvron5* gene's structural region began in position

634,671 and ended in chromosome 5 nucleotide 642,743; a gene (PVX_089530) having a putative function was found in this position (Figure 1A). Such analysis has been indispensable in re-annotating genes such as *pvron4* [25] and *pvrhoph3* [37] where incorrect annotations have been found regarding the start and termination of the gene as well as the number of exons.

It was also found that transcription direction, *pvron5* gene structure regarding *pfron5* and *pkron5* and the presence of 31 exons in each species analyzed was conserved (Figure 1A). *ron5* gene identity (ID) and similarity (SI) values between the three species were above 60%, ID and SI being greater between *P. vivax-P. knowlesi* (92% ID; 99% SI) regarding *P. vivax-P. falciparum* (68% ID; 90% SI); such values agreed with the evolutionary relationships between these parasites. Gene structure, transcription orientation and SI values above 35% were taken into



**Figure 1 In-silico, genomic and transcriptional analysis of the *pvron5* gene in the *Plasmodium vivax* VCG-1 strain. (A)** Schematic representation of the *pvron5* gene (blue) localized in Pv_Sal1_chr05:629000..649500 (21 kb) and comparative analysis with *P. falciparum*: Pf3D7_08_v3:798000..818000 (20 kb) and *P. knowlesi*: Pk_strainH_chr05:663000..682000 (19 kb) and Pk_strainH_chr05:709,700..711,400 (1.7 kB). The transcription direction is shown for each gene and the identity and similarity values between *ron5* and adjacent genes regarding the three *Plasmodium* species. Analysis was made concerning the information available in PlasmoDB [28] **(B)** *pvron5* amplification from gDNA. Above, a representation of the *pvron5* gene and the localization of the three sets of primers used for amplifying the gene are shown, along with the size of the expected products. ~3,404 bp (lane 1), ~1,815 bp (lane 2) and ~3,158 bp (lane 3) bands can be observed on the agarose gel, showing the weight of the expected products for *pvron5*. MWM: molecular weight marker. **(C)** *pvron5* transcription in VCG-1 strain late schizonts. Lane 1: *pvron5* positive RT-PCR. Lane 2: *pvrhoph3* positive RT-PCR. Lane 3: *pvron5* negative RT-PCR.

Arévalo-Pinzón et al. Malaria Journal (2015) 14:106

Page 8 of 14

account for determining the existence of conserved synteny in the chromosome region where *pvron5* was localized [41]. The results revealed conservation regarding the number of introns and exons of the genes upstream and downstream *ron5* as well as SI values extending up to 100% in some genes (Figure 1A), thereby suggesting that the *pvron5* gene is an orthologue of the *pfron5* and *pkron5* genes.

Following bioinformatics analysis, the presence of the *pvron5* gene in the VCG-1 strain genome was investigated by PCR amplification of ~8,076 bp comprising the gene from gDNA (Figure 1B); ~3,404 bp, ~1,815 bp and ~3,158 bp fragments were amplified with three sets of overlapping primers (by about 100 bp), two of which were designed upstream (+51) and downstream (−33) of the gene of interest (Figure 1B).

### *pvron5* gene transcription in the late phase intra-erythrocyte cycle

Merozoite invasion of RBC is a complex process, during which the parasite recognizes its target cell, orientates its apical pole and becomes internalized through the parasite's machinery and RBC membrane invagination [42]. These invasion events are accompanied by a large number of receptor-ligand interactions between proteins localized on/in the membrane or the parasite's apical organelles with RBC membrane proteins [42]. *Plasmodium falciparum* transcriptome studies have shown that ~500 ORFs have a transcription peak in late-schizont stage and that 60 to 90 antigens could be participating in invasion [43]. The *pfron5* gene has a maximum transcription peak after 41 hr of the intra-erythrocyte cycle, this being an appropriate time for its participation in the invasion cycle. In fact, it has been reported that *Pf*RON5 is associated with important antigens involved in invasion, such as RON2 and AMA1 [6,8].

PCR amplification of a product having around 3,477 bp from cDNA synthesized with reverse transcriptase (RT+) confirmed *pvron5* gene transcription (Figure 1C). The *pvrhoph3* gene was amplified as transcription control during schizont stage. Amplification was not obtained from RT negative samples, showing that synthesized cDNA was free of contamination with gDNA (Figure 1C). *pvron5* transcription in the VCG-1 strain agreed with previous studies of the *P. vivax* transcriptome carried out with three clinical isolates, showing that the PVX_089530 gene had a maximum transcription peak between 35 (TP7) and 40 hr (TP8) of the intra-erythrocyte cycle, similar to that reported for proteins which have been well characterized regarding invasion, such as *Pv*200, or new antigens, such as *Pv*RON2 [44]. Large differences regarding the size of the amplified *pvron5* product from gDNA (~8,076 bp) and cDNA (3,477 bp) suggested the presence of intron regions, this being consistent with the bioinformatics prediction (Figure 1).

The *pvron5* cDNA sequence (VCG-1 strain) was deposited in the NCBI (GenBank accession number: KP026121) and was compared to strains distributed throughout different geographic regions, such as India, Brazil, Asia and Africa, taking the Sal-1 strain deposited in PlasmoDB as reference. Analysis at nucleotide level revealed a 27 nt deletion towards the 5′ extreme in the India VII strain, coinciding with the absence of nine amino acids between positions 100 to 108 (Figure 2A and Additional file 1). Six changes were also found, four of which were non-synonymous mutations in positions 544, 547, 730, and 929 at amino acid level (Figure 2A). Such amount of change in *Pv*RON5 is low when compared to that present in other malarial antigens, such as MSP-1 and AMA-1 [45,46]. In fact, amino acids conserved physical-chemical properties in the first three changes mentioned (544, 547 and 730). However, it cannot be ruled out that such changes could have been associated with parasite evasion mechanisms. This is important when designing a completely effective anti-malaria vaccine as antigens having high genetic variability involve the expression of different alleles in different parasite strains, inducing allele-specific responses partly reducing vaccine efficacy [47,48].

### Analyzing RON5 expression and localization in *Plasmodium vivax*

RON5 is a 1,158 residue-long protein in the *P. vivax* VCG-1 strain and, according to SignalP and BaCelLo, it is a secreted protein containing a classical eukaryotic signal sequence towards the amino terminal extreme in the first 21 amino acids, having a short potential site for a type I peptidase between aa 21(S) and 22(R) (Figure 2A). This allows entry to the secretory pathway for traffic from the endoplasmic reticule through the Golgi complex by a conserved pathway before being packaged into the apically located secretory organelles. It also contains two predicted transmembrane domains localized in its sequence in the protein's central portion between residues 555–574 and 643–664 (Figure 2A). The protein's topology in parasite membrane would thus have amino and carboxyl terminal ends facing outwards, probably in contact with the host cell. Previous studies regarding *Pf*RON5 have provided contradictory results regarding the number of transmembrane domains in the sequence. Richard *et al.*, predicted six transmembrane regions (TMs) for *Pf*RON5 based on a hydrophobicity profile analysis [8]. A later study used different bioinformatics tools (Phobius, Polyphobius, TMHMM2.0, ConpredII and TMpred) for constructing a consensus regarding the transmembrane domains in *Pf*RON5 [39]. Such analysis led to concluding that, as well as the different models and statistics involved in using each tool, the dissimilar results may well have been due to protozoan protein sequences having been under-represented in the training data sets of most tools in

Arévalo-Pinzón *et al. Malaria Journal* (2015) 14:106

Page 9 of 14



**Figure 2** (See legend on next page.)

Arévalo-Pinzón *et al. Malaria Journal* (2015) 14:106

Page 10 of 14
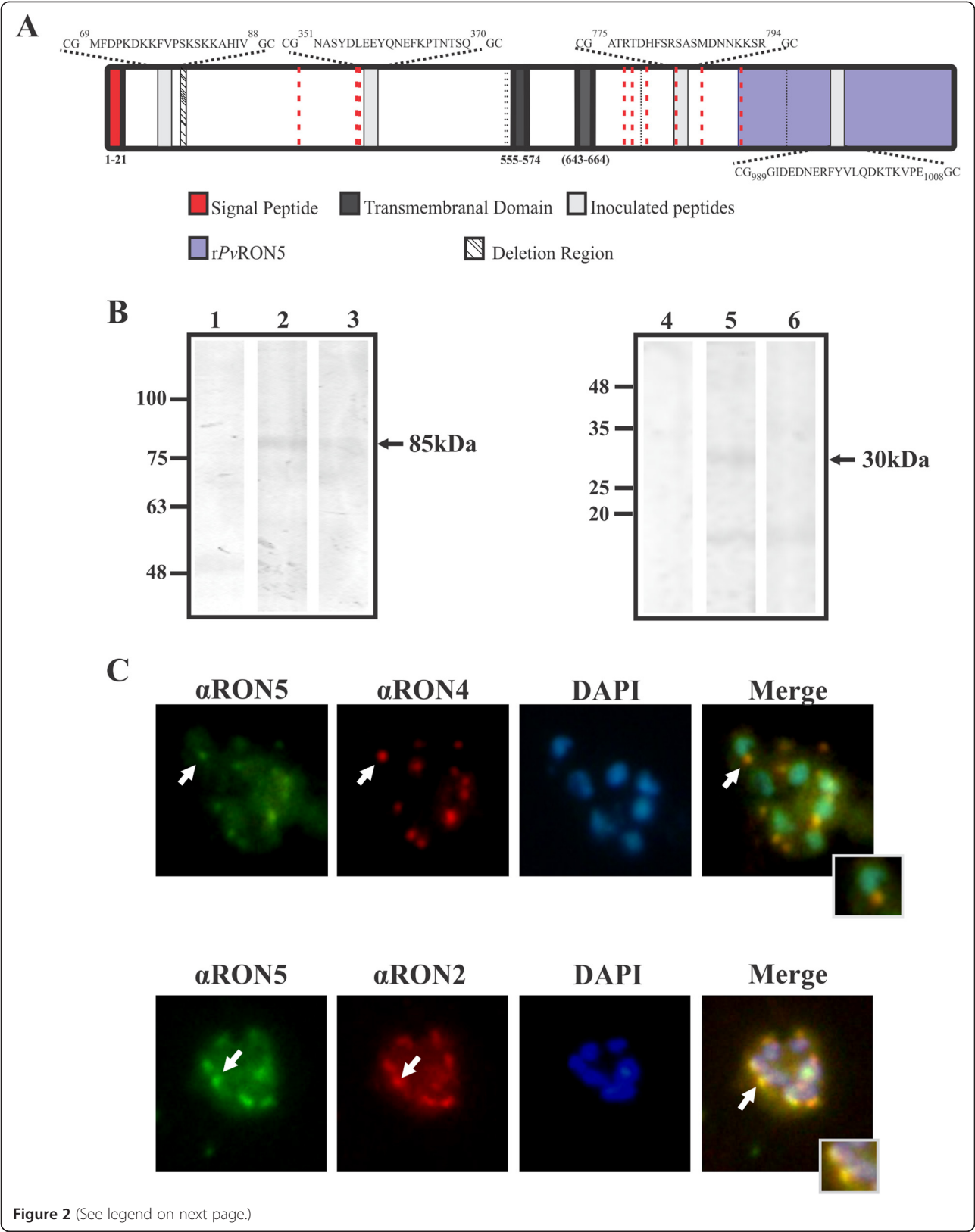
(See figure on previous page.)

**Figure 2 *Pv*RON5 expression in *Plasmodium vivax* schizonts. (A)** Representation to scale of the *P. vivax* RON5 protein. The signal peptide and the two transmembrane domains predicted by bioinformatics tools and the localization and sequence of the linear B-cell epitope peptides selected for polyclonal antibody production are shown. Comparative analysis of amino acid sequences from different *P. vivax* strains revealed the deletion of a nine-residue-long region; black dotted lines show synonymous and non-synonymous changes. Aligning *P. vivax, P. falciparum* and *P. knowlesi* RON5 revealed nine conserved cysteines (red dotted lines). The recombinant protein (r*Pv*RON5) produced in *E. coli* is shown in purple. **(B)** *Pv*RON5 expression in VCG-1 strain schizont lysate. Lane 1, pre-immune serum 60; lane 2, immune serum 60; lane 3, immune serum 60 pre-incubated with peptides 36930 and 36927; lane 4, pre-immune serum 2; lane 5, immune serum 2 and lane 6, immune serum 2 pre-incubated with peptide 39274. **(C)** *Pv*RON5 sub-cellular localization in *P. vivax*-infected RBCs in schizont stage. Green shows serum reactivity for *Pv*RON5, having a dotted pattern similar to that observed for *Pv*RON4 and *Pv*RON2 (red). The arrows show the dotted pattern and the overlaying of the images (merging). DAPI (4′,6-diamidino-2-phenylindole) was used for staining the parasite nucleus.

relation to other eukaryotic sequences, thereby hampering predicting transmembrane domains in these organisms [39]. Regarding *Py*RON5, two transmembrane domains were predicted by Polyphobius which had not been predicted by OCTOPUS and Phobius [49]. Interestingly, ultracentrifuge analysis supported the idea that *Py*RON5 is a protein lacking transmembrane domains, being mostly isolated in the soluble fraction compared to the fractions obtained with triton and SDS [49]. However, if the TJ model proposed by Besterio *et al.,* [9] is taken into account, it may be assumed that the protein should contain at least one hydrophobic region affording passage towards host cell cytoplasm. No repeat sequences or low complexity regions were found in *Pv*RON5, contrasting with that reported for *Pv*RON2 and *Pv*RON4, where several tandem repeats have been detected between both antigens' amino and central regions [24,25]. Repeats in malaria have been associated with evasion of the immune system regarding functionally important regions and the production of low affinity antibodies and independent T-cell activation. Interestingly, nine conserved cysteines were detected in *P. falciparum, P. vivax* and *P. knowlesi* RON5, distributed throughout the protein (Additional file 1), possibly being involved in conserved protein fold (Figure 2A).

Antibodies against *Pv*RON5 peptides were produced in rabbits for investigating the protein's presence and experimental molecular weight in VCG-1 strain late schizonts (Figure 2A). The polyclonal antibodies so obtained had high reactivity (by ELISA) for the inoculated peptides compared to pre-immune sera (p < 0.01). Rabbit 32 and 60 sera recognized a single band of around 85 kDa in schizont protein extract whose intensity became reduced when the antibodies had been previously incubated with the immunized peptides (36930 and 36927) (Figure 2B). This band had a molecular weight which that was below the predicted molecular weight (133 kDa) for *Pv*RON5. Bearing studies about some rhoptry proteins (i.e., *Tg*RON5, *Tg*RON4, *Pv*RON4, *Pv*RON2, *Pf*RAP1 and *Py*RON5) in mind where proteolytic processing was identified and suggested for maturation and/or functional activation [9,24,25,49,50], anti-peptide antibodies were produced against *Pv*RON5 amino- and carboxyl-terminal extremes

for identifying bands from proteolytic cleavages. Sera from rabbit 3 immunized with peptide 39276 localized towards the carboxyl-terminal extreme recognized a single ~85 kDa band, similar to sera 32 and 60 (Figure 2B), while sera from rabbit 2 inoculated with peptide 39274 located in the amino-terminal extreme recognized ~15 and ~30 kDa bands (Figure 2B), the latter band being specifically recognized, as sera previously incubated with peptide 39274 only recognized the ~15 kDa band (Figure 2B, lane 6). The ~85 and ~30 kDa specific products detected in *P. vivax* suggested that *Pv*RON5 is expressed in VCG-1 strain schizonts and undergoes proteolytic processing towards the amino terminal extreme.

Even though processing in RON5 has not been detected to date in *P. falciparum*, recent studies in *T. gondii* have shown that RON5 undergoes a minimum of two cuts, one being mediated by subtilisin 2 (SUB2) [20]. When characterizing RON5 in *P. yoelii*, the authors described a specific 87 kDa band and small ~33, ~31, and ~26 kDa fragments, suggesting physiologically processed products [48]. The *Pv*RON5 sequence was scanned for identifying possible candidate processing sites and evaluating whether they matched the consensus sequences for SUB2 (SφXE where φ was a hydrophobic residue and X any amino acid) [51] and SUB1 (I/L/V/TXG/APaa (not Leu), where X was any residue and Paa tended to be a polar residue) [52]. Two probable cleavage sites were identified for SUB1, one being located in the *Pv*RON5 amino terminal region (VCGQ, residues 261–264). Such cleavage produced two fragments partly coinciding with the electrophoretic migration observed for both products recognized by WB (Figure 2B). Analysis of *Py*RON5 protein sequence (GenBank: CDZ11526.1) revealed two putative cleavage sites for SUB1 which did not coincide with the number of previously shown fragments [49]. Such marked differences in the number of fragments obtained with RON5 in *P. falciparum, P. vivax, P. knowlesi* and *T. gondii* indicated that RON5 has differing cleavage patterns and thus involves the action of different enzymes. It cannot be ruled out that differences in processing may have been due to the particular moment of the parasite's lifecycle when the samples were taken for Western Blot analysis. However, further studies are required for

Arévalo-Pinzón *et al. Malaria Journal* (2015) 14:106

Page 11 of 14

evaluating putative cleavage and function regarding these proteins.

Anti-RON5 polyclonal antibodies produced in rabbits were used for determining RON5 sub-cellular localization in *P. vivax* schizonts. The images revealed that *Pv*RON5 had a dotted pattern characteristic of apical localization (Figure 2C). Including antibodies against proteins localized in the rhoptry neck, such as *Pv*RON2 and *Pv*RON4 in IFA, showed that *Pv*RON5 overlapped with the fluorescence for these two proteins, suggesting that *Pv*RON5 could be localized in the same compartment as *Pv*RON2 and *Pv*RON4 (Figure 2C) and was similar to that reported by electron microscope for *Pf*RON5 [21] and *Py*RON5 [49]. This expression and localization data agreed with antigen transcription time and coincided with the results from a previous study of the VCG-1 strain proteome where *Pv*RON5 peptides in schizont phase were identified [53].

### Determining the antigenicity of a *Pv*RON5 fragment

A ~33 kDa fragment was expressed in *E. coli* and purified by affinity chromatography based on the predicted topology for *Pv*RON5 and findings regarding the function of the RON5 carboxy terminal region in *T. gondii* (Figure 3A). This recombinant protein was used for investigating (by ELISA and WB) antibodies' natural response against *Pv*RON5 in samples from *P. vivax*-infected patients. Preliminary results showed that the sera recognized a 33 kDa band with differing reactivity, which was correlated with ELISA assay data (Figure 3B). The differences so observed in recognition of r*Pv*RON5 by sera from infected patients from different geographical regions in Colombia may have been due to the temporary acquisition of antibodies against the *Pv*RON5 carboxyl-terminal region, as has been described for the RON6 carboxyl terminus in *P. falciparum* regarding sera from patients from Papua New Guinea and Vietnam [54]. Sera from healthy individuals did not recognize r*Pv*RON5. It is worth emphasizing that reactivity was only evaluated regarding the protein's carboxyl-terminal extreme. Future antigenicity studies could deal with evaluating the protein's other regions.

### r*Pv*RON5 bound to samples enriched with human reticulocytes

Designing an anti-malarial vaccine has been based on a functional approach for several years now; this has involved identifying conserved regions from antigens specifically binding to host cell receptors with high affinity. An attempt was made to block regions actively involved in RBC entry and whose sequences have a significant role in invasion characterized by being much more conserved than non-critical regions [55]. This concept has led to the



**Figure 3 r*Pv*RON5 expression and antigenicity studies. (A)** r*Pv*RON5 expression and purification. Lane 1, r*Pv*RON5 purified by affinity chromatography with Coomassie blue staining. A single ~33 kDa band was observed which coincided with the expected molecular weight. Lane 2, WB recognition of r*Pv*RON5 using anti-polyhistidine monoclonal antibody. **(B)** *P. vivax* patients' sera reactivity with r*Pv*RON5. Top panel, recognition of recombinant protein by WB. H: reactivity by monoclonal anti-polyhistidine serum. Lanes 1 to 11, recognition of r*Pv*RON5 by sera from *P. vivax*-infected patients. A single ~33 kDa band can be seen. Lanes 12 to 15, sera from healthy individuals. R: Polyclonal serum 2 reactivity with r*Pv*RON5. Bottom panel, ELISA recognition of r*Pv*RON5 by sera from *P. vivax*-infected patients (grey bars) and healthy individuals (black bars).

Arévalo-Pinzón *et al. Malaria Journal* (2015) 14:106

Page 12 of 14

functional regions of most *P. falciparum* proteins participating in merozoite entry to RBC, having been identified and named HABPs. Interestingly, when HABPs were immunized in *Aotus* monkeys it was found that such conserved HABPs (cHABPs) were poorly immunogenic and thus did not induce protection against experimental challenge. A second approach was adopted which was orientated towards identifying HABP critical residues, which were then modified by replacing them with other amino acids having similar mass but different polarity and called mHABPs; many of these mHABPs were found to be immunogenic and protection-inducing [56]. The explanation for such immunological response was correlated with mHABP binding to purified molecules from the major histocompatibility complex (MHC) and its 3-D structure. This information led to suggesting that changes in cHABPs improve peptide coupling in the MHC thereby optimizing immunological presentation and thus inducing a protective immune response [57].

The lack of a continuous source of reticulocyte-enriched samples regarding *P. vivax* has hampered the identification of regions where *P. vivax* antigens bind to their target cells, using the methodology adopted concerning *P. falciparum*. Binding regions have been identified in three *P. vivax* proteins to date: *Pv*MSP1, *Pv*DBP and *Pv*RBP-1 [58-60]. Two qualitative methodologies have been adopted to make further advances in identifying these regions; they require fewer target cells for evaluating whether the *Pv*RON5 carboxyl terminal region interacts with umbilical cord samples and reticulocyte-enriched samples.

Figure 4A shows that r*Pv*RON5 bound to umbilical cord RBC and reticulocyte-enriched samples. IFA involving reticulocytes labelled with anti-CD71 antibody and polyclonal serum (rabbit 3) against r*Pv*RON5 having high reactivity for the recombinant protein as shown by WB (Figure 3, lane R), were used for determining recombinant protein preference and/or tropism for human reticulocytes or mature RBC. The results showed that r*Pv*RON5 bound to both mature RBC and reticulocytes (Figure 4B). The differences between cell-associated fluorescence measured by Image J 1.48 in RBCs compared to reticulocytes showed that r*Pv*RON5 had greater ability to bind human reticulocytes ($p < 0.01$) than RBCs (as expected), as reticulocytes are target cells for *P. vivax*. This pattern was similar to that reported for *Pv*MSP1 which contains reticulocyte binding HABPs, binding to erythrocytes to a lesser degree [58,61]. The foregoing could depend on the few RON5 receptors on RBC membrane compared to reticulocytes as part of RBC maturation and differentiation [62]. No fluorescence was observed in the negative controls (Additional file 2). All the above data suggested that *Pv*RON5 appears to be an adhesin, which might participate in invasion by binding to reticulocyte surface.

## Conclusions

Identifying and characterizing new antigens in *P. vivax* is an indispensable step for making advances in designing a vaccine against this parasite species. The present study identified the *pvron5* gene consisting of 8,076 bp, which was transcribed during the parasite's intra-erythrocyte cycle and expressed at the apical pole of VCG-1 strain schizonts. The *Pv*RON5 protein contained a hydrophobic signal sequence, two transmembrane domains and was conserved between distinct strains of the parasite distributed around the world. The *Pv*RON5 carboxyl-terminal
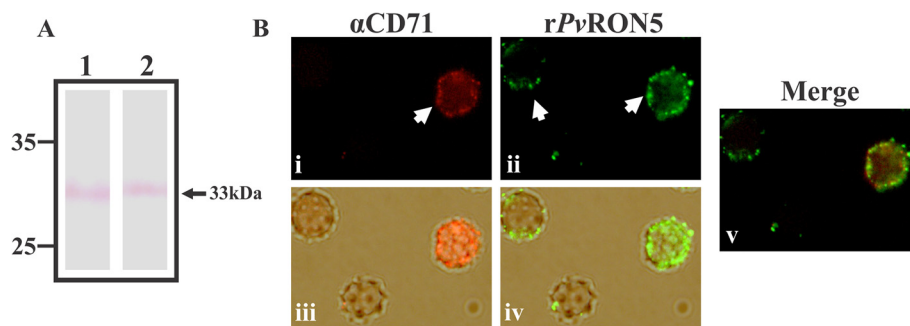


**Figure 4 r*Pv*RON5 binding to human reticulocytes. (A)** Immunoprecipitation and WB assays with reticulocytes (lane 1) and packed RBC (lane 2) with r*Pv*RON5. 15 μg r*Pv*RON5 was incubated with human reticulocytes or packed RBC passed through CF11 columns, followed by separation by dibutyl phthalate gradient. Cell-associated protein was eluted with 1 M NaCl in PBS and the eluted fraction was immunoprecipitated with anti-polyhistidine antibodies. The precipitate was run on an SDS-PAGE gel and revealed with anti-polyhistidine antibodies. **(B)** Indirect immunofluorescence binding studies. **(i)** reticulocyte labelling with antibodies against the transferrin receptor (CD71) which is expressed at high levels during erythroid development phases and is absent in mature cells (RBC). **(ii)** r*Pv*RON5 recognition by polyclonal antibodies directed against the recombinant bound to reticulocytes and RBC. **(iii)** The cells were seen in white light and those which were positive for CD71 (red). **(iv)** The cells were observed in white light simultaneously with r*Pv*RON5 binding (green) to cell membrane. **(v)** Merging between red fluorescence (CD71) and green (r*Pv*RON5). Greater r*Pv*RON5 preference for reticulocytes than mature RBCs was observed.

Arévalo-Pinzón *et al. Malaria Journal* (2015) 14:106

Page 13 of 14

region bound to RBC, having a high preference for human reticulocytes, and was recognized by sera from *P. vivax*-infected patients. All these characteristics led to cataloguing this new antigen as an important candidate to be included in immunogenicity and protection assays in experimental models.

## Additional files

**Additional file 1: RON5 was aligned with *Plasmodium* strains.** Red shows the cysteines which were conserved among *P. vivax*, *P. falciparum* and *P. knowlesi*; blue shows the cysteines which were only conserved between *P. vivax* and *P. knowlesi*.

**Additional file 2: Figure S1.** Negative controls included in rPvRON5 reticulocyte binding assays. This shows the fluorescence obtained for: **a)** reticulocytes or RBC incubated only with polyclonal antibody against rPvRON5 followed by FITC-coupled secondary antibodies; **b)** reticulocytes or RBC incubated with only FITC-coupled secondary antibodies; **c)** reticulocytes or RBC incubated with rPvRON5 followed by incubation with FITC-coupled secondary antibody.

## Competing interests

The authors declare that they have no competing interests.

## Authors' contributions

GAP did the bioinformatics analysis, molecular biology assays and wrote the initial manuscript. MB carried out immunoassays, reticulocyte-enrichment and recombinant protein binding to human reticulocytes assays. HC synthesized and purified the peptides used for rabbit and mice immunizations and analyzed the data. MAP evaluated and coordinated assays and revised the final manuscript. All authors have read and approved the final manuscript.

## Acknowledgements

## References

1. Joiner KA, Roos DS. Secretory traffic in the eukaryotic parasite *Toxoplasma gondii:* less is more. J Cell Biol. 2002;157:557–63.
2. Kats LM, Black CG, Proellocks NI, Coppel RL. *Plasmodium* rhoptries: how things went pear-shaped. Trends Parasitol. 2006;22:269–76.
3. Zuccala ES, Gout AM, Dekiwadia C, Marapana DS, Angrisano F, Turnbull L, et al. Subcompartmentalisation of proteins in the rhoptries correlates with ordered events of erythrocyte invasion by the blood stage malaria parasite. PLoS One. 2012;7:e46160.
4. Riglar DT, Richard D, Wilson DW, Boyle MJ, Dekiwadia C, Turnbull L, et al. Super-resolution dissection of coordinated events during malaria parasite invasion of the human erythrocyte. Cell Host Microbe. 2011;9:9–20.
5. Shen B, Sibley LD. The moving junction, a key portal to host cell invasion by apicomplexan parasites. Curr Opin Microbiol. 2012;15:449–55.
6. Collins CR, Withers-Martinez C, Hackett F, Blackman MJ. An inhibitory antibody blocks interactions between components of the malarial invasion machinery. PLoS Pathog. 2009;5:e1000273.
7. Alexander DL, Mital J, Ward GE, Bradley P, Boothroyd JC. Identification of the moving junction complex of *Toxoplasma gondii:* a collaboration between distinct secretory organelles. PLoS Pathog. 2005;1:e17.
8. Richard D, MacRaild CA, Riglar DT, Chan JA, Foley M, Baum J, et al. Interaction between *Plasmodium falciparum* apical membrane antigen 1 and the rhoptry neck protein complex defines a key step in the erythrocyte invasion process of malaria parasites. J Biol Chem. 2010;285:14815–22.
9. Besteiro S, Michelin A, Poncet J, Dubremetz JF, Lebrun M. Export of a *Toxoplasma gondii* rhoptry neck protein complex at the host cell membrane to form the moving junction during invasion. PLoS Pathog. 2009;5:e1000309.
10. Tonkin ML, Roques M, Lamarque MH, Pugniere M, Douguet D, Crawford J, et al. Host cell invasion by apicomplexan parasites: insights from the co-structure of AMA1 with a RON2 peptide. Science. 2011;333:463–7.
11. Vulliez-Le Normand B, Tonkin ML, Lamarque MH, Langer S, Hoos S, Roques M, et al. Structural and functional insights into the malaria parasite moving junction complex. PLoS Pathog. 2012;8:e1002755.
12. Collins CR, Withers-Martinez C, Bentley GA, Batchelor AH, Thomas AW, Blackman MJ. Fine mapping of an epitope recognized by an invasion-inhibitory monoclonal antibody on the malaria vaccine candidate apical membrane antigen 1. J Biol Chem. 2007;282:7431–41.
13. Coley AM, Gupta A, Murphy VJ, Bai T, Kim H, Foley M, et al. Structure of the malaria antigen AMA1 in complex with a growth-inhibitory antibody. PLoS Pathog. 2007;3:1308–19.
14. Harris KS, Casey JL, Coley AM, Masciantonio R, Sabo JK, Keizer DW, et al. Binding hot spot for invasion inhibitory molecules on *Plasmodium falciparum* apical membrane antigen 1. Infect Immun. 2005;73:6981–9.
15. Srinivasan P, Ekanem E, Diouf A, Tonkin ML, Miura K, Boulanger MJ, et al. Immunization with a functional protein complex required for erythrocyte invasion protects against lethal malaria. Proc Natl Acad Sci U S A. 2014;111:10311–6.
16. Bargieri DY, Andenmatten N, Lagal V, Thiberge S, Whitelaw JA, Tardieux I, et al. Apical membrane antigen 1 mediates apicomplexan parasite attachment but is dispensable for host cell invasion. Nat Comm. 2013;4:2552.
17. Giovannini D, Spath S, Lacroix C, Perazzi A, Bargieri D, Lagal V, et al. Independent roles of apical membrane antigen 1 and rhoptry neck proteins during host cell invasion by apicomplexa. Cell Host Microbe. 2011;10:591–602.
18. Lamarque MH, Roques M, Kong-Hap M, Tonkin ML, Rugarabamu G, Marq JB, et al. Plasticity and redundancy among AMA-RON pairs ensure host cell entry of *Toxoplasma* parasites. Nat Comm. 2014;5:4098.
19. Takemae H, Sugi T, Kobayashi K, Gong H, Ishiwa A, Recuenco FC, et al. Characterization of the interaction between *Toxoplasma gondii* rhoptry neck protein 4 and host cellular beta-tubulin. Sci Rep. 2013;3:3199.
20. Beck JR, Chen AL, Kim EW, Bradley PJ. RON5 is critical for organization and function of the *Toxoplasma moving* junction complex. PLoS Pathog. 2014;10:e1004025.
21. Curtidor H, Patino LC, Arevalo-Pinzon G, Vanegas M, Patarroyo ME, Patarroyo MA. *Plasmodium falciparum* rhoptry neck protein 5 peptides bind to human red blood cells and inhibit parasite invasion. Peptides. 2014;53:210–7.
22. Hossain ME, Dhawan S, Mohmmed A. The cysteine-rich regions of *Plasmodium falciparum* RON2 bind with host erythrocyte and AMA1 during merozoite invasion. Parasitol Res. 2012;110:1711–21.
23. Pico de Coana Y, Rodriguez J, Guerrero E, Barrero C, Rodriguez R, Mendoza M, et al. A highly infective *Plasmodium vivax* strain adapted to *Aotus* monkeys: quantitative haematological and molecular determinations useful for *P. vivax* malaria vaccine development. Vaccine. 2003;21:3930–7.
24. Arevalo-Pinzon G, Curtidor H, Patino LC, Patarroyo MA. PvRON2, a new *Plasmodium vivax* rhoptry neck antigen. Malar J. 2011;10:60.
25. Arevalo-Pinzon G, Curtidor H, Abril J, Patarroyo MA. Annotation and characterization of the *Plasmodium vivax* rhoptry neck protein 4 (PvRON4). Malar J. 2013;12:356.
26. WHO. Word malaria report 2013. Geneva: World Health Organization; 2013.
27. Patarroyo MA, Calderon D, Moreno-Perez DA. Vaccines against *Plasmodium vivax*: a research challenge. Expert Rev Vaccines. 2012;11:1249–60.
28. Plasmo DB. Plasmodium genomics resource. [http://www.plasmodb.org]
29. Altschul SF, Gish W, Miller W, Myers EW, Lipman DJ. Basic local alignment search tool. J Mol Biol. 1990;215:403–10.
30. Burge C, Karlin S. Prediction of complete gene structures in human genomic DNA. J Mol Biol. 1997;268:78–94.
31. Spidey. [http://www.ncbi.nlm.nih.gov/spidey/]
32. Petersen TN, Brunak S, von Heijne G, Nielsen H. SignalP 4.0: discriminating signal peptides from transmembrane regions. Nat Methods. 2011;8:785–6.
33. Kall L, Krogh A, Sonnhammer EL. An HMM posterior decoder for sequence feature prediction that includes homology information. Bioinformatics. 2005;21 Suppl 1:i251–7.

Arévalo-Pinzón *et al. Malaria Journal* (2015) 14:106

Page 14 of 14

34. Pierleoni A, Martelli PL, Fariselli P, Casadio R. BaCelLo: a balanced subcellular localization predictor. Bioinformatics. 2006;22:408–16.

35. Letunic I, Goodstadt L, Dickens NJ, Doerks T, Schultz J, Mott R, et al. Recent improvements to the SMART domain-based sequence annotation resource. Nucleic Acids Res. 2002;30:242–4.

36. Chomczynski P. A reagent for the single-step simultaneous isolation of RNA, DNA and proteins from cell and tissue samples. Biotechniques. 1993;15:532–4.

37. Mongui A, Perez-Leal O, Rojas-Caraballo J, Angel DI, Cortes J, Patarroyo MA. Identifying and characterising the *Plasmodium falciparum* RhopH3 *Plasmodium vivax* homologue. Biochem Biophys Res Commun. 2007;358:861–6.

38. Thompson JD, Higgins DG, Gibson TJ. CLUSTAL W: improving the sensitivity of progressive multiple sequence alignment through sequence weighting, position-specific gap penalties and weight matrix choice. Nucleic Acids Res. 1994;22:4673–80.

39. Curtidor H, Patino LC, Arevalo-Pinzon G, Patarroyo ME, Patarroyo MA. Identification of the *Plasmodium falciparum* rhoptry neck protein 5 (PfRON5). Gene. 2011;474:22–8.

40. Russell B, Suwanarusk R, Borlon C, Costa FT, Chu CS, Rijken MJ, et al. A reliable ex vivo invasion assay of human reticulocytes by *Plasmodium vivax*. Blood. 2011;118:e74–81.

41. Kuzniar A, van Ham RC, Pongor S, Leunissen JA. The quest for orthologs: finding the corresponding gene across genomes. Trends Genet. 2008;24:539–51.

42. Harvey KL, Gilson PR, Crabb BS. A model for the progression of receptor-ligand interactions during erythrocyte invasion by *Plasmodium falciparum*. Int J Parasitol. 2012;42:567–73.

43. Bozdech Z, Llinas M, Pulliam BL, Wong ED, Zhu J, DeRisi JL. The transcriptome of the intraerythrocytic developmental cycle of *Plasmodium falciparum*. PLoS Biol. 2003;1:E5.

44. Bozdech Z, Mok S, Hu G, Imwong M, Jaidee A, Russell B, et al. The transcriptome of *Plasmodium vivax* reveals divergence and diversity of transcriptional regulation in malaria parasites. Proc Natl Acad Sci U S A. 2008;105:16290–5.

45. Escalante AA, Lal AA, Ayala FJ. Genetic polymorphism and natural selection in the malaria parasite *Plasmodium falciparum*. Genetics. 1998;149:189–202.

46. Healer J, Murphy V, Hodder AN, Masciantonio R, Gemmill AW, Anders RF, et al. Allelic polymorphisms in apical membrane antigen-1 are responsible for evasion of antibody-mediated inhibition in *Plasmodium falciparum*. Mol Microbiol. 2004;52:159–68.

47. Ouattara A, Takala-Harrison S, Thera MA, Coulibaly D, Niangaly A, Saye R, et al. Molecular basis of allele-specific efficacy of a blood-stage malaria vaccine: vaccine development implications. J Infect Dis. 2013;207:511–9.

48. Hisaeda H, Yasutomo K, Himeno K. Malaria: immune evasion by parasites. Int J Biochem Cell Biol. 2005;37:700–6.

49. Mutungi JK, Yahata K, Sakaguchi M, Kaneko O. Expression and localization of rhoptry neck protein 5 in merozoites and sporozoites of *Plasmodium yoelii*. Parasitol Int. 2014;63:794–801.

50. Harnyuttanakorn P, McBride JS, Donachie S, Heidrich HG, Ridley RG. Inhibitory monoclonal antibodies recognise epitopes adjacent to a proteolytic cleavage site on the RAP-1 protein of *Plasmodium falciparum*. Mol Biochem Parasitol. 1992;55:177–86.

51. Bradley PJ, Hsieh CL, Boothroyd JC. Unprocessed Toxoplasma ROP1 is effectively targeted and secreted into the nascent parasitophorous vacuole. Mol Biochem Parasitol. 2002;125:189–93.

52. Silmon de Monerri NC, Flynn HR, Campos MG, Hackett F, Koussis K, Withers-Martinez C, et al. Global identification of multiple substrates for *Plasmodium falciparum* SUB1, an essential malarial processing protease. Infect Immun. 2011;79:1086–97.

53. Moreno-Perez DA, Degano R, Ibarrola N, Muro A, Patarroyo MA. Determining the *Plasmodium vivax* VCG-1 strain blood stage proteome. J Proteomics. 2014;113C:268–80.

54. Proellocks NI, Kats LM, Sheffield DA, Hanssen E, Black CG, Waller KL, et al. Characterisation of PfRON6, a *Plasmodium falciparum* rhoptry neck protein with a novel cysteine-rich domain. Int J Parasitol. 2009;39:683–92.

55. Patarroyo ME, Patarroyo MA. Emerging rules for subunit-based, multiantigenic, multistage chemically synthesized vaccines. Acc Chem Res. 2008;41:377–86.

56. Patarroyo ME, Cifuentes G, Vargas LE, Rosas J. Structural modifications enable conserved peptides to fit into MHC molecules thus inducing protection against malaria. Chembiochem. 2004;5:1588–93.

57. Patarroyo ME, Bermudez A, Patarroyo MA. Structural and immunological principles leading to chemically synthesized, multiantigenic, multistage, minimal subunit-based vaccine development. Chem Rev. 2011;111:3459–507.

58. Rodriguez LE, Urquiza M, Ocampo M, Curtidor H, Suarez J, Garcia J, et al. *Plasmodium vivax* MSP-1 peptides have high specific binding activity to human reticulocytes. Vaccine. 2002;20:1331–9.

59. Ocampo M, Vera R, Eduardo Rodriguez L, Curtidor H, Urquiza M, Suarez J, et al. *Plasmodium vivax* Duffy binding protein peptides specifically bind to reticulocytes. Peptides. 2002;23:13–22.

60. Urquiza M, Patarroyo MA, Mari V, Ocampo M, Suarez J, Lopez R, et al. Identification and polymorphism of *Plasmodium vivax* RBP-1 peptides which bind specifically to reticulocytes. Peptides. 2002;23:2265–77.

61. Espinosa AM, Sierra AY, Barrero CA, Cepeda LA, Cantor EM, Lombo TB, et al. Expression, polymorphism analysis, reticulocyte binding and serological reactivity of two *Plasmodium vivax* MSP-1 protein recombinant fragments. Vaccine. 2003;21:1033–43.

62. Liu J, Guo X, Mohandas N, Chasis JA, An X. Membrane remodeling during reticulocyte maturation. Blood. 2010;115:2021–7.

## 5         Caracterización de Interacciones Hospedero-Patógeno en *P. vivax*

La malaria es una enfermedad infecciosa que afecta a las zonas tropicales y subtropicales del mundo, especialmente a niños menores de cinco años y mujeres en estado de embarazo. En los últimos años, según reportes de la OMS, se ha observado una disminución en el número de casos nuevos al año, lo que destaca el esfuerzo internacional en la implementación de medidas de control como el uso combinado de mosquiteros tratados con insecticida (MTI), el rociado residual en interiores y el uso de terapia combinada basada en artemisinina [71]. Pese a ello, el informe de la malaria para el 2016 reportó cerca de 216 millones de casos de paludismo y alrededor de 445.000 muertes a nivel mundial y deja un preocupante balance, donde la tendencia a la reducción en los casos y muertes por malaria se ha estancado, e incluso revertido en las Américas y en algunas regiones de Asia Sudoriental [2, 3]. La aparición de cepas de *Plasmodium* resistentes a cloroquina y artemisinina, la resistencia de los mosquitos *Anopheles* a los insecticidas y la presencia de hipnozoitos (esquizontes hepáticos latentes en *P. vivax*) que ocasionan recaídas y desencadenan infecciones en el estadio intraeritrocítico incluso en ausencia de transmisión continúa, son de los principales obstáculos en el control y eliminación de la malaria [2, 72, 73]. Esto, sumado a la complejidad del ciclo de vida del parásito que involucra múltiples fases, tanto en el vector como en el humano (Figura 3), muestran la necesidad de un control múltiple, que involucre la combinación de fármacos, control de vectores y el desarrollo de una vacuna efectiva.

Diferentes aproximaciones metodológicas para el desarrollo de una vacuna contra la malaria han sido utilizadas, entre las que se incluye el uso del microorganismo completo, como esporozoítos vivos atenuados genéticamente o por radiación [74, 75] o esporozoitos vivos administrados bajo tratamiento con cloroquina [76]. Desafortunadamente, aunque estas vacunas,

son capaces de inducir protección esterilizante, presentan desventajas relacionadas con la producción masiva de esporozoitos para la vacunación [77].

En otra aproximación con *P. falciparum*, el tamizaje de librerías genómicas o de ADN complementario (ADNc) con anticuerpos aislados de pacientes infectados, ha permitido la identificación, purificación, caracterización y evaluación como inmunógenos (aproximación inmunológica) de importantes antígenos derivados del parásito [77]. En esta aproximación, donde se han utilizado antígenos recombinantes, péptidos sintéticos y más recientemente vectores virales, aquellas regiones con capacidad antigénica o inmunogénica son las consideradas candidatas a vacuna [78-80]. Adicionalmente, la era de las ciencias ómicas, ha permitido la identificación masiva de blancos potenciales con capacidad protectiva [77]. En muchos casos, los mismos candidatos a vacuna han sido probados sobre diferentes plataformas, con diferentes adyuvantes, e inclusive en combinación con otros antígenos [81-83], sin embargo, a pesar de los logros con las diferentes propuestas, aún no se encuentra disponible una vacuna contra la malaria para uso en humanos.

Parte del fracaso en el desarrollo de una vacuna contra la malaria puede ser explicado por la presencia de diferentes rutas de invasión que utiliza el *Plasmodium* y por la respuesta inmune alelo-específica que dirige la atención contra epítopes polimórficos no relevantes [84, 85]. De esta forma, una vacuna basada en antígenos polimórficos antigénicos, sería sólo capaz de proteger contra el reto homólogo (respuesta cepa-específica), o en otros casos, sólo servir como una "cortina de humo" para dirigir la respuesta inmune contra las regiones no funcionales [86, 87]. La respuesta alelo-específica podría ser entonces la responsable de la falla observada en muchas formulaciones

que han avanzado a ensayos clínicos, utilizando proteínas como *Pf*AMA1 [88], *Pf*MSP1 [86, 89] y *Pf*CSP [90], entre otros. Basados en estos hechos, aún no es claro en cuáles antígenos se debe priorizar y cómo predecir e identificar las regiones ideales de las distintas proteínas, para ser incluidos en una vacuna multiantígeno, multiestadío contra la malaria.

Utilizando como modelo de estudio la malaria, en la Fundación Instituto de Inmunología de Colombia (FIDIC), se ha establecido una metodología universal para el desarrollo de vacunas [91]. Ésta se enfoca en una aproximación funcional, donde el objetivo principal es generar respuesta inmune contra las regiones conservadas (sin cambios a nivel de aminoácidos) de las proteínas del parásito, que se unen específicamente y con alta afinidad a la célula hospedera durante el proceso de invasión [91, 92]. Estas regiones (20 residuos de longitud), se han denominado péptidos conservados con alta capacidad de unión (cHABPs, del inglés Conserved High Activity Binding Peptides) a eritrocitos y han sido identificados para la mayoría de las proteínas del merozoito y en cerca de 12 proteínas del esporozoito de *P. falciparum* [93-95]. Algunos cHABPs derivados de merozoitos inhiben la invasión de este parásito, lo que indica una asociación importante con algunas de las funciones presentes en la invasión como son: adhesión, reorientación, formación del pre-enlace fuerte o del enlace fuerte [92, 95].

Cuando monos *Aotus* spp. fueron inmunizados con cHABPs, se encontró que la mayoría de estos péptidos carecían de capacidad inmunogénica y protectiva, indicando que estos cHABPs son silentes inmunológicamente, es decir que, en condiciones de infección natural, estas regiones funcionales y críticas en el proceso de invasión, no estimulan la producción de anticuerpos y, por lo tanto, no inducen respuesta inmune protectora. Estudios posteriores, mostraron que parte de este

fenómeno, se explica por el ajuste imperfecto de los cHABPs en el complejo mayor de histocompatibilidad (CMH) clase II, lo que se traduce en un complejo trimérico CMH-péptido-receptor de las células T (RCT) inestable. Para solucionar este problema, cada cHABP fue utilizado como plantilla para el diseño de péptidos análogos, a los cuales se les substituían los residuos críticos en la invasión, de acuerdo a los principios fisicoquímicos previamente definidos [91, 96]. Algunos de estos HABPs modificados (mHABPs, del inglés modified HABPs), fueron capaces de inducir respuesta inmune protectiva frente al reto experimental en monos *Aotus* [97, 98]. La determinación de la estructura tridimensional de cada péptido, así como la unión de algunos cHABPs y mHABPs a moléculas purificadas del HLA-DRβ1 humano, mostró que las modificaciones hechas sobre la secuencia de los cHABPs inducían cambios estructurales que le permitían un mejor ajuste dentro del CMH y que se correlacionaban con la protección en monos *Aotus* [97, 99]. De esta forma, los cHABPs se estarían convirtiendo en estructuras proteicas inductoras de protección inmune (IMPIPS, del inglés IMmune Protection-Inducing Protein Structures) y serían las subunidades a ser incluidas en una vacuna contra la malaria [97, 100].

En *P. falciparum* han sido identificados y modificados todos los componentes mínimos necesarios para bloquear la invasión a nivel de esporozoito y merozoito en las distintas poblaciones humanas (restricción genética de los haplotipos del antígeno leucocitario humano), donde *P. falciparum* es prevalente [97]. En *P. vivax*, tan solo tres proteínas: *Pv*MSP-1 [101], *Pv*DBP [102] y *Pv*RBP-1 [101], han sido incluidas en ensayos de interacción receptor-ligando para identificar las regiones relacionadas con la unión a la célula hospedera: cHABPs. Por consiguiente, el descubrimiento de nuevos antígenos y la caracterización e identificación de las regiones

funcionales que se unen a los reticulocitos, son de vital importancia para el desarrollo de una vacuna contra *P. vivax*.

Desafortunadamente, la realización de estudios funcionales de adhesión en *P. vivax* se encuentra limitada por la dificultad en la obtención y enriquecimiento de reticulocitos humanos, que ocupan cerca del 1 al 2% del total de sangre periférica. Esta limitante, impone retos a la hora de utilizar la misma metodología aplicada en *P. falciparum* para identificar cHABPs en *P. vivax*. Los estudios hechos con las proteínas *Pv*DBP, *Pv*MSP1 y *Pv*RBP-1 se realizaron con sangre de un paciente con β-talasemia, que mantenía alrededor de un 85% de reticulocitos en sangre periférica [101, 102]. Sin embargo, el acceso a estos pacientes y las implicaciones de su enfermedad, les impiden la donación constante de sangre.

Es por esto, que diferentes fuentes de reticulocitos humanos han sido exploradas, entre las que se incluyen la producción de reticulocitos a partir de células madre hematopoyéticas (CMHem) o embriónicas (CME), uso de sangre de animales (primates o ratones) con anemia inducida, o sangre de cordón umbilical (SCU) [103]. El uso de estas fuentes, ha sido combinado con varios métodos de enriquecimiento, como el uso de gradientes de densidad, soluciones hipotónicas y separación inmunomagnética [104]. Aunque se han obtenido distintos rendimientos y volúmenes de reticulocitos a partir de las diferentes fuentes mencionadas [16, 104], el uso de SCU combinado con gradientes de densidad o separación inmunomagnética, promete ser la fuente más asequible, económica y con rendimientos aceptables [104, 105]. La SCU contiene alrededor del 3 al 8% de reticulocitos y es capaz de soportar el crecimiento de *P. vivax* por periodos cortos de tiempo [106]. Cuando se comparan a nivel proteómico las células eritroides de adultos con las células de cordón

umbilical, sólo se han observado pequeñas diferencias relacionadas a los perfiles de expresión de las globinas, anhidrasas carbónicas y acuaporina 1 [63].

Teniendo como objetivo la caracterización de regiones conservadas de unión de las proteínas de *P. vivax* a reticulocitos humanos, el diseño experimental consistió en buscar técnicas que requiriesen la menor cantidad de reticulocitos para el ensayo. De esta forma, se estandarizó un protocolo de enriquecimiento de reticulocitos a partir de SCU, para evaluar la unión de una región conservada de la proteína *Pv*RON5 a reticulocitos humanos, mediante inmunofluorescencia cuantitativa e inmunoprecipitación. El ensayo de inmunoprecipitación mostró que la proteína recombinante (r*Pv*RON5) es capaz de unirse tanto a normocitos como a reticulocitos. Al comparar la fluorescencia asociada a reticulocitos (marcados con CD71) versus eritrocitos (negativos para CD71), se encontró que r*Pv*RON5 se unió más a reticulocitos que a normocitos, lo que muestra una preferencia de unión de esta proteína por las células hospederas de *P. vivax*. Estos resultados fueron publicados en el artículo titulado "The *Plasmodium vivax* rhoptry neck protein 5 is expressed in the apical pole of *Plasmodium vivax* VCG-1 strain schizonts and binds to human reticulocytes" [70], adjunto arriba.

Para avanzar en la caracterización de las regiones mínimas de unión en *P. vivax*, las proteínas *Pv*AMA-1 (*Pv*AMA1, *Pv*AMA-DI-II y *Pv*AMA-DII-III) y *Pv*RON4 fueron expresadas sobre la membrana de las células COS-7 e incubadas con SCU. Este ensayo, evalúa la asociación directa de los eritrocitos con las células COS-7 que expresan las proteínas de *P. vivax* sobre la membrana, lo que lleva a la formación de rosetas. La expresión de las proteínas del parásito en células eucariotas, asegura un adecuado plegamiento de las proteínas, similar a como se expresan en el parásito.

Una vez evaluadas las regiones de interacción positiva, se obtuvieron las proteínas recombinantes en *E. coli* (*Pv*AMA1, *Pv*AMA-DI-II, *Pv*AMA-DII-III, *Pv*RON2-RI, *Pv*RON2-RII y *Pv*RON4) y se purificaron mediante cromatografía de afinidad. Estas proteínas fueron incubadas con SCU y la interacción proteína-reticulocito fue medida por citometría de flujo. En este ensayo, se utilizaron anticuerpos anti-histidina acoplados a fluoresceína (FITC, del inglés Fluorescein Isotiocyanate) para reconocer las proteínas recombinantes, mientras que para reconocer a los reticulocitos, se utilizó un anticuerpo anti-CD71 acoplado a APC-H7, y se incluyó un anticuerpo anti-CD45 acoplado a aloficocianina (APC, del inglés Allophycocyanin) para reconocer y descartar de la población aquellos linfocitos activados CD71$^+$. Posteriormente, con las proteínas *Pv*RON2-RI, *Pv*RON2-RII y *Pv*RON4, se determinó si la unión a reticulocitos es específica, radiomarcando las proteínas e incubándolas en presencia o ausencia de la misma proteína no-radiomarcada. Para determinar la región mínima de interacción de las proteínas *Pv*AMA1-DI-II, *Pv*RON2-RI y *Pv*RON4, se sintetizaron los péptidos conservados que cubrían las secuencias de cada proteína recombinante. Cada péptido fue utilizado en un ensayo de competición, en el cual se incubó cada uno con la proteína recombinante correspondiente. Los péptidos que inhibieron la unión de la proteína recombinante, fueron incluidos en un ensayo de interacción receptor-ligando, para evaluar si correspondían a cHABPs.

A partir de estos ensayos, se encontró que los péptidos 21270 (derivado de *Pv*AMA-DI-II), 40305 (derivado de *Pv*RON4) y 40595 (derivado de *Pv*RON2-RI), correspondían a regiones mínimas conservadas de unión (cHABPs), que eran capaces de inhibir la unión de la proteína recombinante y que, a su vez, se unían con alta afinidad y especificidad a los eritrocitos, de acuerdo a las condiciones previamente reportadas [95]

Aunque, en términos generales, se espera que la mayoría de los eventos de invasión e interacción entre *P. falciparum* y *P. vivax* sean similares debido a la cantidad de genes ortólogos entre estas dos especies, con los resultados encontrados en este estudio [107] y los derivados de trabajos previos [101], se puede sugerir que cada parásito utiliza diferentes regiones de las mismas proteínas para interactuar con la célula hospedera. Es así como en *P. falciparum* la proteína AMA1 utiliza el dominio III para interactuar con la membrana de los eritrocitos [37], mientras que en *P. vivax* se utiliza de preferencia el dominio I [107]. Por otro lado, mientras *P. falciparum* utiliza la región carboxi-terminal de la proteína *Pf*RON2 para unirse [38], *P. vivax* con su ortólogo utiliza la región central. Este hallazgo define, en parte, la existencia de especificidad de cada uno de los parásitos por sus respectivas células hospederas, y pone de manifiesto que las regiones que se incluyan en el diseño de una vacuna contra *P. falciparum*, deben ser diferentes a las incluidas para *P. vivax*.

Los resultados de esta investigación fueron reportados en dos artículos científicos titulados: "*Plasmodium vivax* ligand-receptor interaction: *Pv*AMA-1 domain I contains the minimal regions for specific interaction with CD71+ reticulocytes" publicado en la revista Scientific Reports y el artículo "Receptor-ligand and parasite protein-protein interactions in *Plasmodium vivax*: analysing rhoptry neck proteins 2 and 4" publicado en la revista Cellular Microbiology, los cuales se muestran a continuación.

# SCIENTIFIC REP**O**RTS

**OPEN**

# *Plasmodium vivax* ligand-receptor interaction: *Pv*AMA-1 domain I contains the minimal regions for specific interaction with CD71+ reticulocytes

Gabriela Arévalo-Pinzón[1,2], Maritza Bermúdez[1,3], Diana Hernández[1], Hernando Curtidor[1,4] & Manuel Alfonso Patarroyo [1,4]

The malarial parasite's invasion is complex, active and coordinated, involving many low and high affinity interactions with receptors on target cell membrane. Proteomics analysis has described around 40 proteins in *P. vivax* which could be involved in reticulocyte invasion; few have been studied with the aim of elucidating how many of them establish specific interactions with their respective host cells. Given the importance of knowing which of the parasite's protein regions are functionally important for invasion, minimum regions mediating specific interaction between *Plasmodium vivax* apical membrane antigen 1 (*Pv*AMA-1) and its host cell were here elucidated. The region covering *Pv*AMA-1 domains I and II (*Pv*AMA-DI-II) specifically bound to the CD71+ red blood cell subpopulation. A 20 residue-long region (⁸¹EVENAKYRIPAGRCPVFGKG¹⁰⁰) located in domain I was capable of inhibiting *Pv*AMA-DI-II recombinant protein binding to young reticulocytes (CD71+CD45−) and rosette formation. This conserved peptide specifically interacted with high affinity with reticulocytes (CD71+) through a neuraminidase- and chymotrypsin-treatment sensitive receptor. Such results showed that, despite AMA-1 having universal functions during late *Plasmodium* invasion stages, *Pv*AMA-1 had reticulocyte-preferring binding regions, suggesting that *P. vivax* target cell selection is not just restricted to initial interactions but maintained throughout the erythrocyte invasion cycle, having important implications for designing a specific anti-*P. vivax* vaccine.

*Plasmodium vivax* is one of five species causing human malaria; it is responsible for more than half the cases reported outside Africa, accounting for ~100 million cases and around 2.5 billion people at risk of infection[1, 2]. In spite of this, worldwide malaria control strategies and advances regarding vaccine design have mainly been focused on *P. falciparum*[3]. However, clinical, epidemiological and biological differences between these two species regarding infection severity, blood phase dynamics, geographical distribution, type of target cell and disease transmission dynamics[2–4] suggest that *P. falciparum*-related control mechanisms might not be effective against *P. vivax* and provide an initiative for in-depth research concerning *P. vivax* biology directed towards developing drugs and vaccines against this species.

One of the main thrusts of research is concerned with elucidating the repertoire of receptor-ligand complexes used by *P. vivax* to enter host cells. Four steps define multistep erythrocyte invasion; there is initial contact with the host cell followed by merozoite (Mrz) reorientation of the apical pole to ensure direct contact with the membrane, leading to high affinity interactions being established for forming a strong bond/tight junction (TJ) acting as anchor so that myosin actin motor can enable parasite sliding within a nascent parasitophorous vacuole

¹Fundación Instituto de Inmunología de Colombia (FIDIC), Carrera 50 # 26-20, Bogotá, Colombia. ²PhD Program in Biomedical and Biological Sciences, Universidad del Rosario, Carrera 24 #, 63C-69, Bogotá, Colombia. ³MSc Program in Biological Sciences, Pontificia Universidad Javeriana, Carrera 7 # 40-62, Bogotá, Colombia. ⁴School of Medicine and Health Sciences, Universidad del Rosario, Carrera 24 #, 63C-69, Bogotá, Colombia. Gabriela Arévalo-Pinzón and Maritza Bermúdez contributed equally to this work. Correspondence and requests for materials should be addressed to M.A.P. (email: mapatarr.fidic@gmail.com)

in which it resides and multiplies[5]. Merozoite surface protein-1 (MSP-1) interaction with heparin[6] has been described for *P. falciparum*, followed by its interaction with band 3[7] and glycophorin A on erythrocyte surface[8] which is continued by interaction between erythrocyte binding antigens (EBA-175, EBA-140, EBA-181 and EBL-1) and/or reticulocyte-binding-like homologues (*Pf*Rh2a, *Pf*Rh2b and *Pf*Rh4) with receptors such as glycophorin A[9], glycophorin C[10], protein 4.1[11], glycophorin B[12] and complement receptor-1 (CR1)[13]. EBA and Rh proteins define one of the main *P. falciparum* evasion mechanisms depending on receptor availability and/or changes in the expression of such antigens, forcing the parasite to alternate between invasion pathways[14, 15]. Afterwards, Rh5 interaction with Basigin triggers rhoptry content release associated with calcium flux on parasite/host interface[5], followed by an interaction between apical membrane antigen-1 (AMA-1) and rhoptry neck protein-2 (RON2) leading to TJ formation, facilitating parasite penetration[16].

Such host-parasite interactions are poorly understood in *P. vivax*. The main interactions evaluated regarding this species are orientated towards proteins involved in Duffy-positive reticulocytes' initial contact and selection as target cells. Research published in 1994 showed that Duffy binding protein (DBP) region II was involved in interaction with the Duffy antigen receptor for chemokines (DARC)[17] while Galinski *et al.*, described two members from the reticulocyte binding protein (RBP) family (RBP-1 and RBP-2) having reticulocyte specificity and binding to yet-to-be-defined receptors[18]. Moreover, *Pv*MSP-1 also contains specific regions involved in interaction with reticulocytes[19]. *P. vivax* genome sequencing has revealed new RBP family members believed to provide recognition and specificity in reticulocyte binding[4] and which could be involved in an alternative pathway in an attempt to justify the presence of *P. vivax* in Duffy-negative patients[20]. However, flow cytometry-based erythrocyte-binding assays have shown that *Pv*RBP2a recognizes a receptor on both reticulocytes and mature erythrocytes[21] while RBP1a (known earlier as RBP1) and RBP1b recombinant proteins only bind to reticulocytes[22]; on the contrary, another study showed that RBP1a and RBP1b displayed preferential normocyte binding[21]. A novel protein named erythrocyte binding protein-2 (EBP-2), representing a new member of the DBP family, preferentially binds to young (CD71^{high}) Duffy-positive reticulocytes and has minimal Duffy-negative reticulocyte binding capability, suggesting that EBP-2 mediates a Duffy-independent infection pathway[23]. Recent research has highlighted a molecule expressed in rhoptries named *Pv*RON5 which, despite binding to all RBC, displayed a marked preference for human reticulocytes[24].

AMA-1, one of the leading blood stage vaccine candidates involved in later contact events during *P. falciparum* Mrz and sporozoite (Spz) invasion, was selected to increase knowledge about specific interactions between *P. vivax* and reticulocytes[25, 26]. AMA-1 is a micronemal type I transmembrane protein which is translocated to parasite surface via the rhoptry neck just prior to or during host cell invasion and is conserved among apicomplexan parasites[27, 28]. This protein forms the ectodomain within which 16 conserved cysteines contribute to eight disulphide bonds folding the protein into three major domains (DI; DII and DIII)[29]. *Plasmodium spp*. and *T. gondii* AMA-1 crystal structures have shown that core domains I and II are based on the Plasminogen Apple Nematode (PAN) folding motif, defining a superfamily of protein folding implicated in receptor binding[30] and hydrophobic pocket formation[31, 32].

The 83 kDa precursor protein (*Pf*AMA-1_{83}) becomes converted to *Pf*AMA-1_{66}[33] during Mrz release and erythrocyte invasion; this protein undergoes two C-terminal cleavages during invasion, giving rise to 48-kDa and 44-kDa soluble forms[34]. No viable parasites were obtained when the gene encoding *Pf*AMA-1 was disrupted in *P. falciparum* asexual blood stages and/or other *Plasmodium* species, indicating that the encoded protein has an essential function during this part of the parasite cycle[27, 35]. Several studies have implicated *Plasmodium* AMA-1 in erythrocyte binding[36–38] as well as *P. knowlesi* Mrz reorientation on RBC surface[39] and more recently in mediating TJ formation together with rhoptry-derived proteins (RON proteins)[16, 40]. *Pf*AMA-1 conditional expression during the intra-erythrocyte cycle has directly or indirectly involved this protein in resealing erythrocytes at the end of invasion[41]. *T. gondii Tg*AMA-1-depleted tachyzoites have significant defects regarding rhoptry secretion, compromising their ability to invade host cells[42].

Even though it is still not completely clear how this protein mediates and integrates all these tasks during invasion, monoclonal antibodies or synthetic peptides binding close to or in the *Pf*AMA-1 hydrophobic pocket inhibit erythrocyte invasion, some of them blocking interaction between *Pf*AMA-1 and *Pf*RON2[43–46]. Immunization with AMA-1 induced invasion-inhibiting antibodies, conferring protection in animals[47–49]; however, this protection has shown to be strain specific. In fact, immunizing mice with *P. chabaudi* DS strain-derived AMA-1 has conferred complete protection against homologous challenge but poor protection has been observed regarding challenge with *P. chabaudi* 556KA strain[50]. Likewise, naturally-acquired antibodies against *Pf*AMA-1 has strongly inhibited 3D7 strain Mrz invasion but has had a poor effect on other *P. falciparum* strains[51]. Naturally-acquired immunity to *Pv*AMA-1 is associated with the appearance of cytophilic antibodies (IgG1 and IgG3) related to protection[52]. Different AMA-1 formulations found during vaccine clinical development have been based on one or two *P. falciparum* strains inducing strain-specific protective responses[53, 54] or, in some cases, the vaccine has not been efficient even against homologous parasites[55]. Although AMA-1 is the major target in naturally-acquired invasion inhibitory antibodies, this protein has a high degree of allelic diversity[56, 57]; several studies analyzing AMA-1 sequences from different geographical regions have shown that the *ama-1* gene is under balancing selection, thereby posing a challenge when designing a vaccine based on this antigen[58–61]. Even though different authors have suggested including multiple alleles in a vaccine to induce antibodies having wide-scale reactivity and thus covering the parasite population's global genetic diversity[62, 63], it is also important to ascertain which AMA-1 regions are involved in this protein's vital functions to guide any immune response towards these regions thereby leading to developing control methods covering *Plasmodium*'s broad allele spectrum.

Within the framework of developing a specific vaccine against *P. vivax* there is enormous interest in identifying and characterizing the functional binding regions which this parasite uses to invade its target cells. Taking into account the important experimental antecedents mentioned above, a series of experiments was thus carried out; this led to identifying a conserved region of *Pv*AMA-1 located in domain I (DI) specifically interacting
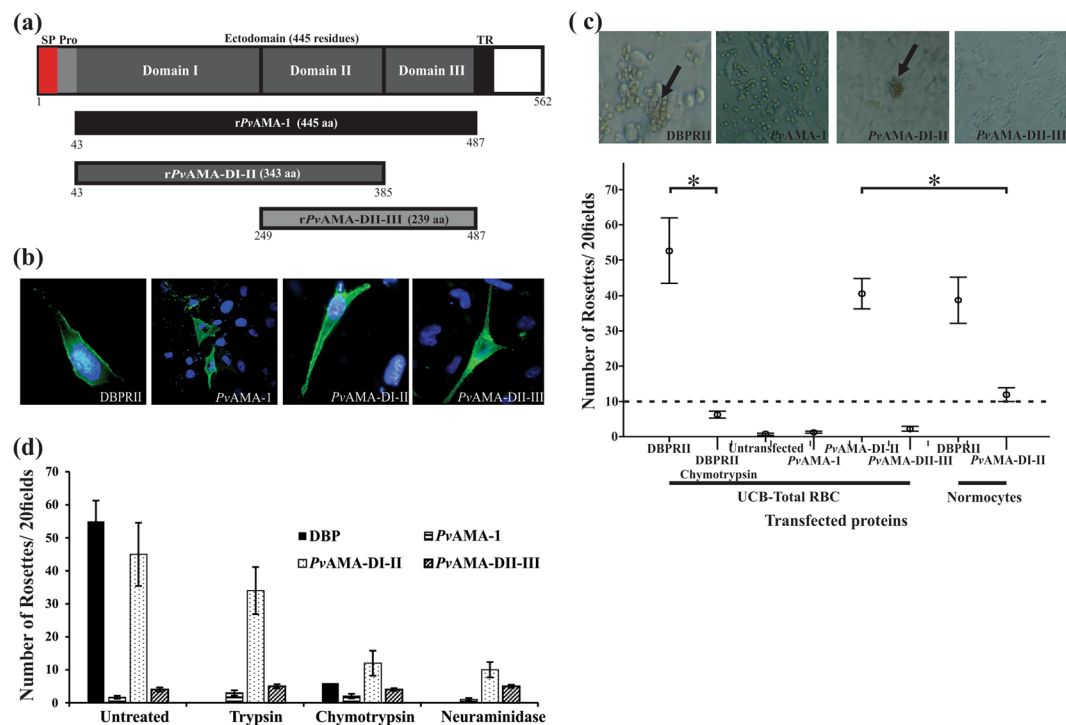
2

**Figure 1.** COS7 cells expressing *Pv*AMA-DI-DII bound to UCB RBC. (**a**) Schematic representation of *Pv*AMA-1 primary structure. Signal peptide (SP) is indicated in red, pro-sequence (Pro) in light grey, ectodomain (consisting of domain I (DI), domain II (DII) and domain III (DIII)) in dark grey, transmembrane region (TR) in black and cytoplasmic tail in white. The three fragments were expressed both on COS-7 cell membrane and as soluble recombinant proteins in *E. coli*. Black shows the complete *Pv*AMA-1 ectodomain (r*Pv*AMA-1), dark grey represents domains I-II (r*Pv*AMA-DI-II) and light grey domains II–III (r*Pv*AMA-DII-III). The first and last residues in each region are indicated. (**b**) Immunofluorescence assay. Each of the three *Pv*AMA-1 fragments was cloned in the pRE4 vector and expressed on COS-7 cell membrane. The presence of HSV gD protein signal peptide and transmembrane domain in pRE4 vector enabled the expression of each fragment on cells surface, as shown by green fluorescence. Cell nuclei were stained with DAPI. (**c**) Rosette formation assays. The binding assay was performed with UCB RBC or reticulocyte-depleted normocytes. Only *Pv*AMA-DI-DII and DBPRII transfected cells could form rosettes (black arrows). The amount of rosettes for each protein expressed on COS-7 cells is shown. DBPRII was used as positive control while non-transfected cells and DBPRII binding to chymotrypsin-treated UCB were used as negative controls. (**d**) Trypsin-, chymotrypsin- and neuraminidase-treated UCB RBC binding assays. It can be seen that the amount of rosettes became reduced with *Pv*DI-DII protein when RBC were treated with chymotrypsin and neuraminidase. Only intact erythrocyte and chymotrypsin-treated DBPRII binding was evaluated. At least three independent experiments (with replicates) were performed for all experiments. The error bars indicate the standard deviation.

with reticulocytes which could be used as template for inclusion in a synthetic multistage, multi-antigen vaccine against *P. vivax*.

## Results

**PvAMA-DI-II bound to total RBC.** The full *Pv*AMA-1 ectodomain, *Pv*AMA-DI-II and *Pv*AMA-DII-III (Fig. 1a) were expressed on the COS-7 cell surface (Fig. 1b) to evaluate whether *Pv*AMA-1 bound to human RBC. The herpes simplex virus (HSV) gD gene's signal peptide and transmembrane domain, included in pRE4 mammalian expression vector[64], allowed different *Pv*AMA-1 constructs to become translocated to the surface of transfected COS-7 cells. Immunofluorescence assays using non-permeabilized transfected COS-7 using DL6[17] or F8.12.19[65] antibodies confirmed these proteins' correct orientation on COS-7 cell surface (Fig. 1b); no staining with these antibodies was observed in non-transfected cells. Transfection efficiency was seen to be 4%-5% for all constructs, including transfection of the pHVDR22 plasmid which expresses DBPRII used as a positive control[17] (Fig. 1b), agreeing with transfection efficiency obtained in other studies with *Plasmodium* antigens[66, 67]. The transfected cells incubated with umbilical cord blood (UCB) (about 5–7% of reticulocytes) showed that only *Pv*AMA-1 domains I and II (*Pv*AMA-DI-II) bound to RBC, although the amount of rosettes was lower than for the DBPRII construct (p > 0.05) (Fig. 1c). Negative controls with either non-transfected COS-7 with human RBC or COS-7 expressing DBPRII with chymotrypsin-treated RBC (which removes the Duffy antigen receptor)[68] gave no rosettes or significantly decreased (p < 0.05) the amount of rosettes compared to untreated RBC (Fig. 1c). No significant amount of rosettes was found for the full *Pv*AMA-1 ectodomain or *Pv*AMA-DII-III, suggesting that

the domain I and II region is responsible for *Pv*AMA-1 binding. *Pv*AMA-DI-II binding was affected regarding neuraminidase- or chymotrypsin-treated RBC, being reduced by 71% or 73%, respectively, while limited impact on binding was observed concerning trypsin-treated RBC (Fig. 1d). Enzyme treatment of RBC led to no significant change in the amount of rosettes for either of the other two *Pv*AMA-1 fragments, different from what has been reported for *Pf*AMA-1 domain III which only binds to its receptor (known as Kx) on trypsin-treated erythrocytes[38].

Taking into account that *P. vivax* preferentially infects reticulocytes, an evaluation was made of whether *Pv*AMA-DI-II binding concerns interaction with all RBC populations or only a minor subpopulation (reticulocytes). As purified intact reticulocytes (>99%) could not be obtained, peripheral blood (containing only 1% reticulocytes) depleted in white blood cells and reticulocytes was used to obtain only normocytes and determine binding properties regarding the latter cells. The amount of rosettes decreased with normocytes regarding UCB (p = 0.01) for COS-7 expressing *Pv*AMA-DI-II (Fig. 1d), suggesting that these domains bound to a specific non-normocyte RBC sub-population while only a slight reduction in the el amount of rosettes was observed for DBP region II thereby agreeing with that published previously for this region[23].

### CD71+ cells were the main *Pv*AMA-DI-II binding targets.

Previous studies have shown that immature reticulocytes (CD71+, I-II-III stages) are the major *P. vivax* target cells, whereas older CD71− (IV stage) reticulocytes were rarely invaded[69]. A cytometry-based erythrocyte-binding assay was thus used to evaluate whether *Pv*AMA-DI-II binding was dependent on a specific RBC subpopulation (i.e. reticulocytes (CD71+)). Three soluble recombinant proteins (r*Pv*AMA-1, r*Pv*AMA-DI-II and r*Pv*AMA-DII-III) (Fig. 1a) were obtained in *E. coli* and purified by affinity chromatography (Fig. 2a). These proteins displayed a molecular mass of ~54 kDa (r*Pv*AMA-1), ~40 kDa (r*Pv*AMA-DI-II) and ~27 kDa (r*Pv*AMA-DII-III) in SDS-PAGE, and were recognized by WB with a monoclonal anti-histidine antibody (Fig. 2a). r*Pv*AMA-1 and r*Pv*AMA-DII-III were recognized by mAb F8.12.19 in dot blot and ELISA assays, confirming correct recombinant protein folding (Fig. 2a). This mAb recognized a conformational epitope on full-*Pv*AMA-1, specifically in domain III[65].

Each recombinant protein was incubated with UCB and reticulocytes were stained with transferrin receptor (CD71) antibodies; this receptor is known to be expressed during the earliest erythroid precursor stages and becomes progressively depleted during reticulocyte maturation into normocytes[70]. It has also been found in activated lymphocytes[71]; an antibody against the CD45 marker (found in all leukocytes) having greater expression in lymphocytes was thus included to rule out this population from the binding study (Supplementary Fig. S1). The study population thus consisted of CD71+CD45− cells (mean 2.07%: 3.58% maximum and 1.54% minimum) (Fig. 2b) corresponding to the population of preference in *P. vivax* invasion. Each recombinant protein's binding to CD71+CD45− cells was detected with a phycoerythrin-conjugated anti-histidine monoclonal antibody. The histograms show that soluble recombinant DBPRII bound to CD71+CD45−cells *(*16.1% ± 2.5) as did r*Pv*AMA-DI-II (9.3% ± 1.2) whereas only 2.5% ± 0.6 binding was found for r*Pv*AMA-1 and 2.9 ± 0.5 for r*Pv*AMA-DII-III (p < 0.05) (Fig. 2b and c). Only 0.8% binding of DBPRIII-IV was found; earlier studies have shown that this fragment did not bind to either normocytes or reticulocytes, so it was considered as a negative control[17, 72]. r*Pv*AMA-DI-II binding activity was shown to increase in a concentration-dependent manner and was saturated at 50 μg/mL, similar to DBPRII (Fig. 2d). Only 0.03% to 0.3% binding was found when each *Pv*AMA-1 recombinants' binding to the CD71−CD45− population (normocytes and stage IV reticulocytes) was evaluated (Supplementary Fig. S2). 3.4% ± 0.5 binding was found for *Pv*DBP RII thereby agreeing with previous work showing that DBPRII-DARC interaction is more abundant with reticulocytes than total RBC[23].

### Conserved peptide 21270 had binding properties which were CD71+ reticulocyte-specific for the *Pv*AMA-DI-II regIón.

Seventeen peptides covering the whole *Pv*AMA-1 domains I and II (residues 41 to 380) were chemically synthesized and included in a CD71+ cell binding inhibition experiment where each peptide competed with r*Pv*AMA-DI-II to delineate the specific region within *Pv*AMA-DI-II involved in CD71+ reticulocyte interaction. Figure 3a shows that adding peptide 21270 (located in DI) produced a 52% reduction regarding r*Pv*AMA-DI-II binding to CD71+CD45−cells and 14% concerning 21289 (located in DII).

We have previously reported a sensitive and specific binding test for detecting receptor-ligand interactions between peptides and receptors on RBC surface[73]. Each synthetic peptide derived from malarial Spz and Mrz antigens was radiolabeled and incubated with human hepatocytes or RBC in the presence or absence of the same unlabeled peptide. The specific binding plot was obtained from the difference between total binding (binding in the absence of non-radiolabeled peptide) and unspecific binding (binding in the presence of non-radiolabeled peptide) plots[74]. Peptides having ≥0.02 slope specific binding plot were considered high activity binding peptides (HABPs) and used as templates for designing an anti-malarial vaccine[75]. Some HABPs were conserved (no amino acid sequence variation) and others had genetic variability and elicited a strain-specific immune response allowing malarial parasites to escape vaccine-induced immunity, meaning that they were discarded from further immunological studies[74].

Taking into account that AMA-1 is significantly polymorphic in all *Plasmodium* species[60, 76], the specific binding activity of *Pv*AMA-1 peptides which did not have amino acid changes was measured (Supplementary Fig. S2) to describe this protein's conserved functional regions involved in interaction with specific target cells. Five conserved peptides were selected, three of them in DI and two in DII, peptides 21268 and 21270 being found to be HABPs having ≥2% specific binding activity (Fig. 3b). Only 0.7% to 1.2% specific binding (not surpassing the ≥2% threshold) was found when these peptides were assayed for normocyte binding showing that the specific binding activity measured for these two peptides was directed towards their interaction with reticulocytes, as already shown by cytometry (Fig. 2).

Due to HABP 21270 being able to inhibit recombinant protein interaction by more than 50% (1:20 molar ratio) (Fig. 3a), it was evaluated whether it could inhibit rosette formation. Adding UCB RBCs pre-incubated
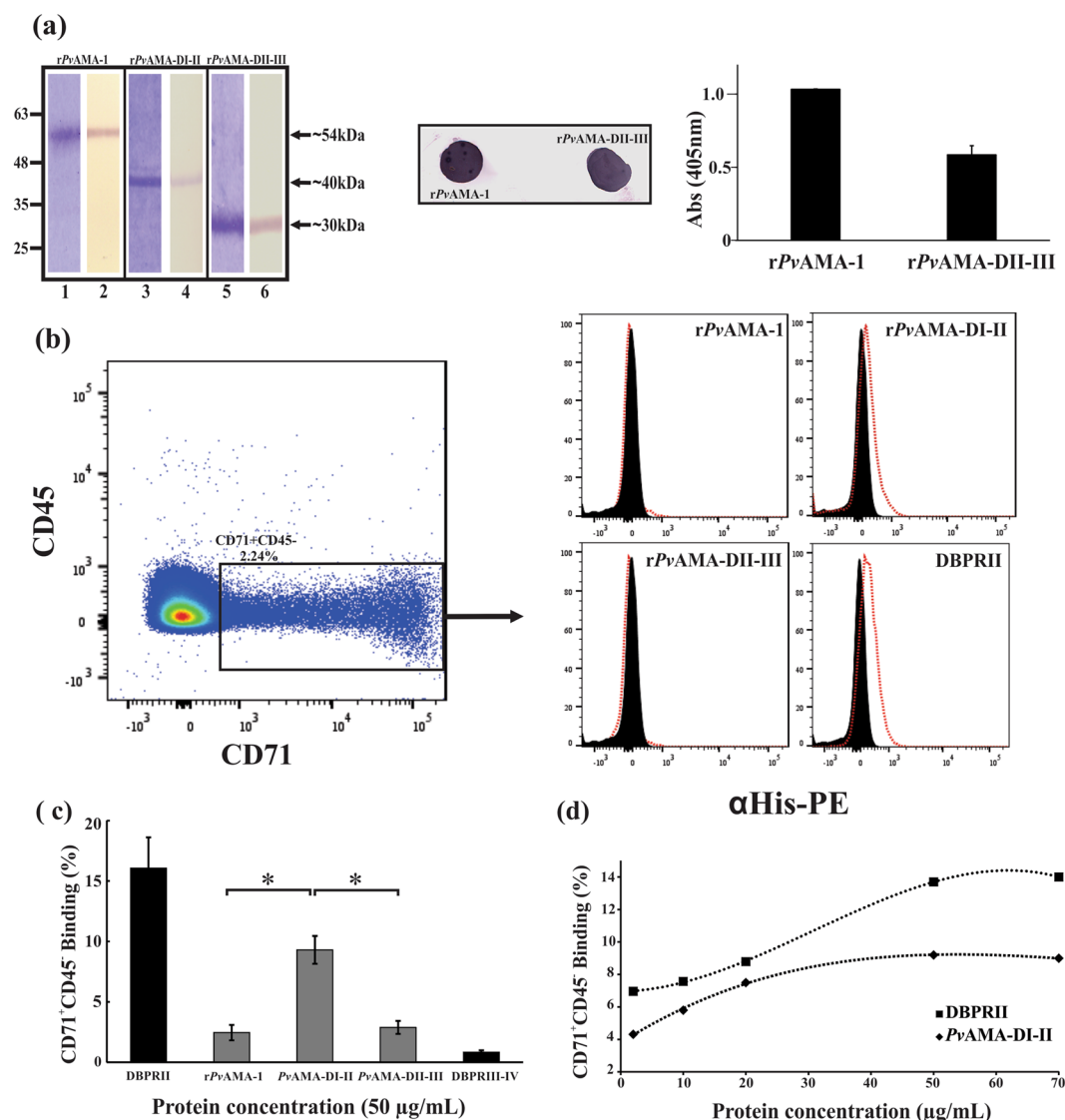
**Figure 2.** Soluble recombinant protein *Pv*AMA-DI-II only interacted with CD71$^+$ reticulocytes. (**a**) Three soluble *Pv*AMA-1 recombinant fragments were obtained and purified by affinity chromatography. Lanes 1, 3 and 5 show recombinant proteins resolved by SDS-PAGE followed by Coomassie blue staining. A single expected molecular weight band was observed for each protein fragment. Lanes 2, 4 and 6 show Western blot recognition of each recombinant protein by anti-histidine tag monoclonal antibody. (**b**) Dot plot showing the CD71$^+$CD45$^-$ study population (black box). This population was used for determining each recombinant protein's binding. Histograms showing each recombinant protein's binding to CD71$^+$CD45$^-$ cells (reticulocytes). Each protein's cell binding was detected with PE conjugated anti-His Tag antibodies. Displacement (red lines) regarding control was observed in r*Pv*AMA-DI-II and DBPRII histograms. (**c**) CD71$^+$CD45$^-$ cell binding percentages for each protein evaluated on the X axis. At least three independent experiments (with replicates) were performed for all experiments. The error bars indicate the standard deviation. Soluble recombinant protein DBPRII was used as positive binding control and DBPRIII-IV as negative binding control. (**d**) Saturation assay showing r*Pv*AMA-DI-II and DBPRII total binding at different protein concentrations.

with peptide 21270 to COS-7 cells expressing *Pv*AMA-DI-II inhibited the amount of rosettes by 87% compared to control (Fig. 3c). Measuring HABP 21270 binding to UCB RBC at different radiolabeled peptide concentrations in the presence or absence of unlabeled peptide yielded a $1.9 \pm 0.34\,\mu M$ $K_d$, Hill coefficient $= 3.0 \pm 0.47$ indicating positive cooperativity (Fig. 3d).

HABP 21270-CD71$^+$ reticulocyte interaction was sensitive to treatment with neuraminidase and chymotrypsin (Fig. 3e), similar to the pattern observed for the whole of domains I-II, suggesting that this peptide located in domain I had *Pv*AMA-1-specific binding properties.
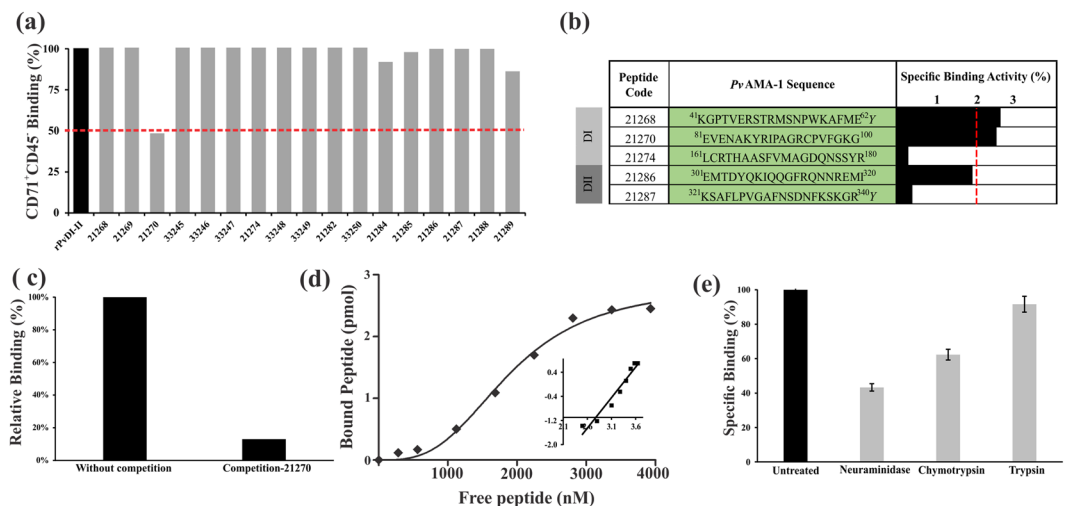
**Figure 3.** *Pv*AMA-1 domain I contained peptides specifically interacting with reticulocytes. (**a**) Flow cytometry inhibition experiments. 20 residue-long synthetic peptides covering the complete *Pv*AMA-1 domain I and II sequence were used. Peptide numbers were assigned according to FIDIC's serial numbering system. Each peptide was pre-incubated with UCB RBC and then incubated with r*Pv*AMA-DI-II. Recombinant protein binding percentages were detected with PE conjugated anti-Histidine tag antibodies. (**b**) Binding profile of conserved peptides within *Pv*AMA-1 domains I-II to UCB RBC. Black bars represent percentage binding activity defined as the amount of peptide (picomoles) binding specifically per added peptide (picomoles). Peptides having ≥2 binding percentage (red line) were considered HABPs, according to previously described criteria[74]. Each assay was carried out in triplicate. A tyrosine residue was added at the C-terminus of peptides 21268 and 21287 to enable radiolabeling. (**c**) Inhibition experiments involving rosetting assay. Peptide 21270 was pre-incubated with UCB RBC; RBC were then incubated with COS-7 cells expressing the *Pv*AMA-DI-II region. The values show *Pv*AMA-DI-II average relative UCB RBC binding percentage in the absence (100%) or presence of peptide 21270. (**d**) HABP 21270 saturation curves. The curve represents specific binding. The x-axis in the Hill plot (inset) shows log F = free peptide and the y-axis log (B/Bmax−B), where B is the amount of bound peptide and Bmax the maximum amount of bound peptide. (**e**) The effect of enzyme treatment on HABP 21270 binding to RBC. Each bar represents peptide 21270 specific binding activity percentages upon incubation with neuraminidase-, chymotrypsin- and trypsin-treated RBC. Untreated RBC were used as control (black). Standard deviations were below 5%.

**PvAMA-1 HABPs were located near the hydrophobic binding Groove.** The *Pv*AMA-1 structure was solved by Pizarro *et al.*[31], who described three domains comprising the antigen's ectodomain. When HABPs 21268 and 21270 were located on *Pv*AMA-1 structure it was found that both peptides were located on the same face (Fig. 4), opposite to the face where most polymorphic sites which contribute towards *Pv*AMA-1's overall diversity[61] were found.

## Discussion

Determining *P. vivax* antigens' functional regions could be one of the best strategies for blocking this parasite's biological functions during host cell entry. Comparative studies involving *P. falciparum* have led to a significant amount of new antigens being identified in *P. vivax*[77]; in spite of this, few studies have emphasized the identification of *P. vivax* proteins' functional regions during invasion, mainly due to this species preferentially invading reticulocytes (low concentration in peripheral blood) together with the inherent characteristics in each *P. vivax* strain impeding the development of a continuous culture *in vitro*[78]. Even though short-term cultures have been developed, it has been observed that parasite density becomes reduced as intra-erythrocytic cycles advance, even when adding fresh reticulocytes[79]. The foregoing, plus variability concerning parasitemia percentages depending on the isolate[79, 80], could lead to a poor interpretation of the role played by a particular antigen during *P. vivax* Mrz invasion.

Evaluating some *P. vivax* proteins' binding to human reticulocytes represents an approach to begin describing the possible antigens involved in host cell invasion. Some regions having specific binding to and high affinity for receptors on reticulocyte membrane suggested the participation of the proteins evaluated here in some steps related to host cell invasion. Using recombinant proteins and reticulocytes in host-pathogen interaction has provided one of the best alternatives to date[21, 22, 81].

Bearing in mind that obtaining pure reticulocytes in high amounts for binding assays is extremely difficult due to their low concentration in blood and little stability, UCB RBC or reticulocyte-depleted normocytes were here used for characterizing specific *Pv*AMA-1 reticulocyte binding properties using three different receptor-ligand interaction techniques. Rosette formation led to recombinant expression in a mammalian system containing all the machinery for the correct *P. vivax* protein folding. Flow cytometry was used for determining which specific RBC population each recombinant protein assayed here bound to and which short regions might be mediating
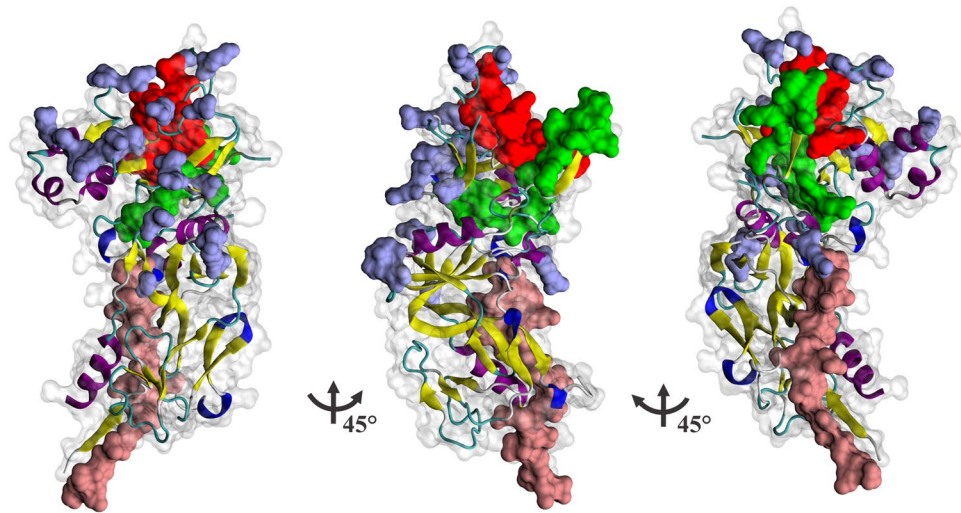
**Figure 4.** HABP 21270 formed part of the *Pv*AMA-1 hydrophobic trough. Surface view of the *Pv*AMA-1 ectodomain, showing HABP 21268 (pink) and HABP 21270 (green) localization. Red shows part of the hydrophobic trough formed between both PAN domains and grey shows the cluster of polymorphic residues in *Pv*AMA-1 contained in domain I and II[61]. The molecule's secondary structure is shown, yellow highlighting the β-sheets, violet the *a*-helices, blue the turns and white shows random structure. This representation was built in the VMD (Visual Molecular Dynamics) software, taking PDB 1W81 as source[31].

such binding. Finally, a robust methodology was used for confirming peptide-cell interaction specificity and determining physicochemical parameters.

Binding assays using the aforementioned methodologies (including soluble recombinant proteins and proteins expressed on COS-7 cell membrane) showed that *Pv*AMA-DI-II recognized a receptor just on CD71+ reticulocytes (i.e. a *P. vivax* target cell) (Fig. 1 and 2). Receptor-ligand interaction was affected by treating UCB RBC with chymotrypsin and neuraminidase. The same enzymatic profile observed for *Pv*AMA-DI-II has been described for glycophorin B which is a receptor for erythrocyte binding ligand-1 (EBL-1)[12] and the receptor for Rh1 binding; however, future experiments should explore the identity of the *Pv*AMA-DI-II receptor. "Why do only AMA-1 domains I and II bind to CD71+ reticulocytes if the full *Pv*AMA-1 ectodomain contains domains I-II-III?" represents an interesting question which emerged from the binding assays. Miss-folding could explain this pattern; however, these fragments were expressed in COS-7 ensuring correct protein folding (Fig. 1). mAb F8.12.19 which recognized a conformational epitope in DIII[65] recognized both complete r*Pv*AMA-1 and r*Pv*AMA-DII-III (Fig. 2a). Some studies have shown that different AMA-1 recombinant domain combinations (i.e. DI-DII or DIII only) maintain the same structure as the complete AMA-1 protein[32].

A previous study found that *Pf*AMA-1 domain III was the only fragment which could specifically interact with a receptor on RBC membrane, only becoming exposed when RBC were treated with trypsin, while the complete ectodomain did not interact. The authors suggested that this might have been due to *Pf*AMA-1 cleavage and that DIII acts as a receptor for invasion[38]. Even though the presence of fragments has not been determined for *Pv*AMA-1, it cannot be ruled out that the protein undergoes proteolytic processing similar to that for *Pf*AMA-1 and that the resulting fragments play a role in binding. A similar pattern has been described for *Pf*MSP-1 and its cleavage products[8, 82].

It has been suggested that AMA-1 participates in the invasion stage which is conserved for most apicomplexa, as well as having similar tertiary structure in *Plasmodium spp.*[60]; however, different binding properties have been reported for its homologues. It has been reported through rosetting assays that different *Pf*AMA-1 domains did not bind to intact human RBC[38]; however, DIII have bound to human erythrocytes pre-treated with trypsin[38] while *Py*AMA-1 DI-DII has only interacted with intact mouse and rat erythrocytes but not with trypsin- or chymotrypsin-treated erythrocytes[37]. Complementing other authors' reports[32], the results presented here suggested that AMA-1 recognizes specific receptors on different *Plasmodium* host cells in close relationship with target cell preference.

Comparative analysis of the proteome of human RBC and reticulocytes has shown that membrane or cytosol protein detected thereby was not unique to just erythrocytes or reticulocytes[83]. The difference between these two cells thus lying in the abundance of each protein, having around 500 membrane proteins, being lower in erythrocytes than in reticulocytes[83]. It seems that such differences could be critical for *P. vivax* to have tropism regarding reticulocytes compared to normocytes; however, it is still not clear whether *P. vivax* selectivity for its target cells could be just mediated during initial invasion stages where low affinity interactions occur, or whether this happens during late stages where high affinity interactions are established or simply that selectivity is maintained throughout reticulocyte invasion.

When defining domain I and II regions responsible for binding to CD71+ reticulocytes it was found that peptide 21270 located between residues[81]E to[100]G in domain I significantly inhibited the soluble recombinant protein (r*Pv*AMA-DI-II) binding and rosette formation, strongly suggesting that this peptide has *Pv*AMA-1 binding

properties. Furthermore, to reinforce this inhibition experiment, it was found that peptide 21270 is a HABP which binds specifically and with high affinity to reticulocytes, having an enzyme binding profile similar to that reported for the soluble recombinant protein (rPvAMA-DI-II). Interestingly, this peptide's amino acid sequence is conserved among strains having various geographical origins. Several studies have shown that AMA-1's polymorphic nature prevents it being considered a vaccine candidate[61]; in fact, the results of different PfAMA-1 formulations assayed at clinical level have shown that a protective response has been strain specific. Thus, finding conserved regions of PvAMA-1 having a binding function could be used for resolving one of the parasite's main evasion mechanisms: antigenic polymorphism[84]. No binding peptides were found in PvAMA-1 domain II; it has been found in other species, such as P. falciparum, that AMA-1 domain II does not participate in binding to RBC[38] but does play a role during PfRON2 interaction-related invasion[16, 85]. Structural studies have suggested that DII protects a significant portion of the binding site in AMA-1 against a host's immune response and can be readily displaced to extend the hydrophobic groove for effective binding to PfRON2[16]. Such structural changes regarding AMA-1-RON2 interaction have been used for explaining invasion inhibiting antibodies (i.e. 4G2) which have recognised the base of a loop in PfAMA-1 ectodomain DII[43]. MAb 4G2 binding has prevented DII loop displacement for effective PfRON2 binding, thereby affecting tight junction formation during parasite invasion[16]. Even though such interactions have not been studied in P. vivax, PvAMA-1 DII participation in invasion cannot be ruled out.

A methodology based on identifying conserved sequences having high specific host cell binding capability has been used with P. falciparum and other microorganisms such as Mycobacterium tuberculosis during the last 25 years for characterizing conserved HABPs (cHABP) directly involved in target cell binding[73, 86].

Regarding P. falciparum it has been described that many cHABPs form niches or clefts where they or the receptors can bind[87]. For example, PfAMA-1 cHABPs 4313 ([134]DAEVAGTQYRLPSGKCPVFG[153]) and 4325 ([374]MIKSAFLPTGAFKADRYKSH[393]) formed a channel where a yet-to-be characterized receptor bound during Mrz invasion. P. falciparum circumsporozoite (PfCSP) cHABP 4397 formed a hydrophobic cavity where hepatocyte heparan sulphate proteoglycans (HSPG) bound, while cHABP 3279, located in the P. falciparum thrombospondin-related anonymous protein (PfTRAP) von Willebrand domain, folded to create a cavity where the cholesterol molecule bound during Spz invasion[87].

Previous studies have highlighted AMA-1's role as adhesin during invasion[36]. It has been described recently that P. falciparum and T. gondii AMA-1 DI-II domains interact with a RON2-derived protein which might be mediating TJ formation[16, 88]. Structural and inhibition studies regarding this interaction have supported the argument concerning TJ/complex formation being crucial for parasite entry[16, 40]. However, AMA-1 conditional knockout studies have shown that modified parasites can form the characteristic TJ ring[89], suggesting varied roles for AMA-1 during invasion. The present work thus found that PvAMA-1 domain I and II were interacting with reticulocytes, i.e. acting as an adhesin.

Two P. vivax cHABPs were identified here (both located in PvAMA-1 domain I) having structural differences regarding their localization; cHABP 21270 formed part of the trough formed between PAN domains and (as in PfAMA-1) could be the critical pocket where the receptor binds. Out of the 8 HABPs identified previously in the whole PfAMA-1 ectodomain[36], cHABP 4313 was a homolog of cHABP 21270, having 95% similarity. Interestingly, cHABP 4313 inhibited Mrz invasion of erythrocytes by 75%[36] suggesting that this region´s critical role during this stage of the cycle. However, this region does not participate as adhesin during Spz invasion of hepatocytes; rather, the parasite uses different PfAMA-1 regions to interact[90]. P. vivax cHABP 21268 was located on the same face as HABP 21270 but opposite the trough; even though this cHABP did not inhibit rPvAMA-DI-II binding by flow cytometry in 1:20 molar ratio, it displayed a low inhibition of rosette formation (by 25%) (Supplementary Fig. S4).

Bearing cHABP 21268 location in mind and its low inhibitory capacity, it can be suggested that, even though it might specifically interact with a receptor on reticulocyte membrane, it is not the determinant region in protein binding. When PvAMA-1 polymorphisms were located on the 3D structure, it was found that most were located on the opposite face of the identified cHABPs, suggesting that one face of PvAMA-1 is more exposed to the immune system than others[60]. It has been reported that different microorganisms hide relevant regions from the immune system while exposing immunodominant (but non-functional) regions under immune pressure, to protect antigen function during invasion[91].

To date, PvMSP-1[19], PvRBP-1a[92] and PvDBP[72] HABPs have been identified which bind specifically to reticulocytes; this, together with characterizing PvAMA-1 regions, has increased current knowledge about P. vivax Mrz specific binding properties used for invading reticulocytes. Future work should address evaluating naturally-acquired antibodies capability for blocking PvAMA-1 binding to reticulocytes and correlate the results with some degree of protection. Future work should also be aimed at identifying critical binding residues which could be modified (mHABP) to increase cHABP immunogenicity and protection-inducing capability, following the methodology proposed for developing a vaccine against P. falciparum[93].

## Methods

**Constructing recombinant plasmids.** Three PvAMA-1 fragments corresponding to the ectodomain (residues 43-487), domain I and II (residues 43-386) and domain II and III (249-487) were amplified from Plasmodium vivax VCG-I strain genomic DNA for PvAMA-1 expression as a recombinant protein and expression on COS-7 cells (American Type Culture Collection CRL-1651). Gene specific primers were designed using the PvAMA-1 genomic sequence (PVX_092275) available in PlasmoDB[93] as template. Each fragment was amplified using a KAPA HiFi HotStart ReadyMix PCR kit at 25 μL final reaction volume, containing 12.5 μL 2x KAPA HiFi Ready Mix, 1.5 μL of each primer (Supplementary Table S1) at 5 μM concentration and 7.5 μL of nuclease-free water. The amplification conditions for the three products consisted of one 5-min cycle at 95 °C followed by 35 cycles lasting 20 sec at 98 °C, 45 sec at 56 °C and 2 min at 72 °C with a final extension cycle lasting 5 min at 72 °C. Purified products were digested with DraI or PvuII and ApaI restriction enzymes and cloned in pRE4 vector[64]

in frame with the HSVgD signal sequence and transmembrane segment[17] to express these fragments on COS-7 cells membrane or digested with BamHI and SalI and cloned in pQE30 vector in frame with histidine tag at the N-terminal to be expressed in *E. coli*. Each construct was transformed in JM109 cells and selected on Luria Bertani (LB) plates containing ampicillin and confirmed by sequencing. The resulting plasmids were labelled pRE4-*Pv*AMA-1, pRE4-*Pv*AMA-DI-II, pRE4-*Pv*AMA-DII-III, pQE30-*Pv*AMA-1, pQE30-*Pv*AMA-DI-II and pQE30-*Pv*AMA-DII-III.

**COS-7 cell culture and transfection.** COS-7 cells were cultured in Dulbecco-Modified Eagle Medium (DMEM) with 10% FCS in a humidified 5% $CO_2$ incubator at 37 °C. For all transfection experiments, $3 \times 10^4$ cells were seeded in 3.5-cm diameter wells (40–60% confluent) and then transfected with 300 ng of each recombinant plasmid using FuGENE HD transfection reagent (Promega), following the manufacturer's protocol, in the presence of OptiMEM medium for 48 h in a humidified 5% $CO_2$ incubator at 37 °C. The cells were grown on coverslips for use in immunofluorescence to verify the correct protein expression on COS-7 cell surface.

**Immunofluorescence assay.** Transfected cells grown on coverslips were washed in phosphate buffered saline (PBS), fixed with 2% formaldehyde (in PBS) for 15 min at room temperature (RT) and blocked with 10% FCS in PBS for 1 hr to verify correct protein expression on COS-7 cell surface. The cells were stained overnight with anti-DL6 antibodies (Santa Cruz) in 1:1,000 dilution at 4 °C which recognized a proline-rich region adjacent to the mature HSV gD protein transmembrane segment or F8.12.19 monoclonal antibody which recognized a conformational epitope in *Pv*AMA-1 domain III[65]. Fluorescein-conjugated goat anti-mouse antibodies were used as secondary antibodies. Cell nuclei were stained with 4′,6-diamidino-2-phenylindole (DAPI) and fluorescence was visualized by fluorescence microscope (Olympus BX51) using an Olympus DP2 camera and Fiji software. Transfection efficiency (%) was calculated as total amount of fluorescent COS-7 cells × 100/total amount of COS-7 cells counted in 30 fields, as described previously[67].

**COS-7 cells used for erythrocyte binding assays.** Human RBC from UCB containing about 5–7% reticulocytes were washed three times in PBS (pH 7.4) and then treated with neuraminidase, chymotrypsin or trypsin, as described earlier[94]. Briefly, an erythrocyte suspension (60% haematocrit) was incubated at 37 °C for 60 min with either neuraminidase (150 μU/mL; ICN 900-67-6), trypsin (1 mg/mL; Sigma T-1005) or chymotrypsin (1 mg/mL; Sigma C-4129). Erythrocytes were then washed twice by spinning with PBS at 2,500 × g for 5 min. The UCB blood used in this study came from Bogotá's District Blood Bank (Colombia).

COS-7 cells were tested 48 h after transfection with pRE4-*Pv*AMA-1, pRE4-*Pv*AMA-DI-II or pRE4-*Pv*AMA-DII-III plasmids regarding their binding to normal, neuraminidase-treated, chymotrypsin-treated and trypsin-treated human RBC from UCB (10%) or reticulocyte-depleted erythrocytes (10% haematocrit) from peripheral blood without any treatment for 2 hr at 37 °C. Regarding competition assays, UCB (10%) was pre-incubated with 10 μL peptide 21270 (1 mg/mL) for 1 hr at 37 °C followed by two washes with incomplete DMEM and then added to transfected COS-7 cells. After incubation, the cells were washed twice with PBS. The COS-7 cells with adherent erythrocytes or normocytes (i.e. rosettes) were scored in 20 randomly-chosen fields at 200× magnification. Rosettes were considered positive when adherent erythrocytes covered more than 50% of COS-7 cell surface. COS-7 cells transfected with plasmid pHVDR22 (which expressed DBP RII) were used as positive control[17] while non-transfected cells were used as negative control. At least three independent experiments were performed with replicates.

**Soluble recombinant expression and purification.** *E. coli* (JM109) recombinant proteins transformed with pQE30-*Pv*AMA-1, pQE30-*Pv*AMA-DI-II or pQE30-*Pv*AMA-DII-III were grown in 25 mL LB broth supplemented with 0.1 mg/mL ampicillin and 0.1% D-glucose for 12 hr at 37 °C with constant shaking. This starting culture was used to inoculate 475 mL LB broth containing 0.1 mg/mL ampicillin and 0.1% D-glucose maintained at 37 °C with constant shaking until reaching 0.6–0.8 optical density (OD) at 620 nm. Recombinant protein expression was induced with isopropyl β-D1-thioglactopyranoside (IPTG) at 1 mM final concentration. The cultures were grown for another 16 hr at 30 °C and *E. coli* cells were harvested by centrifugation. The cell pellet was suspended in lysis buffer (50 mM Tris pH 8.0, 300 mM NaCl, 25 mM imidazole) supplemented with 15 mM 2-β-mercaptoethanol, 0.1 mM ethylene glycol-bis (β-aminoethyl ether)-N,N,N',N'-tetraacetic acid (EGTA), 0.1 mg/mL lysozyme, 0.5% Tween 20 and a protease inhibitor cocktail. Bacterial cells were lysed by sonication (Torebeo Ultrasonic Processor 36800). The lysate was spun at 15,000 × g for 30 min at 4 °C and the supernatant was incubated with nickel-nitrylotriacetic acid ($Ni^{2+}$-NTA) agarose resin for purifying recombinant proteins by affinity chromatography. Bound protein was eluted with increasing imidazole gradients (50–500 mM). The eluates were analyzed on SDS-PAGE and by Western Blot and the fractions containing the recombinant protein having a clear single band were pooled. Protein concentration was determined using the BioRad protein assay system (BCA method) and a standard bovine serum albumin (BSA) curve.

**ELISA and dot blot assays.** The ELISA assay described elsewhere[40] had some modifications. Briefly, 1 μg recombinant protein (r*Pv*AMA-1 or r*Pv*AMA-DII-III) was pre-absorbed onto 96-well plates in coating buffer (15 mM sodium carbonate and 35 mM sodium bicarbonate) and then blocked with 5% BSA in PBS and 1% Tween 20 at 37 °C. The plates were incubated for 1 hr with F8.12.19 monoclonal antibody in 1:16,000 dilution at 37 °C, followed by three washes with 1% PBS-Tween. Peroxidase-conjugated anti mouse IgG was used as secondary antibody, diluted 1:5,000 for 1 hr. Antigen-antibody reaction was detected using a TMB Microwell peroxidase substrate system kit (KPL Laboratories). The reaction was stopped after 10 min incubation with 1 M phosphoric acid. Absorbance was measured at 405 nm using a microtiter reader.

The dot blot assay involved seeding 10 μL r*Pv*AMA-1 or r*Pv*AMA-DII-III on nitrocellulose membrane and then incubating for 15 min in a damp chamber at 37 °C. The membrane was blocked with 5% milk in 0.5%

PBS-Tween for 30 min; the membrane was then incubated with F8.12.19 monoclonal antibody (1:16,000) for 1 hr. Alkaline phosphatase conjugated anti-mouse antibody was used as secondary antibody. A BCIP/NBT (Promega) kit was used for revealing the reaction, according to the manufacturer's instructions.

**Flow cytometry assays.** The flow cytometry-based RBC-binding assay was performed as previously described, with the following modifications[21]. Twenty-five micrograms of each recombinant protein were incubated with 500 μL UCB suspension overnight at 4 °C with constant shaking. Competition assays involved adding each *Pv*AMA-1 DI- and DII-derived synthetic peptide (>99% purity) in a 1:20 (protein:peptide) molar ratio. The erythrocytes were washed with 1% BSA/PBS and then incubated with anti-human CD45 allophycocyanin (APC) (Becton Dickinson) and anti-human CD71-APC-H7 monoclonal antibodies (Becton Dickinson) for 20 min at RT following incubation with mouse anti-histidine phycoerythrin conjugated monoclonal antibody (Miltenyi Biotec). RBC were washed and suspended in 2 mL PBS. One million events were read on a FACSCanto II (BD Bioscience) and the results were analyzed using FlowJo software (TreeStar). DBPRII recombinant soluble protein was used as positive binding control and DBPRIII-IV as negative control. At least three independent experiments were performed with different UCB samples.

***Pv*AMA-1 peptide synthesis and radio-labeling.** *Pv*AMA-1 domain I and II (PVX_092275) were synthesized in sequential peptides (20-mer) using the t-Boc amino-acid strategy and p methylbenzhydrylamine resin (0.5 mequiv/g, Bachem), following solid-phase multiple peptide synthesis methodology[95, 96]. Peptides were cleaved by the low–high hydrogen fluoride technique and analyzed by RP-HPLC and MALDI-TOF mass spectrometry (Bruker Daltonics). Conserved peptides were radiolabeled using 3 μL -Na$^{125}$I (100 mCi/mL; ARC) and 15 μL chloramine T (2.75 mg/mL). The reaction was stopped after 15 min by adding 15 μL sodium metabisulphite (2.3 mg/mL), as described previously[97]. Radiolabeled peptides were separated by size-exclusion chromatography on a Sephadex G-25 column (Pharmacia). Each eluted fraction was then analyzed by gamma counter (Packard Cobra II).

**Radiolabeled peptide binding assays.** $2 \times 10^7$ RBC from UCB were incubated at RT for 90 min with different concentrations of each radiolabeled peptide (0–800 nM) in the absence (total binding) or presence (non-specific binding) of the same unlabeled peptide dissolved in 4-(2-hydroxyethyl)-1-piperazineethanesulphonic acid buffered saline (HBS; 200 μL final volume). Following incubation, cells were washed twice with HBS and the amount of cell-bound radiolabeled peptide was quantified on an automatic gamma counter.

Peptides' specific binding activity was evaluated in a binding assay with enzyme-treated RBC from UCB. The RBC were treated as described in the COS-7 cell RBC binding assay. $2 \times 10^7$ untreated RBC and trypsin-, chymotrypsin- or neuraminidase-treated RBC were incubated at RT for 90 min with 400 nM of each radiolabeled peptide in the absence or presence of the same unlabelled peptide, as described previously[97].

**Determining dissociation constants.** Modified binding assays were used for determining HABP 21270 dissociation constants ($K_d$), and Hill coefficients ($n$H). Briefly, $1.5 \times 10^7$ RBC were incubated with increasing concentrations of radiolabeled peptide (0–4,000 nM) in the absence or presence of unlabelled peptide (20 μM), using a 255 μL final volume. Cell-bound radioactivity was quantified as in binding assays[97]. GraphPad Prism software v5 was used for calculating $K_d$ and $n$H, following an interaction model, one by one.

**Statistical analysis.** SPSS v20.0 was used for statistical analysis of RBC-binding assays. Comparative statistics were reported from non-parametric univariate analysis. Differences between means were compared by Kruskal-Wallis tests when comparing multiple groups or Mann-Whitney U-test for comparing two groups.

**Ethics approval and consent to participate.** All parents from the donors of umbilical cord samples here used signed an informed consent form after receiving detailed information regarding the study's goals. The umbilical cord samples were collected by Bogotá's District Blood Centre (Colombia), following the protocols established by this institution, in accordance with Colombian laws and regulations. All procedures were approved by FIDIC's ethics committee.

## References

1. Gething, P. W. *et al*. A long neglected world malaria map: *Plasmodium vivax* endemicity in 2010. *PLoS Negl Trop Dis* **6**, e1814, doi:10.1371/journal.pntd.0001814 (2012).
2. Howes, R. E. *et al*. Global Epidemiology of Plasmodium vivax. *Am J Trop Med Hyg*. doi:10.4269/ajtmh.16-0141 (2016).
3. Mueller, I. *et al*. Key gaps in the knowledge of *Plasmodium vivax*, a neglected human malaria parasite. *Lancet Infect Dis* **9**, 555–566, doi:10.1016/S1473-3099(09)70177-X (2009).
4. Carlton, J. M. *et al*. Comparative genomics of the neglected human malaria parasite *Plasmodium vivax*. *Nature* **455**, 757–763, doi:10.1038/nature07327 (2008).
5. Weiss, G. E. *et al*. Revealing the sequence and resulting cellular morphology of receptor-ligand interactions during *Plasmodium falciparum* invasion of erythrocytes. *PLoS Pathog* **11**, e1004670, doi:10.1371/journal.ppat.1004670 (2015).
6. Boyle, M. J., Richards, J. S., Gilson, P. R., Chai, W. & Beeson, J. G. Interactions with heparin-like molecules during erythrocyte invasion by *Plasmodium falciparum* merozoites. *Blood* **115**, 4559–4568, doi:10.1182/blood-2009-09-243725 (2010).
7. Goel, V. K. *et al*. Band 3 is a host receptor binding merozoite surface protein 1 during the *Plasmodium falciparum* invasion of erythrocytes. *Proc Natl Acad Sci USA* **100**, 5164–5169, doi:10.1073/pnas.0834959100 (2003).
8. Baldwin, M. R., Li, X., Hanada, T., Liu, S. C. & Chishti, A. H. Merozoite surface protein 1 recognition of host glycophorin A mediates malaria parasite invasion of red blood cells. *Blood* **125**, 2704–2711, doi:10.1182/blood-2014-11-611707 (2015).
9. Camus, D. & Hadley, T. J. A *Plasmodium falciparum* antigen that binds to host erythrocytes and merozoites. *Science* **230**, 553–556 (1985).
10. Lobo, C. A., Rodriguez, M., Reid, M. & Lustigman, S. Glycophorin C is the receptor for the *Plasmodium falciparum* erythrocyte binding ligand PfEBP-2 (baebl). *Blood* **101**, 4628–4631, doi:10.1182/blood-2002-10-3076 (2003).

11. Lanzillotti, R. & Coetzer, T. L. The 10 kDa domain of human erythrocyte protein 4.1 binds the *Plasmodium falciparum* EBA-181 protein. *Malar J* **5**, 100, doi:10.1186/1475-2875-5-100 (2006).

12. Mayer, D. C. *et al.* Glycophorin B is the erythrocyte receptor of *Plasmodium falciparum* erythrocyte-binding ligand, EBL-1. *Proc Natl Acad Sci USA* **106**, 5348–5352, doi:10.1073/pnas.0900878106 (2009).

13. Tham, W. H. *et al.* Complement receptor 1 is the host erythrocyte receptor for *Plasmodium falciparum* PfRh4 invasion ligand. *Proc Natl Acad Sci USA* **107**, 17327–17332, doi:10.1073/pnas.1008151107 (2010).

14. Stubbs, J. *et al.* Molecular mechanism for switching of P. falciparum invasion pathways into human erythrocytes. *Science* **309**, 1384–1387, doi:10.1126/science.1115257 (2005).

15. Lopaticki, S. *et al.* Reticulocyte and erythrocyte binding-like proteins function cooperatively in invasion of human erythrocytes by malaria parasites. *Infect Immun* **79**, 1107–1117, doi:10.1128/IAI.01021-10 (2011).

16. Vulliez-Le Normand, B. *et al.* Structural and functional insights into the malaria parasite moving junction complex. *PLoS Pathog* **8**, e1002755, doi:10.1371/journal.ppat.1002755 (2012).

17. Chitnis, C. E. & Miller, L. H. Identification of the erythrocyte binding domains of *Plasmodium vivax* and *Plasmodium knowlesi* proteins involved in erythrocyte invasion. *J Exp Med* **180**, 497–506 (1994).

18. Galinski, M. R., Medina, C. C., Ingravallo, P. & Barnwell, J. W. A reticulocyte-binding protein complex of *Plasmodium vivax* merozoites. *Cell* **69**, 1213–1226 (1992).

19. Rodriguez, L. E. *et al. Plasmodium vivax* MSP-1 peptides have high specific binding activity to human reticulocytes. *Vaccine* **20**, 1331–1339 (2002).

20. Gunalan, K. *et al.* Role of *Plasmodium vivax* Duffy-binding protein 1 in invasion of Duffy-null Africans. *Proc Natl Acad Sci USA* **113**, 6271–6276, doi:10.1073/pnas.1606113113 (2016).

21. Franca, C. T. *et al. Plasmodium vivax* Reticulocyte Binding Proteins Are Key Targets of Naturally Acquired Immunity in Young Papua New Guinean Children. *PLoS Negl Trop Dis* **10**, e0005014, doi:10.1371/journal.pntd.0005014 (2016).

22. Han, J. H. *et al.* Identification of a reticulocyte-specific binding domain of *Plasmodium vivax* reticulocyte-binding protein 1 that is homologous to the PfRh4 erythrocyte-binding domain. *Sci Rep* **6**, 26993, doi:10.1038/srep26993 (2016).

23. Ntumngia, F. B. *et al.* A Novel Erythrocyte Binding Protein of *Plasmodium vivax* Suggests an Alternate Invasion Pathway into Duffy-Positive Reticulocytes. *MBio* **7**, doi:10.1128/mBio.01261-16 (2016).

24. Arevalo-Pinzon, G., Bermudez, M., Curtidor, H. & Patarroyo, M. A. The *Plasmodium vivax* rhoptry neck protein 5 is expressed in the apical pole of *Plasmodium vivax* VCG-1 strain schizonts and binds to human reticulocytes. *Malar J* **14**, 106, doi:10.1186/s12936-015-0619-1 (2015).

25. Silvie, O. *et al.* A role for apical membrane antigen 1 during invasion of hepatocytes by *Plasmodium falciparum* sporozoites. *J Biol Chem* **279**, 9490–9496, doi:10.1074/jbc.M311331200 (2004).

26. Peterson, M. G. *et al.* Integral membrane protein located in the apical complex of *Plasmodium falciparum*. *Mol Cell Biol* **9**, 3151–3154 (1989).

27. Triglia, T. *et al.* Apical membrane antigen 1 plays a central role in erythrocyte invasion by *Plasmodium* species. *Mol Microbiol* **38**, 706–718 (2000).

28. Donahue, C. G., Carruthers, V. B., Gilk, S. D. & Ward, G. E. The *Toxoplasma* homolog of *Plasmodium* apical membrane antigen-1 (AMA-1) is a microneme protein secreted in response to elevated intracellular calcium levels. *Mol Biochem Parasitol* **111**, 15–30 (2000).

29. Hodder, A. N. *et al.* The disulfide bond structure of *Plasmodium* apical membrane antigen-1. *J Biol Chem* **271**, 29446–29452 (1996).

30. Tordai, H., Banyai, L. & Patthy, L. The PAN module: the N-terminal domains of plasminogen and hepatocyte growth factor are homologous with the apple domains of the prekallikrein family and with a novel domain found in numerous nematode proteins. *FEBS Lett* **461**, 63–67 (1999).

31. Pizarro, J. C. *et al.* Crystal structure of the malaria vaccine candidate apical membrane antigen 1. *Science* **308**, 408–411, doi:10.1126/science.1107449 (2005).

32. Bai, T. *et al.* Structure of AMA-1 from *Plasmodium falciparum* reveals a clustering of polymorphisms that surround a conserved hydrophobic pocket. *Proc Natl Acad Sci USA* **102**, 12736–12741, doi:10.1073/pnas.0501808102 (2005).

33. Narum, D. L. & Thomas, A. W. Differential localization of full-length and processed forms of PF83/AMA-1 an apical membrane antigen of *Plasmodium falciparum* merozoites. *Mol Biochem Parasitol* **67**, 59–68 (1994).

34. Howell, S. A. *et al.* A single malaria merozoite serine protease mediates shedding of multiple surface proteins by juxtamembrane cleavage. *J Biol Chem* **278**, 23890–23898, doi:10.1074/jbc.M302160200 (2003).

35. Giovannini, D. *et al.* Independent roles of apical membrane antigen 1 and rhoptry neck proteins during host cell invasion by apicomplexa. *Cell Host Microbe* **10**, 591–602, doi:10.1016/j.chom.2011.10.012 (2011).

36. Urquiza, M. *et al. Plasmodium falciparum* AMA-1 erythrocyte binding peptides implicate AMA-1 as erythrocyte binding protein. *Vaccine* **19**, 508–513 (2000).

37. Fraser, T. S., Kappe, S. H., Narum, D. L., VanBuskirk, K. M. & Adams, J. H. Erythrocyte-binding activity of *Plasmodium yoelii* apical membrane antigen-1 expressed on the surface of transfected COS-7 cells. *Mol Biochem Parasitol* **117**, 49–59 (2001).

38. Kato, K., Mayer, D. C., Singh, S., Reid, M. & Miller, L. H. Domain III of *Plasmodium falciparum* apical membrane antigen 1 binds to the erythrocyte membrane protein Kx. *Proc Natl Acad Sci USA* **102**, 5552–5557, doi:10.1073/pnas.0501594102 (2005).

39. Mitchell, G. H., Thomas, A. W., Margos, G., Dluzewski, A. R. & Bannister, L. H. Apical membrane antigen 1, a major malaria vaccine candidate, mediates the close attachment of invasive merozoites to host red blood cells. *Infect Immun* **72**, 154–158 (2004).

40. Srinivasan, P. *et al.* Binding of *Plasmodium* merozoite proteins RON2 and AMA-1 triggers commitment to invasion. *Proc Natl Acad Sci USA* **108**, 13275–13280, doi:10.1073/pnas.1110303108 (2011).

41. Yap, A. *et al.* Conditional expression of apical membrane antigen 1 in *Plasmodium falciparum* shows it is required for erythrocyte invasion by merozoites. *Cell Microbiol* **16**, 642–656, doi:10.1111/cmi.12287 (2014).

42. Mital, J., Meissner, M., Soldati, D. & Ward, G. E. Conditional expression of *Toxoplasma gondii* apical membrane antigen-1 (TgAMA1) demonstrates that *Tg*AMA-1 plays a critical role in host cell invasion. *Mol Biol Cell* **16**, 4341–4349, doi:10.1091/mbc.E05-04-0281 (2005).

43. Collins, C. R. *et al.* Fine mapping of an epitope recognized by an invasion-inhibitory monoclonal antibody on the malaria vaccine candidate apical membrane antigen 1. *J Biol Chem* **282**, 7431–7441, doi:10.1074/jbc.M610562200 (2007).

44. Collins, C. R., Withers-Martinez, C., Hackett, F. & Blackman, M. J. An inhibitory antibody blocks interactions between components of the malarial invasion machinery. *PLoS Pathog* **5**, e1000273, doi:10.1371/journal.ppat.1000273 (2009).

45. Richard, D. *et al.* Interaction between *Plasmodium falciparum* apical membrane antigen 1 and the rhoptry neck protein complex defines a key step in the erythrocyte invasion process of malaria parasites. *J Biol Chem* **285**, 14815–14822, doi:10.1074/jbc.M109.080770 (2010).

46. Dutta, S. *et al.* Mode of action of invasion-inhibitory antibodies directed against apical membrane antigen 1 of *Plasmodium falciparum*. *Infect Immun* **73**, 2116–2122, doi:10.1128/IAI.73.4.2116-2122.2005 (2005).

47. Deans, J. A. *et al.* Vaccination trials in rhesus monkeys with a minor, invariant, *Plasmodium knowlesi* 66 kD merozoite antigen. *Parasite Immunol* **10**, 535–552 (1988).

48. Mahdi Abdel Hamid, M. *et al.* Vaccination with *Plasmodium knowlesi* AMA-1 formulated in the novel adjuvant co-vaccine HT protects against blood-stage challenge in rhesus macaques. *PLoS One* **6**, e20547, doi:10.1371/journal.pone.0020547 (2011).

49. Gentil, F. *et al*. A recombinant vaccine based on domain II of *Plasmodium vivax* Apical Membrane Antigen 1 induces high antibody titres in mice. *Vaccine* **28**, 6183–6190, doi:10.1016/j.vaccine.2010.07.017 (2010).

50. Crewther, P. E., Matthew, M. L., Flegg, R. H. & Anders, R. F. Protective immune responses to apical membrane antigen 1 of *Plasmodium chabaudi* involve recognition of strain-specific epitopes. *Infect Immun* **64**, 3310–3317 (1996).

51. Hodder, A. N., Crewther, P. E. & Anders, R. F. Specificity of the protective antibody response to apical membrane antigen 1. *Infect Immun* **69**, 3286–3294, doi:10.1128/IAI.69.5.3286-3294.2001 (2001).

52. Wickramarachchi, T. *et al*. Natural human antibody responses to *Plasmodium vivax* apical membrane antigen 1 under low transmission and unstable malaria conditions in Sri Lanka. *Infect Immun* **74**, 798–801, doi:10.1128/IAI.74.1.798-801.2006 (2006).

53. Roestenberg, M. *et al*. Safety and immunogenicity of a recombinant *Plasmodium falciparum* AMA-1 malaria vaccine adjuvanted with Alhydrogel, Montanide ISA 720 or AS02. *PLoS One* **3**, e3960, doi:10.1371/journal.pone.0003960 (2008).

54. Thera, M. A. *et al*. A field trial to assess a blood-stage malaria vaccine. *N Engl J Med* **365**, 1004–1013, doi:10.1056/NEJMoa1008115 (2011).

55. Ouattara, A. *et al*. Lack of allele-specific efficacy of a bivalent AMA-1 malaria vaccine. *Malar J* **9**, 175, doi:10.1186/1475-2875-9-175 (2010).

56. Drew, D. R. *et al*. A novel approach to identifying patterns of human invasion-inhibitory antibodies guides the design of malaria vaccines incorporating polymorphic antigens. *BMC Med* **14**, 144, doi:10.1186/s12916-016-0691-6 (2016).

57. Dutta, S., Lee, S. Y., Batchelor, A. H. & Lanar, D. E. Structural basis of antigenic escape of a malaria vaccine candidate. *Proc Natl Acad Sci USA* **104**, 12488–12493, doi:10.1073/pnas.0701464104 (2007).

58. Escalante, A. A. *et al*. Polymorphism in the gene encoding the apical membrane antigen-1 (AMA-1) of *Plasmodium falciparum*. X. Asembo Bay Cohort Project. *Mol Biochem Parasitol* **113**, 279–287 (2001).

59. Polley, S. D. & Conway, D. J. Strong diversifying selection on domains of the *Plasmodium falciparum* apical membrane antigen 1 gene. *Genetics* **158**, 1505–1512 (2001).

60. Chesne-Seck, M. L. *et al*. Structural comparison of apical membrane antigen 1 orthologues and paralogues in apicomplexan parasites. *Mol Biochem Parasitol* **144**, 55–67, doi:10.1016/j.molbiopara.2005.07.007 (2005).

61. Arnott, A. *et al*. Global Population Structure of the Genes Encoding the Malaria Vaccine Candidate, *Plasmodium vivax* Apical Membrane Antigen 1 (PvAMA1). *PLoS Negl Trop Dis* **7**, e2506, doi:10.1371/journal.pntd.0002506 (2013).

62. Remarque, E. J., Faber, B. W., Kocken, C. H. & Thomas, A. W. A diversity-covering approach to immunization with *Plasmodium falciparum* apical membrane antigen 1 induces broader allelic recognition and growth inhibition responses in rabbits. *Infect Immun* **76**, 2660–2670, doi:10.1128/IAI.00170-08 (2008).

63. Faber, B. W. *et al*. Production, Quality Control, Stability and Pharmacotoxicity of a Malaria Vaccine Comprising Three Highly Similar *Pf*AMA-1 Protein Molecules to Overcome Antigenic Variation. *PLoS One* **11**, e0164053, doi:10.1371/journal.pone.0164053 (2016).

64. Cohen, G. H. *et al*. Expression of herpes simplex virus type 1 glycoprotein D deletion mutants in mammalian cells. *J Virol* **62**, 1932–1940 (1988).

65. Igonet, S. *et al*. Cross-reactivity studies of an anti-*Plasmodium vivax* apical membrane antigen 1 monoclonal antibody: binding and structural characterisation. *J Mol Biol* **366**, 1523–1537, doi:10.1016/j.jmb.2006.12.028 (2007).

66. Hossain, M. E., Dhawan, S. & Mohmmed, A. The cysteine-rich regions of *Plasmodium falciparum* RON2 bind with host erythrocyte and AMA-1 during merozoite invasion. *Parasitol Res* **110**, 1711–1721, doi:10.1007/s00436-011-2690-z (2012).

67. Gao, X. *et al*. Antibodies targeting the *Pf*RH1 binding domain inhibit invasion of *Plasmodium falciparum* merozoites. *PLoS Pathog* **4**, e1000104, doi:10.1371/journal.ppat.1000104 (2008).

68. Barnwell, J. W., Nichols, M. E. & Rubinstein, P. *In vitro* evaluation of the role of the Duffy blood group in erythrocyte invasion by *Plasmodium vivax*. *J Exp Med* **169**, 1795–1802 (1989).

69. Malleret, B. *et al*. *Plasmodium vivax*: restricted tropism and rapid remodeling of CD71-positive reticulocytes. *Blood* **125**, 1314–1324, doi:10.1182/blood-2014-08-596015 (2015).

70. Dong, H. Y., Wilkes, S. & Yang, H. CD71 is selectively and ubiquitously expressed at high levels in erythroid precursors of all maturation stages: a comparative immunochemical study with glycophorin A and hemoglobin A. *Am J Surg Pathol* **35**, 723–732, doi:10.1097/PAS.0b013e31821247a8 (2011).

71. Caruso, A. *et al*. Flow cytometric analysis of activation markers on stimulated T cells and their correlation with cell proliferation. *Cytometry* **27**, 71–76 (1997).

72. Ocampo, M. *et al*. *Plasmodium vivax* Duffy binding protein peptides specifically bind to reticulocytes. *Peptides* **23**, 13–22 (2002).

73. Patarroyo, M. E. & Patarroyo, M. A. Emerging rules for subunit-based, multiantigenic, multistage chemically synthesized vaccines. *Acc Chem Res* **41**, 377–386, doi:10.1021/ar700120t (2008).

74. Rodriguez, L. E. *et al*. Intimate molecular interactions of *P. falciparum* merozoite proteins involved in invasion of red blood cells and their implications for vaccine design. *Chem Rev* **108**, 3656–3705, doi:10.1021/cr068407v (2008).

75. Curtidor, H., Patarroyo, M. E. & Patarroyo, M. A. Recent advances in the development of a chemically synthesised anti-malarial vaccine. *Expert Opin Biol Ther* **15**, 1567–1581, doi:10.1517/14712598.2015.1075505 (2015).

76. Takala, S. L. *et al*. Extreme polymorphism in a vaccine antigen and risk of clinical malaria: implications for vaccine development. *Sci Transl Med* **1**, 2ra5, doi:10.1126/scitranslmed.3000257 (2009).

77. Patarroyo, M. A., Calderon, D. & Moreno-Perez, D. A. Vaccines against *Plasmodium vivax*: a research challenge. *Expert Rev Vaccines* **11**, 1249–1260, doi:10.1586/erv.12.91 (2012).

78. Noulin, F., Borlon, C., Van Den Abbeele, J., D'Alessandro, U. & Erhart, A. 1912-2012: a century of research on *Plasmodium vivax in vitro* culture. *Trends Parasitol* **29**, 286–294, doi:10.1016/j.pt.2013.03.012 (2013).

79. Panichakul, T. *et al*. Production of erythropoietic cells *in vitro* for continuous culture of *Plasmodium vivax*. *Int J Parasitol* **37**, 1551–1557, doi:10.1016/j.ijpara.2007.05.009 (2007).

80. Chotivanich, K. *et al*. Ex-vivo short-term culture and developmental assessment of *Plasmodium vivax*. *Trans R Soc Trop Med Hyg* **95**, 677–680 (2001).

81. Cheng, Y. *et al*. *Plasmodium vivax* GPI-anchored micronemal antigen (*Pv*GAMA) binds human erythrocytes independent of Duffy antigen status. *Sci Rep* **6**, 35581, doi:10.1038/srep35581 (2016).

82. Li, X. *et al*. A co-ligand complex anchors *Plasmodium falciparum* merozoites to the erythrocyte invasion receptor band 3. *J Biol Chem* **279**, 5765–5771, doi:10.1074/jbc.M308716200 (2004).

83. Wilson, M. C. *et al*. Comparison of the Proteome of Adult and Cord Erythroid Cells, and Changes in the Proteome Following Reticulocyte Maturation. *Mol Cell Proteomics* **15**, 1938–1946, doi:10.1074/mcp.M115.057315 (2016).

84. Healer, J. *et al*. Allelic polymorphisms in apical membrane antigen-1 are responsible for evasion of antibody-mediated inhibition in *Plasmodium falciparum*. *Mol Microbiol* **52**, 159–168, doi:10.1111/j.1365-2958.2003.03974.x (2004).

85. Delgadillo, R. F., Parker, M. L., Lebrun, M., Boulanger, M. J. & Douguet, D. Stability of the *Plasmodium falciparum* AMA1-RON2 Complex Is Governed by the Domain II (DII) Loop. *PLoS One* **11**, e0144764, doi:10.1371/journal.pone.0144764 (2016).

86. Obando-Martinez, A. Z. *et al*. Conserved high activity binding peptides are involved in adhesion of two detergent-resistant membrane-associated merozoite proteins to red blood cells during invasion. *J Med Chem* **53**, 3907–3918, doi:10.1021/jm901474p (2010).

87. Patarroyo, M. E., Arevalo-Pinzon, G., Reyes, C., Moreno-Vranich, A. & Patarroyo, M. A. Malaria Parasite Survival Depends on Conserved Binding Peptides' Critical Biological Functions. *Curr Issues Mol Biol* **18**, 57–78 (2016).

88. Tonkin, M. L. *et al*. Host cell invasion by apicomplexan parasites: insights from the co-structure of AMA-1 with a RON2 peptide. *Science* **333**, 463–467, doi:10.1126/science.1204988 (2011).

89. Bargieri, D. Y. *et al*. Apical membrane antigen 1 mediates apicomplexan parasite attachment but is dispensable for host cell invasion. *Nat Commun* **4**, 2552, doi:10.1038/ncomms3552 (2013).

90. Valbuena, J. *et al*. Synthetic peptides from *Plasmodium falciparum* apical membrane antigen 1 (AMA-1) specifically interacting with human hepatocytes. *Biochimie* **88**, 1447–1455, doi:10.1016/j.biochi.2006.05.005 (2006).

91. Farooq, F. & Bergmann-Leitner, E. S. Immune Escape Mechanisms are *Plasmodium's* Secret Weapons Foiling the Success of Potent and Persistently Efficacious Malaria Vaccines. *Clin Immunol* **161**, 136–143, doi:10.1016/j.clim.2015.08.015 (2015).

92. Urquiza, M. *et al*. Identification and polymorphism of *Plasmodium vivax* RBP-1 peptides which bind specifically to reticulocytes. *Peptides* **23**, 2265–2277 (2002).

93. Patarroyo, M. E. *et al*. IMPIPS: the immune protection-inducing protein structure concept in the search for steric-electron and topochemical principles for complete fully-protective chemically synthesised vaccine development. *PLoS One* **10**, e0123249, doi:10.1371/journal.pone.0123249 (2015).

94. Curtidor, H. *et al*. *Plasmodium falciparum* rhoptry neck protein 5 peptides bind to human red blood cells and inhibit parasite invasion. *Peptides* **53**, 210–217, doi:10.1016/j.peptides.2013.07.028 (2014).

95. Houghten, R. A. General method for the rapid solid-phase synthesis of large numbers of peptides: specificity of antigen-antibody interaction at the level of individual amino acids. *Proc Natl Acad Sci USA* **82**, 5131–5135 (1985).

96. Merrifield, R. B. Solid phase peptide synthesis. I. The synthesis of a tetrapeptide. *Journal of American Chemical Society* **85**, 2149–2154 (1963).

97. Arevalo-Pinzon, G. *et al*. Rh1 high activity binding peptides inhibit high percentages of *Plasmodium falciparum* FVO strain invasion. *Vaccine* **31**, 1830–1837, doi:10.1016/j.vaccine.2013.01.052 (2013).

## Acknowledgements

## Author Contributions

G.A.P. designed the experiments, expressed the recombinant proteins, performed binding experiments and wrote the initial manuscript. M.B. carried out COS7 culture, rosetting assays and inhibition experiments. D.H. contributed to work on recombinant protein expression. H.C. synthesized and purified the peptides and M.A.P. designed the experiments, evaluated and coordinated the assays and revised the final version of the manuscript.

## Additional Information

# Receptor-ligand and protein-protein interactions in *Plasmodium vivax*: analysing rhoptry neck proteins 2 and 4.

Maritza Bermúdez [1, ¶], Gabriela Arévalo-Pinzón [1, 2, ¶], Laura Rubio [1], Olivier Chaloin [3], Sylviane Muller [3, 4], Hernando Curtidor [1, 5], Manuel Alfonso Patarroyo [1, 5 *]

[1] Fundación Instituto de Inmunología de Colombia (FIDIC), Carrera 50 # 26-20, Bogotá, Colombia

[2] PhD Programme in Biomedical and Biological Sciences, Universidad del Rosario, Carrera 24 # 63C-69, Bogotá, Colombia

[3] CNRS, Immunopathology and therapeutic chemistry/Laboratory of excellence Medalis, Institut de Biologie Moléculaire et Cellulaire (IBMC), 15 rue René Descartes, 67000 Strasbourg, France

[4] University of Strasbourg Institute for Advanced Study (USIAS), 5 allée du Général Rouvillois, 67083 Strasbourg, France

[5] School of Medicine and Health Sciences, Universidad del Rosario, Carrera 24 # 63C-69, Bogotá, Colombia

[*]Corresponding author: mapatarr.fidic@gmail.com, +57 1 3244672 ext. 141

[¶] Equal contributors

Running title: *Pv*RON2 and *Pv*RON4 participate in parasite-host interactions

**Summary**

Elucidating receptor-ligand and protein-protein interactions represents an attractive alternative for designing effective *Plasmodium vivax* control methods. This article describes the ability of *P. vivax* rhoptry neck proteins 2 and 4 (RON2 and RON4) to bind to human reticulocytes. Biochemical and cellular studies showed that two conserved regions of *Pv*RON2 and *Pv*RON4 specifically interact with protein receptors on CD71$^+$CD45$^-$ reticulocytes. Mapping each protein fragment's binding region led to defining the specific participation of two 20 amino acid-long regions selectively competing for *Pv*RON2 and *Pv*RON4 binding to reticulocytes. Binary interactions between *Pv*RON2 (ligand) and other parasite proteins, such as *Pv*RON4, *Pv*RON5 and apical membrane antigen 1 (AMA1) were evaluated and characterised by surface plasmon resonance (SPR). The results revealed that both *Pv*RON2 cysteine-rich regions strongly interact with *Pv*AMA1 domains II and III (equilibrium constants in the nanomolar range) and at a lower extent with the complete *Pv*AMA1 ectodomain and domains I and II. These results strongly support that these proteins participate in *P. vivax*'s complex invasion process, thus providing new pertinent targets for blocking *P. vivax* merozoites' specific entry to their target cells.

**Introduction**

The invasion cycle of parasites from the phylum Apicomplexa (i.e. *Toxoplasma gondii* or *Plasmodium* spp), represents one of the most complex pathogen invasion processes which is actively orchestrated by the parasite itself through a series of events involving a diverse set of molecular interactions [1; 2]. Such process requires a sequence of coordinated activities, including recognition, host cell attachment, protein secretion (from micronemes and rhoptries) and motility, supported by an actin/myosin-based gliding in apicomplexan parasites [3]. One of its most outstanding features concerns the formation of stable, high-avidity merozoite (Mz) apex binding to a host cell, resembling a form of ring moving progressively (moving junction - MJ) from the apical pole towards the back of the parasite, propelling it into a nascent parasitophorous vacuole, thereby allowing it to survive and replicate within a target cell [4].

Studies orientated towards identifying the components forming the circumferential ring have shown that it appears to be mainly formed by a multimeric protein complex, involving the parasite's apical membrane antigen 1 (AMA1) and rhoptry neck (RON) proteins -2, -4, -5 and -8 (the latter only in *T. gondii*) [5; 6; 7; 8]. The RON/AMA1 complex acts independently of host cell receptors as Apicomplexans secrete RON proteins into a host cell, using RON2 as receptor on target cell membrane. RON2 is anchored to host cell surface and the carboxyl terminal region remains exposed for binding to AMA1 which acts as parasite ligand [5; 9; 10]. Regarding the other RONs, it has been described that RON5 and RON8 in *T. gondii* are involved in stabilising and organising the complex in a host cell [11; 12]. It has been found that conditional knockdown involving a loss of *Tg*RON5 has led to the complete degradation of *Tg*RON2 and mistargeting of *Tg*RON4 [11], whilst a loss of *Tg*RON4 has significantly reduced

3

*Tg*RON5 and *Tg*RON2 levels [13]. It has also been shown that four host proteins (ALIX-CD2AP-CIN85 and TSG101) are specifically recruited to the MJ through specific binding motifs present on *Tg*RON proteins [13].

Structural studies of the complex formed between AMA1 and a RON2 peptide have shown the participation of the AMA1 hydrophobic trough, so that a binding pocket accepts the RON2 critical loop region, having significant shape and complementary charge [14; 15; 16]. This interaction's importance in *P. falciparum* has been established by using antibodies, peptides or small molecules directed against the *Pf*AMA1-*Pf*RON2 complex interface, thereby significantly inhibiting invasion [8; 9; 17]. Immunising mice with the AMA1-RON2L complex (but not with individual antigens) has induced qualitatively higher growth inhibitory antibodies capable of protecting mice against experimental challenge with a lethal *P. yoelii* strain, highlighting such protein–protein interaction's important role during invasion [18].

AMA1 was initially identified in *P. knowlesi* [19] and then found throughout all Apicomplexa, being essential for *T. gondii* and *P. falciparum* survival [20; 21]. Regarding AMA1's function in MJ formation, various roles involved in *P. falciparum* invasion have been attributed to it, including Mz reorientation on red blood cell (RBC) surface [22], participation in resealing RBC at the end of invasion [23], interaction with aldolase which provides extracellular linkage for the actin/myosin motor [24] and interaction with receptors on RBC surface [25; 26]. Previous observations showed that tachyzoites (Tz) and sporozoites (Spz) having conditional knockouts for AMA1 were capable of invading a host cell and appeared to form normal MJ, suggesting that AMA1 was acting independently of RONs and that AMA1-RON2 interaction was not essential [27; 28]. However, later studies showed that Tz used paralogues of the generic AMA1-RON2 pair as substitutes, partially compensating for the loss of *Tg*AMA1 [29]. Alternative pathways for the lack of AMA1 and RON2 have not been reported in *P.*

*falciparum* [29], unlike that observed in other invasion steps (such as reorientation) using functionally redundant proteins, such as erythrocyte binding antigens (EBAs) and reticulocyte-binding-like protein homologues (RH) [30]. This would suggest that whilst it might be a conserved mechanism amongst Apicomplexa, differences concerning regulation of MJ components, composition and interaction regions could partly define selectivity by their respective host cells.

*P. falciparum* RONs were identified by co-immunoprecipitation assays showing AMA1 association with high molecular weight components located in the rhoptry neck [31] homologues of those reported in *T. gondii* [32; 33; 34]. Even though there is no clear evidence of *Pf*RON2, *Pf*RON4 and *Pf*RON5 translocation across/onto host cell membrane and RBC cytosol in *P. falciparum*, previous studies have shown that *Pf*RON2 uses a cysteine-rich region (*Pf*RON2-C) located in the carboxyl terminal extreme for interacting with receptors on a host cell; these are sensitive to treatment with trypsin and neuraminidase [35]. However, the cysteine-rich region located in *Pf*RON2's central portion (*Pf*RON2-M) and the *Pf*RON2-C region interact with *Pf*AMA1 [35]. *Pf*RON5 contains peptides having high affinity binding to receptors on RBC which are capable of inhibiting Mz entry to target cells. Such data highlight RON and AMA1 participation in establishing receptor-ligand and protein-protein interactions [36; 37].

Regarding *P. vivax*, the geographically most widespread cause of human malaria [38], there is little information concerning the proteins participating in binding (ligand-receptor interaction) or protein-protein interactions, partly due to difficulties in culturing *P. vivax in-vitro* thereby impeding genetic approaches for studying proteins' role during the cycle of invasion of reticulocytes. Such limitations have been a barrier to studying the biological, clinical and immunological characteristics necessary for designing control measures against

*P. vivax*. Using *P. vivax* strains adapted in non-human primates [39] or infected patients' blood [40] has enabled comparative approaches with other *Plasmodium* species [41] or using omic sciences [42; 43] to identify a significant amount of proteins expressed in *P. vivax* schizonts (Sch) and Mz [41]. *Pv*RON2 [44], *Pv*RON4 [45] and *Pv*RON5 [46] have been identified recently; these are homologous to those identified in *P. falciparum* which are located in the apical extreme of *P. vivax* Colombia Guaviare 1 (VCG-1) strain Sch. Different biochemical techniques have been used to report a conserved *Pv*RON5 fragment located towards the carboxyl-terminal extreme interacting with RBC, having a preference for $CD71^+$ cells [46], suggesting that RONs could be participating in host-parasite interactions, similar to that found in *P. falciparum*. *Pv*RON2 and *Pv*RON4 ability to interact specifically with RBC was thus evaluated to advance the functional characterisation of *P. vivax* RONs; this was followed by determining binary interactions between *Pv*RON2, *Pv*RON4, *Pv*RON5 and *Pv*AMA1 by surface plasmon resonance (SPR). The data indicate that the *Pv*RON2 central region and *Pv*RON4 carboxyl terminal region specifically interact with protein receptors on $CD71^+CD45^-$ reticulocyte membrane. It was also shown here that *Pv*RON2 also participates in interaction with other parasite proteins, such as *Pv*AMA1, *Pv*RON4 and *Pv*RON5, highlighting *P. vivax* RON participation in establishing several protein-protein and host-pathogen interactions.

**Results and Discussion**

*The* Pv*RON4 carboxyl terminal region interacted with umbilical cord blood RBC*

Recombinant plasmids were constructed based on evidence regarding two *P. falciparum* RON2 cysteine-rich regions' binding and interaction activity [9; 35]; they contained the regions encoding the *P. vivax* central (*Pv*RON2-RI) and carboxyl terminal (*Pv*RON2-RII) regions (Figure 1A). A *Pv*RON4 region located towards the carboxyl terminal extreme was amplified (Figure 1A); it is highly conserved at intra- and inter-species level and is under purifying selection, contrary to that reported for the amino terminal region having extensive size polymorphism [47]. Selected regions were cloned in pRE4 vector in frame with herpes simplex virus (HSV) glycoprotein D signal peptide and transmembrane domain thereby enabling proteins to be expressed and anchored to cell membrane [48]. Following transfection and immunofluorescent studies on non-permeabilised cells, it was found that only *Pv*RON4 was correctly and efficiently expressed on COS-7 cell membrane (Figure 1B).

The *P. vivax* infection has been seen to be limited to Duffy (Fy) positive reticulocytes, also known as the Duffy antigen/receptor for chemokines (DARC). Such preference seems to be mediated by specific receptor-ligand interactions between the DBP protein expressed by the parasite and the DARC receptor on RBC membrane [49]. DBP-DARC interaction was taken as positive control based on the above information where *Pv*DBP cysteine-rich region II was expressed on COS-7 cell membrane (Figure 1B). As expected, *Pv*DBPRII interacted with DARC whilst having low negative Duffy cell binding capacity (ANOVA-Tukey: $F_{(3,12)}=24.8$, $p<0.0001$) (Figure 1B and 1C). The *Pv*RON4 C-terminal cysteine-rich region (pRE4-*Pv*RON4 construct) bound to umbilical cord blood (UCB) RBC having different Duffy phenotypes, although their binding activity was lower than that found for *Pv*DBP-RII (Figure 1B and 1C). *Pv*RON4 binding to Fya$^+$Fyb$^-$ had statistically significant differences

regarding binding to Fya⁻Fyb⁻ RBC (ANOVA-Tukey: $F_{(3,12)}=4.26$, p=0.020). When *Pv*RON4 binding to RBC ($m=34\pm2.7$) was compared to binding to normocytes ($m=11\pm1.4$) it was observed that the amount of rosettes compared to normocytes became significantly reduced (t-test: $t_{(10)}=18.68$, p=0.001) (Figure 1B and C). This suggested that *Pv*RON4 binding to RBC depends on a more immature RBC population, similar to that reported for other *P. vivax* antigens, such as *Pv*AMA1 [50], *Pv*GAMA [51] and EBP2 [52], whilst *Pv*DBPRII bound to both RBC and normocytes (Figure 1C).

Several reports have shown that different *P. falciparum* strains differ regarding their ability to invade RBC treated with different enzymes, such as trypsin, chymotrypsin and neuraminidase, removing different receptors from RBC surface [53; 54]. Such assays enabled ascertaining that proteins like erythrocyte binding antigen 175 (EBA175) recognised the sialic acid component in glycophorin A [55] whilst EBA 140 bound to glycophorin C [56]. It has been reported (and also found here) that *Pv*DBP binding to DARC was susceptible to enzymatic treatment with chymotrypsin [57] (t-test: $t_{(4)}=24.4$, p=0.001) (Figure 1D). It has also been reported that *Pv*AMA1 binding was susceptible to neuraminidase and chymotrypsin action [50]. Interestingly, it was found here that *Pv*RON4 interacted with RBC membrane protein receptors susceptible to treatment with the three enzymes evaluated (ANOVA-Tukey: $F_{(3,8)}=59$, p=0.001) (Figure 1D). Such binding profile did not fit any enzymatic behaviour typical of previously-described malaria receptors.

Concerning other parasites such as *T. gondii*, a 17kDa region in *Tg*RON4 proximal C-terminus was sufficient for binding to host cell β-tubulin carboxyl-terminal region [58]. Even though the overall similarity between *T. gondii*, *P. falciparum* or *P. vivax* RON4 is not very high (Supplementary Material), a pattern of conservation could be observed towards these proteins' carboxyl terminal region. This suggested that functional RON4 binding region was

located towards this region, even though receptor type differed according to species, as shown by *Tg*RON4 [58] and *Pv*RON4 interaction results (Figure 1). Although it is still not clear whether RON4 is exported towards host cell cytosol, its participation in MJ formation is crucial for target cell invasion by *T. gondii* and *P. falciparum* [27]. Recent studies have found that the *Pv*RON4 central region contained a sterease/lipase domain which could be associated with ester bonds rupture in the phospholipids constituting host cell membrane [47]. This suggested the presence of several functional domains in RON4, where the C-terminal region could interact with RBC membrane whilst the sterease/lipase (central region) domain could then enable RON4 internalisation. Future studies aimed at elucidating such functional domains' coordinated involvement in invasion should be carried out.


*Pv*RON4 and *Pv*RON2-RII bound specifically to CD71^{+}CD45^{-} cells

Three protein fragments were obtained in recombinant form in *E. coli* for determining *Pv*RON4-RBC interaction specificity and evaluating *Pv*RON2-RI and *Pv*RON2-RII specific binding capability (Figure 1A); these regions were then purified by affinity chromatography. A single band was found for each fragment by western blot and Coomassie blue staining, coinciding with the expected molecular weights (Figure 2A-left). Every recombinant fragment was radiolabelled, quantified and incubated in a UCB RBC competition assay with high concentrations of the same non-radiolabelled recombinant protein. The results showed that even though the three fragments did bind (total binding), only *Pv*RON4 and *Pv*RON2-RI bound specifically to RBC, since radiolabelled protein binding became reduced (by ~55%) in the presence of non-radiolabelled protein (non-specific binding) (Figure 2A-right). When graphing specific binding it was observed that *Pv*RON4 and *Pv*RON2-RI specific binding

activity was 1%-*Pv*RON4 to 2.6%-*Pv*RON2-RI (curve slope) compared to *Pv*RON2-RI 0.22% specific activity (Figure 2A-right).

As *P. vivax* Mrz have a strong preference for reticulocytes expressing transferrin receptor 1 (CD71) (becoming sequentially lost as reticulocytes mature), cytometry was used for determining whether *Pv*RON4 and *Pv*RON2-RI binding was restricted to interaction with this type of immature cell (reticulocyte stages I-III). Figure 2B shows that *Pv*RON2-RI had 6.56% binding to $CD71^+CD45^-$ cells ($m=7.6\pm0.94\%$: 5.2-9.9) and *Pv*RON4 5.60% ($m=5.15\pm0.55\%$: 3.7-6.5), whilst low $CD71^-CD45^-$ cell interaction (~0.1%) was found (data not shown). *Pv*DBPRII recombinant protein had 10.5% binding (positive control) ($m=12.3\pm1.47\%$: 8.6-15.95 95%CI) whilst *Pv*DBPRIII-IV recombinant protein, expressing regions III and IV (negative control), had low binding capacity ($m=1.0\pm0.55\%$: -0.3-2.4), thereby coinciding with previous studies showing that these regions do not participate in target cell binding [59; 60].

It has been reported that the *Pf*RON2 fragment involved in interaction with RBC is located in the carboxyl-terminal region [35], different to that found for *Pv*RON2 where, even though both regions bound, only the region located towards the protein's central portion (called *Pv*RON2-RI here) specifically interacted with UCB RBC (Figure 2). Such data, added to that available for *P. vivax* proteins (e.g. *Pv*MSP1, *Pv*AMA1 [50] and now *Pv*RON2), has shown that some *P. vivax* proteins having orthologues in *P. falciparum* have different functional regions, which could partly be responsible for the specificity of the interaction with respective target cells.

It is still not clear why *P. vivax* has tropism for $CD71^+$ reticulocytes; the interaction defined between DBP and DARC was initially considered essential for parasite binding; however, DARC is expressed on both reticulocytes and erythrocytes. Recent studies have managed to

show that DARC epitope recognised by DBP has increased its exposure during early stages of reticulocyte maturation and decreased it during maturation into normocytes [61]. DARC epitope exposure during reticulocyte stages I-III enables greater DBP association with CD71$^{high}$/TO$^{high}$ reticulocytes, but not in mature reticulocytes or erythrocytes, partly explaining *P. vivax* tropism for reticulocytes [61]. It is worth noting that specific tropism for CD71$^+$ reticulocytes has also been shown for other *P. vivax* proteins, including those studied here. Receptor remodelling during reticulocyte maturation, added to the fact that proteins have distinct binding domains in each species, could complement each parasite's selectivity for its respective host cell.

*20-residue-long peptides were capable of specifically competing for* Pv*RON4 and* Pv*RON2 binding*

Competition assays were carried out between peptides covering radiolabelled protein and recombinant protein fragments' amino acid sequences to define the regions responsible for *Pv*RON2 and *Pv*RON4 interaction with CD71$^+$CD45$^-$ cells. The results showed that *Pv*RON4 fragment-derived peptides 40305, 40306, 40312 and 40313 could inhibit recombinant protein binding by 40% (40305) (Figure 3A). Three peptides (40592, 40593 and 40595) inhibited *Pv*RON2-RI radiolabelled protein binding by up to 41% (Figure 3B).

Peptides 40305, 40313, 40592 and 40595 were radiolabelled and tested in a RBC binding assay, in the presence or absence of non-radiolabelled peptide for characterising *Pv*RON4 and *Pv*RON2-RI specific binding activity as such peptides were capable of inhibiting recombinant protein binding. This method required peptides having ≥0.02 or 2% specific binding activity (according to the specific binding curve, named here high activity binding peptides - HABPs) [62]. This assay gave *Pv*RON4 peptide 40305 and *Pv*RON2-RI 40595 slopes

greater than 2% (Figure 3C and 3D), thereby cataloguing them as HABPs. Flow cytometry showed that HABP 40305 could inhibit protein binding to $CD71^+CD45^-$ reticulocytes by up to 23% and HABP 40495 by 40% (Figure 3C and 3D). HABP 40305 was also able to inhibit rosette formation by 41% compared to negative control (absence of peptide) (Figure 3C).

A significant amount of HABPs have been identified in most *P. falciparum* proteins participating in Spz and Mz invasion of their respective target cells [62; 63]. After HABPs have undergone a series of chemical modifications and structural and immunological studies, they have been able to induce a strong protection-inducing immune response in experimental challenge in a non-human primate animal model [64]. Such HABPs have now been defined as immune protection-inducing protein structures (IMPIPS) and some of them are strong candidates for a multi-antigen, multi-stage, subunit-based anti-*P. falciparum* vaccine [65]. The ~40 proteins identified in *P. vivax* could play important roles during reticulocyte invasion [41]; *Pv*DBP [60], *Pv*MSP1 [66], *Pv*RBP1 [67] and *Pv*AMA1 [50] HABPs had only been identified to date but now *Pv*RON2 and *Pv*RON4 can be added to the list.


*Both* Pv*RON2 regions had a high affinity interaction with* Pv*AMA1 domain II and III*

Previous *P. falciparum* and *T. gondii* immunoprecipitation and confocal microscopy studies have defined an AMA1-RON2-RON4-RON5 macromolecular complex participating in MJ formation (plus RON8 in *T. gondii*). Studies about this complex's stability in denaturing conditions (including sodium dodecyl sulphate) have shown that only the interaction between AMA1 and RON2 is maintained [5]. It has been reported that a 39-residue-long peptide derived from *Pf*RON2, *Tg*RON2 and *Pv*RON2 externally-exposed regions specifically interacts with the AMA1 hydrophobic groove [14; 15; 16].

SPR was used for determining the parameters for *Pv*RON2-RI and *Pv*RON2-RII (immobilised ligands) binding to *Pv*AMA1, *Pv*AMA-DI-II, *Pv*AMA-DII-III, *Pv*RON4 and *Pv*RON5 (as analytes). Equilibrium binding constant (kD) was calculated from association rate constant ($k_{on}$) and dissociation rate constant ($k_{off}$); both *Pv*RON2-RI and *Pv*RON2-RII both bound specifically to *Pv*AMA1 domains II and III (i.e. *Pv*AMA-DII-III) with kD of 11.7nM and 19.8nM, respectively (Figure 4, Table 1), indicating both *Pv*RON2 regions could independently establish a specific interaction with *Pv*AMA1, having greater affinity for *Pv*AMA-DII-III than for the whole *Pv*AMA1 ectodomain or *Pv*AMA-DI-II (Table 1).

Previous structural work concerning *P. falciparum*, *P. vivax* and *T. gondii* AMA1 relationship with RON2 has convincingly shown AMA1 domain II loop and some domain I residues participating in interaction with RON2 located in the carboxyl terminal extreme (RON2sp1) [14; 15; 16]. Such data has led to establishing that the domain II loop causes an important conformational change, revealing a RON2 binding site and becomes responsible for complex stability during invasion [68]. It should be stressed that even though *Pv*RON2-RII (containing *Pv*RON2sp1 binding to *Pv*AMA1) [15] bound specifically to *Pv*AMA1 (1.74µM kD) (Table 1) in the present work, such interaction had less affinity than that reported for the *Pv*RON2sp1-*Pv*AMA1 complex (50nM kD) [15]. However, a stronger interaction was found for *Pv*AMA-DII-III with *Pv*RON2, suggesting other *Pv*AMA1 regions' participation in the interaction with *Pv*RON2. It should also be stressed that another *Pv*RON2 functional region located towards the central region participates in interaction with reticulocytes (Figure 2) and also interacts strongly with *Pv*AMA1 (Figure 4, Table 1), as also proposed for *P. falciparum* [35].

Guided by *Pf*AMA1-*Pf*RON2 structural studies, where some *Pf*AMA1 (Phe183 and Tyr234) residues were seen to be key elements in the interaction with *Pf*RON2sp1 [16], the *Pv*AMA1

Phe128 or Tyr179 homologous residues' functional importance was evaluated regarding interaction with $Pv$RON2-RI and $Pv$RON2-RII. Two soluble recombinant proteins were generated and purified by affinity chromatography (Supplementary Material). Both mutant recombinant proteins were then used as analytes against $Pv$RON2-RI or $Pv$RON2-RII immobilised on sensor chip. Interestingly, both $Pv$AMA1 mutants displayed an order of magnitude increase in binding by SPR ($10^{-7}$ kD vs $10^{-8}$ kD) (Table 1), which suggested that such residues are not essential for the interaction with $Pv$RON2, as opposed to what has been reported for their $P.$ $falciparum$ counterparts ($Pf$AMA1-$Pf$RON2) [16].

It was found that both $Pv$RON2 regions interacted with $Pv$RON4 and $Pv$RON5 but with lower affinity than that reported for interaction with $Pv$AMA-DII-III. Previous $T.$ $gondii$ studies have shown that $Tg$RON5 stabilised $Tg$RON2 and that a loss of TgRON4 significantly reduced $Tg$RON5 and $Tg$RON2 levels. Although it is not clear during which process such interaction might occur, the three proteins were located in the same compartment and released together during invasion. This does not rule out a transitory interaction during their stay in the rhoptry necks and subsequent organisation in host cell cytosol.

Altogether, these results highlight $Pv$RON2 and $Pv$RON4 importance in active $P.$ $vivax$ receptor-ligand and protein-protein complex formation as they could be key elements during parasite invasion. It was clear that $P.$ $vivax$ functional regions could be different to those involved in $P.$ $falciparum$, despite these proteins' conservation in most Apicomplexa; this highlights important implications for designing an effective synthetic vaccine against $P.$ $vivax$.

**Experimental procedures**

*Recombinant plasmids*

A gene fragment encoding a *Pv*RON4 region (residues 403-680) and two fragments encoding *Pv*RON2 (residues 957-1288 encoding RI and residues 1850-2085 RII) were amplified from *Plasmodium vivax* VCG-I strain complementary DNA (cDNA) for *Pv*RON4 and *Pv*RON2 expression as recombinant proteins in *E. coli* or expression on COS-7 cell membrane (American Type Culture Collection CRL-1651). Gene specific primers were designed using *pvron4* (PVX_091434) and *pvron2* cDNA sequences (PVX_117880) available in PlasmoDB as template [69]. A KAPA HiFi HotStart ReadyMix PCR kit was used for amplifying each fragment at 25 µL final reaction volume, containing 12.5 µL 2x KAPA HiFi Ready Mix, 1.5 µL of each primer (Supplementary Table S1) at 5 µM and 7.5 µL of nuclease-free water. The amplification conditions for the three products consisted of one 5-min cycle at 95°C, followed by 35 cycles lasting 20 sec at 98°C, 45 sec at 56°C for *Pv*RON2 fragments or 60°C for *Pv*RON4 fragments and 2 min at 72°C with a final extension cycle lasting 5 min at 72°C.

Purified products were digested with PvuII and ApaI restriction enzymes and cloned in pRE4 vector [48] in frame with the HSVgD signal sequence and transmembrane segment [59] to express these fragments on COS-7 cell membrane or digested with BamHI and SalI for *Pv*RON4 or BamHI and PstI for the *Pv*RON2-RII fragment. They were then cloned in pQE30 in frame with a histidine tag at the N-terminal to be expressed in *E. coli* whilst the *Pv*RON2-RI amplified product was cloned in pEXP5-CT/TOPO expression vector using TOPO TA cloning in frame with a histidine tag at the C-terminus. Each construct was transformed in JM109 cells and selected on Luria Bertani (LB) plates containing ampicillin and confirmed

by sequencing. Only the *Pv*RON2-RI plasmid was used to transform BL21DE3 cells and selected on LB plus ampicillin. The resulting plasmids were labelled pRE4-*Pv*RON4, pRE4-*Pv*RON2RI, pRE4-*Pv*RON2RII, pQE30-*Pv*RON4, pQE30-*Pv*RON2RII and pEXP5-*Pv*RON2RI.

Recombinant plasmids encoding *Pv*AMA1 ectodomain, domain I and II (*Pv*AMA1-DI-II), domain II and III (*Pv*AMA-DII-III) and the C-terminal fragment of *Pv*RON5 were taken from previous studies to express such fragments in *E. coli* [46; 50]. The pHVDR22 plasmid was used to express the Duffy-binding region II on COS7 cell membrane as positive control (*Pv*DBP-RII) [59].

*Transfecting COS7 cells and immunofluorescence assays*

COS-7 cells were cultured in Dulbecco-Modified Eagle Medium (DMEM) with 10% FCS in a humidified 5% CO2 incubator at 37°C. All transfection experiments involved using $3 \times 10^4$ cells seeded in 3.5-cm diameter wells (40%-60% confluent) and then transfected with 300ng of each recombinant plasmid using FuGENE HD transfection reagent (Promega), following the manufacturer's protocol. Transfected cells grown on coverslips were washed with phosphate buffered saline (PBS) and the immunofluorescence assay was done as described in previous studies [50; 59]. Fluorescence was visualised by fluorescence microscope (Olympus BX51) using an Olympus DP2 camera and Fiji software. Transfection efficiency (%) was calculated as total amount of fluorescent COS-7 cells x 100 / total amount of COS-7 cells counted in 30 fields, as described previously [70].

*Rosetting assays*

Human UCB RBC, containing about 5%-7% reticulocytes ($Fya^+Fyb^-$), were washed three times in PBS (pH 7.4) and then treated with neuraminidase, chymotrypsin or trypsin, as

described earlier [71]. Briefly, an erythrocyte suspension (60% haematocrit) was incubated at 37°C for 60 min with either neuraminidase (150µU/mL; ICN 900-67-6), trypsin (1mg/mL; Sigma T-1005) or chymotrypsin (1mg/mL; Sigma C-4129). Erythrocytes were then washed twice by spinning with PBS at 2,500×$g$ for 5 min. Untreated RBC having Fya$^+$Fyb$^+$; Fya$^-$Fyb$^+$; Fya$^+$Fyb$^-$; Fya$^-$Fyb$^-$ Duffy phenotypes were used for binding assays. The UCB used in this study came from Bogotá's Instituto Distrital de Ciencia, Biotecnología e Innovación en Salud (IDCBIS).

COS-7 cells, 48 hr after transfection with pRE4-$Pv$RON4 or pHVDR22 plasmids, were tested for binding to normal, neuraminidase-treated, chymotrypsin-treated and trypsin-treated human UCB RBC (10%) or reticulocyte-depleted erythrocytes (10% haematocrit) from peripheral blood without any treatment for 2 hr at 37°C. Competition assays involved UCB (10%) pre-incubated with 10 µL peptide 40305 (1mg/mL) for 1 hr at 37°C followed by two washes with incomplete DMEM and then added to transfected COS-7 cells, as previously described [50]. COS-7 cells with adherent erythrocytes or normocytes (i.e. rosettes) were scored in 20 randomly-chosen fields at 200× magnification. Rosettes were considered positive when adherent erythrocytes covered more than 50% of COS-7 cell surface. COS-7 cells expressing $Pv$DBP-RII on membrane were used as positive control [59] whilst the same cells but incubated with chymotrypsin-treated RBC or non-transfected cells were used as negative control. At least three independent experiments were performed with replicates.

*Obtaining and purifying recombinant proteins*

*E. coli* (JM109) transformed with pQE30-$Pv$AMA-1, pQE30-$Pv$AMA-DI-II, pQE30-$Pv$AMA-DII-III, pQE30-$Pv$RON4 or pQE30-$Pv$RON2RII and *E. coli* BL21DE3 strain

transformed with pEXP5-*Pv*RON2RI or M15 cells transformed with pQE30-rRON5 were grown in 25 mL LB broth supplemented with 0.1 mg/mL ampicillin (JM109-BL21DE3-M15 cells), 25 μg/mL kanamycin (M15 cells) and 0.1% D-glucose for 12 hr at 37°C with constant shaking. This starting culture was used to inoculate 475 mL LB broth containing 0.1 mg/mL ampicillin, 25 μg/mL kanamycin and 0.1% D-glucose maintained at 37°C with constant shaking until reaching 0.6–0.8 optical density (OD) at 620 nm. Recombinant protein expression was induced with isopropyl β-D1-thiogalactopyranoside (IPTG) at 1 mM final concentration.

Recombinant proteins r*Pv*AMA-1, r*Pv*AMA1-DI-II and r*Pv*AMA1-DII-III were obtained in soluble form, following previously described conditions [50]; r*Pv*RON4, r*Pv*RON5, r*Pv*RON2-RI and r*Pv*RON2-RII were expressed and purified according to a previous study [46], with some modifications. Briefly, 4-5 hr after IPTG induction, cell cultures were spun at 10,000×g for 30 min at 4°C and the bacterial pellet containing the protein in inclusion bodies was washed twice with buffer A (20 mM Tris–HCl pH 8.0, 1 mM EDTA, 1 mM iodoacetamide, 1 mM PMSF and 1 μg/mL leupeptin) supplemented with lysozyme, followed by cell disruption using a sonicator (Branson); 20 mM EDTA, 2% Triton X100 and 0.5 M NaCl were then added. Inclusion bodies were recovered by spinning at 10,000×g for 30 min at 4°C and washed once with buffer A. The recombinant protein was then solubilised with lysis buffer containing 10 mM Tris–HCl, 100 mM NaH$_2$PO$_4$, 4 M urea, 10 mM imidazole and 10% glycerol. Western blot, using an anti-polyhistidine monoclonal antibody (Sigma), was used for recognising recombinant proteins in supernatant.

The supernatant was incubated with nickel-nitrilotriacetic acid (Ni$^{2+}$-NTA) agarose resin for purifying recombinant proteins by affinity chromatography. Bound protein was eluted with

increasing imidazole gradients (50-500 mM). The eluates were analysed on SDS-PAGE and by western Blot and the fractions containing the recombinant protein having a clear single band were pooled. Soluble proteins and those obtained with urea were exhaustively dialysed against 1X PBS. Protein concentration was determined using the BioRad protein assay system (Bicinchoninic Acid Kit) and a standard bovine serum albumin (BSA) curve.

Pv*RON2- and* Pv*RON4-derived peptide synthesis and purification*

Twenty-residue-long, non-overlapping peptides derived from *Pv*RON4 (15 peptides) and *Pv*RON2 (17 peptides) sequences (Supplementary Material) were chemically synthesised using solid-phase, multiple peptide synthesis, 4-methylbenzhydrylamine hydrochloride resin (0.5 meq/g), and t-Boc protected amino acids (Bachem) [72; 73]. The synthetic peptides were cleaved using low-high hydrogen fluoride cleavage. Peptides having greater than 99% purity were obtained by combining analytical reversed-phase high-performance liquid chromatography (RP-HPLC), semi-preparative RP-HPLC and matrix-assisted laser desorption/ionisation time-of-flight mass spectrometry (MALDI-ToF MS) (Bruker Daltonics).

*Radiolabelling recombinant proteins and synthetic peptides*

Briefly, 15µg *Pv*RON2-RI or *Pv*RON2-RII recombinant proteins were radiolabelled with 4 µL de Na$^{125}$I (100 mCi/mL; ARC) and Iodination Beads (Pierce-Thermo Scientific), following the manufacturer's instructions. Following 12 minutes' incubation, radiolabelled recombinant proteins were separated by solution throughout on a SigmaSpin column; 3 µL - Na$^{125}$I (100 mCi/mL; ARC) and 25 µL chloramine T (2.75 mg/mL) were used for radiolabelling the synthetic peptides. The reaction was stopped after 15 min by adding 25 µL

sodium metabisulphite (2.3 mg/mL), as described previously [74]. Radiolabelled peptides were separated by size-exclusion chromatography on a Sephadex G-25 column (Pharmacia). Each eluted fraction was then analysed by gamma counter (Packard Cobra II).

*Radiolabelling proteins and peptide binding assays*

Briefly, $2 \times 10^7$ UCB RBC were incubated at room temperature (RT) for 90 min with different concentrations of each radiolabelled recombinant protein (0-400nM) or radiolabelled peptide (0–800 nM) in the absence (total binding) or presence (non-specific binding) of the same unlabelled recombinant protein or unlabelled peptide (200 μL final volume). Competition assays involved adding each *Pv*RON4 and *Pv*RON2-RI-derived synthetic peptide (Supplementary Material), at a 1:100 (labelled protein:unlabelled peptide) molar ratio. Following incubation, cells were washed twice with HBS and the amount of cell-bound radiolabelled recombinant protein or peptide was quantified on an automatic gamma counter.

Peptides' specific binding activity was evaluated in a binding assay with enzyme-treated UCB RBC; $2 \times 10^7$ untreated RBC and trypsin-, chymotrypsin- or neuraminidase-treated RBC were incubated at RT for 90 min with 400 nM of each radiolabelled peptide in the absence or presence of the same unlabelled peptide, as described previously [74].

*Flow cytometry binding assays*

Flow cytometry assays were carried out according to previously described protocols [50; 75]. Briefly, 25 μg *Pv*RON4 or *Pv*RON2-RI recombinant protein were incubated with 5% UCB RBC and then incubated with antibodies against the transferrin receptor (CD71) on reticulocytes, against cluster of differentiation 45 (CD45) in leukocytes (some activated

leukocytes are CD71$^+$, but reticulocytes are CD45$^-$, so the reticulocyte population selected was CD71$^+$ CD45$^-$) and antibodies against the 6X-His-tag in recombinant proteins. UCB RBC were pre-incubated with peptides before adding recombinant protein for competition assays with peptides 40305 and 40595. The events were acquired on a FACSCanto II (BD Bioscience); results were analysed using FlowJo software (TreeStar). DBP-RII recombinant soluble protein was used as positive binding control and DBP-RIII-IV as negative control. At least three independent experiments were performed with different UCB samples.

*Surface plasmon resonance (SPR)*

SPR involved using BIACORE 3000 system (Uppsala, Sweden), sensor chip CM5 (GE Healthcare Life Sciences), surfactant P20 and amine coupling kit containing N-hydroxysuccinimide (NHS) and N-Ethyl-N'-dimethylaminopropyl carbodiimide (EDC). All biosensor assays were performed with HEPES-buffered saline (HBS-P) as running buffer (10 mM HEPES, 150mM sodium acetate, 3mM magnesium acetate, 0.005% surfactant P20 and 5mM CaCl2, pH 7.4). Compounds were dissolved in running buffer. Immobilisations were performed by injecting 40 µL *Pv*RON2-RI and *Pv*RON2-RII (100 µg/mL in formate buffer, pH 4.3) onto a CM5 sensor chip's activated surface by EDC/NHS, giving 300 RU (*Pv*RON2-RI) and 1,500 (*Pv*RON2-RII) RU signal, followed by 20 µL ethanolamine hydrochloride, pH 8.5, to saturate the matrix's free activated sites.

Increasing concentrations of each purified analyte (*Pv*AMA1, *Pv*AMA-DI-II, *Pv*AMA-DII-III, *Pv*RON4, *Pv*AMA1$^{F128A}$, *Pv*AMA1$^{Y179A}$ and *Pv*RON5) were injected at constant 30 µL/min flow rate at 25°C. The sensor chip surface was regenerated after each experiment by injecting 20 µL 10mM HCl. BIAeval 4.1 software was used for calculating kinetic

parameters. A simple Langmuir binding model was used for overall analysis. The specific binding profiles were obtained after subtracting the response signal from the channel control (activated/deactivated by ethanolamine). Fitting to each model was judged by reduced chi square test values and residue distribution randomness.

*Statistical analysis*

SPSS v20.0 was used for statistical analysis of RBC-binding assays. Mean values and standard deviations (SD) were calculated from the measurements of three independent experiments. Student's t-test and analysis of variance (ANOVA) were used for comparing the means of each experimental group using a 0.05 significance level for testing a stated hypothesis. Tukey's multiple comparison test was used for multiple comparison of experimental group means to those for control.

*Ethical approval and consent to participate*

All the parents of the donors of the UCB samples used here signed an informed consent form after receiving detailed information regarding the study's goals. The UCB samples were collected by Bogotá's Instituto Distrital de Ciencia, Biotecnología e Innovación en Salud (IDCBIS), following the protocols established by this institution, and in accordance with Colombian laws and regulations. All procedures were approved by FIDIC's ethics committee.

**Conflict of interest statement**

The authors declare that the research was conducted in the absence of any commercial or financial relationships that could be construed as a potential conflict of interest.

**Acknowledgements**

# References

1.	Weiss, G. E., Crabb, B. S. & Gilson, P. R. (2016). Overlaying Molecular and Temporal Aspects of Malaria Parasite Invasion. *Trends Parasitol* **32**, 284-95.

2.	Carruthers, V. B. (2002). Host cell invasion by the opportunistic pathogen Toxoplasma gondii. *Acta Trop* **81**, 111-22.

3.	Weiss, G. E., Gilson, P. R., Taechalertpaisarn, T., Tham, W. H., de Jong, N. W., Harvey, K. L., Fowkes, F. J., Barlow, P. N., Rayner, J. C., Wright, G. J., Cowman, A. F. & Crabb, B. S. (2015). Revealing the sequence and resulting cellular morphology of receptor-ligand interactions during Plasmodium falciparum invasion of erythrocytes. *PLoS Pathog* **11**, e1004670.

4.	Aikawa, M., Miller, L. H., Johnson, J. & Rabbege, J. (1978). Erythrocyte entry by malarial parasites. A moving junction between erythrocyte and parasite. *J Cell Biol* **77**, 72-82.

5.	Besteiro, S., Michelin, A., Poncet, J., Dubremetz, J. F. & Lebrun, M. (2009). Export of a Toxoplasma gondii rhoptry neck protein complex at the host cell membrane to form the moving junction during invasion. *PLoS Pathog* **5**, e1000309.

6.	Straub, K. W., Cheng, S. J., Sohn, C. S. & Bradley, P. J. (2009). Novel components of the Apicomplexan moving junction reveal conserved and coccidia-restricted elements. *Cell Microbiol* **11**, 590-603.

7.	Alexander, D. L., Mital, J., Ward, G. E., Bradley, P. & Boothroyd, J. C. (2005). Identification of the moving junction complex of Toxoplasma gondii: a collaboration between distinct secretory organelles. *PLoS Pathog* **1**, e17.

8.	Collins, C. R., Withers-Martinez, C., Hackett, F. & Blackman, M. J. (2009). An inhibitory antibody blocks interactions between components of the malarial invasion machinery. *PLoS Pathog* **5**, e1000273.

9.	Lamarque, M., Besteiro, S., Papoin, J., Roques, M., Vulliez-Le Normand, B., Morlon-Guyot, J., Dubremetz, J. F., Fauquenoy, S., Tomavo, S., Faber, B. W., Kocken, C. H., Thomas, A. W., Boulanger, M. J., Bentley, G. A. & Lebrun, M. (2011). The RON2-AMA1 interaction is a critical step in moving junction-dependent invasion by apicomplexan parasites. *PLoS Pathog* **7**, e1001276.

10.	Srinivasan, P., Beatty, W. L., Diouf, A., Herrera, R., Ambroggio, X., Moch, J. K., Tyler, J. S., Narum, D. L., Pierce, S. K., Boothroyd, J. C., Haynes, J. D. & Miller, L. H. (2011). Binding of Plasmodium merozoite proteins RON2 and AMA1 triggers commitment to invasion. *Proc Natl Acad Sci U S A* **108**, 13275-80.

11.	Beck, J. R., Chen, A. L., Kim, E. W. & Bradley, P. J. (2014). RON5 is critical for organization and function of the Toxoplasma moving junction complex. *PLoS Pathog* **10**, e1004025.

12.	Straub, K. W., Peng, E. D., Hajagos, B. E., Tyler, J. S. & Bradley, P. J. (2011). The moving junction protein RON8 facilitates firm attachment and host cell invasion in Toxoplasma gondii. *PLoS Pathog* **7**, e1002007.

13.	Guerin, A., Corrales, R. M., Parker, M. L., Lamarque, M. H., Jacot, D., El Hajj, H., Soldati-Favre, D., Boulanger, M. J. & Lebrun, M. (2017). Efficient invasion by Toxoplasma depends on the subversion of host protein networks. *Nat Microbiol*.

14.	Tonkin, M. L., Roques, M., Lamarque, M. H., Pugniere, M., Douguet, D., Crawford, J., Lebrun, M. & Boulanger, M. J. (2011). Host cell invasion by apicomplexan parasites: insights from the co-structure of AMA1 with a RON2 peptide. *Science* **333**, 463-7.

15.	Vulliez-Le Normand, B., Saul, F. A., Hoos, S., Faber, B. W. & Bentley, G. A. (2017). Cross-reactivity between apical membrane antgen 1 and rhoptry neck protein 2 in P. vivax and P. falciparum: A structural and binding study. *PLoS One* **12**, e0183198.

16.	Vulliez-Le Normand, B., Tonkin, M. L., Lamarque, M. H., Langer, S., Hoos, S., Roques, M., Saul, F. A., Faber, B. W., Bentley, G. A., Boulanger, M. J. & Lebrun, M. (2012). Structural and

functional insights into the malaria parasite moving junction complex. *PLoS Pathog* **8**, e1002755.

17. Srinivasan, P., Yasgar, A., Luci, D. K., Beatty, W. L., Hu, X., Andersen, J., Narum, D. L., Moch, J. K., Sun, H., Haynes, J. D., Maloney, D. J., Jadhav, A., Simeonov, A. & Miller, L. H. (2013). Disrupting malaria parasite AMA1-RON2 interaction with a small molecule prevents erythrocyte invasion. *Nat Commun* **4**, 2261.

18. Srinivasan, P., Ekanem, E., Diouf, A., Tonkin, M. L., Miura, K., Boulanger, M. J., Long, C. A., Narum, D. L. & Miller, L. H. (2014). Immunization with a functional protein complex required for erythrocyte invasion protects against lethal malaria. *Proc Natl Acad Sci U S A* **111**, 10311-6.

19. Deans, J. A., Alderson, T., Thomas, A. W., Mitchell, G. H., Lennox, E. S. & Cohen, S. (1982). Rat monoclonal antibodies which inhibit the in vitro multiplication of Plasmodium knowlesi. *Clin Exp Immunol* **49**, 297-309.

20. Mital, J., Meissner, M., Soldati, D. & Ward, G. E. (2005). Conditional expression of Toxoplasma gondii apical membrane antigen-1 (TgAMA1) demonstrates that TgAMA1 plays a critical role in host cell invasion. *Mol Biol Cell* **16**, 4341-9.

21. Triglia, T., Healer, J., Caruana, S. R., Hodder, A. N., Anders, R. F., Crabb, B. S. & Cowman, A. F. (2000). Apical membrane antigen 1 plays a central role in erythrocyte invasion by Plasmodium species. *Mol Microbiol* **38**, 706-18.

22. Mitchell, G. H., Thomas, A. W., Margos, G., Dluzewski, A. R. & Bannister, L. H. (2004). Apical membrane antigen 1, a major malaria vaccine candidate, mediates the close attachment of invasive merozoites to host red blood cells. *Infect Immun* **72**, 154-8.

23. Yap, A., Azevedo, M. F., Gilson, P. R., Weiss, G. E., O'Neill, M. T., Wilson, D. W., Crabb, B. S. & Cowman, A. F. (2014). Conditional expression of apical membrane antigen 1 in Plasmodium falciparum shows it is required for erythrocyte invasion by merozoites. *Cell Microbiol* **16**, 642-56.

24. Diaz, S. A., Martin, S. R., Howell, S. A., Grainger, M., Moon, R. W., Green, J. L. & Holder, A. A. (2016). The Binding of Plasmodium falciparum Adhesins and Erythrocyte Invasion Proteins to Aldolase Is Enhanced by Phosphorylation. *PLoS One* **11**, e0161850.

25. Kato, K., Mayer, D. C., Singh, S., Reid, M. & Miller, L. H. (2005). Domain III of Plasmodium falciparum apical membrane antigen 1 binds to the erythrocyte membrane protein Kx. *Proc Natl Acad Sci U S A* **102**, 5552-7.

26. Urquiza, M., Suarez, J. E., Cardenas, C., Lopez, R., Puentes, A., Chavez, F., Calvo, J. C. & Patarroyo, M. E. (2000). Plasmodium falciparum AMA-1 erythrocyte binding peptides implicate AMA-1 as erythrocyte binding protein. *Vaccine* **19**, 508-13.

27. Giovannini, D., Spath, S., Lacroix, C., Perazzi, A., Bargieri, D., Lagal, V., Lebugle, C., Combe, A., Thiberge, S., Baldacci, P., Tardieux, I. & Menard, R. (2011). Independent roles of apical membrane antigen 1 and rhoptry neck proteins during host cell invasion by apicomplexa. *Cell Host Microbe* **10**, 591-602.

28. Bargieri, D. Y., Andenmatten, N., Lagal, V., Thiberge, S., Whitelaw, J. A., Tardieux, I., Meissner, M. & Menard, R. (2013). Apical membrane antigen 1 mediates apicomplexan parasite attachment but is dispensable for host cell invasion. *Nat Commun* **4**, 2552.

29. Lamarque, M. H., Roques, M., Kong-Hap, M., Tonkin, M. L., Rugarabamu, G., Marq, J. B., Penarete-Vargas, D. M., Boulanger, M. J., Soldati-Favre, D. & Lebrun, M. (2014). Plasticity and redundancy among AMA-RON pairs ensure host cell entry of Toxoplasma parasites. *Nat Commun* **5**, 4098.

30. Lopaticki, S., Maier, A. G., Thompson, J., Wilson, D. W., Tham, W. H., Triglia, T., Gout, A., Speed, T. P., Beeson, J. G., Healer, J. & Cowman, A. F. (2011). Reticulocyte and erythrocyte

binding-like proteins function cooperatively in invasion of human erythrocytes by malaria parasites. *Infect Immun* **79**, 1107-17.

31. Curtidor, H., Patino, L. C., Arevalo-Pinzon, G., Patarroyo, M. E. & Patarroyo, M. A. (2011). Identification of the Plasmodium falciparum rhoptry neck protein 5 (PfRON5). *Gene* **474**, 22-8.

32. Bradley, P. J., Ward, C., Cheng, S. J., Alexander, D. L., Coller, S., Coombs, G. H., Dunn, J. D., Ferguson, D. J., Sanderson, S. J., Wastling, J. M. & Boothroyd, J. C. (2005). Proteomic analysis of rhoptry organelles reveals many novel constituents for host-parasite interactions in Toxoplasma gondii. *J Biol Chem* **280**, 34245-58.

33. Cao, J., Kaneko, O., Thongkukiatkul, A., Tachibana, M., Otsuki, H., Gao, Q., Tsuboi, T. & Torii, M. (2009). Rhoptry neck protein RON2 forms a complex with microneme protein AMA1 in Plasmodium falciparum merozoites. *Parasitol Int* **58**, 29-35.

34. Alexander, D. L., Arastu-Kapur, S., Dubremetz, J. F. & Boothroyd, J. C. (2006). Plasmodium falciparum AMA1 binds a rhoptry neck protein homologous to TgRON4, a component of the moving junction in Toxoplasma gondii. *Eukaryot Cell* **5**, 1169-73.

35. Hossain, M. E., Dhawan, S. & Mohmmed, A. (2012). The cysteine-rich regions of Plasmodium falciparum RON2 bind with host erythrocyte and AMA1 during merozoite invasion. *Parasitol Res* **110**, 1711-21.

36. Counihan, N. A., Kalanon, M., Coppel, R. L. & de Koning-Ward, T. F. (2013). Plasmodium rhoptry proteins: why order is important. *Trends Parasitol* **29**, 228-36.

37. Remarque, E. J., Faber, B. W., Kocken, C. H. & Thomas, A. W. (2008). Apical membrane antigen 1: a malaria vaccine candidate in review. *Trends Parasitol* **24**, 74-84.

38. Howes, R. E., Battle, K. E., Mendis, K. N., Smith, D. L., Cibulskis, R. E., Baird, J. K. & Hay, S. I. (2016). Global Epidemiology of Plasmodium vivax. *Am J Trop Med Hyg* **95**, 15-34.

39. Pico de Coana, Y., Rodriguez, J., Guerrero, E., Barrero, C., Rodriguez, R., Mendoza, M. & Patarroyo, M. A. (2003). A highly infective Plasmodium vivax strain adapted to Aotus monkeys: quantitative haematological and molecular determinations useful for P. vivax malaria vaccine development. *Vaccine* **21**, 3930-7.

40. Bozdech, Z., Mok, S., Hu, G., Imwong, M., Jaidee, A., Russell, B., Ginsburg, H., Nosten, F., Day, N. P., White, N. J., Carlton, J. M. & Preiser, P. R. (2008). The transcriptome of Plasmodium vivax reveals divergence and diversity of transcriptional regulation in malaria parasites. *Proc Natl Acad Sci U S A* **105**, 16290-5.

41. Patarroyo, M. A., Calderon, D. & Moreno-Perez, D. A. (2012). Vaccines against Plasmodium vivax: a research challenge. *Expert Rev Vaccines* **11**, 1249-60.

42. Moreno-Perez, D. A., Degano, R., Ibarrola, N., Muro, A. & Patarroyo, M. A. (2014). Determining the Plasmodium vivax VCG-1 strain blood stage proteome. *J Proteomics* **113C**, 268-280.

43. Venkatesh, A., Patel, S. K., Ray, S., Shastri, J., Chatterjee, G., Kochar, S. K., Patankar, S. & Srivastava, S. (2016). Proteomics of Plasmodium vivax malaria: new insights, progress and potential. *Expert Rev Proteomics* **13**, 771-82.

44. Arevalo-Pinzon, G., Curtidor, H., Patino, L. C. & Patarroyo, M. A. (2011). PvRON2, a new Plasmodium vivax rhoptry neck antigen. *Malar J* **10**, 60.

45. Arevalo-Pinzon, G., Curtidor, H., Abril, J. & Patarroyo, M. A. (2013). Annotation and characterization of the Plasmodium vivax rhoptry neck protein 4 (PvRON4). *Malar J* **12**, 356.

46. Arevalo-Pinzon, G., Bermudez, M., Curtidor, H. & Patarroyo, M. A. (2015). The Plasmodium vivax rhoptry neck protein 5 is expressed in the apical pole of Plasmodium vivax VCG-1 strain schizonts and binds to human reticulocytes. *Malar J* **14**, 106.

47. Buitrago, S. P., Garzon-Ospina, D. & Patarroyo, M. A. (2016). Size polymorphism and low sequence diversity in the locus encoding the Plasmodium vivax rhoptry neck protein 4 (PvRON4) in Colombian isolates. *Malar J* **15**, 501.

48. Cohen, G. H., Wilcox, W. C., Sodora, D. L., Long, D., Levin, J. Z. & Eisenberg, R. J. (1988). Expression of herpes simplex virus type 1 glycoprotein D deletion mutants in mammalian cells. *J Virol* **62**, 1932-40.

49. Miller, L. H., Mason, S. J., Clyde, D. F. & McGinniss, M. H. (1976). The resistance factor to Plasmodium vivax in blacks. The Duffy-blood-group genotype, FyFy. *N Engl J Med* **295**, 302-4.

50. Arevalo-Pinzon, G., Bermudez, M., Hernandez, D., Curtidor, H. & Patarroyo, M. A. (2017). Plasmodium vivax ligand-receptor interaction: PvAMA-1 domain I contains the minimal regions for specific interaction with CD71+ reticulocytes. *Sci Rep* **7**, 9616.

51. Baquero, L. A., Moreno-Perez, D. A., Garzon-Ospina, D., Forero-Rodriguez, J., Ortiz-Suarez, H. D. & Patarroyo, M. A. (2017). PvGAMA reticulocyte binding activity: predicting conserved functional regions by natural selection analysis. *Parasit Vectors* **10**, 251.

52. Ntumngia, F. B., Thomson-Luque, R., Torres Lde, M., Gunalan, K., Carvalho, L. H. & Adams, J. H. (2016). A Novel Erythrocyte Binding Protein of Plasmodium vivax Suggests an Alternate Invasion Pathway into Duffy-Positive Reticulocytes. *MBio* **7**.

53. Duraisingh, M. T., Triglia, T., Ralph, S. A., Rayner, J. C., Barnwell, J. W., McFadden, G. I. & Cowman, A. F. (2003). Phenotypic variation of Plasmodium falciparum merozoite proteins directs receptor targeting for invasion of human erythrocytes. *EMBO J* **22**, 1047-57.

54. DeSimone, T. M., Jennings, C. V., Bei, A. K., Comeaux, C., Coleman, B. I., Refour, P., Triglia, T., Stubbs, J., Cowman, A. F. & Duraisingh, M. T. (2009). Cooperativity between Plasmodium falciparum adhesive proteins for invasion into erythrocytes. *Mol Microbiol* **72**, 578-89.

55. Duraisingh, M. T., Maier, A. G., Triglia, T. & Cowman, A. F. (2003). Erythrocyte-binding antigen 175 mediates invasion in Plasmodium falciparum utilizing sialic acid-dependent and -independent pathways. *Proc Natl Acad Sci U S A* **100**, 4796-801.

56. Gilberger, T. W., Thompson, J. K., Triglia, T., Good, R. T., Duraisingh, M. T. & Cowman, A. F. (2003). A novel erythrocyte binding antigen-175 paralogue from Plasmodium falciparum defines a new trypsin-resistant receptor on human erythrocytes. *J Biol Chem* **278**, 14480-6.

57. Barnwell, J. W., Nichols, M. E. & Rubinstein, P. (1989). In vitro evaluation of the role of the Duffy blood group in erythrocyte invasion by Plasmodium vivax. *J Exp Med* **169**, 1795-802.

58. Takemae, H., Sugi, T., Kobayashi, K., Gong, H., Ishiwa, A., Recuenco, F. C., Murakoshi, F., Iwanaga, T., Inomata, A., Horimoto, T., Akashi, H. & Kato, K. (2013). Characterization of the interaction between Toxoplasma gondii rhoptry neck protein 4 and host cellular beta-tubulin. *Sci Rep* **3**, 3199.

59. Chitnis, C. E. & Miller, L. H. (1994). Identification of the erythrocyte binding domains of Plasmodium vivax and Plasmodium knowlesi proteins involved in erythrocyte invasion. *J Exp Med* **180**, 497-506.

60. Ocampo, M., Vera, R., Eduardo Rodriguez, L., Curtidor, H., Urquiza, M., Suarez, J., Garcia, J., Puentes, A., Lopez, R., Trujillo, M., Torres, E. & Patarroyo, M. E. (2002). Plasmodium vivax Duffy binding protein peptides specifically bind to reticulocytes. *Peptides* **23**, 13-22.

61. Ovchynnikova, E., Aglialoro, F., Bentlage, A. E. H., Vidarsson, G., Salinas, N. D., von Lindern, M., Tolia, N. H. & van den Akker, E. (2017). DARC extracellular domain remodeling in maturating reticulocytes explains Plasmodium vivax tropism. *Blood* **130**, 1441-1444.

62. Rodriguez, L. E., Curtidor, H., Urquiza, M., Cifuentes, G., Reyes, C. & Patarroyo, M. E. (2008). Intimate molecular interactions of P. falciparum merozoite proteins involved in invasion of red blood cells and their implications for vaccine design. *Chem Rev* **108**, 3656-705.

63. Curtidor, H., Vanegas, M., Alba, M. P. & Patarroyo, M. E. (2011). Functional, immunological and three-dimensional analysis of chemically synthesised sporozoite peptides as components of a fully-effective antimalarial vaccine. *Curr Med Chem* **18**, 4470-502.

64. Curtidor, H., Patarroyo, M. E. & Patarroyo, M. A. (2015). Recent advances in the development of a chemically synthesised anti-malarial vaccine. *Expert Opin Biol Ther* **15**, 1567-81.

65. Patarroyo, M. E., Bermudez, A., Alba, M. P., Vanegas, M., Moreno-Vranich, A., Poloche, L. A. & Patarroyo, M. A. (2015). IMPIPS: the immune protection-inducing protein structure concept in the search for steric-electron and topochemical principles for complete fully-protective chemically synthesised vaccine development. *PLoS One* **10**, e0123249.

66. Rodriguez, L. E., Urquiza, M., Ocampo, M., Curtidor, H., Suarez, J., Garcia, J., Vera, R., Puentes, A., Lopez, R., Pinto, M., Rivera, Z. & Patarroyo, M. E. (2002). Plasmodium vivax MSP-1 peptides have high specific binding activity to human reticulocytes. *Vaccine* **20**, 1331-9.

67. Urquiza, M., Patarroyo, M. A., Mari, V., Ocampo, M., Suarez, J., Lopez, R., Puentes, A., Curtidor, H., Garcia, J., Rodriuez, L. E., Vera, R., Torres, A., Laverde, M., Robles, A. P. & Patarroyo, M. E. (2002). Identification and polymorphism of Plasmodium vivax RBP-1 peptides which bind specifically to reticulocytes. *Peptides* **23**, 2265-77.

68. Delgadillo, R. F., Parker, M. L., Lebrun, M., Boulanger, M. J. & Douguet, D. (2016). Stability of the Plasmodium falciparum AMA1-RON2 Complex Is Governed by the Domain II (DII) Loop. *PLoS One* **11**, e0144764.

69. PlasmoDB: Plasmodium genomics resource.

70. Gao, X., Yeo, K. P., Aw, S. S., Kuss, C., Iyer, J. K., Genesan, S., Rajamanonmani, R., Lescar, J., Bozdech, Z. & Preiser, P. R. (2008). Antibodies targeting the PfRH1 binding domain inhibit invasion of Plasmodium falciparum merozoites. *PLoS Pathog* **4**, e1000104.

71. Curtidor, H., Patino, L. C., Arevalo-Pinzon, G., Vanegas, M., Patarroyo, M. E. & Patarroyo, M. A. (2014). Plasmodium falciparum rhoptry neck protein 5 peptides bind to human red blood cells and inhibit parasite invasion. *Peptides* **53**, 210-7.

72. Merrifield, R. B. (1963). Solid phase peptide synthesis. I. The synthesis of a tetrapeptide. *Journal of American Chemical Society* **85**, 2149 - 2154.

73. Houghten, R. A. (1985). General method for the rapid solid-phase synthesis of large numbers of peptides: specificity of antigen-antibody interaction at the level of individual amino acids. *Proc Natl Acad Sci U S A* **82**, 5131-5.

74. Arevalo-Pinzon, G., Curtidor, H., Munoz, M., Suarez, D., Patarroyo, M. A. & Patarroyo, M. E. (2013). Rh1 high activity binding peptides inhibit high percentages of *Plasmodium falciparum* FVO strain invasion. *Vaccine* **31**, 1830-7.

75. Moreno-Perez, D. A., Baquero, L. A., Chitiva-Ardila, D. M. & Patarroyo, M. A. (2017). Characterising PvRBSA: an exclusive protein from Plasmodium species infecting reticulocytes. *Parasit Vectors* **10**, 243.

**Figure legends**

**Figure 1.** *Pv*RON4 binding to RBCs. **(a).** *Pv*RON2 and *Pv*RON4 schematic representation. Each protein's main characteristics are shown. Signal sequence (dark blue), transmembrane domains (black), coiled-coil domains (grey) and cysteine residues conserved amongst *P. vivax* strains (dotted red lines) [44; 45]. The locations are shown of two *Pv*RON2 fragments (*Pv*RON2-RI and *Pv*RON2-RII) and one *Pv*RON4 fragment, which were cloned in vectors to be expressed in COS-7 cells and *E. coli*. **(b).** *Pv*DBPRII and *Pv*RON4 expression and location on COS-7 eukaryote cell surface. Above: Green shows expressed proteins and blue shows DAPI-stained cell nuclei. Transfection efficiency was ~5% which was used for normalising the rosetting data. Below: an example of a rosette indicating RBC bound to COS-7 cell surface. **(c).** Rosette formation assay. Computation of the amount of rosettes counted in 20 fields using UCB RBC from different Duffy phenotypes with COS-7 cells transfected with *Pv*DBPRII or *Pv*RON4. A rosette assay involving normocytes having $Fya^+Fyb^-$ phenotype was also included **(d).** Enzyme treatment assays. The amount of rosettes formed between cells transfected with *Pv*DBPRII or *Pv*RON4 and UCB RBC treated with different enzymes is shown. All rosetting assays were performed three times in triplicate.

**Figure 2.** *Pv*RON2-RI and *Pv*RON4 proteins interacted specifically with $CD71^+$ reticulocytes. (a) *Pv*RON2 and *Pv*RON4 expression and specific binding to UCB RBC. Left-hand side: protein recognition by western blot (1) with monoclonal anti-histidine antibody and Coomassie blue staining (2) after the purification of the three proteins obtained in *E. coli*. Right-hand side: specific binding assays. All recombinant proteins were radio-labelled with $Na^{125}I$ and made to compete for binding to UCB RBC in the absence (total binding) or presence of the same non-radio-labelled protein (non-specific binding). A specific binding curve was obtained from the two curves. CPM: counts per minute. Data is shown as the mean values (± SD) of at least 3 independent experiments. (b) *Pv*RON2-RI and *Pv*RON4 binding to $CD71^+ CD45^-$ as measured by flow cytometry. Dot plots show the evaluated recombinant proteins' binding to a $CD71^+ CD45^-$ reticulocyte population. Binding was detected by a PE-conjugated monoclonal anti-histidine antibody. The percentage obtained for negative control (cells without recombinant protein) was subtracted from each binding assay. The bar graph

represents each protein's average binding to $CD71^+CD45^-$ cells obtained in three assays performed in triplicate.

**Figure 3.** Ascertaining *Pv*RON2-RI and *Pv*RON4 RBC binding regions. (a) Competition assays between synthetic peptides and *Pv*RON4 recombinant protein (left) or *Pv*RON2-RI (right) regarding RBC binding. RBC binding percentage in the absence (100% binding) or presence of each synthetic peptide covering each recombinant protein complete sequence (inhibition). Peptides were numbered according to our institute's serial system. Data is shown as mean values (±SD) regarding at least 3 independent experiments. (b) Determining *Pv*RON4 and *Pv*RON2 HABPs and competition studies. *Pv*RON4-derived peptides 40305 and 40313 and *Pv*RON2-RI-derived 40592 and 40595 binding profiles. Horizontal black bar length indicates each peptide's specific binding activity. The location of each sequence in *Pv*RON4 or *Pv*RON2 is also shown in superscript. Peptides having specific binding activity equal to or greater than 2% were considered HABPs [62]. (c) Flow cytometry competition assays. Dot plots of *Pv*RON4 or *Pv*RON2-RI binding to $CD71^+CD45^-$ cells in the presence of HABPs 40305 and 40595. Inhibition percentages are indicated regarding protein total binding (100%). (d) Peptide 40305 inhibition of rosette formation on COS-7 cells transfected with *Pv*RON4.

**Figure 4.** Measuring *Pv*RON2-RI and *Pv*RON2-RII interactions with *Pv*AMA-DII-III by surface plasmon resonance. (a) Sensorgrams showing *Pv*AMA-DII-III (analyte) binding to *Pv*RON2-RI (immobilised). *Pv*AMA-DII-III concentrations are indicated for each curve (nM). (b). Sensorgrams showing *Pv*AMA-DII-III (analyte) binding to *Pv*RON2-RII (immobilised), *Pv*AMA-DII-III with concentrations indicated.

**Supplementary Material**

**Figure S1.** Aligning *Pf*RON4, *Pv*RON4 and *Tg*RON4 amino acid sequences. Grey shows the carboxyl-terminal region; black shows the sterease/lipase domain in just *Pf*RON4 and *Pv*RON4 sequences. Aligned sequences' access codes: PlasmoDB accession numbers PF3D7_1116000 for *Pf*RON4, PVX_091434 for *Pv*RON4 and ToxoDB accession number TGME49_229010 for *Tg*RON4.

**Figure S2.** *Pv*AMA1-F128A and *Pv*AMA1-Y179A mutant protein expression and purification. Four primers (A, B, C and D) were designed for amplifying mutant fragments; B and C contained mutations for changing F128A (mutant 1) or Y179A (mutant 2) (Table S1). A Taq polymerase KAPA HiFi HotStart (Kapa Biosystems) kit was used for amplifying the mutants, according to the manufacturer's recommendations, and VCG-1 strain DNA. Two initial PCRs were run for each mutant to amplify F1 (primers A-B) and F2 products (primers C-D). 1μL of each fragment (FI and FII) in 1/10 dilution was used as template for obtaining the *Pv*AMA1 construct with the specific mutation. Each purified product was ligated in pEXP5-CT/TOPO vector by TOPO TA cloning. Each construct confirmed by sequencing was used for transforming *E. coli* BL21DE3. Expression was achieved after IPTG induction. The protein so obtained was purified by affinity chromatography. Western blot revealed a single expected molecular weight band (51kDa) recognised by anti-histidine antibodies. A single band was also observed by Coomassie blue staining.

**Table 1.** Dissociation equilibrium constants (kD) obtained from interactions between *Pv*RON2-RI and *Pv*RON2-RII as ligands having different *P. vivax* analytes

| Ligand: *Pv*RON2-RI | | | |
|---|---|---|---|
| **Analyte** | **$K_{on}$, 1/Ms** [1] | **$K_{off}$, 1/s** [2] | **kD, M** [3] |
| *Pv*AMA-DII-III | $5.07 \times 10^5$ | $5.96 \times 10^{-3}$ | **$1.17 \times 10^{-8}$** |
| *Pv*AMA-DI-II | $4.21 \times 10^3$ | $2.29 \times 10^{-3}$ | $5.44 \times 10^{-7}$ |
| *Pv*AMA1 | $5.31 \times 10^4$ | $6.09 \times 10^{-3}$ | $1.15 \times 10^{-7}$ |
| *Pv*RON4 | $1.30 \times 10^3$ | $4.62 \times 10^{-3}$ | $3.56 \times 10^{-6}$ |
| *Pv*RON5 | 577 | $1.91 \times 10^{-3}$ | $3.31 \times 10^{-6}$ |
| *Pv*AMA1 F128A | $1.47 \times 10^5$ | $5.0 \times 10^{-3}$ | $3.4 \times 10^{-8}$ |
| *Pv*AMA1 Y179A | $1.28 \times 10^5$ | $4.93 \times 10^{-3}$ | $3.86 \times 10^{-8}$ |
| Ligand: *Pv*RON2-RII | | | |
| **Analyte** | **$K_{on}$, 1/Ms** | **$K_{off}$, 1/s** | **kD, M** |
| *Pv*AMA-DII-III | $3.49 \times 10^5$ | $6.69 \times 10^{-3}$ | **$1.92 \times 10^{-8}$** |
| *Pv*AMA1 | $8.64 \times 10^3$ | $1.15 \times 10^{-2}$ | $1.74 \times 10^{-6}$ |
| *Pv*RON4 | $6.44 \times 10^3$ | $2.92 \times 10^{-3}$ | $4.54 \times 10^{-7}$ |
| *Pv*RON5 | $2.19 \times 10^3$ | $7.93 \times 10^{-3}$ | $3.62 \times 10^{-6}$ |
| *Pv*AMA1 F128A | $3.18 \times 10^5$ | $2.49 \times 10^{-3}$ | $7.83 \times 10^{-9}$ |
| *Pv*AMA1 Y179A | $7.68 \times 10^5$ | $6.33 \times 10^{-3}$ | $8.24 \times 10^{-8}$ |

[1]: complex formation rate is represented by association constant ($K_{on}$)
[2]: complex decay rate is represented by the dissociation constant ($K_{off}$)
[3]: interaction dissociation constant (kD) was calculated from $K_{on}$ and $K_{off}$
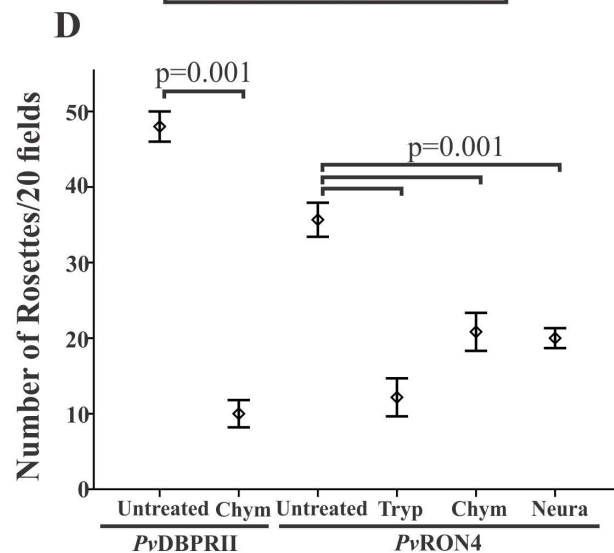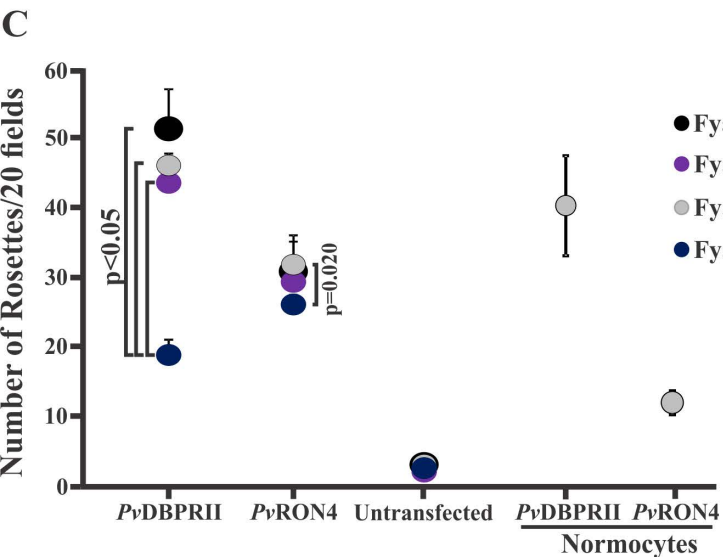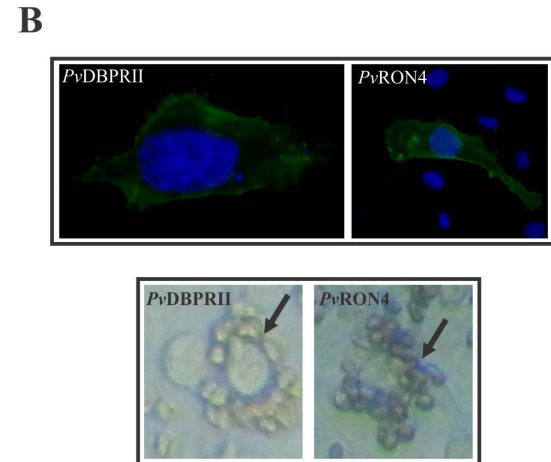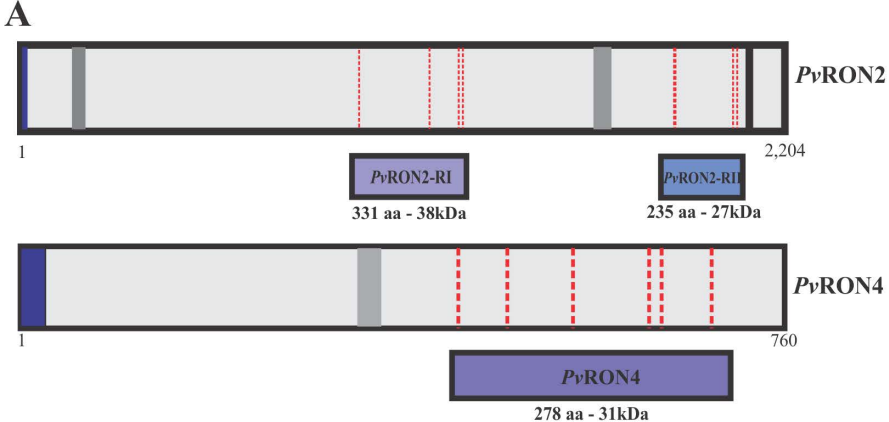
**Figure 1**
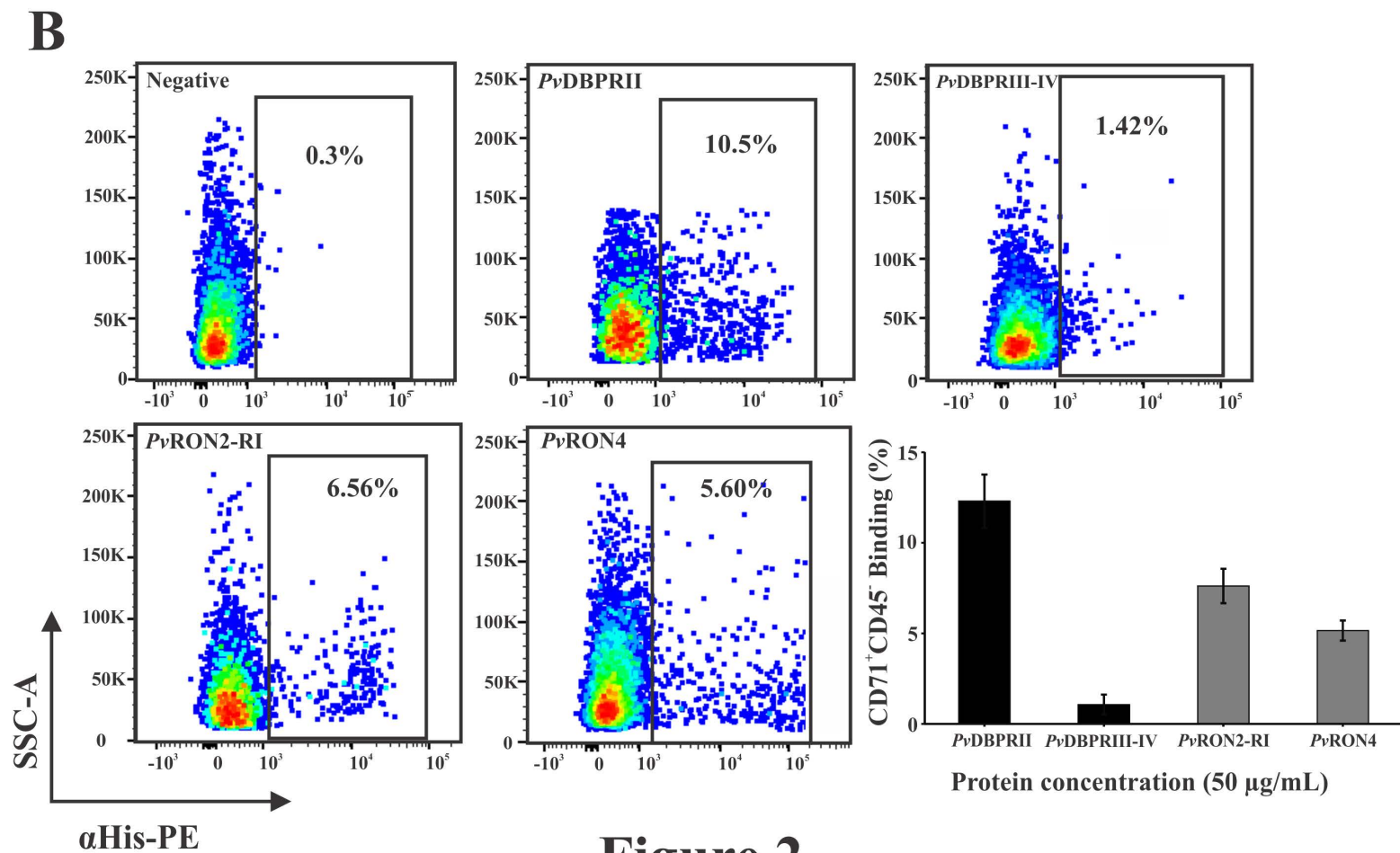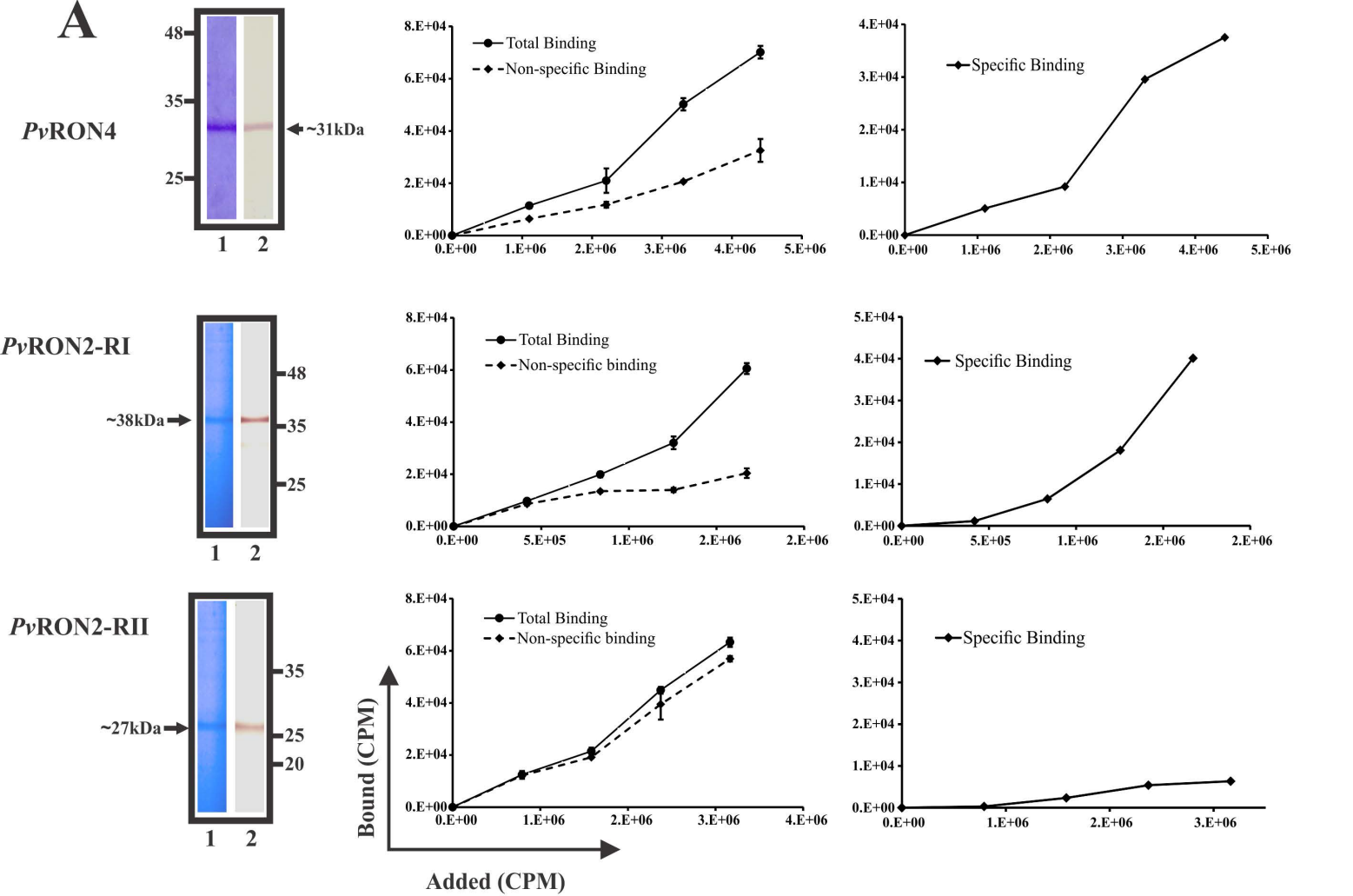
**Figure 2**

**A**
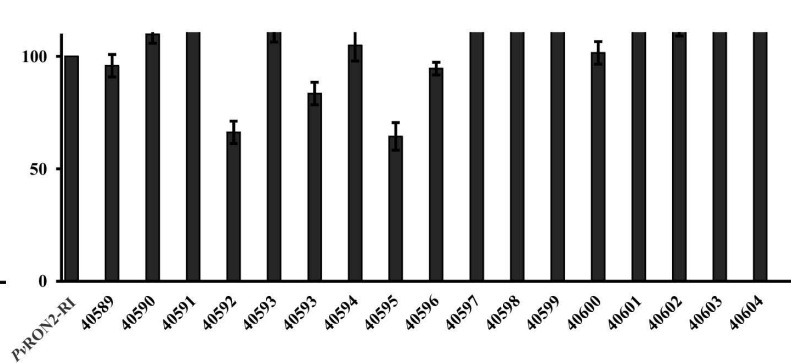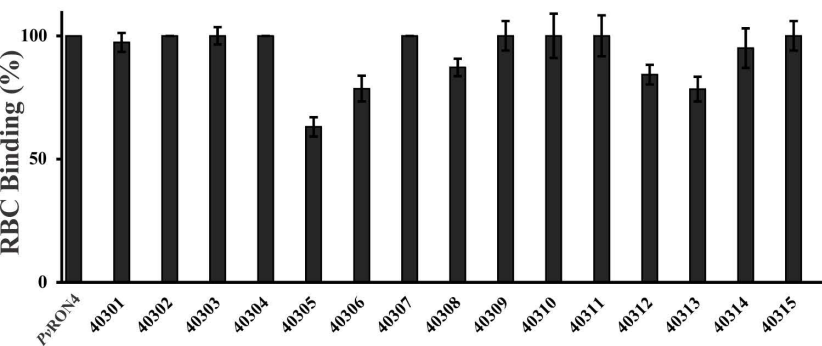
**B**

| Peptide Code | *Pv*RON4 Sequence | Specific Binding Activity (%) | | |
|---|---|---|---|---|
| | | 1 | 2 | 3 |
| 40305 | [501]VQQWKYYQNMLGFETGNEHA[520] | | | |
| 40313 | [661]LNMQGRRVLQPLVKMSFLGA[680]Y | | | |

| Peptide Code | *Pv*RON2 Sequence | Specific Binding Activity (%) | | |
|---|---|---|---|---|
| | | 1 | 2 | 3 |
| 40592 | [1037]DAYEDKSFISEANSFRNEEM[1056] | | | |
| 40595 | [1097]LIEPIRRKYNKLASSSVGLN[1116] | | | |

**C**
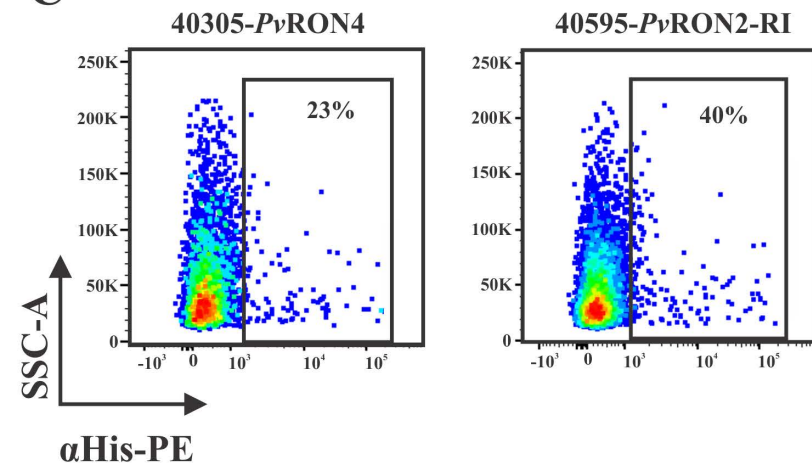
**D**
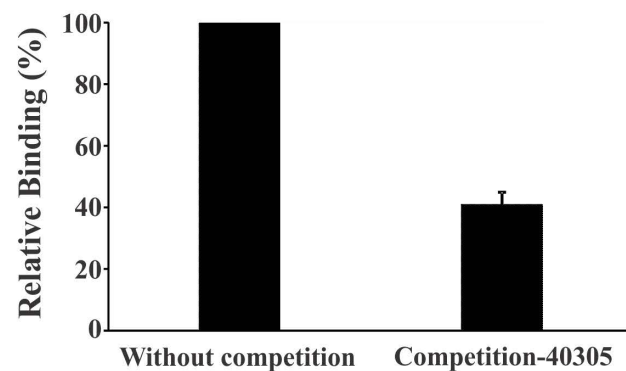
# Figure 3

**A** *Pv*AMA-DII-III on *Pv*RON2-RI

SPR signal (RU)

22nM
11nM
5.5nM
2.8nM
1.4nM

time (s)

**B** *Pv*AMA-DII-III on *Pv*RON2-RII

SPR signal (RU)

88nM
44nM
22nM
11nM
5.5nM

time (s)
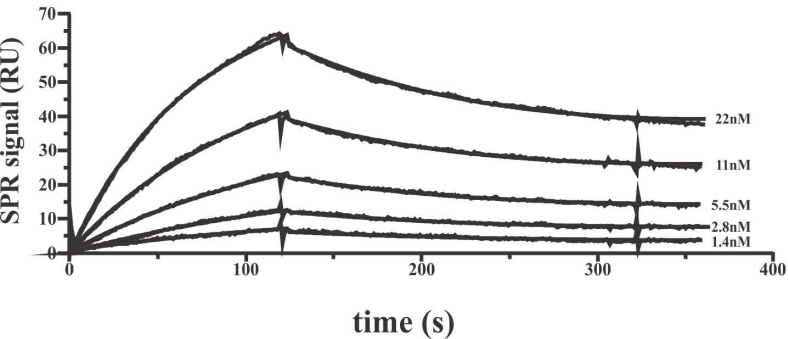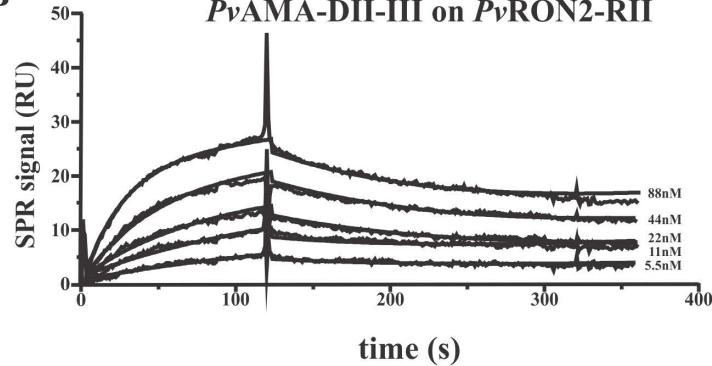
# Figure 4

### 6. Caracterización de Interacciones Proteína-Proteína en *P. vivax*

Las interacciones proteína-proteína (IPP) juegan un rol esencial en prácticamente todos los procesos biológicos, incluidos los relacionados con el proceso de invasión de los microorganismos a sus células hospederas. En malaria, se ha encontrado que, además del amplio repertorio de interacciones receptor-ligando necesarios para la invasión [29, 52, 108], el panorama podría ser aún más complejo. Hay un creciente número de evidencias sobre la formación de complejos macromoleculares entre los ligandos de *P. falciparum* [109-111], que podrían favorecer e incrementar la fuerza de interacción con los receptores sobre el eritrocito [112, 113]. Análisis cromatográficos y estudios de interacción muestran que *Pf*MSP1 es una plataforma de unión para la mayoría de las proteínas solubles que forman una variedad de complejos de diferentes tamaños sobre la superficie del merozoito [111, 114]. Así, *Pf*MSP1 es capaz de formar un macrocomplejo con las proteínas *Pf*MSP6, *Pf*MSP7, la proteína de alto peso molecular de las roptrias 3 (*Pf*RhopH3, del inglés High molecular weight Rhoptry Protein 3), la proteína asociada a las roptrias 1 (RAP1, del inglés Rhoptry-Associated Protein-1), *Pf*RAP2, *Pf*MSP1DBL1, *Pf*MSP1DBL2 y un complejo co-ligando con la proteína *Pf*MSP9, mientras diferentes fragmentos de *Pf*MSP1 interactúan con glicoforina A, banda 3 y otros receptores asociados a la membrana del eritrocito aún no identificados [109-111, 114-116] (Figura 5). De otra parte, la proteína soluble *Pf*Rh5, secretada desde las roptrias, forma un complejo con el antígeno protectivo rico en cisteínas (*Pf*CyRPA, del inglés Cysteine-Rich Protective Antigen), que se ancla a la superficie del parásito a través de la proteína *Pf*P113 vía glicosilfosfatidilinositol (GPI, del inglés Glycosylphosphatidylinositol). De esta forma, la proteína *Pf*Rh5 interactúa con el receptor Basigina sobre la membrana de los eritrocitos [117-119]. El uso de anticuerpos policlonales IgG

contra *Pf*RH5 y CyRPA, inhiben fuertemente la invasión de cepas de *P. falciparum* con diferentes

fenotipos de invasión [118], lo que indica el papel crucial de la formación del complejo y de la

interacción con el receptor.
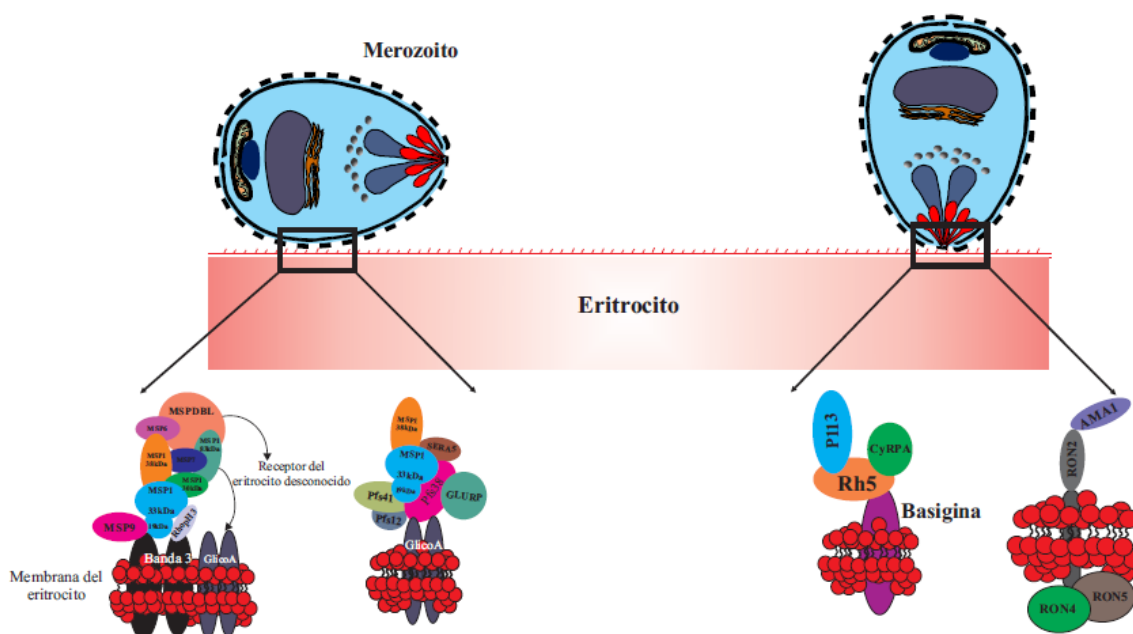


***Figura 5. Interacciones proteína-proteína descritas en* P. falciparum.**
*Se muestran los complejos proteicos más representativos identificados en* P. falciparum*. Dos ellos se han identificado en la fase de adhesión al eritrocito donde participa varias proteínas del parásito entre ellas los diferentes fragmentos de la proteína MSP1 y los otros dos complejos se forman luego de la reorientación y están implicados en la formación del pre-enlace fuerte (Rh5-CyRPA-P113) y enlace fuerte (AMA1-RONs).*

Como se mencionó previamente, el enlace fuerte también es formado por un macrocomplejo de

proteínas liberadas desde las roptrias y micronemas, donde AMA1, RON2, RON4 y RON5 son

importantes [34, 35, 56, 120]. A diferencia de otras fases durante el proceso de invasión, donde se

reporta redundancia funcional entre las proteínas del parásito, en *Plasmodium falciparum*, sólo

existe una copia de AMA1 y RON2 y no se han reportado proteínas que complementen la función

de las mismas. En contraste, *T. gondii* contiene dentro de su genoma varias proteínas parálogas

que complementan la función de RON2, RON4 y AMA1 [58, 121]. A través de varios ensayos de

interacción entre AMA-1 y RON2 en *P. falciparum*, *T. gondii* y más recientemente, en *P. vivax*,

se ha encontrado que un péptido localizado en la región conservada carboxi-terminal de la proteína RON2, interactúa específicamente con el canal hidrofóbico de la proteína AMA-1 [122-124]. Estudios estructurales de esta interacción han sido fundamentales para describir la acción del anticuerpo inhibitorio de la invasión 4G2, el cual interactúa con el DII de *Pf*AMA1, impidiendo cambios conformacionales en *Pf*AMA1 que bloquean su interacción con *Pf*RON2 [34]. El péptido R1, derivado de una librería de expresión en fagos, es conocido por ser un potente inhibidor de la entrada de los merozoitos a los eritrocitos y lo hace a través de su interacción con el bolsillo hidrofóbico de *Pf*AMA1 [34, 35]. Adicionalmente, se han identificado pequeñas moléculas derivadas de una librería de 21.000 compuestos, que tienen la habilidad de bloquear la invasión, previniendo la formación del enlace fuerte. Los compuestos se unen a *Pf*AMA1 y bloquean su interacción directa con *Pf*RON2 [36]. Estos datos indican, que el bloqueo de los puntos calientes de la interacción pueden ser utilizados como una nueva estrategia para impedir la invasión de los parásitos de la malaria [36, 109, 114]. Estudios previos han mostrado que la inmunización de ratones con el complejo AMA1-RON2, pero no con AMA1 sola, indujo una completa protección en los animales frente a reto experimental homólogo con una cepa letal de *P. yoelii* [125]. De manera interesante, el análisis de interacción con mutantes de la proteína *Pf*RON2, mostró que los residuos [2041]R, [2044]P, [2038]F y [2033]P son críticos para su interacción con *Pf*AMA1, mientras que los residuos [251]Y, [234]Y y [183]F, localizados en el canal hidrofóbico de *Pf*AMA1, son esenciales para la interacción con el péptido de *Pf*RON2 [124].

Aunque no está completamente elucidado cómo las proteínas RON4 y RON5 están interactuando dentro del complejo RONs/AMA1, estudios previos en *T. gondii*, muestran que estas proteínas se localizan en el citosol de la célula hospedera y son capaces de reclutar e interactuar

cooperativamente con componentes de la maquinaria del complejo de clasificación endosomal requerido para el transporte (ESCRT, del inglés Endosomal Sorting Complexes Required for Transport) para acceder y forzar el acceso a la célula blanco [126]. Adicionalmente, se ha reportado que el *knockdown* o *knockout* condicional de las proteínas del complejo RONs/AMA1 reducen significativamente la capacidad de invasión de los parásitos [120, 127]; así mismo, el *knockdown* de *Tg*RON4 o *Tg*RON5 afecta la expresión y estabilidad de los otros componentes del complejo como *Tg*RON2, lo que indica la dependencia de cada proteína en la formación del complejo [120, 126]. En resumen, existe una amplia evidencia acerca de la importancia de la formación del complejo RONs/AMA1 durante el proceso de invasión de los parásitos *Apicomplexa*, que lo hace un blanco para la búsqueda de métodos de control y de ampliar su estudio en otros parásitos como *P. vivax*.

En *P. vivax* aún no se han explorado los complejos macromoleculares que se forman durante el proceso de invasión a reticulocitos. Sin embargo, un estudio reciente de IPP con 37 proteínas de *P. vivax*, mediante tamizaje de interacción extracelular basado en avidez (AVEXIS, del inglés AVidity-based EXtracellular Interaction Screen), reportó la presencia de interacciones entre las proteínas P12-P41, P12-PVX_110945 y MSP3.10-MSP7.1 [128]. Hasta el momento, no se conoce exactamente el papel funcional de estas proteínas ni de sus interacciones dentro del proceso de invasión de *P. vivax* a los reticulocitos. Para incrementar el conocimiento en esta área básica de *P. vivax* y, basados en los antecedentes sobre el complejo RONs/AMA1, en este trabajo se evalúo la interacción entre RON2 de *P. vivax* y las proteínas *Pv*RON4, *Pv*RON5 y *Pv*AMA1, utilizando resonancia de plasmones de superficie (SPR, del inglés Surface Plasmon Resonance). Mediante esta técnica, se encontró que las dos regiones de *Pv*RON2 (*Pv*RON2-RI y *Pv*RON2-RII) tienen la

habilidad de interactuar con *Pv*AMA1, *Pv*AMA-DI-II, *Pv*AMA-DII-III, *Pv*RON4 y *Pv*RON5, siendo la interacción entre los dos fragmentos de *Pv*RON2 con *Pv*AMA-DII-III la que presentó mayor afinidad y constantes de disociación (kD, del inglés dissociation equilibrium constant) que se encuentran en el rango nanomolar. Al evaluar la importancia de los residuos $^{128}$F y $^{179}$Y de *Pv*AMA1 en su interacción con *Pv*RON2, se encontró que estos residuos no son esenciales para la interacción, contrario a lo reportado para la interacción entre *Pf*AMA1-*Pf*RON2 [124], sugiriendo que, si bien ciertas interacciones intermoleculares son comunes entre AMA1/RON2 en *P. falciparum* y *P. vivax* [123, 124], otras son exclusivas para cada especie, similar a lo encontrado para las interacciones hospedero-patógeno. Estos resultados fueron publicados en la revista Cellular Microbiology en un artículo titulado "Receptor-ligand and parasite protein-protein interactions in *Plasmodium vivax*: analysing rhoptry neck proteins 2 and 4", que se mostró en el capítulo anterior.

A partir de los resultados obtenidos en este trabajo, se propone un modelo de interacciones receptor-ligando y proteína-proteína en *P. vivax* basados en las proteínas *Pv*RON2, *Pv*RON4, *Pv*RON5 y *Pv*AMA1 (Figura 6). En este modelo, la proteína *Pv*RON2 anclada a la membrana del merozoito vía un dominio transmembranal (DT) [42], interactúa específicamente a través de la región central rica en cisteínas (*Pv*RON2-RI) con un receptor (desconocido) sobre la membrana del reticulocito. A su vez, el dominio I de *Pv*AMA1, y las regiones carboxi-terminal de *Pv*RON4 y *Pv*RON5 (ancladas mediante DT), interactúan con receptores de tipo proteico sobre la membrana del merozoito [70]. Finalmente, las dos regiones ricas en cisteína de *Pv*RON2 interactúan con el dominio II y III de *Pv*AMA1 y con *Pv*RON4 y *Pv*RON5 (Figura 6). Aunque no es claro si estas interacciones ocurren al mismo tiempo, la interacción hospedero-patógeno puede abrir la puerta

para la translocación de las proteínas RONs al citosol de la célula hospedera, que podría servirle de anclaje a la proteína *Pv*AMA1 para formar el enlace fuerte durante el proceso de invasión de los merozoitos de *P. vivax* a los reticulocitos.
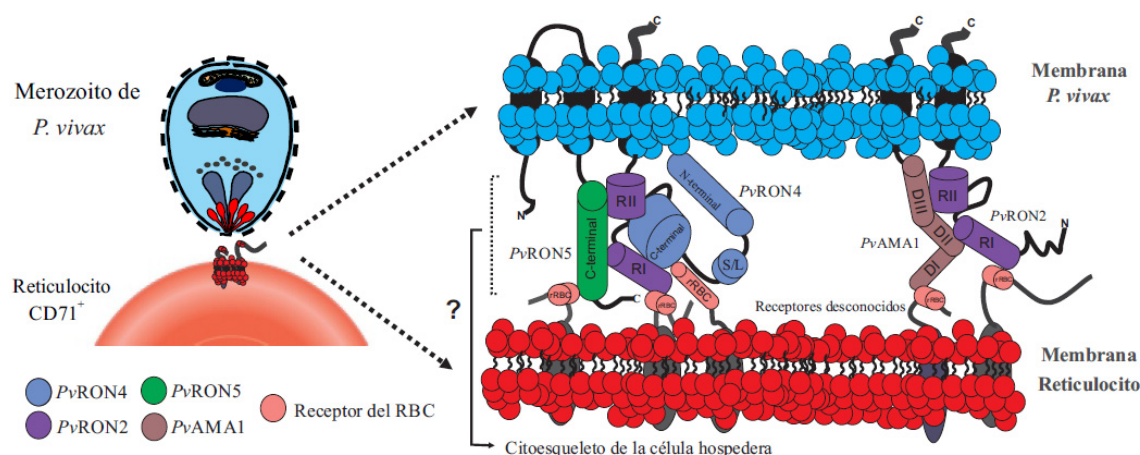


*Figura 6. Modelo propuesto para las interacciones hospedero-patógeno y proteína-proteína durante la invasión de merozoitos de* **P. vivax** *a reticulocitos humanos.*
*Se muestra la membrana del merozoito (azul) y la membrana del reticulocito (rojo)*

## 6.1 Aplicando arreglos de proteínas programable de ácidos nucleicos para medir interacciones proteína-proteína en *P. vivax*

Diferentes técnicas genéticas, celulares y bioquímicas han sido desarrolladas en los últimos años para la detección *in vivo* e *in vitro* de las IPP [129-131]. Las aproximaciones *in vivo* incluyen el sistema de dos híbridos y sus variantes, que permiten la identificación de interacciones binarias [132, 133], mientras la transferencia de energía de resonancia fluorescente (FRET, del inglés fluorescence resonance energy transfer) y la resonancia de energía bioluminiscente (BRET, del inglés bioluminescence resonance energy transfer), miden las IPP en células vivas en tiempo real [134, 135]. Las técnicas *in vitro* incluyen purificación en tándem [136], co-inmunoprecipitación [56], resonancia de plasmones de superficie (SPR, del inglés Surface Plasmon Resonance) [137], espectrometría de masas [138] y microarreglos de proteínas [139, 140], entre otros.

Los arreglos de proteínas han surgido como una herramienta útil para el análisis simultáneo a larga escala de cientos de proteínas a nivel miniaturizado, permitiendo el análisis de varios parámetros en un solo experimento [141]. La estrategia más común para la fabricación de los microarreglos, consiste en la inmovilización de proteínas purificadas sobre soportes sólidos, que son luego expuestas a muestras que contienen las moléculas de unión [142, 143]. Estos microarreglos han sido útiles en investigación clínica para el descubrimiento de biomarcadores [144, 145], estudios de niveles de proteínas con sus respectivas modificaciones postraduccionales (glicosilación, fosforilación, acetilación), enfermedades autoinmunes [146, 147] y han sido aplicados para evaluar la respuesta inmune humoral en enfermedades infecciosas causadas por *Pseudomonas aeruginosa*, *P. falciparum* y *Mycobacterium tuberculosis*, entre otros [148-150]. Recientes desarrollos en el campo de los microarreglos, muestran aplicaciones como la evaluación enzimática [151] e interacciones DNA-proteína y proteína-proteína [131].

Los microarreglos presentan como ventaja importante (además de la medición multiparamétrica), la capacidad de detectar proteínas en baja abundancia, lo que incrementa la sensibilidad y especificidad, respecto a otras técnicas de medición de IPP. La sensibilidad se incrementa debido a que la reacción de unión y de captura del complejo presa-cebo ocurre sobre la más alta concentración de blanco inmovilizado en una pequeña área del microarreglo, incrementando la señal de interacción [141]. Sin embargo, los microarreglos presentan algunas desventajas que limitan su uso a nivel de proteínas. Típicamente, la expresión y purificación de proteínas incluye la clonación de cada gen dentro de un vector de expresión, que se utiliza para transformar un sistema de expresión heterólogo (comúnmente *E. coli*) e inducir la expresión y producción de la

proteína recombinante, seguido de un laborioso proceso de purificaciones por cromatografía de afinidad, intercambio o exclusión por tamaño. Este proceso, aunque eficiente a baja escala, puede resultar en problemas relacionados con diferencias hasta de 1.000 veces en la producción de una proteína a otra; además, estas proteínas requieren una cadena de frio para no perder su actividad, lo que limita la vida media de la proteína. En muchos casos, el sistema de expresión carece de la maquinaria necesaria para proveer las modificaciones postraduccionales requeridas para una adecuada actividad y plegamiento de la proteína. Por último, la expresión, purificación y la impresión sobre la placa de miles de proteínas recombinantes es una tarea laboriosa que eleva su costo, reduce su reproducibilidad y limita su utilización [152-154].

Como alternativa a estos inconvenientes, en los últimos años, se han desarrollado varios microarreglos con expresión de proteínas *in-situ*, tales como: impresión de arreglos de proteínas a partir de ADN (DAPA, del inglés printing protein arrays from DNA), arreglos de proteínas *in-situ* (PISA, del inglés Protein *in situ* arrays), y arreglos de proteínas programables de ácidos nucleicos (NAPPA, del inglés Nucleic Acids Programmable Protein Arrays). Estos microarreglos utilizan diversos extractos libres de células eucariotas, que proporcionan la maquinaria transcripcional y de traducción necesaria para obtener proteínas funcionales. Dentro de esta aproximación, se ha utilizado exitosamente el extracto de reticulocitos de conejo (RRL, del inglés Rabbit Reticulocyte Lysate), extracto de germen de trigo (WGE, del inglés Wheat Germ Extract) y el extracto de células HeLa [140, 155-157].

Uno de los microarreglos funcionales más novedosos es el NAPPA, una tecnología de alto rendimiento, que se ha utilizado para evaluar IPP [131, 158-160]. El NAPPA es construido a partir de la impresión sobre láminas funcionalizadas de ADNc que codifican para la proteína de interés,

y clonados en marco con una cola de afinidad como la glutatión S-transferasa (GST, del inglés Glutathione S-Transferase) [156]. El ADNc impreso es entonces transcrito y traducido con un sistema libre de células, que contiene la maquinaria necesaria para la producción de proteínas funcionales. Una vez la proteína es expresada, esta es capturada por un anticuerpo anti-GST que se encuentra también impreso sobre el microarreglo [152, 156]. De esta forma, las proteínas estarían fijas sobre el microarreglo listas para llevar a cabo los estudios de interacción (Figura 7).
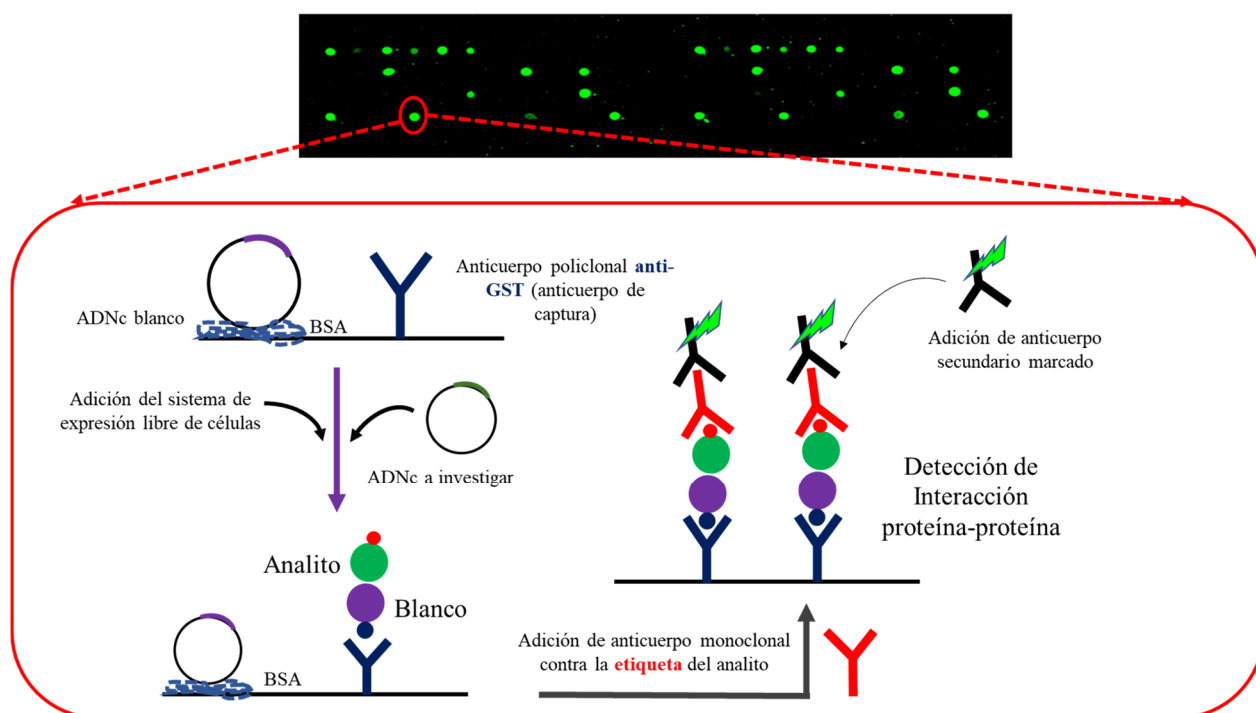


**Figura 7. Esquema general de NAPPA.**
*Se muestran los pasos a seguir en la determinación de interacciones entre proteínas utilizando el microarreglo NAPPA. Albúmina Sérica Bovina (BSA, del inglés Bovine Serum Albumin).*

Adicionalmente, esta técnica permite expresar, junto con la proteína blanco, la proteína con la que deseamos conocer la interacción (Analito). Para esto, el ADNc soluble que codifica para el analito, es simultáneamente co-expresado con los diferentes blancos inmovilizados sobre el microarreglo. Este paso se lleva a cabo usando el mismo sistema de expresión libre de células, pero el analito se expresa en marco con una etiqueta diferente a la de la proteína blanco (Figura 7). Posteriormente, se adiciona un anticuerpo contra la etiqueta del analito, seguido de la adición de un anticuerpo

secundario marcado; si la interacción blanco-analito ocurre, una señal positiva de fluorescencia revelará la posición de la interacción dentro del microarreglo.

Teniendo en cuenta que es indispensable ampliar el conocimiento en la red de interacciones proteína-proteína en *P. vivax* y basados en las ventajas que ofrece el NAPPA, se diseñó un estudio preliminar para aplicar esta tecnología a la evaluación de IPP en *P. vivax*, a partir de la clonación de 20 de genes que codifican para proteínas de *P. vivax* que se expresan en el estadio intraeritrocítico. Para validar este microarreglo, se utilizó como analito la proteína P12 de *P. vivax*, que se ha encontrado interactúa específicamente con la proteína P41 mediante la técnica AVEXIS y resonancia de plasmones de superficie [128]. Los resultados mostraron que la mayoría de las proteínas fueron expresadas *in-situ* y capturadas sobre el array. La co-expresión de la proteína P12 sobre el array, mostró una señal de interacción con cuatro proteínas de *P. vivax* tales como P41 (reportado previamente), *Pv*RBP1a (región II y IV), *Pv*MSP1$_{42kDa}$, *Pv*MSP8 y *Pv*RAP1. Estos resultados muestran la factibilidad y viabilidad de NAPPA para medir interacciones en patógenos como *P. vivax*. Los datos de esta investigación fueron reunidos en una publicación titulada "Self-assembling functional programmable protein array for studying protein-protein interactions in malaria parasites", que fue sometida y se encuentra en evaluación por pares en la revista Malaria Journal (Anexo 1).

## CONCLUSIONES

1. Los genes *pvron4* y *pvron5* están presentes en el genoma de la cepa VCG-1 de *P. vivax* y se transcriben durante el estadio de esquizontes.

2. Los genes *pvron4* y *pvron5* codifican para proteínas de alto peso molecular y se localizan en el polo apical (roptrias) de esquizontes tardíos de la cepa VCG-1.

3. La región carboxi-terminal de la proteína *Pv*RON5 es reconocida por sueros de pacientes con infección natural por *P. vivax*

4. La región carboxi-terminal de la proteína *Pv*RON5 se une a normocitos y reticulocitos CD71 positivos, con preferencia de unión por los reticulocitos.

5. El dominio I y II de *Pv*AMA-1, la región central de la proteína *Pv*RON2 y la región carboxi-terminal de la proteína *Pv*RON4, se unen específicamente a reticulocitos $CD71^+CD45^-$.

6. Los péptidos 21270 (derivado de *Pv*AMA-DI-II), 40305 (derivado de *Pv*RON4) y 40595 (derivado de *Pv*RON2-RI), son las regiones de unión mínimas de interacción con reticulocitos humanos $CD71^+$.

7. Las dos regiones ricas en cisteínas de la proteína *Pv*RON2, establecen interacciones de alta afinidad con el dominio II y III de la proteína *Pv*AMA1.

8. Se estandarizó una metodología secuencial para la determinación de regiones de unión de proteínas de *P. vivax* a reticulocitos humanos.

9. Se aplicó el NAPPA como una técnica de alto rendimiento para identificar IPP en *P. vivax*.

10. Se amplió el conocimiento de las interacciones hospedero-patógeno y de las interacciones proteína-proteína en *P. vivax*.

**PERSPECTIVAS GENERALES**

Teniendo en cuenta que el uso combinado de técnicas de interacción hospedero-patógeno en *P. vivax* puede ampliar el conocimiento de las regiones mínimas de interacción de las proteínas con reticulocitos humanos, las perspectivas futuras se pueden orientar a:

1. Incluir más proteínas que se expresen durante el ciclo intraeritrocítico de *P. vivax* en ensayos de interacción con reticulocitos humanos, siguiendo la metodología planteada en este trabajo doctoral. La elucidación de estas regiones, es clave para avanzar en el diseño de una vacuna contra *P. vivax*, siguiendo una metodología similar a la ya planteada para *P. falciparum*.

2. Evaluar la capacidad de los cHABPs 21270, 40305 y 40595 de inhibir la invasión de merozoitos de *P. vivax* a reticulocitos humanos mediante un cultivo a corto plazo. De esta forma, se podría confirmar el papel funcional de estas regiones durante el proceso de invasión.

3. Determinar los residuos críticos que participan en la unión de los cHABPs 21270, 40305 y 40595 a reticulocitos humanos, que permitan guiarnos para la modificación hacia moléculas IMPIPs.

4. Aplicar diferentes técnicas de identificación de receptores, para hallar las proteínas de los reticulocitos con las que interactúan *Pv*AMA-1, *Pv*RON2, *Pv*RON4 y *Pv*RON5.

Respecto a las IPP dentro del parásito, se plantea como perspectiva:

1. La elucidación de los puntos calientes de la interacción entre la proteína *Pv*RON2 y *Pv*AMA-1, para el diseño de métodos de control que bloqueen la invasión.

# REFERENCIAS BIBLIOGRÁFICAS

1.  Organización Mundial de la Salud: **Informe Mundial sobre Paludismo 2016.** Organización Mundial de la Salud; 2017.
2.  Organización Mundial de la Salud: **Informe Mundial sobre el Paludismo 2017.** Organización Mundial de la Salud; 2017.
3.  Organización Panamericana de la Salud / Organización Mundial de la Salud: **Alerta Epidemiológica: Aumento de casos de malaria.** Organización Panamericana de la Salud / Organización Mundial de la Salud.; 2017.
4.  Guerra CA, Snow RW, Hay SI: **Mapping the global extent of malaria in 2005.** *Trends Parasitol* 2006, **22:**353-358.
5.  Gupta H, Dhunputh P, Bhatt AN, Satyamoorthy K, Umakanth S: **Cerebral malaria in a man with Plasmodium vivax mono-infection: a case report.** *Trop Doct* 2016, **46:**241-245.
6.  Mueller I, Galinski MR, Baird JK, Carlton JM, Kochar DK, Alonso PL, del Portillo HA: **Key gaps in the knowledge of Plasmodium vivax, a neglected human malaria parasite.** *Lancet Infect Dis* 2009, **9:**555-566.
7.  Rahimi BA, Thakkinstian A, White NJ, Sirivichayakul C, Dondorp AM, Chokejindachai W: **Severe vivax malaria: a systematic review and meta-analysis of clinical studies since 1900.** *Malar J* 2014, **13:**481.
8.  Krotoski WA, Collins WE, Bray RS, Garnham PC, Cogswell FB, Gwadz RW, Killick-Kendrick R, Wolf R, Sinden R, Koontz LC, Stanfill PS: **Demonstration of hypnozoites in sporozoite-transmitted Plasmodium vivax infection.** *Am J Trop Med Hyg* 1982, **31:**1291-1293.
9.  Carlton JM, Sina BJ, Adams JH: **Why is Plasmodium vivax a neglected tropical disease?** *PLoS Negl Trop Dis* 2011, **5:**e1160.
10. Bassat Q, Velarde M, Mueller I, Lin J, Leslie T, Wongsrichanalai C, Baird JK: **Key Knowledge Gaps for Plasmodium vivax Control and Elimination.** *Am J Trop Med Hyg* 2016, **95:**62-71.
11. Nomura T, Carlton JM, Baird JK, del Portillo HA, Fryauff DJ, Rathore D, Fidock DA, Su X, Collins WE, McCutchan TF, et al: **Evidence for different mechanisms of chloroquine resistance in 2 Plasmodium species that cause human malaria.** *J Infect Dis* 2001, **183:**1653-1661.
12. Gavin AC, Bosche M, Krause R, Grandi P, Marzioch M, Bauer A, Schultz J, Rick JM, Michon AM, Cruciat CM, et al: **Functional organization of the yeast proteome by systematic analysis of protein complexes.** *Nature* 2002, **415:**141-147.
13. Paing MM, Tolia NH: **Multimeric assembly of host-pathogen adhesion complexes involved in apicomplexan invasion.** *PLoS Pathog* 2014, **10:**e1004120.
14. Woodson SA: **Macromolecular complexes: how RNA and protein get together.** *Curr Biol* 1996, **6:**23-25.
15. Panichakul T, Sattabongkot J, Chotivanich K, Sirichaisinthop J, Cui L, Udomsangpetch R: **Production of erythropoietic cells in vitro for continuous culture of Plasmodium vivax.** *Int J Parasitol* 2007, **37:**1551-1557.
16. Noulin F, Borlon C, Van Den Abbeele J, D'Alessandro U, Erhart A: **1912-2012: a century of research on Plasmodium vivax in vitro culture.** *Trends Parasitol* 2013, **29:**286-294.

17. Pico de Coana Y, Rodriguez J, Guerrero E, Barrero C, Rodriguez R, Mendoza M, Patarroyo MA: **A highly infective Plasmodium vivax strain adapted to Aotus monkeys: quantitative haematological and molecular determinations useful for P. vivax malaria vaccine development.** *Vaccine* 2003, **21:**3930-3937.

18. Armistead JS, Adams JH: **Advancing Research Models and Technologies to Overcome Biological Barriers to Plasmodium vivax Control.** *Trends Parasitol* 2017.

19. Bozdech Z, Mok S, Hu G, Imwong M, Jaidee A, Russell B, Ginsburg H, Nosten F, Day NP, White NJ, et al: **The transcriptome of Plasmodium vivax reveals divergence and diversity of transcriptional regulation in malaria parasites.** *Proc Natl Acad Sci U S A* 2008, **105:**16290-16295.

20. Patarroyo MA, Calderon D, Moreno-Perez DA: **Vaccines against Plasmodium vivax: a research challenge.** *Expert Rev Vaccines* 2012, **11:**1249-1260.

21. Flannery EL, Wang T, Akbari A, Corey VC, Gunawan F, Bright AT, Abraham M, Sanchez JF, Santolalla ML, Baldeviano GC, et al: **Next-Generation Sequencing of Plasmodium vivax Patient Samples Shows Evidence of Direct Evolution in Drug-Resistance Genes.** *ACS Infect Dis* 2015, **1:**367-379.

22. Roobsoong W, Roytrakul S, Sattabongkot J, Li J, Udomsangpetch R, Cui L: **Determination of the Plasmodium vivax schizont stage proteome.** *J Proteomics* 2011, **74:**1701-1710.

23. Moreno-Perez DA, Degano R, Ibarrola N, Muro A, Patarroyo MA: **Determining the Plasmodium vivax VCG-1 strain blood stage proteome.** *J Proteomics* 2014, **113C:**268-280.

24. Bourgard C, Albrecht L, Kayano A, Sunnerhagen P, Costa FTM: **Plasmodium vivax Biology: Insights Provided by Genomics, Transcriptomics and Proteomics.** *Front Cell Infect Microbiol* 2018, **8:**34.

25. Moreno-Perez DA, Mongui A, Soler LN, Sanchez-Ladino M, Patarroyo MA: **Identifying and characterizing a member of the RhopH1/Clag family in Plasmodium vivax.** *Gene* 2011, **481:**17-23.

26. Mongui A, Angel DI, Moreno-Perez DA, Villarreal-Gonzalez S, Almonacid H, Vanegas M, Patarroyo MA: **Identification and characterization of the Plasmodium vivax thrombospondin-related apical merozoite protein.** *Malar J* 2010, **9:**283.

27. Mongui A, Angel DI, Gallego G, Reyes C, Martinez P, Guhl F, Patarroyo MA: **Characterization and antigenicity of the promising vaccine candidate Plasmodium vivax 34kDa rhoptry antigen (Pv34).** *Vaccine* 2009, **28:**415-421.

28. Bozdech Z, Llinas M, Pulliam BL, Wong ED, Zhu J, DeRisi JL: **The transcriptome of the intraerythrocytic developmental cycle of Plasmodium falciparum.** *PLoS Biol* 2003, **1:**E5.

29. Weiss GE, Gilson PR, Taechalertpaisarn T, Tham WH, de Jong NW, Harvey KL, Fowkes FJ, Barlow PN, Rayner JC, Wright GJ, et al: **Revealing the sequence and resulting cellular morphology of receptor-ligand interactions during Plasmodium falciparum invasion of erythrocytes.** *PLoS Pathog* 2015, **11:**e1004670.

30. Counihan NA, Kalanon M, Coppel RL, de Koning-Ward TF: **Plasmodium rhoptry proteins: why order is important.** *Trends Parasitol* 2013, **29:**228-236.

31. Cao J, Kaneko O, Thongkukiatkul A, Tachibana M, Otsuki H, Gao Q, Tsuboi T, Torii M: **Rhoptry neck protein RON2 forms a complex with microneme protein AMA1 in Plasmodium falciparum merozoites.** *Parasitol Int* 2009, **58:**29-35.

32. Curtidor H, Patino LC, Arevalo-Pinzon G, Patarroyo ME, Patarroyo MA: **Identification of the Plasmodium falciparum rhoptry neck protein 5 (PfRON5).** *Gene* 2011, **474:**22-28.

33. Morahan BJ, Sallmann GB, Huestis R, Dubljevic V, Waller KL: **Plasmodium falciparum: genetic and immunogenic characterisation of the rhoptry neck protein PfRON4.** *Exp Parasitol* 2009, **122:**280-288.

34. Collins CR, Withers-Martinez C, Hackett F, Blackman MJ: **An inhibitory antibody blocks interactions between components of the malarial invasion machinery.** *PLoS Pathog* 2009, **5:**e1000273.

35. Srinivasan P, Beatty WL, Diouf A, Herrera R, Ambroggio X, Moch JK, Tyler JS, Narum DL, Pierce SK, Boothroyd JC, et al: **Binding of Plasmodium merozoite proteins RON2 and AMA1 triggers commitment to invasion.** *Proc Natl Acad Sci U S A* 2011, **108:**13275-13280.

36. Srinivasan P, Yasgar A, Luci DK, Beatty WL, Hu X, Andersen J, Narum DL, Moch JK, Sun H, Haynes JD, et al: **Disrupting malaria parasite AMA1-RON2 interaction with a small molecule prevents erythrocyte invasion.** *Nat Commun* 2013, **4:**2261.

37. Kato K, Mayer DC, Singh S, Reid M, Miller LH: **Domain III of Plasmodium falciparum apical membrane antigen 1 binds to the erythrocyte membrane protein Kx.** *Proc Natl Acad Sci U S A* 2005, **102:**5552-5557.

38. Hossain ME, Dhawan S, Mohmmed A: **The cysteine-rich regions of Plasmodium falciparum RON2 bind with host erythrocyte and AMA1 during merozoite invasion.** *Parasitol Res* 2012, **110:**1711-1721.

39. Curtidor H, Patino LC, Arevalo-Pinzon G, Vanegas M, Patarroyo ME, Patarroyo MA: **Plasmodium falciparum rhoptry neck protein 5 peptides bind to human red blood cells and inhibit parasite invasion.** *Peptides* 2014, **53:**210-217.

40. Tonkin ML, Boulanger MJ: **The shear stress of host cell invasion: exploring the role of biomolecular complexes.** *PLoS Pathog* 2015, **11:**e1004539.

41. Riglar DT, Richard D, Wilson DW, Boyle MJ, Dekiwadia C, Turnbull L, Angrisano F, Marapana DS, Rogers KL, Whitchurch CB, et al: **Super-resolution dissection of coordinated events during malaria parasite invasion of the human erythrocyte.** *Cell Host Microbe* 2011, **9:**9-20.

42. Arevalo-Pinzon G, Curtidor H, Patino LC, Patarroyo MA: **PvRON2, a new Plasmodium vivax rhoptry neck antigen.** *Malar J* 2011, **10:**60.

43. Sinnis P, Coppi A: **A long and winding road: the Plasmodium sporozoite's journey in the mammalian host.** *Parasitol Int* 2007, **56:**171-178.

44. Miller LH, Baruch DI, Marsh K, Doumbo OK: **The pathogenic basis of malaria.** *Nature* 2002, **415:**673-679.

45. White NJ, Pukrittayakamee S, Hien TT, Faiz MA, Mokuolu OA, Dondorp AM: **Malaria.** *Lancet* 2014, **383:**723-735.

46. Gaur D, Chitnis CE: **Molecular interactions and signaling mechanisms during erythrocyte invasion by malaria parasites.** *Curr Opin Microbiol* 2011, **14:**422-428.

47. Hill AV: **Vaccines against malaria.** *Philos Trans R Soc Lond B Biol Sci* 2011, **366:**2806-2814.

48. Dvorak JA, Miller LH, Whitehouse WC, Shiroishi T: **Invasion of erythrocytes by malaria merozoites.** *Science* 1975, **187:**748-750.

49.     Boyle MJ, Richards JS, Gilson PR, Chai W, Beeson JG: **Interactions with heparin-like molecules during erythrocyte invasion by Plasmodium falciparum merozoites.** *Blood* 2010, **115:**4559-4568.

50.     Barnwell JW, Nichols ME, Rubinstein P: **In vitro evaluation of the role of the Duffy blood group in erythrocyte invasion by Plasmodium vivax.** *J Exp Med* 1989, **169:**1795-1802.

51.     Adams JH, Blair PL, Kaneko O, Peterson DS: **An expanding ebl family of Plasmodium falciparum.** *Trends Parasitol* 2001, **17:**297-299.

52.     Lopaticki S, Maier AG, Thompson J, Wilson DW, Tham WH, Triglia T, Gout A, Speed TP, Beeson JG, Healer J, Cowman AF: **Reticulocyte and erythrocyte binding-like proteins function cooperatively in invasion of human erythrocytes by malaria parasites.** *Infect Immun* 2011, **79:**1107-1117.

53.     Ord RL, Rodriguez M, Yamasaki T, Takeo S, Tsuboi T, Lobo CA: **Targeting sialic acid dependent and independent pathways of invasion in Plasmodium falciparum.** *PLoS One* 2012, **7:**e30251.

54.     Bradley PJ, Ward C, Cheng SJ, Alexander DL, Coller S, Coombs GH, Dunn JD, Ferguson DJ, Sanderson SJ, Wastling JM, Boothroyd JC: **Proteomic analysis of rhoptry organelles reveals many novel constituents for host-parasite interactions in Toxoplasma gondii.** *J Biol Chem* 2005, **280:**34245-34258.

55.     Aikawa M, Miller LH, Johnson J, Rabbege J: **Erythrocyte entry by malarial parasites. A moving junction between erythrocyte and parasite.** *J Cell Biol* 1978, **77:**72-82.

56.     Besteiro S, Michelin A, Poncet J, Dubremetz JF, Lebrun M: **Export of a Toxoplasma gondii rhoptry neck protein complex at the host cell membrane to form the moving junction during invasion.** *PLoS Pathog* 2009, **5:**e1000309.

57.     Straub KW, Peng ED, Hajagos BE, Tyler JS, Bradley PJ: **The moving junction protein RON8 facilitates firm attachment and host cell invasion in Toxoplasma gondii.** *PLoS Pathog* 2011, **7:**e1002007.

58.     Lamarque MH, Roques M, Kong-Hap M, Tonkin ML, Rugarabamu G, Marq JB, Penarete-Vargas DM, Boulanger MJ, Soldati-Favre D, Lebrun M: **Plasticity and redundancy among AMA-RON pairs ensure host cell entry of Toxoplasma parasites.** *Nat Commun* 2014, **5:**4098.

59.     Malleret B, Li A, Zhang R, Tan KS, Suwanarusk R, Claser C, Cho JS, Koh EG, Chu CS, Pukrittayakamee S, et al: **Plasmodium vivax: restricted tropism and rapid remodeling of CD71-positive reticulocytes.** *Blood* 2015, **125:**1314-1324.

60.     Thomson-Luque R, Shaw Saliba K, Kocken CHM, Pasini EM: **A Continuous, Long-Term Plasmodium vivax In Vitro Blood-Stage Culture: What Are We Missing?** *Trends Parasitol* 2017, **33:**921-924.

61.     Chitnis CE, Sharma A: **Targeting the Plasmodium vivax Duffy-binding protein.** *Trends Parasitol* 2008, **24:**29-34.

62.     Galinski MR, Medina CC, Ingravallo P, Barnwell JW: **A reticulocyte-binding protein complex of Plasmodium vivax merozoites.** *Cell* 1992, **69:**1213-1226.

63.     Wilson MC, Trakarnsanga K, Heesom KJ, Cogan N, Green C, Toye AM, Parsons SF, Anstee DJ, Frayne J: **Comparison of the Proteome of Adult and Cord Erythroid Cells, and Changes in the Proteome Following Reticulocyte Maturation.** *Mol Cell Proteomics* 2016, **15:**1938-1946.

64. Gunalan K, Lo E, Hostetler JB, Yewhalaw D, Mu J, Neafsey DE, Yan G, Miller LH: **Role of Plasmodium vivax Duffy-binding protein 1 in invasion of Duffy-null Africans.** *Proc Natl Acad Sci U S A* 2016, **113:**6271-6276.

65. Carlton JM, Adams JH, Silva JC, Bidwell SL, Lorenzi H, Caler E, Crabtree J, Angiuoli SV, Merino EF, Amedeo P, et al: **Comparative genomics of the neglected human malaria parasite Plasmodium vivax.** *Nature* 2008, **455:**757-763.

66. Moreno-Perez DA, Montenegro M, Patarroyo ME, Patarroyo MA: **Identification, characterization and antigenicity of the Plasmodium vivax rhoptry neck protein 1 (PvRON1).** *Malar J* 2011, **10:**314.

67. Moreno-Perez DA, Saldarriaga A, Patarroyo MA: **Characterizing PvARP, a novel Plasmodium vivax antigen.** *Malar J* 2013, **12:**165.

68. Angel DI, Mongui A, Ardila J, Vanegas M, Patarroyo MA: **The Plasmodium vivax Pv41 surface protein: identification and characterization.** *Biochem Biophys Res Commun* 2008, **377:**1113-1117.

69. Arevalo-Pinzon G, Curtidor H, Abril J, Patarroyo MA: **Annotation and characterization of the Plasmodium vivax rhoptry neck protein 4 (PvRON4).** *Malar J* 2013, **12:**356.

70. Arevalo-Pinzon G, Bermudez M, Curtidor H, Patarroyo MA: **The Plasmodium vivax rhoptry neck protein 5 is expressed in the apical pole of Plasmodium vivax VCG-1 strain schizonts and binds to human reticulocytes.** *Malar J* 2015, **14:**106.

71. Cibulskis RE, Alonso P, Aponte J, Aregawi M, Barrette A, Bergeron L, Fergus CA, Knox T, Lynch M, Patouillard E, et al: **Malaria: Global progress 2000 - 2015 and future challenges.** *Infect Dis Poverty* 2016, **5:**61.

72. Djouaka R, Riveron JM, Yessoufou A, Tchigossou G, Akoton R, Irving H, Djegbe I, Moutairou K, Adeoti R, Tamo M, et al: **Multiple insecticide resistance in an infected population of the malaria vector Anopheles funestus in Benin.** *Parasit Vectors* 2016, **9:**453.

73. Dondorp AM, Yeung S, White L, Nguon C, Day NP, Socheat D, von Seidlein L: **Artemisinin resistance: current status and scenarios for containment.** *Nat Rev Microbiol* 2010, **8:**272-280.

74. Hoffman SL, Goh LM, Luke TC, Schneider I, Le TP, Doolan DL, Sacci J, de la Vega P, Dowler M, Paul C, et al: **Protection of humans against malaria by immunization with radiation-attenuated Plasmodium falciparum sporozoites.** *J Infect Dis* 2002, **185:**1155-1164.

75. Kumar KA, Baxter P, Tarun AS, Kappe SH, Nussenzweig V: **Conserved protective mechanisms in radiation and genetically attenuated uis3(-) and uis4(-) Plasmodium sporozoites.** *PLoS One* 2009, **4:**e4480.

76. Roestenberg M, McCall M, Hopman J, Wiersma J, Luty AJ, van Gemert GJ, van de Vegte-Bolmer M, van Schaijk B, Teelen K, Arens T, et al: **Protection against a malaria challenge by sporozoite inoculation.** *N Engl J Med* 2009, **361:**468-477.

77. Tuju J, Kamuyu G, Murungi LM, Osier FHA: **Vaccine candidate discovery for the next generation of malaria vaccines.** *Immunology* 2017, **152:**195-206.

78. Malkin E, Hu J, Li Z, Chen Z, Bi X, Reed Z, Dubovsky F, Liu J, Wang Q, Pan X, et al: **A phase 1 trial of PfCP2.9: an AMA1/MSP1 chimeric recombinant protein vaccine for Plasmodium falciparum malaria.** *Vaccine* 2008, **26:**6864-6873.

79. Sagara I, Ellis RD, Dicko A, Niambele MB, Kamate B, Guindo O, Sissoko MS, Fay MP, Guindo MA, Kante O, et al: **A randomized and controlled Phase 1 study of the safety**

and immunogenicity of the AMA1-C1/Alhydrogel + CPG 7909 vaccine for Plasmodium falciparum malaria in semi-immune Malian adults.** *Vaccine* 2009, **27:**7292-7298.

80.    Audran R, Cachat M, Lurati F, Soe S, Leroy O, Corradin G, Druilhe P, Spertini F: **Phase I malaria vaccine trial with a long synthetic peptide derived from the merozoite surface protein 3 antigen.** *Infect Immun* 2005, **73:**8017-8026.

81.    Arama C, Troye-Blomberg M: **The path of malaria vaccine development: challenges and perspectives.** *J Intern Med* 2014, **275:**456-466.

82.    Plebanski M, Locke E, Kazura JW, Coppel RL: **Malaria vaccines: into a mirror, darkly?** *Trends Parasitol* 2008, **24:**532-536.

83.    Goodman AL, Draper SJ: **Blood-stage malaria vaccines - recent progress and future challenges.** *Ann Trop Med Parasitol* 2010, **104:**189-211.

84.    Volkman SK, Hartl DL, Wirth DF, Nielsen KM, Choi M, Batalov S, Zhou Y, Plouffe D, Le Roch KG, Abagyan R, Winzeler EA: **Excess polymorphisms in genes for membrane proteins in Plasmodium falciparum.** *Science* 2002, **298:**216-218.

85.    Flanagan KL, Wilson KL, Plebanski M: **Polymorphism in liver-stage malaria vaccine candidate proteins: immune evasion and implications for vaccine design.** *Expert Rev Vaccines* 2016, **15:**389-399.

86.    Takala SL, Coulibaly D, Thera MA, Dicko A, Smith DL, Guindo AB, Kone AK, Traore K, Ouattara A, Djimde AA, et al: **Dynamics of polymorphism in a malaria vaccine antigen at a vaccine-testing site in Mali.** *PLoS Med* 2007, **4:**e93.

87.    Ouattara A, Barry AE, Dutta S, Remarque EJ, Beeson JG, Plowe CV: **Designing malaria vaccines to circumvent antigen variability.** *Vaccine* 2015, **33:**7506-7512.

88.    Takala SL, Coulibaly D, Thera MA, Batchelor AH, Cummings MP, Escalante AA, Ouattara A, Traore K, Niangaly A, Djimde AA, et al: **Extreme polymorphism in a vaccine antigen and risk of clinical malaria: implications for vaccine development.** *Sci Transl Med* 2009, **1:**2ra5.

89.    Thera MA, Doumbo OK, Coulibaly D, Diallo DA, Sagara I, Dicko A, Diemert DJ, Heppner DG, Jr., Stewart VA, Angov E, et al: **Safety and allele-specific immunogenicity of a malaria vaccine in Malian adults: results of a phase I randomized trial.** *PLoS Clin Trials* 2006, **1:**e34.

90.    Neafsey DE, Juraska M, Bedford T, Benkeser D, Valim C, Griggs A, Lievens M, Abdulla S, Adjei S, Agbenyega T, et al: **Genetic Diversity and Protective Efficacy of the RTS,S/AS01 Malaria Vaccine.** *N Engl J Med* 2015, **373:**2025-2037.

91.    Patarroyo ME, Patarroyo MA: **Emerging rules for subunit-based, multiantigenic, multistage chemically synthesized vaccines.** *Acc Chem Res* 2008, **41:**377-386.

92.    Patarroyo ME, Arevalo-Pinzon G, Reyes C, Moreno-Vranich A, Patarroyo MA: **Malaria Parasite Survival Depends on Conserved Binding Peptides' Critical Biological Functions.** *Curr Issues Mol Biol* 2016, **18:**57-78.

93.    Calvo M, Guzman F, Perez E, Segura CH, Molano A, Patarroyo ME: **Specific interactions of synthetic peptides derived from P. falciparum merozoite proteins with human red blood cells.** *Pept Res* 1991, **4:**324-333.

94.    Curtidor H, Vanegas M, Alba MP, Patarroyo ME: **Functional, immunological and three-dimensional analysis of chemically synthesised sporozoite peptides as components of a fully-effective antimalarial vaccine.** *Curr Med Chem* 2011, **18:**4470-4502.

95. Rodriguez LE, Curtidor H, Urquiza M, Cifuentes G, Reyes C, Patarroyo ME: **Intimate molecular interactions of P. falciparum merozoite proteins involved in invasion of red blood cells and their implications for vaccine design.** *Chem Rev* 2008, **108:**3656-3705.

96. Berzofsky JA, Ahlers JD, Belyakov IM: **Strategies for designing and optimizing new generation vaccines.** *Nat Rev Immunol* 2001, **1:**209-219.

97. Patarroyo ME, Bermudez A, Patarroyo MA: **Structural and immunological principles leading to chemically synthesized, multiantigenic, multistage, minimal subunit-based vaccine development.** *Chem Rev* 2011, **111:**3459-3507.

98. Espejo F, Cubillos M, Salazar LM, Guzman F, Urquiza M, Ocampo M, Silva Y, Rodriguez R, Lioy E, Patarroyo ME: **Structure, Immunogenicity, and Protectivity Relationship for the 1585 Malarial Peptide and Its Substitution Analogues.** *Angew Chem Int Ed Engl* 2001, **40:**4654-4657.

99. Guzman F, Jaramillo K, Salazar LM, Torres A, Rivera A, Patarroyo ME: **1H-NMR structures of the Plasmodium falciparum 1758 erythrocyte binding peptide analogues and protection against malaria.** *Life Sci* 2002, **71:**2773-2785.

100. Patarroyo ME, Patarroyo MA, Pabon L, Curtidor H, Poloche LA: **Immune protection-inducing protein structures (IMPIPS) against malaria: the weapons needed for beating Odysseus.** *Vaccine* 2015, **33:**7525-7537.

101. Rodriguez LE, Urquiza M, Ocampo M, Curtidor H, Suarez J, Garcia J, Vera R, Puentes A, Lopez R, Pinto M, et al: ***Plasmodium vivax* MSP-1 peptides have high specific binding activity to human reticulocytes.** *Vaccine* 2002, **20:**1331-1339.

102. Ocampo M, Vera R, Eduardo Rodriguez L, Curtidor H, Urquiza M, Suarez J, Garcia J, Puentes A, Lopez R, Trujillo M, et al: **Plasmodium vivax Duffy binding protein peptides specifically bind to reticulocytes.** *Peptides* 2002, **23:**13-22.

103. Moreno-Perez DA, Ruiz JA, Patarroyo MA: **Reticulocytes: Plasmodium vivax target cells.** *Biol Cell* 2013, **105:**251-260.

104. Russell B, Suwanarusk R, Borlon C, Costa FT, Chu CS, Rijken MJ, Sriprawat K, Warter L, Koh EG, Malleret B, et al: **A reliable ex vivo invasion assay of human reticulocytes by Plasmodium vivax.** *Blood* 2011, **118:**e74-81.

105. Chu TTT, Sinha A, Malleret B, Suwanarusk R, Park JE, Naidu R, Das R, Dutta B, Ong ST, Verma NK, et al: **Quantitative mass spectrometry of human reticulocytes reveal proteome-wide modifications during maturation.** *Br J Haematol* 2018, **180:**118-133.

106. Udomsangpetch R, Somsri S, Panichakul T, Chotivanich K, Sirichaisinthop J, Yang Z, Cui L, Sattabongkot J: **Short-term in vitro culture of field isolates of Plasmodium vivax using umbilical cord blood.** *Parasitol Int* 2007, **56:**65-69.

107. Arevalo-Pinzon G, Bermudez M, Hernandez D, Curtidor H, Patarroyo MA: **Plasmodium vivax ligand-receptor interaction: PvAMA-1 domain I contains the minimal regions for specific interaction with CD71+ reticulocytes.** *Sci Rep* 2017, **7:**9616.

108. Stubbs J, Simpson KM, Triglia T, Plouffe D, Tonkin CJ, Duraisingh MT, Maier AG, Winzeler EA, Cowman AF: **Molecular mechanism for switching of P. falciparum invasion pathways into human erythrocytes.** *Science* 2005, **309:**1384-1387.

109. Lin CS, Uboldi AD, Marapana D, Czabotar PE, Epp C, Bujard H, Taylor NL, Perugini MA, Hodder AN, Cowman AF: **The merozoite surface protein 1 complex is a platform for binding to human erythrocytes by Plasmodium falciparum.** *J Biol Chem* 2014, **289:**25655-25669.

110. Kauth CW, Woehlbier U, Kern M, Mekonnen Z, Lutz R, Mucke N, Langowski J, Bujard H: **Interactions between merozoite surface proteins 1, 6, and 7 of the malaria parasite Plasmodium falciparum.** *J Biol Chem* 2006, **281:**31517-31527.

111. Ranjan R, Chugh M, Kumar S, Singh S, Kanodia S, Hossain MJ, Korde R, Grover A, Dhawan S, Chauhan VS, et al: **Proteome analysis reveals a large merozoite surface protein-1 associated complex on the Plasmodium falciparum merozoite surface.** *J Proteome Res* 2011, **10:**680-691.

112. Wanaguru M, Crosnier C, Johnson S, Rayner JC, Wright GJ: **Biochemical analysis of the Plasmodium falciparum erythrocyte-binding antigen-175 (EBA175)-glycophorin-A interaction: implications for vaccine design.** *J Biol Chem* 2013, **288:**32106-32117.

113. Batchelor JD, Malpede BM, Omattage NS, DeKoster GT, Henzler-Wildman KA, Tolia NH: **Red blood cell invasion by Plasmodium vivax: structural basis for DBP engagement of DARC.** *PLoS Pathog* 2014, **10:**e1003869.

114. Lin CS, Uboldi AD, Epp C, Bujard H, Tsuboi T, Czabotar PE, Cowman AF: **Multiple Plasmodium falciparum Merozoite Surface Protein 1 Complexes Mediate Merozoite Binding to Human Erythrocytes.** *J Biol Chem* 2016, **291:**7703-7715.

115. Li X, Chen H, Oo TH, Daly TM, Bergman LW, Liu SC, Chishti AH, Oh SS: **A co-ligand complex anchors Plasmodium falciparum merozoites to the erythrocyte invasion receptor band 3.** *J Biol Chem* 2004, **279:**5765-5771.

116. Baldwin MR, Li X, Hanada T, Liu SC, Chishti AH: **Merozoite surface protein 1 recognition of host glycophorin A mediates malaria parasite invasion of red blood cells.** *Blood* 2015, **125:**2704-2711.

117. Crosnier C, Bustamante LY, Bartholdson SJ, Bei AK, Theron M, Uchikawa M, Mboup S, Ndir O, Kwiatkowski DP, Duraisingh MT, et al: **Basigin is a receptor essential for erythrocyte invasion by Plasmodium falciparum.** *Nature* 2011, **480:**534-537.

118. Reddy KS, Amlabu E, Pandey AK, Mitra P, Chauhan VS, Gaur D: **Multiprotein complex between the GPI-anchored CyRPA with PfRH5 and PfRipr is crucial for Plasmodium falciparum erythrocyte invasion.** *Proc Natl Acad Sci U S A* 2015, **112:**1179-1184.

119. Galaway F, Drought LG, Fala M, Cross N, Kemp AC, Rayner JC, Wright GJ: **P113 is a merozoite surface protein that binds the N terminus of Plasmodium falciparum RH5.** *Nat Commun* 2017, **8:**14333.

120. Beck JR, Chen AL, Kim EW, Bradley PJ: **RON5 is critical for organization and function of the Toxoplasma moving junction complex.** *PLoS Pathog* 2014, **10:**e1004025.

121. Guerin A, El Hajj H, Penarete-Vargas D, Besteiro S, Lebrun M: **RON4L1 is a new member of the moving junction complex in Toxoplasma gondii.** *Sci Rep* 2017, **7:**17907.

122. Tonkin ML, Roques M, Lamarque MH, Pugniere M, Douguet D, Crawford J, Lebrun M, Boulanger MJ: **Host cell invasion by apicomplexan parasites: insights from the co-structure of AMA1 with a RON2 peptide.** *Science* 2011, **333:**463-467.

123. Vulliez-Le Normand B, Saul FA, Hoos S, Faber BW, Bentley GA: **Cross-reactivity between apical membrane antgen 1 and rhoptry neck protein 2 in P. vivax and P. falciparum: A structural and binding study.** *PLoS One* 2017, **12:**e0183198.

124. Vulliez-Le Normand B, Tonkin ML, Lamarque MH, Langer S, Hoos S, Roques M, Saul FA, Faber BW, Bentley GA, Boulanger MJ, Lebrun M: **Structural and functional insights into the malaria parasite moving junction complex.** *PLoS Pathog* 2012, **8:**e1002755.

125.	Srinivasan P, Ekanem E, Diouf A, Tonkin ML, Miura K, Boulanger MJ, Long CA, Narum DL, Miller LH: **Immunization with a functional protein complex required for erythrocyte invasion protects against lethal malaria.** *Proc Natl Acad Sci U S A* 2014, **111:**10311-10316.

126.	Guerin A, Corrales RM, Parker ML, Lamarque MH, Jacot D, El Hajj H, Soldati-Favre D, Boulanger MJ, Lebrun M: **Efficient invasion by Toxoplasma depends on the subversion of host protein networks.** *Nat Microbiol* 2017, **2:**1358-1366.

127.	Giovannini D, Spath S, Lacroix C, Perazzi A, Bargieri D, Lagal V, Lebugle C, Combe A, Thiberge S, Baldacci P, et al: **Independent roles of apical membrane antigen 1 and rhoptry neck proteins during host cell invasion by apicomplexa.** *Cell Host Microbe* 2011, **10:**591-602.

128.	Hostetler JB, Sharma S, Bartholdson SJ, Wright GJ, Fairhurst RM, Rayner JC: **A Library of Plasmodium vivax Recombinant Merozoite Proteins Reveals New Vaccine Candidates and Protein-Protein Interactions.** *PLoS Negl Trop Dis* 2015, **9:**e0004264.

129.	Petschnigg J, Snider J, Stagljar I: **Interactive proteomics research technologies: recent applications and advances.** *Curr Opin Biotechnol* 2011, **22:**50-58.

130.	Auerbach D, Thaminy S, Hottiger MO, Stagljar I: **The post-genomic era of interactive proteomics: facts and perspectives.** *Proteomics* 2002, **2:**611-623.

131.	Manzano-Roman R, Dasilva N, Diez P, Diaz-Martin V, Perez-Sanchez R, Orfao A, Fuentes M: **Protein arrays as tool for studies at the host-pathogen interface.** *J Proteomics* 2013, **94:**387-400.

132.	Fields S, Song O: **A novel genetic system to detect protein-protein interactions.** *Nature* 1989, **340:**245-246.

133.	Vasavada HA, Ganguly S, Germino FJ, Wang ZX, Weissman SM: **A contingent replication assay for the detection of protein-protein interactions in animal cells.** *Proc Natl Acad Sci U S A* 1991, **88:**10686-10690.

134.	Miyawaki A, Tsien RY: **Monitoring protein conformations and interactions by fluorescence resonance energy transfer between mutants of green fluorescent protein.** *Methods Enzymol* 2000, **327:**472-500.

135.	Chan FK, Holmes KL: **Flow cytometric analysis of fluorescence resonance energy transfer: a tool for high-throughput screening of molecular interactions in living cells.** *Methods Mol Biol* 2004, **263:**281-292.

136.	Burckstummer T, Bennett KL, Preradovic A, Schutze G, Hantschel O, Superti-Furga G, Bauch A: **An efficient tandem affinity purification procedure for interaction proteomics in mammalian cells.** *Nat Methods* 2006, **3:**1013-1019.

137.	Natsume T, Nakayama H, Isobe T: **BIA-MS-MS: biomolecular interaction analysis for functional proteomics.** *Trends Biotechnol* 2001, **19:**S28-33.

138.	Kikuchi J, Furukawa Y, Hayashi N: **Identification of novel p53-binding proteins by biomolecular interaction analysis combined with tandem mass spectrometry.** *Mol Biotechnol* 2003, **23:**203-212.

139.	Manzano-Roman R, Diaz-Martin V, Gonzalez-Gonzalez M, Matarraz S, Alvarez-Prado AF, LaBaer J, Orfao A, Perez-Sanchez R, Fuentes M: **Self-assembled protein arrays from an Ornithodoros moubata salivary gland expression library.** *J Proteome Res* 2012, **11:**5972-5982.

140. He M, Taussig MJ: **Single step generation of protein arrays from DNA by cell-free expression and in situ immobilisation (PISA method).** *Nucleic Acids Res* 2001, **29:**E73-73.

141. Templin MF, Stoll D, Schrenk M, Traub PC, Vohringer CF, Joos TO: **Protein microarray technology.** *Drug Discov Today* 2002, **7:**815-822.

142. Zhu H, Bilgin M, Bangham R, Hall D, Casamayor A, Bertone P, Lan N, Jansen R, Bidlingmaier S, Houfek T, et al: **Global analysis of protein activities using proteome chips.** *Science* 2001, **293:**2101-2105.

143. Ramani SR, Tom I, Lewin-Koh N, Wranik B, Depalatis L, Zhang J, Eaton D, Gonzalez LC: **A secreted protein microarray platform for extracellular protein interaction discovery.** *Anal Biochem* 2012, **420:**127-138.

144. Natesan M, Ulrich RG: **Protein microarrays and biomarkers of infectious disease.** *Int J Mol Sci* 2010, **11:**5165-5183.

145. Takeda A, Shimada H, Nakajima K, Imaseki H, Suzuki T, Asano T, Ochiai T, Isono K: **Monitoring of p53 autoantibodies after resection of colorectal cancer: relationship to operative curability.** *Eur J Surg* 2001, **167:**50-53.

146. Weber MS, Hemmer B, Cepok S: **The role of antibodies in multiple sclerosis.** *Biochim Biophys Acta* 2011, **1812:**239-245.

147. Nokoff NJ, Rewers M, Cree Green M: **The interplay of autoimmunity and insulin resistance in type 1 diabetes.** *Discov Med* 2012, **13:**115-122.

148. Montor WR, Huang J, Hu Y, Hainsworth E, Lynch S, Kronish JW, Ordonez CL, Logvinenko T, Lory S, LaBaer J: **Genome-wide study of Pseudomonas aeruginosa outer membrane protein immunogenicity using self-assembling protein microarrays.** *Infect Immun* 2009, **77:**4877-4886.

149. Kunnath-Velayudhan S, Salamon H, Wang HY, Davidow AL, Molina DM, Huynh VT, Cirillo DM, Michel G, Talbot EA, Perkins MD, et al: **Dynamic antibody responses to the Mycobacterium tuberculosis proteome.** *Proc Natl Acad Sci U S A* 2010, **107:**14703-14708.

150. Nnedu ON, O'Leary MP, Mutua D, Mutai B, Kalantari-Dehaghi M, Jasinskas A, Nakajima-Sasaki R, John-Stewart G, Otieno P, Liang X, et al: **Humoral immune responses to Plasmodium falciparum among HIV-1-infected Kenyan adults.** *Proteomics Clin Appl* 2011, **5:**613-623.

151. Arenkov P, Kukhtin A, Gemmell A, Voloshchuk S, Chupeeva V, Mirzabekov A: **Protein microchips: use for immunoassay and enzymatic reactions.** *Anal Biochem* 2000, **278:**123-131.

152. Qiu J, LaBaer J: **Nucleic acid programmable protein array a just-in-time multiplexed protein expression and purification platform.** *Methods Enzymol* 2011, **500:**151-163.

153. Saul J, Petritis B, Sau S, Rauf F, Gaskin M, Ober-Reynolds B, Mineyev I, Magee M, Chaput J, Qiu J, LaBaer J: **Development of a full-length human protein production pipeline.** *Protein Sci* 2014, **23:**1123-1135.

154. Grabski AC: **Advances in preparation of biological extracts for protein purification.** *Methods Enzymol* 2009, **463:**285-303.

155. Goshima N, Kawamura Y, Fukumoto A, Miura A, Honma R, Satoh R, Wakamatsu A, Yamamoto J, Kimura K, Nishikawa T, et al: **Human protein factory for converting the transcriptome into an in vitro-expressed proteome.** *Nat Methods* 2008, **5:**1011-1017.

156. Ramachandran N, Hainsworth E, Bhullar B, Eisenstein S, Rosen B, Lau AY, Walter JC, LaBaer J: **Self-assembling protein microarrays.** *Science* 2004, **305:**86-90.
157. Angenendt P, Kreutzberger J, Glokler J, Hoheisel JD: **Generation of high density protein microarrays by cell-free in situ expression of unpurified PCR products.** *Mol Cell Proteomics* 2006, **5:**1658-1666.
158. Ramachandran N, Raphael JV, Hainsworth E, Demirkan G, Fuentes MG, Rolfs A, Hu Y, LaBaer J: **Next-generation high-density self-assembling functional protein arrays.** *Nat Methods* 2008, **5:**535-538.
159. Yu X, Bian X, Throop A, Song L, Moral LD, Park J, Seiler C, Fiacco M, Steel J, Hunter P, et al: **Exploration of panviral proteome: high-throughput cloning and functional implications in virus-host interactions.** *Theranostics* 2014, **4:**808-822.
160. Yu X, Decker KB, Barker K, Neunuebel MR, Saul J, Graves M, Westcott N, Hang H, LaBaer J, Qiu J, Machner MP: **Host-pathogen interaction profiling using self-assembling human protein arrays.** *J Proteome Res* 2015, **14:**1920-1936.

**ANEXOS**

**Anexo 1 "Self-assembling functional programmable protein array for studying protein-protein interactions in malaria parasites"**

# Malaria Journal

## Self-assembling functional programmable protein array for studying protein-protein interactions in malaria parasites
### --Manuscript Draft--

| | |
|---|---|
| Manuscript Number: | |
| Full Title: | Self-assembling functional programmable protein array for studying protein-protein interactions in malaria parasites |
| Article Type: | Research |

| Abstract: | Background<br>Plasmodium vivax is the most widespread malarial species, causing significant morbidity worldwide. Knowledge is limited regarding the molecular mechanism of invasion due to the lack of a continuous in vitro culture system for these species. Since protein-protein and host-cell interactions play an essential role in the microorganism's invasion and replication, elucidating protein function during invasion is critical when developing more effective control methods. Nucleic acid programmable protein array (NAPPA) has thus become a suitable technology for studying protein-protein and host-protein interactions since producing proteins through the in vitro transcription/translation (IVTT) method overcomes most of the drawbacks encountered to date, such as heterologous protein production, stability and purification.<br><br>Results<br>Twenty P. vivax proteins on merozoite surface or in secretory organelles were selected and successfully cloned using gateway technology. Most constructs were displayed in the array expressed in situ, using the IVTT method. The Pv12 protein was used as bait for evaluating array functionality and co-expressed with P. vivax cDNA display in the array. It was found that Pv12 interacted with Pv41 (as previously described), as well as PvMSP142kDa, PvRBP1a, PvMSP8 and PvRAP1.<br><br>Conclusions<br>NAPPA is a high-performance technique enabling co-expression of bait and query in situ, thereby enabling interactions to be analysed rapidly and reproducibly. It offers a fresh alternative for studying protein-protein and ligand-receptor interactions regarding a parasite which is difficult to cultivate (i.e. P. vivax). |
|---|---|

| Corresponding Author: | Manuel Fuentes, Ph.D.<br>Instituto de Biologia Molecular y Celular del Cancer<br>SPAIN |
|---|---|
| Corresponding Author Secondary Information: | |

| Corresponding Author's Institution: | Instituto de Biologia Molecular y Celular del Cancer |
| --- | --- |
| Corresponding Author's Secondary Institution: | |
| First Author: | Gabriela Arévalo Pinzón |
| First Author Secondary Information: | |
| Order of Authors: | Gabriela Arévalo Pinzón |
| | María González-González |
| | Carlos Fernando Suárez |
| | Hernando Curtidor |
| | Javier Carabias-Sánchez |
| | Antonio Muro |
| | Joshua LaBaer |
| | Manuel Alfonso Patarroyo, M.D., Dr.Sc. |
| | Manuel Fuentes |
| Order of Authors Secondary Information: | |
| Suggested Reviewers: | Asif Mohmmed<br>ICGEB, New Delhi, India<br>amohd@icgeb.res.in<br>Expert in the field. |
| | Olivier Chaloin<br>French National Centre for Scientific Research-CNRS-IBMC<br>o.chaloin@unistra.fr<br>Expert in the field. |
| | Brigitte Vulliez-Le Normand<br>Institut Pasteur<br>bvulliez@pasteur.fr<br>Expert in the field. |
| | Agustín Benito<br>Instituto de Salud Carlos III<br>abenito@isciii.es<br>Expert in the field. |
| | Sanjeeva Srivastava<br>Indian Institute of Technology Bombay<br>sanjeeva@iitb.ac.in<br>Expert in the field. |
| | Mitch Magee<br>Texas Center for Infectious Diseases<br>mitch.magee@asu.edu<br>Expert in the field. |

| Additional Information: | |
| --- | --- |
| Question | Response |
| <b>Is this study a clinical trial?</b><hr><i>A clinical trial is defined by the Word Health Organisation as 'any research study that prospectively assigns human participants or groups of humans to one or more health-related interventions to evaluate the effects on health outcomes'.</i> | No |

# Self-assembling functional programmable protein array for studying protein-protein interactions in malaria parasites

Gabriela Arévalo-Pinzón [1,2], María González-González [3,4], Carlos Fernando Suárez [1,5], Hernando Curtidor [1,6], Javier Carabias-Sánchez [3], Antonio Muro [7], Joshua LaBaer [8], Manuel Alfonso Patarroyo [1,6], Manuel Fuentes [3, 4*]

[1] Fundación Instituto de Inmunología de Colombia (FIDIC), Carrera 50 # 26-20, Bogotá, Colombia

[2] PhD Programme in Biomedical and Biological Sciences, Universidad del Rosario, Carrera 24 # 63C-69, Bogotá, Colombia

[3] Proteomics Unit, Cancer Research Centre (IBMCC/CSIC/USAL/IBSAL), Salamanca 37007, Spain

[4] Department of Medicine and General Cytometry Service-Nucleus, Cancer Research Centre (IBMCC/CSIC/USAL/IBSAL), Salamanca 37007, Spain

[5] Universidad de Ciencias Aplicadas y Ambientales (U.D.C.A.), Calle 222 # 55 - 37, Bogotá, Colombia

[6] School of Medicine and Health Sciences, Universidad del Rosario, Carrera 24 # 63C-69, Bogotá, Colombia

[7] Unidad de Investigación Enfermedades Infecciosas y Tropicales (e-INTRO), Instituto de Investigación Biomédica de Salamanca-Centro de Investigación de Enfermedades Tropicales de la Universidad de Salamanca (IBSAL-CIETUS), Facultad de Farmacia, Universidad de Salamanca, Campus Universitario Miguel de Unamuno s/n, E-37007 Salamanca, Spain

[8] Virginia G. Piper Center for Personalized Diagnostics, Biodesign Institute, Arizona State University, Tempe, Arizona


*Corresponding author

E-mail addresses:

GAP gabarpi@gmail.com
MGG mariagg@usal.es
CFS cfsuarezm@gmail.com
HC hernando.curtidor@urosario.edu.co
JCS jcarabias@usal.es
AM ama@usal.es
JL jlabaer@asu.edu
MAP mapatarr.fidic@gmail.com
MF mfuentes@usal.es

**Abstract**

**Background**

*Plasmodium vivax* is the most widespread malarial species, causing significant morbidity worldwide. Knowledge is limited regarding the molecular mechanism of invasion due to the lack of a continuous *in vitro* culture system for these species. Since protein-protein and host-cell interactions play an essential role in the microorganism's invasion and replication, elucidating protein function during invasion is critical when developing more effective control methods. Nucleic acid programmable protein array (NAPPA) has thus become a suitable technology for studying protein-protein and host-protein interactions since producing proteins through the *in vitro* transcription/translation (IVTT) method overcomes most of the drawbacks encountered to date, such as heterologous protein production, stability and purification.

**Results**

Twenty *P. vivax* proteins on merozoite surface or in secretory organelles were selected and successfully cloned using gateway technology. Most constructs were displayed in the array expressed *in situ*, using the IVTT method. The *Pv*12 protein was used as bait for evaluating array functionality and co-expressed with *P. vivax* cDNA display in the array. It was found that *Pv*12 interacted with *Pv*41 (as previously described), as well as *Pv*MSP1$_{42kDa}$, *Pv*RBP1a, *Pv*MSP8 and *Pv*RAP1.

**Conclusions**

NAPPA is a high-performance technique enabling co-expression of bait and query *in situ*, thereby enabling interactions to be analysed rapidly and reproducibly. It offers a fresh alternative for studying protein-protein and ligand-receptor interactions regarding a parasite which is difficult to cultivate (i.e. *P. vivax*).

2

68

**Background**

Most pathogen invasion processes are mediated by protein-protein interactions (PPI) leading to the formation of stable or transitory molecular complexes between pathogen and host proteins which are necessary for successful invasion and replication. PPI networks have thus been studied in pathogens such as *Bacillus anthracis*, *Francisella tularensis* and *Yersinia pestis* with human proteins for defining a target/bait set of proteins for understanding pathogenicity mechanisms [1]; such study has revealed how the different pathogens interact with crucial host pathways involved in inflammation and immunity [1].

Reports concerning *P. falciparum* (a protozoan parasite responsible for most mortality caused by malaria worldwide) have reported that a significant amount of proteins being expressed in specialised apical organelles and on cell membrane interact with host cell receptors during sporozoite (Spz) invasion of hepatocytes and merozoite (Mrz) invasion of red blood cells (RBC) [2-4]. Such interactions are indispensable for parasite entry and establishment within parasitophorous vacuoles where the parasite resides during its development within a host cell [5].

*Plasmodium* parasites have a diverse ligand repertoire [3] and adapt to differing conditions [6, 7]; however, the scenario is much more complex. Evidence has grown regarding macromolecular complex formation between ligands [8-10] and host surface molecule multimeric assemblies which could favour and increase the strength of any receptor-ligand interaction [11, 12]. It has been seen for *P. falciparum* (the best characterised *Plasmodium* species) that the major Mrz surface protein (*Pf*MSP1) has macromolecular interactions with *Pf*MSP6, *Pf*MSP7, *Pf*RhopH3, *Pf*RAP1, *Pf*RAP2, *Pf*MSP1DBL1, *Pf*MSP1DBL2 and forms

4

93  a co-ligand complex with *Pf*MSP9, whilst different *Pf*MSP1 fragments interact with

94  glycophorin A and Band3 and other not-yet-identified receptors on RBC membrane [8-10,

95  13-15].

96

97  Chromatographic and interaction analyses have shown that MSP1 is a binding platform for

98  several soluble proteins forming a variety of different-sized MSP1 complexes on Mrz

99  surface [10, 14]. Protein complexes which might play a role in Mrz invasion have been

100  isolated and purified from detergent-resistant membranes (DRMs), such as low (RAP1/2

101  and RAP1/3) and high molecular weight rhoptry complexes (RhopH1/H2/H3) and the

102  invasion motor complex (GAP45/GAP50/myosinA), as well as from proteins like MSP1,

103  *Pf*P113, *Pf*P12 and *Pf*41 [16]. It has been reported recently that *P. falciparum* reticulocyte

104  homologue 5 (*Pf*RH5, a conserved parasite soluble ligand) forms a multi-protein complex

105  with cysteine-rich protective antigen-CyRPA and the membrane-anchored parasite P113

106  protein, thereby enabling *Pf*RH5 to remain anchored to Mrz surface to interact with basigin

107  on RBC [17-19]. It is known that apical membrane antigen-1 (AMA-1) forms a

108  macromolecular complex with rhoptry neck (RON) proteins participating in tight junction

109  (TJ) or moving junction (MJ) formation [20-23], an essential step during which irreversible

110  and high-affinity interactions are maintained for parasite entry to RBC or hepatocytes [24].

111  This involves RON proteins being secreted into a host cell where RON2 spans the

112  membrane serving as ligand for AMA on parasite surface whilst RON4 and RON5 stabilise

113  the complex from host cell cytosol [25, 26]. Inhibitory antibody targets/baits from different

114  forms of the complexes formed by MSP1 and AMA-1 or peptides directed against AMA1-

115  RON2 complex interaction hotspots provide evidence that targeting critically important

116     regions in the core of these complexes could be used as a new strategy for blocking *P.*

117     *falciparum* invasion [8, 14, 27].

118

119     Little is known about macromolecular complexes and host-pathogen interactions

120     concerning *P. vivax*, the second most important species causing malaria worldwide [28].

121     Some proteins' functions have been speculated about to date on the basis of their

122     counterparts in other species [29]. Although *P. vivax* invasion is thought to be similar to

123     that of *P. falciparum*, some biological differences condition disease severity and hamper its

124     biological study [30, 31]. This is mainly related to this specie preferentially invading young

125     RBC, meaning that no continuous *in-vitro* culture is available for real-time evaluation of

126     protein interactions during invasion [31].

127

128     Genetic, cellular and biochemical approaches have been developed during the last few

129     years for *in vivo* and *in vitro* detection of protein-protein interactions [32, 33]; it should be

130     stressed that interactions must be identified for a better understanding of invasion and

131     characterising the specific molecular mechanisms involved in pathogen invasion and

132     survival within a target host cell [34, 35]. The increased amount of genomes sequenced to

133     date has led to designing high-performance techniques for analysing a large amount of

134     samples and resolving problems associated with proteins' traditional expression (cell-based

135     systems) and the use of different purification methods [36-38].

136

137     Protein microarrays enable direct detection of interactions on a proteomic scale, mainly

138     being used for identifying biomarkers, PPI and in enzymatic assays [39-41]. However,

139     conventional protein arrays pose several challenges, including the need for producing and

6

140    purifying a large amount of proteins having good yield and purity as well as maintaining

141    protein stability. Most protein cell expression methods require heterologous systems (i.e.

142    *Escherichia coli)* which could cause differences regarding protein yield; post-translational

143    modification status is highly dependent on the cell system used and such protocols are

144    extremely time-consuming.

145

146    Cell-free protein expression systems (CFPS) are thus an alternative for creating new arrays,

147    aimed at avoiding some of the aforementioned problems. CFPS are based on PCR products

148    or plasmids for *in vitro* protein synthesis using cell extracts (i.e. *E. coli*, wheat germ extract,

149    rabbit reticulocyte lysate (RRL), HeLa, etc.) which provide the required machinery for

150    individual protein transcription and translation [37, 42-44]. CFPS have been used with

151    different protein microarrays (i.e. NAPPA). NAPPA produces protein microarrays using

152    CFPS (mainly RRL) to transcribe and translate cDNA-encoded bait proteins directly onto

153    glass slides [45, 46]. *De novo* synthesised proteins are directly captured by anti-tag

154    antibodies co-spotted with specific cDNA. A target/bait *in vitro* transcription/translation

155    (IVTT) expressed protein is thus captured onto the surface ready for functional assays; this

156    approach has been successfully used in applications such as vaccine development and

157    evaluating autoimmune responses and protein-protein interactions [47-49]. A query protein

158    is simultaneously IVTT co-expressed with target/bait proteins in protein interaction assays;

159    however, this approach requires a different C-terminal tag. Such approach has been

160    successfully used in several applications, i.e. determining *Legionella pneumophila* effector

161    (SidM and LidA) interaction network with 10,000 unique human proteins [49] and

162    evaluating anti-serum profiles and protein interactions in a cDNA expression library from

163    *Ornithodoros moubata* salivary glands [50].

164    The difficulty of maintaining a continuous *P. vivax* culture hampers evaluating protein-

165    protein interactions when using functional approaches such as knockouts (total, conditional

166    with or without complementation) [6, 51], knockdowns or inhibition assays [52].

167    Alternatives are needed and NAPPA technology thus stands out as a very good choice for

168    studying *P. vivax* host-pathogen and protein-protein interactions. The present study

169    involved designing and developing a NAPPA array constructed by non-contact printing of

170    20 *P. vivax* key genes encoding proteins which might be involved in Mrz invasion of

171    reticulocytes. Each gene was sub-cloned in a vector compatible with the IVTT expression

172    system encoding a C-terminal tag. Such array has been optimised and fully-characterised to

173    study *in situ* protein interactions enabling new insights regarding the macromolecular

174    complexes involved in *P. vivax* protein-protein interactions.

175

176

**Methods**

177

**Primer design**

178

179    Primers containing a partial *attB* recombination sequence flanking a gene-specific sequence

180    were used for amplifying genes of interest from *P. vivax* cDNA or gDNA (Table S1). For

181    example, the forward primer 5'-

182    **AAAGCAGGCT**TC*GAAGGAGATAGAACCATG*<u>GAAACAGAAAGTTATAAGCAGC-</u>

183    <u>3'</u>, having the partial *attB* sequence (in bold) included a gene-specific portion (underlined)

184    and Shine Dalgarno and Kozak consensus sequences to enable protein expression (italics);

185    the reverse primer 5'-**AGAAAGCTGGGT**CTCC<u>TGTTGTTCCAGGCTGTACC</u>-3'

186    included a partial *attB* sequence and the gene-specific portion. The stop codon was

187    removed to enable the PCR product to be fused in frame with a C-terminal GST tag. A set

188    of universal primers containing complete *attB1*

189    (GGGGACAAGTTTGTACAAA<u>AAAGCAGGCTTCGAAGGAGAT</u>) and *attB2*

190    (GGGGACCACTTTGTACA<u>AGAAAGCTGGGTCTCC</u>) sequences were also synthesised.

191    Regions overlapping the partial *attB* sequence from gene-specific primers are underlined.

192

193    To fuse *Pv*12 in frame with an N-terminal Halo tag, gene specific primers (underlined)

194    were designed with the complete *attB* recombination sequence (in bold) (forward 5'-

195    **GGGGACAAGTTTGTACAAAAAAGCAGGCT**CC<u>ACGTGCGATTTTAATG</u>-3';

196    reverse 5'-

197    **GGGGACCACTTTGTACAAGAAAGCTGGGT**C*CTA*<u>GCCCTGCAGAACATTCGC</u>-

198    3'). The initiation (ATG) codon was deleted in each forward primer and the stop codon was

199    maintained in all reverse primers (in italics).

9

200  The region encoding the ectodomain was selected for each gene, excluding signal peptide,

201  transmembrane domain and glycosylphosphatidylinositol (GPI) anchor sequences (when

202  present). For some proteins (such as *Pv*MSP1, *Pv*RBP1a, *Pv*DBP and *Pv*RON2), several

203  fragments based on functional or previously studied regions were amplified (Table 1).

**Cloning and subcloning**

205  The first round of PCR involved 50 µL containing 25 µL 2x KAPA HiFi Ready Mix, 3.0

206  µL of each specific primer (5 µM concentration partial attB recombination sequence), 15

207  µL nuclease-free water and *P. vivax* cDNA or gDNA as template. PCR conditions for each

208  gene involved an initial denaturing step at 95°C for 3 min, followed by 35 cycles consisting

209  of denaturing at 98°C for 20 sec, annealing at 58-60°C for 30 sec and an extension step at

210  72°C for 1-2 min. A final extension cycle lasted 5 min at 72°C. The product obtained from

211  each gene was purified by Wizard SV Gel and PCR Clean-Up System (Promega),

212  according to the manufacturer's specifications. The second round of PCR involved 50 µL

213  reaction including a set of universal primers (5 µM concentration), 25 µL 2x KAPA HiFi

214  Ready Mix, 15 µL nuclease-free water and the purified product obtained in the first PCR to

215  introduce the remainder of the *attB* sequence needed for recombination using the Gateway

216  system (Invitrogen) [53]. The product obtained from each gene was purified and then used

217  for BP recombination.

218

219  Obtaining the pDONR constructs involved transferring 100 fmol of each purified insert into

220  the *attP* sequence-containing pDONR221 entry vector (150 ng/µL) in 2 µL BP clonase

221  (Invitrogen). The reaction was incubated for 4 h at 25°C and then used to transform One

222  Shot TOP10 chemically competent *E. coli* (Invitrogen). The cells were plated onto LB

223  agar-kanamycin and colonies were screened by PCR to identify positive clones. Five

224 positive clones were sequenced with M13 forward and reverse primers to confirm the

225 presence of the *P. vivax attL* gene-specific sequence.

226

227 LR reactions for transferring the pDONR221-containing *attL* sequence into *attR*-containing

228 pANT7-cGST or PJFT7-nHalo involved 20 µL LR enzyme (Invitrogen) 1:1 ratio

229 (donor:destination vector, each at 150 ng/µL) for 1-4 h at 25°C. Transfer reactions were

230 used to transform the DH5α competent *E. coli* strain (Invitrogen) which was then plated

231 onto LB agar-ampicillin.

232

**233 Plasmid sequencing**

234 The University of Salamanca's (CSIC) Cancer Research Centre (Spain) sequenced all

235 pANT7-cGST inserts in both strands using primers flanking the recombination regions

236 (forward: 5'-TAATACGACTCACTATAG-3'; reverse: 5'-

237 CCGCAAGCTTGTCATCAACCACTT-3'). Ten plasmids from the expression library

238 were randomly selected to assess insert presence by restriction with BsrGI (New England)

239 and to discard plasmid degradation.

240 The *pv12* gene cloned into pJFT7-nHalo was sequenced in both strands by using primers

241 flanking the recombination regions (forward: 5'-CCCATTGTATGGGATCTGATC-3';

242 reverse: 5'-TGTTTCGCCATTTATCACCTTC-3') at the sequencing service of the Cancer

243 Research Centre (University of Salamanca-CSIC, Spain).

244

**245 Sample preparation, substrate functionalisation and array printing**

246 Sample preparation involved seeding 3 µg of each purified plasmid DNA in a 384-well

247 microtitre plate and then incubating overnight at 40°C to allow the DNA to dry; 12 µL

11

248  master mix solution (containing 33.3 mg/mL bovine serum albumin (BSA), 2.5 mg/mL

249  rabbit polyclonal anti-GST antibody and 2 mM Bis-(sulfosuccinimidyl) suberate (BS3))

250  was added to each precipitated plasmid DNA and then incubated for 30min at 37°C,

251  following previously described protocols [48, 50]. Microscope glass substrates were

252  functionalised with aminosilane, as previously described [54, 55].

253

254  The 384-well-plates and functionalised substrate slides were loaded into an Ultra Marathon

255  robotic microarray spotter (Arrayjet Inc.) configured for simultaneously printing 48

256  samples (including the plasmid from each selected antigen and control samples), producing

257  150µm features. cDNA-containing master mix samples (500pl per sample containing

258  approximately 3 ng plasmid DNA/spot) were printed by non-contact inkjet printer

259  (UltraMarathon, Arrayjet). The printer was set up to print sub-arrays in 8 rows x 6 columns.

260  Sixteen sub-arrays were printed per slide and each sub-array contained 29 cDNAs encoding

261  *P. vivax* proteins and one cDNA encoding a *P. falciparum* protein. The printed arrays were

262  then stored at room temperature in an airtight container with silica packets and protected

263  from light. Several features were included in the array as negative controls, such as clean

264  buffer, master mix without cDNA and master mix components independently (BSA or BS3

265  or anti-GST antibody).

266

267  ***In situ* protein expression using the NAPPA approach**

268  Once the array had been constructed and cDNA evaluated, proteins were expressed using

269  two CFPS protocols: a rabbit reticulocyte lysate (RRL) (Promega) or 1-step human coupled

270  *in vitro* translation (HCIVT) (Thermo Scientific) systems. The IVTT lysate master mix was

271  prepared with 200 µL reticulocyte lysate (Promega) containing 16 µL TNT buffer, 8 µL T7

272 polymerase, 4 µL -Met, 4 µL -Leu or -Cys, 8 µL RNaseOut (Invitrogen Inc) and 160 µL

273 DEPC water, following the manufacturer's instructions. The master mix for HCIVT was

274 prepared by mixing 88 µL HeLa lysate, 5.2 µL accessory proteins, 10.8 µL reaction mix, 1

275 µL leupeptin and 1 µL aprotinin (both at 1 µg/mL final concentration), as described by the

276 manufacturer.

277

278 A HybriWell (Grace Biolabs Inc.) gasket was pressed onto the slides and each lysate master

279 mix was individually added onto a slide through the gasket port. The HybriWell was gently

280 massaged to spread the mix uniformly onto the array. Port seals were applied to both ports

281 on the HybriWell to avoid evaporation. The arrays were incubated for 90 min at 30°C and

282 30 min at 15°C for protein expression and capture by the anti-GST polyclonal antibody.

283 The HybriWell was then removed and the array washed three times with PBS for 5 min on

284 a rocking platform.

285

286 **Analysing cDNA and protein display onto the arrays**

287 Prior to functional assays, some control experiments were performed to ensure the quality

288 of printing and protein expression on the arrays (QC assays).

289

290 Printed arrays were washed with phosphate-buffered saline (PBS), pH 7.4, for 15 min with

291 gentle shaking, followed by a brief washing step with deionised water for 1 min. The array

292 surface was blocked with 20 mL Superblock PBS for 1 h at room temperature (RT) with

293 gentle shaking followed by a 5 min wash with deionised water. The arrays were dried under

294 a stream of filtered compressed air [40]. Blocked slides were incubated with 150 µL/slide

295 of 1:600 (v/v) diluted PicoGreen dye (Invitrogen Inc.) for staining the cDNA to evaluate

13

296 DNA printing quality. The slides were scanned using a ProScanArray HT scanner (Perkin-

297 Elmer) and the resulting images were analysed and quantified using GenePix Software

298 version 6.0 (GenePix).

299

300 The slides were then incubated with Superblock PBS (Pierce) for 1 h at RT to ascertain

301 whether protein expression had been universal throughout the whole array and then

302 incubated with mouse anti-GST antibody (Cell Signaling Technologies Inc.) in Superblock

303 PBS at 1:200 (v/v) dilution for 1 h at RT to evaluate protein expression throughout the

304 whole array. After three 5-min washes with washing buffer (PBS 5% milk+0.2% tween

305 20), the slides were incubated with HRP-linked anti-mouse IgG (Amersham) for 1 h at

306 1:200 dilution and washed again three times with PBS (5 min/wash). Signal was developed

307 by incubating with 200 μL/slide tyramide signal amplification reagent (Perkin-Elmer) for

308 10 min at RT. The slides were then rinsed with deionised water, dried using compressed air

309 and scanned (array images were analysed as described above).

310

311 Query cDNA was co-expressed by supplementing the IVTT master mix (for RRL) with 1

312 μg of cDNA encoding the *Pv*12 protein with a Halo tag to check *in situ* expressed *P. vivax*

313 protein functionality (Table 1 and Table S1); the interaction was then indirectly detected by

314 incubation with anti-Halo antibody (Promega).

315

**Processing microarray data and statistical analysis**

317 Computational processing of arrays began by acquiring the images, followed by analysing

318 each spot [56]. Data was normalised (taking sub-array as analysis unit) by dividing the

319 mean for the master mix (corrected for sub-array) by the difference in value of the spot's

14

320 total fluorescence minus the average value for empty spot and/or master mix. If such value

321 was >1 this meant the presence of DNA or protein in the spot. The mean of the previously

322 normalised values was also obtained for analysing each clone's expression; if this was >1 it

323 indicated protein presence [48, 50, 56].

324

325 **Results**

326 **Designing a *P. vivax* NAPPA**

327 Thirty-five PCR products were obtained from 20 selected *P. vivax* gene fragments, 29 of

328 which were successfully cloned using Gateway technology (83% efficiency) (Table 1 and

329 Figure S1). This methodology used pDONR221 and two destination vectors (pANT7-cGST

330 or PJFT7-nHalo) to transfer encoding sequences from the first plasmid to the second one

331 (Figure 1). pANT7-cGST contained a GST protein enabling nascent protein capture by a

332 fixed polyclonal antibody against GST on the array, whilst query protein was cloned in

333 pJFT7-nHalo (N-terminus Halo tag) and detected by monoclonal anti-Halo tag antibodies

334 (Figure 1).

335

336 This experimental approach has more advantages than traditional cloning methods because

337 it does not require the use of restriction enzymes and site-specific recombination enables

338 DNA fragments to be correctly cloned in frame with GST or Halo tags, thereby simplifying

339 cloning [57, 58]. All the clones from this expression library were full-sequence validated

340 and their sequences were analysed by BLAST to confirm their identity. A set of 10 clones

341 (randomly selected from the expression library) were digested by BsrGI to verify insert

342 presence and ascertain plasmid DNA quality (Figure 2A). Expression library quality was

343 validated and the clones were then ready for designing the NAPPA array.

344 Glycerol concentration and drop number were tested (data not shown) to homogenise and

345 avoid aberrant effects as master mix component complexity (BSA, cDNA, cross-linkers,

346 anti-tag antibody, etc.) could affect non-contact deposition and because viscosity plays a

347 critical role. Optimal conditions were found to be 50% (v/v) glycerol and 5 drops per spot.

348 The cDNA staining signal in these arrays was >1 in all the spots after normalisation against

349 control spots (master mix components without cDNA). This meant that all cDNAs in the

350 expression library had been successfully deposited on the array by the non-contact strategy.

351 For example, cDNA staining signal Duffy Binding Protein region-1 (DBP-RI) was detected

352 in 94% of the spots.

353

354 The normalised signal obtained from printed cDNA was then evaluated across intra- and

355 inter-arrays to evaluate robustness and reproducibility (Figure 2), good intra-array

356 ($R^2$=0.80) and inter-array reproducibility ($R^2$=0.75) being observed (Figure 2). These

357 results should guarantee consistent reproducibility levels for further studies with this *P.*

358 *vivax* expression library.

359

**360 Self-assembling protein array displaying *Plasmodium vivax* proteins**

361 Spotted *P. vivax* cDNA was expressed *in situ* with RRL and protein presence was detected

362 by anti-GST monoclonal antibody (as described in the Materials and Methods section).

363 This led to signals being detected for all cDNAs in the *P. vivax* expression library in all

364 printed cDNA (100% efficiency) (Figure 1, Figure 3A and 3B). A second HeLa lysate-

365 based *in vitro* expression system (HCIVT) was used with the same NAPPA *P. vivax* array.

366 Nascent protein (C-terminal GST tag) was also detected by anti-GST monoclonal

367 antibodies (as described in the Materials and Methods section). Figure 3B depicts the

368    HCIVT system normalised signal; no expression was detected using this system although a

369    signal was detected in 10% of the spots for the following 17 proteins ( normalised signal >

370    1): (*Pf*MSP1$_{83}$, *Pv*41, *Pv*MSP10, *Pv*MSP1$_{42}$, *Pv*MSP4, *Pv*MSP5, *Pv*MSP8, *Pv*RAP2,

371    *Pv*RBP1a-RIV, *Pv*RBP1a-RI, *Pv*RBP1a-RII, *Pv*RBP1a-RIII, *Pv*RON1, *Pv*RON2-RII,

372    *Pv*RON2-RIII, *Pv*RON4 and *Pv*RON5C).

373

374    ***Plasmodium vivax* in *situ* protein-protein interaction studies**

375    Recent protein-protein interaction screening has involved using Avidity-based extracellular

376    interaction screening (AVEXIS) technology to characterise interaction between 34 *P. vivax*

377    Mrz proteins (bait and preys) [59]. This intra-library AVEXIS was only able to identify

378    three *P. vivax* protein-protein interactions in bait-prey orientation, one such being *Pv*12

379    interaction with *Pv*41 protein. *Pv*12 protein interaction was then tested with *P. vivax*

380    proteins displayed on the array to evaluate whether NAPPA was working properly; *Pv*12 is

381    a GPI-anchored 6-Cys protein expressed on parasite schizont surface and associated with

382    DRM complexes [60], this being where the formation of several of the parasite's protein

383    complexes involved in host cell interactions take place [16].

384

385    *Pv*12 was then cloned and sub-cloned (pDONR221 and pJFT7-nHalo) as described in the

386    Materials and Methods section (Table 1 and Table S1). *Pv*12 as query protein was co-IVTT

387    expressed with a *P. vivax* cDNA library array for *in situ* protein interaction studies;

388    interactions were detected by anti-Halo tag antibody (Figure 1), showing that *Pv*12

389    interacted with five *P. vivax* proteins located on surface membrane and in rhoptry

390    organelles, mainly with *Pv*RBP1a region IV and *Pv*41 proteins (Figure 4).

391

**Discussion**

392

393    Most pathogen (i.e. *Plasmodium*) invasion is PPI-mediated, leading to stable or transient

394    molecular complex formation [61]. Identifying and characterising these types of interaction

395    strongly suggests a functional relationship between participating proteins and enables

396    understanding the biological mechanisms (replication, transcription, metabolism and

397    invasion) used by microorganisms for invading and infecting target cells. Blocking PPI has

398    been suggested as a target for action against pathogens by designing new drugs or small

399    binding molecules targeting cell surface or the contact region between proteins [27, 62].

400

401    NAPPA is one of the chosen methodologies for characterising PPIs. The first step in this

402    study was thus the rational selection of content and query and evaluating whether a variety

403    of such *P. vivax* proteins could be displayed by this format (Figure 1). Twenty proteins

404    were selected based on *P. vivax* transcriptomic and proteomic data [63-67] and functional

405    evidence of these antigens in *P. vivax* and other species (i.e., *P. falciparum*) during Mrz

406    invasion of target cells [29].

407

408    Selected antigens (Table 1) were subdivided into three groups according to their subcellular

409    location on Mrz surface proteins and proteins located in the micronemes and in the

410    rhoptries. Mrz surface proteins are primarily exposed on Mrz plasma membrane during

411    invasion and some of them are involved in weak, low-affinity interactions with receptors on

412    RBC membrane for selecting a specific target cell [3, 68]. Four proteins were selected from

413    the Mrz surface (MSP) group (*Pv*MSP-1, -4, -8 and -10); all of them are membrane-

414    anchored via glycosylphosphatidylinositol (GPI) and expressed on *P. vivax* schizonts [69-

415    71]. MSP1 is the major MSP and has been implicated in many *P. falciparum* receptor-

18

416  ligand (glycophorin A, Band 3 and heparin) and protein-protein interactions (MSP6-MSP7-

417  RhopH3-RAPs) [9, 10, 13]. It has been the object of significant antigenic and

418  immunological studies highlighting its importance as *P. falciparum* and *P. vivax* vaccine

419  antigen candidate [72, 73]. The other surface antigen group selected here included the

420  *Plasmodium*-specific 6-Cys family containing a cysteine-rich domain, the 6-cysteine or

421  s48/45 domain [74]. This *Plasmodium*-specific family's proteins are expressed in a stage-

422  specific manner and perform important functions during life-cycle (gamete, Spz or Mrz)

423  stages. P12 and P41 proteins have been characterised as blood-stage 6-Cys proteins in *P.*

424  *falciparum* and *P. vivax* and have been seen to form a stable complex on the infective

425  DRM-associated Mrz surface [59, 75].

426

427  Microneme and RON proteins are involved in high-affinity interactions initiating parasite

428  entry to RBC. Native *Pv*RBP1a is colocalised on Mrz microneme with *Pv*DBP [76]; whilst

429  RBP proteins are responsible for the specificity of *P. vivax* Mrz binding to reticulocytes,

430  *Pv*DBP is involved in *P. vivax* selectivity for invading Duffy antigen cells expressed on

431  reticulocyte surface [77]; both proteins have been considered important vaccine candidates

432  [72]. The AMA-1 protein has been implicated in macro-complex formation, together with

433  RON2, -4 and -5 proteins for establishing the TJ necessary for parasite mobilisation inside

434  its target cell [23]. The content of the rhoptries involved in PV formation is then discharged

435  onto a host/target cell for successful entry [78]. Many proteins have been seen to be

436  involved in this last step during Mrz invasion, such as RhopH3, RAP1 and RAP2. *P.*

437  *falciparum* RAP1, RAP2 and RAP3 form a low molecular weight complex in the bulb of

438  the rhoptries, this being invasion-inhibitory monoclonal antibodies' target *in vitro* [79].

439  Other proteins such as *Pv*TRAMP, *Pv*RON1 and *Pv*ARP have been recently identified and

19

440 characterised in *P. vivax* schizonts and have been recognised by *P. vivax*-infected

441 individuals' serum [80-82].

442

443 The array was designed to display cDNA encoding *P. vivax* proteins several times so as to

444 have several replicates but mostly to avoid cross-contamination across features and highly

445 homogeneous spot morphology. A non-contact printer was used to create these arrays

446 which, apart from the requirements described above, had an advantage regarding the

447 amount of cDNA per master mix (3µg) compared to 10-15 µg cDNA/master mix

448 previously reported in arrays constructed by microcontact printers [50].

449

450 One of the greatest challenges when evaluating protein function is being able to obtain

451 soluble proteins and maintain their stability and functionality during purification; however,

452 cell-based expression systems have limitations regarding obtaining soluble *Plasmodium*

453 proteins, mainly due to codon usage bias and large repeats in antigenic protein sequences

454 [83]. Cell-based expression systems may well be valuable for studying many proteins'

455 structure but their use for large-scale analysis is limited; developing CFPS offers an

456 efficient alternative for developing protein arrays. All *P. vivax* antigens were efficiently

457 expressed with the RRL system compared to that found when proteins were expressed

458 using the HCIVT system (based on HeLa cell lysates) (Figure 3).

459

460 The RRL system is one of the most used NAPPA expression systems, producing hundreds

461 of proteins including various microorganisms' proteomes and more than 1,000 human

462 proteins [45, 49, 84]. However, further experiments are required to optimise HCIVT-

463 expressed array performance regarding *P. vivax*; this could include increasing lysate

464 concentration, expression time, temperature or adding protease inhibitors. Previous studies

465 have shown NAPPA feasibility by using the HCIVT system, >2,000 proteins being

466 successfully expressed from various microorganisms (i.e. *Vibrio cholera* and *Bacillus*

467 *anthracis*) and antigenic human proteins [58].

468

469 Malarial proteins expressed in cell-free *E. coli* or wheat germ extracts and analysed on flat

470 solid arrays with immune sera is one of the main uses for malaria-related large-scale CFPS

471 [85, 86]. However, previous *P. vivax* protein expression studies using wheat germ and *E.*

472 *coli* systems have revealed significant differences regarding production, scalability and

473 stability, depending on the antigen being expressed. Some studies have indicated that

474 proteins expressed in a wheat germ cell-free system are more suitable for such analysis as

475 they are mostly soluble and have retained enzymatic activity [87]. The present study has

476 shown the feasibility of producing *P. vivax* antigens from surface membrane, rhoptries and

477 micronemes in array format with the RRL system.

478

479 When *P. vivax* protein-protein interactions were measured it was found that *Pv*12 protein

480 used as bait interacted with *Pv*41, as previously described using AVEXIS technology [59].

481 AVEXIS is based on measuring protein-protein interactions between bait (biotinylated and

482 captured by streptavidin-coated wells) and prey proteins (enzymatically tagged and

483 containing a pentamerisation domain to increase interaction avidity) [88]. This technology

484 has been used to ascertain Rh5 interaction with the Basigin receptor [17], Rh5 interaction

485 with *Pf*113 protein [19] and recently for evaluating *P. vivax* protein-protein interactions

486 [59]. These studies were only able to detect three interactions between 34 bait and prey

487 proteins (i.e. very few interactions compared to those identified in *P. falciparum*) [59, 89].

488 Although AVEXYS can increase avidity, prey pentamerisation can cause steric hindrance

489 affecting real detection of protein-protein interactions.

490

491 NAPPA detected interaction between *Pv*12 and other MSP (in addition to *Pv*12-*Pv*41

492 interaction), such as *Pv*MSP1$_{42kDa}$ and *Pv*MSP8 and proteins located in the apical

493 organelles, such as *Pv*RAP1 and *Pv*RBP1a (Figure 4). Previous studies have described

494 *Pv*12 forming part of DRMs [60], a platform where many Mrz invasion-associated proteins

495 are organised into multi-protein complexes [16], thereby suggesting that *Pv*12 could be

496 involved in forming a complex between parasite proteins. It is worth stressing that, in

497 addition to NAPPA's advantages regarding expression, in situ co-expression of analyte and

498 query and RT storage, it has higher sensitivity than other protein-protein interaction

499 measurement techniques, mainly because the protein-protein complex is only found in the

500 small microspot area, resulting in increased high local signal. Although few molecules can

501 be captured in the microspot, high density molecules can be obtained in it [90].

502

503 **Conclusions**

504 NAPPA is a high-performance technique for evaluating interactions in *P. vivax*, offering a

505 new and useful alternative for studying the biology of this difficult-to-culture parasite. It

506 enables bait and query co-expression *in situ*, thereby enabling interactions to be analysed

507 rapidly and reproducibly. NAPPA seems to be a flexible approach for identifying key PPI

508 in full- or targeted-proteomes. This article has highlighted the NAPPA and RRL-based

509 expression system for the successful and reproducible expression of *P. vivax* proteins which

510 might be involved in *P. vivax* Mrz protein-protein interactions. The query protein (*Pv*12)

511 was able to interact with parasite surface membrane- and apical organelle-derived Mrz

512 proteins. This technique will facilitate studying therapeutic targets and clarifying protein-

513 protein interaction mechanisms.

514

515 **Declarations**

516 **Ethics approval and consent to participate**

517 Not required.

518

519 **Consent for publication**

520 Not applicable.

521

522 **Availability of data and material**

523 All data generated or analysed during this study is included within this article.

524

525 **Competing interests**

526 The authors declare that they have no competing interests.

527

528 **Funding**

23

540

**Authors' contributions**

542 GAP carried out the molecular biology assays, participated in NAPPA assays and wrote the

543 initial manuscript. MGG and JCS carried out NAPPA assay. CS and HC processed and

544 analysed NAPPA data. AM, MAP, JL and MF participated in coordinating and designing

545 the assays. MAP evaluated and coordinated the molecular biology assays and revised the

546 final manuscript. MF evaluated and coordinated the NAPPA assays and revised the final

547 manuscript. All authors have read and approved the final version of this manuscript.

548

551

552

**References**

1. Dyer MD, Neff C, Dufford M, Rivera CG, Shattuck D, Bassaganya-Riera J, Murali TM, Sobral BW: **The human-bacterial pathogen protein interaction networks of Bacillus anthracis, Francisella tularensis, and Yersinia pestis.** *PLoS One* 2010, **5:**e12089.

2. Malpede BM, Tolia NH: **Malaria adhesins: structure and function.** *Cell Microbiol* 2014, **16:**621-631.

3. Weiss GE, Gilson PR, Taechalertpaisarn T, Tham WH, de Jong NW, Harvey KL, Fowkes FJ, Barlow PN, Rayner JC, Wright GJ, et al: **Revealing the sequence and resulting cellular morphology of receptor-ligand interactions during Plasmodium falciparum invasion of erythrocytes.** *PLoS Pathog* 2015, **11:**e1004670.

4. Garcia JE, Puentes A, Patarroyo ME: **Developmental biology of sporozoite-host interactions in Plasmodium falciparum malaria: implications for vaccine design.** *Clin Microbiol Rev* 2006, **19:**686-707.

5. Singh S, Alam MM, Pal-Bhowmick I, Brzostowski JA, Chitnis CE: **Distinct external signals trigger sequential release of apical organelles during erythrocyte invasion by malaria parasites.** *PLoS Pathog* 2010, **6:**e1000746.

6. Lopaticki S, Maier AG, Thompson J, Wilson DW, Tham WH, Triglia T, Gout A, Speed TP, Beeson JG, Healer J, Cowman AF: **Reticulocyte and erythrocyte binding-like proteins function cooperatively in invasion of human erythrocytes by malaria parasites.** *Infect Immun* 2011, **79:**1107-1117.

7. Stubbs J, Simpson KM, Triglia T, Plouffe D, Tonkin CJ, Duraisingh MT, Maier AG, Winzeler EA, Cowman AF: **Molecular mechanism for switching of P. falciparum invasion pathways into human erythrocytes.** *Science* 2005, **309:**1384-1387.

8. Lin CS, Uboldi AD, Marapana D, Czabotar PE, Epp C, Bujard H, Taylor NL, Perugini MA, Hodder AN, Cowman AF: **The merozoite surface protein 1 complex is a platform for binding to human erythrocytes by Plasmodium falciparum.** *J Biol Chem* 2014, **289:**25655-25669.

583    9.    Kauth CW, Woehlbier U, Kern M, Mekonnen Z, Lutz R, Mucke N, Langowski J,

584          Bujard H: **Interactions between merozoite surface proteins 1, 6, and 7 of the**

585          **malaria parasite Plasmodium falciparum.** *J Biol Chem* 2006, **281:**31517-31527.

586    10.    Ranjan R, Chugh M, Kumar S, Singh S, Kanodia S, Hossain MJ, Korde R, Grover

587          A, Dhawan S, Chauhan VS, et al: **Proteome analysis reveals a large merozoite**

588          **surface protein-1 associated complex on the Plasmodium falciparum merozoite**

589          **surface.** *J Proteome Res* 2011, **10:**680-691.

590    11.    Wanaguru M, Crosnier C, Johnson S, Rayner JC, Wright GJ: **Biochemical analysis**

591          **of the Plasmodium falciparum erythrocyte-binding antigen-175 (EBA175)-**

592          **glycophorin-A interaction: implications for vaccine design.** *J Biol Chem* 2013,

593          **288:**32106-32117.

594    12.    Batchelor JD, Malpede BM, Omattage NS, DeKoster GT, Henzler-Wildman KA,

595          Tolia NH: **Red blood cell invasion by Plasmodium vivax: structural basis for**

596          **DBP engagement of DARC.** *PLoS Pathog* 2014, **10:**e1003869.

597    13.    Li X, Chen H, Oo TH, Daly TM, Bergman LW, Liu SC, Chishti AH, Oh SS: **A co-**

598          **ligand complex anchors Plasmodium falciparum merozoites to the erythrocyte**

599          **invasion receptor band 3.** *J Biol Chem* 2004, **279:**5765-5771.

600    14.    Lin CS, Uboldi AD, Epp C, Bujard H, Tsuboi T, Czabotar PE, Cowman AF:

601          **Multiple Plasmodium falciparum Merozoite Surface Protein 1 Complexes**

602          **Mediate Merozoite Binding to Human Erythrocytes.** *J Biol Chem* 2016,

603          **291:**7703-7715.

604    15.    Baldwin MR, Li X, Hanada T, Liu SC, Chishti AH: **Merozoite surface protein 1**

605          **recognition of host glycophorin A mediates malaria parasite invasion of red**

606          **blood cells.** *Blood* 2015, **125:**2704-2711.

607    16.    Sanders PR, Cantin GT, Greenbaum DC, Gilson PR, Nebl T, Moritz RL, Yates JR,

608          3rd, Hodder AN, Crabb BS: **Identification of protein complexes in detergent-**

609          **resistant membranes of Plasmodium falciparum schizonts.** *Mol Biochem*

610          *Parasitol* 2007, **154:**148-157.

611    17.    Crosnier C, Bustamante LY, Bartholdson SJ, Bei AK, Theron M, Uchikawa M,

612          Mboup S, Ndir O, Kwiatkowski DP, Duraisingh MT, et al: **Basigin is a receptor**

613 **essential for erythrocyte invasion by Plasmodium falciparum.** *Nature* 2011,
614 **480:**534-537.

615 18. Reddy KS, Amlabu E, Pandey AK, Mitra P, Chauhan VS, Gaur D: **Multiprotein**
616 **complex between the GPI-anchored CyRPA with PfRH5 and PfRipr is crucial**
617 **for Plasmodium falciparum erythrocyte invasion.** *Proc Natl Acad Sci U S A*
618 2015, **112:**1179-1184.

619 19. Galaway F, Drought LG, Fala M, Cross N, Kemp AC, Rayner JC, Wright GJ: **P113**
620 **is a merozoite surface protein that binds the N terminus of Plasmodium**
621 **falciparum RH5.** *Nat Commun* 2017, **8:**14333.

622 20. Besteiro S, Michelin A, Poncet J, Dubremetz JF, Lebrun M: **Export of a**
623 **Toxoplasma gondii rhoptry neck protein complex at the host cell membrane to**
624 **form the moving junction during invasion.** *PLoS Pathog* 2009, **5:**e1000309.

625 21. Collins CR, Withers-Martinez C, Hackett F, Blackman MJ: **An inhibitory**
626 **antibody blocks interactions between components of the malarial invasion**
627 **machinery.** *PLoS Pathog* 2009, **5:**e1000273.

628 22. Tonkin ML, Roques M, Lamarque MH, Pugniere M, Douguet D, Crawford J,
629 Lebrun M, Boulanger MJ: **Host cell invasion by apicomplexan parasites: insights**
630 **from the co-structure of AMA1 with a RON2 peptide.** *Science* 2011, **333:**463-
631 467.

632 23. Vulliez-Le Normand B, Tonkin ML, Lamarque MH, Langer S, Hoos S, Roques M,
633 Saul FA, Faber BW, Bentley GA, Boulanger MJ, Lebrun M: **Structural and**
634 **functional insights into the malaria parasite moving junction complex.** *PLoS*
635 *Pathog* 2012, **8:**e1002755.

636 24. Aikawa M, Miller LH, Johnson J, Rabbege J: **Erythrocyte entry by malarial**
637 **parasites. A moving junction between erythrocyte and parasite.** *J Cell Biol*
638 1978, **77:**72-82.

639 25. Beck JR, Chen AL, Kim EW, Bradley PJ: **RON5 is critical for organization and**
640 **function of the Toxoplasma moving junction complex.** *PLoS Pathog* 2014,
641 **10:**e1004025.

642 26. Srinivasan P, Beatty WL, Diouf A, Herrera R, Ambroggio X, Moch JK, Tyler JS,
643 Narum DL, Pierce SK, Boothroyd JC, et al: **Binding of Plasmodium merozoite**

644      **proteins RON2 and AMA1 triggers commitment to invasion.** *Proc Natl Acad Sci*

645      *U S A* 2011, **108:**13275-13280.

646    27.    Srinivasan P, Yasgar A, Luci DK, Beatty WL, Hu X, Andersen J, Narum DL, Moch

647      JK, Sun H, Haynes JD, et al: **Disrupting malaria parasite AMA1-RON2**

648      **interaction with a small molecule prevents erythrocyte invasion.** *Nat Commun*

649      2013, **4:**2261.

650    28.    Vogel G: **The forgotten malaria.** *Science* 2013, **342:**684-687.

651    29.    Patarroyo MA, Calderon D, Moreno-Perez DA: **Vaccines against Plasmodium**

652      **vivax: a research challenge.** *Expert Rev Vaccines* 2012, **11:**1249-1260.

653    30.    Mueller I, Galinski MR, Baird JK, Carlton JM, Kochar DK, Alonso PL, del Portillo

654      HA: **Key gaps in the knowledge of Plasmodium vivax, a neglected human**

655      **malaria parasite.** *Lancet Infect Dis* 2009, **9:**555-566.

656    31.    Noulin F, Borlon C, Van Den Abbeele J, D'Alessandro U, Erhart A: **1912-2012: a**

657      **century of research on Plasmodium vivax in vitro culture.** *Trends Parasitol*

658      2013, **29:**286-294.

659    32.    Petschnigg J, Snider J, Stagljar I: **Interactive proteomics research technologies:**

660      **recent applications and advances.** *Curr Opin Biotechnol* 2011, **22:**50-58.

661    33.    Dasilva N, Diez P, Gonzalez-Gonzalez M, Matarraz S, Sayagues JM, Orfao A,

662      Fuentes M: **Protein microarrays: technological aspects, applications and**

663      **intellectual property.** *Recent Pat Biotechnol* 2013, **7:**142-152.

664    34.    Kenworthy AK: **Imaging protein-protein interactions using fluorescence**

665      **resonance energy transfer microscopy.** *Methods* 2001, **24:**289-296.

666    35.    Suter B, Kittanakom S, Stagljar I: **Two-hybrid technologies in proteomics**

667      **research.** *Curr Opin Biotechnol* 2008, **19:**316-323.

668    36.    Isaksson L, Enberg J, Neutze R, Goran Karlsson B, Pedersen A: **Expression**

669      **screening of membrane proteins with cell-free protein synthesis.** *Protein Expr*

670      *Purif* 2012, **82:**218-225.

671    37.    Hillebrecht JR, Chong S: **A comparative study of protein synthesis in in vitro**

672      **systems: from the prokaryotic reconstituted to the eukaryotic extract-based.**

673      *BMC Biotechnol* 2008, **8:**58.

28

674   38.   Tuckey C, Asahara H, Zhou Y, Chong S: **Protein synthesis using a reconstituted**
675         **cell-free system.** *Curr Protoc Mol Biol* 2014, **108:**16 31 11-22.

676   39.   Ramachandran N, Anderson KS, Raphael JV, Hainsworth E, Sibani S, Montor WR,
677         Pacek M, Wong J, Eljanne M, Sanda MG, et al: **Tracking humoral responses**
678         **using self assembling protein microarrays.** *Proteomics Clin Appl* 2008, **2:**1518-
679         1527.

680   40.   Ramachandran N, Srivastava S, Labaer J: **Applications of protein microarrays for**
681         **biomarker discovery.** *Proteomics Clin Appl* 2008, **2:**1444-1459.

682   41.   Casado-Vela J, Fuentes M, Franco-Zorrilla JM: **Screening of protein-protein and**
683         **protein-DNA interactions using microarrays: applications in biomedicine.** *Adv*
684         *Protein Chem Struct Biol* 2014, **95:**231-281.

685   42.   Hino M, Kataoka M, Kajimoto K, Yamamoto T, Kido J, Shinohara Y, Baba Y:
686         **Efficiency of cell-free protein synthesis based on a crude cell extract from**
687         **Escherichia coli, wheat germ, and rabbit reticulocytes.** *J Biotechnol* 2008,
688         **133:**183-189.

689   43.   Gonzalez-Gonzalez M, Jara-Acevedo R, Matarraz S, Jara-Acevedo M, Paradinas S,
690         Sayagues JM, Orfao A, Fuentes M: **Nanotechniques in proteomics: protein**
691         **microarrays and novel detection platforms.** *Eur J Pharm Sci* 2012, **45:**499-506.

692   44.   Manzano-Roman R, Dasilva N, Diez P, Diaz-Martin V, Perez-Sanchez R, Orfao A,
693         Fuentes M: **Protein arrays as tool for studies at the host-pathogen interface.** *J*
694         *Proteomics* 2013, **94:**387-400.

695   45.   Ramachandran N, Raphael JV, Hainsworth E, Demirkan G, Fuentes MG, Rolfs A,
696         Hu Y, LaBaer J: **Next-generation high-density self-assembling functional**
697         **protein arrays.** *Nat Methods* 2008, **5:**535-538.

698   46.   Carlson ED, Gan R, Hodgman CE, Jewett MC: **Cell-free protein synthesis:**
699         **applications come of age.** *Biotechnol Adv* 2012, **30:**1185-1194.

700   47.   Montor WR, Huang J, Hu Y, Hainsworth E, Lynch S, Kronish JW, Ordonez CL,
701         Logvinenko T, Lory S, LaBaer J: **Genome-wide study of Pseudomonas**
702         **aeruginosa outer membrane protein immunogenicity using self-assembling**
703         **protein microarrays.** *Infect Immun* 2009, **77:**4877-4886.

704  48.  Henjes F, Lourido L, Ruiz-Romero C, Fernandez-Tajes J, Schwenk JM, Gonzalez-

705  Gonzalez M, Blanco FJ, Nilsson P, Fuentes M: **Analysis of autoantibody profiles**

706  **in osteoarthritis using comprehensive protein array concepts.** *J Proteome Res*

707  2014, **13:**5218-5229.

708  49.  Yu X, Decker KB, Barker K, Neunuebel MR, Saul J, Graves M, Westcott N, Hang

709  H, LaBaer J, Qiu J, Machner MP: **Host-pathogen interaction profiling using self-**

710  **assembling human protein arrays.** *J Proteome Res* 2015, **14:**1920-1936.

711  50.  Manzano-Roman R, Diaz-Martin V, Gonzalez-Gonzalez M, Matarraz S, Alvarez-

712  Prado AF, LaBaer J, Orfao A, Perez-Sanchez R, Fuentes M: **Self-assembled**

713  **protein arrays from an Ornithodoros moubata salivary gland expression**

714  **library.** *J Proteome Res* 2012, **11:**5972-5982.

715  51.  Yap A, Azevedo MF, Gilson PR, Weiss GE, O'Neill MT, Wilson DW, Crabb BS,

716  Cowman AF: **Conditional expression of apical membrane antigen 1 in**

717  **Plasmodium falciparum shows it is required for erythrocyte invasion by**

718  **merozoites.** *Cell Microbiol* 2014, **16:**642-656.

719  52.  Williams AR, Douglas AD, Miura K, Illingworth JJ, Choudhary P, Murungi LM,

720  Furze JM, Diouf A, Miotto O, Crosnier C, et al: **Enhancing blockade of**

721  **Plasmodium falciparum erythrocyte invasion: assessing combinations of**

722  **antibodies against PfRH5 and other merozoite antigens.** *PLoS Pathog* 2012,

723  **8:**e1002991.

724  53.  Smallwood SE, Rahman MM, Werden SJ, Martino MF, McFadden G: **Production**

725  **of Myxoma virus gateway entry and expression libraries and validation of viral**

726  **protein expression.** *Curr Protoc Microbiol* 2011, **Chapter 14:**Unit 14A 12.

727  54.  Link AJ, Labaer J: **Construction of Nucleic Acid Programmable Protein Arrays**

728  **(NAPPA) 1: Coating Glass Slides with Amino Silane.** *CSH Protoc* 2008,

729  **2008:**pdb prot5056.

730  55.  Gonzalez-Gonzalez M, Bartolome R, Jara-Acevedo R, Casado-Vela J, Dasilva N,

731  Matarraz S, Garcia J, Alcazar JA, Sayagues JM, Orfao A, Fuentes M: **Evaluation**

732  **of homo- and hetero-functionally activated glass surfaces for optimized**

733  **antibody arrays.** *Anal Biochem* 2014, **450:**37-45.

734 56. Diez P, Dasilva N, Gonzalez-Gonzalez M, Matarraz S, Casado-Vela J, Orfao A,
735 Fuentes M: **Data Analysis Strategies for Protein Microarrays.** *Microarrays*
736 *(Basel)* 2012, **1:**64-83.

737 57. Katzen F: **Gateway((R)) recombinational cloning: a biological operating system.**
738 *Expert Opin Drug Discov* 2007, **2:**571-589.

739 58. Hunt I: **From gene to protein: a review of new and enabling technologies for**
740 **multi-parallel protein expression.** *Protein Expr Purif* 2005, **40:**1-22.

741 59. Hostetler JB, Sharma S, Bartholdson SJ, Wright GJ, Fairhurst RM, Rayner JC: **A**
742 **Library of Plasmodium vivax Recombinant Merozoite Proteins Reveals New**
743 **Vaccine Candidates and Protein-Protein Interactions.** *PLoS Negl Trop Dis* 2015,
744 **9:**e0004264.

745 60. Moreno-Perez DA, Areiza-Rojas R, Florez-Buitrago X, Silva Y, Patarroyo ME,
746 Patarroyo MA: **The GPI-anchored 6-Cys protein Pv12 is present in detergent-**
747 **resistant microdomains of Plasmodium vivax blood stage schizonts.** *Protist*
748 2013, **164:**37-48.

749 61. Paing MM, Tolia NH: **Multimeric assembly of host-pathogen adhesion**
750 **complexes involved in apicomplexan invasion.** *PLoS Pathog* 2014, **10:**e1004120.

751 62. Wells JA, McClendon CL: **Reaching for high-hanging fruit in drug discovery at**
752 **protein-protein interfaces.** *Nature* 2007, **450:**1001-1009.

753 63. Moreno-Perez DA, Degano R, Ibarrola N, Muro A, Patarroyo MA: **Determining**
754 **the Plasmodium vivax VCG-1 strain blood stage proteome.** *J Proteomics* 2014,
755 **113C:**268-280.

756 64. Lu F, Li J, Wang B, Cheng Y, Kong DH, Cui L, Ha KS, Sattabongkot J, Tsuboi T,
757 Han ET: **Profiling the humoral immune responses to Plasmodium vivax**
758 **infection and identification of candidate immunogenic rhoptry-associated**
759 **membrane antigen (RAMA).** *J Proteomics* 2014, **102:**66-82.

760 65. Acharya P, Pallavi R, Chandran S, Dandavate V, Sayeed SK, Rochani A, Acharya
761 J, Middha S, Kochar S, Kochar D, et al: **Clinical proteomics of the neglected**
762 **human malarial parasite Plasmodium vivax.** *PLoS One* 2011, **6:**e26623.

763 66. Acharya P, Pallavi R, Chandran S, Chakravarti H, Middha S, Acharya J, Kochar S,
764 Kochar D, Subudhi A, Boopathi AP, et al: **A glimpse into the clinical proteome of**

765　　　**human malaria parasites Plasmodium falciparum and Plasmodium vivax.**
766　　　*Proteomics Clin Appl* 2009, **3:**1314-1325.

767　67.　Roobsoong W, Roytrakul S, Sattabongkot J, Li J, Udomsangpetch R, Cui L:
768　　　**Determination of the Plasmodium vivax schizont stage proteome.** *J Proteomics*
769　　　2011, **74:**1701-1710.

770　68.　Beeson JG, Drew DR, Boyle MJ, Feng G, Fowkes FJ, Richards JS: **Merozoite**
771　　　**surface proteins in red blood cell invasion, immunity and vaccines against**
772　　　**malaria.** *FEMS Microbiol Rev* 2016, **40:**343-372.

773　69.　Perez-Leal O, Sierra AY, Barrero CA, Moncada C, Martinez P, Cortes J, Lopez Y,
774　　　Salazar LM, Hoebeke J, Patarroyo MA: **Identifying and characterising the**
775　　　**Plasmodium falciparum merozoite surface protein 10 Plasmodium vivax**
776　　　**homologue.** *Biochem Biophys Res Commun* 2005, **331:**1178-1184.

777　70.　Perez-Leal O, Sierra AY, Barrero CA, Moncada C, Martinez P, Cortes J, Lopez Y,
778　　　Torres E, Salazar LM, Patarroyo MA: **Plasmodium vivax merozoite surface**
779　　　**protein 8 cloning, expression, and characterisation.** *Biochem Biophys Res*
780　　　*Commun* 2004, **324:**1393-1399.

781　71.　Black CG, Barnwell JW, Huber CS, Galinski MR, Coppel RL: **The Plasmodium**
782　　　**vivax homologues of merozoite surface proteins 4 and 5 from Plasmodium**
783　　　**falciparum are expressed at different locations in the merozoite.** *Mol Biochem*
784　　　*Parasitol* 2002, **120:**215-224.

785　72.　Lopez C, Yepes-Perez Y, Hincapie-Escobar N, Diaz-Arevalo D, Patarroyo MA:
786　　　**What Is Known about the Immune Response Induced by Plasmodium vivax**
787　　　**Malaria Vaccine Candidates?** *Front Immunol* 2017, **8:**126.

788　73.　Singh S, Miura K, Zhou H, Muratova O, Keegan B, Miles A, Martin LB, Saul AJ,
789　　　Miller LH, Long CA: **Immunity to recombinant plasmodium falciparum**
790　　　**merozoite surface protein 1 (MSP1): protection in Aotus nancymai monkeys**
791　　　**strongly correlates with anti-MSP1 antibody titer and in vitro parasite-**
792　　　**inhibitory activity.** *Infect Immun* 2006, **74:**4573-4580.

793　74.　Arredondo SA, Cai M, Takayama Y, MacDonald NJ, Anderson DE, Aravind L,
794　　　Clore GM, Miller LH: **Structure of the Plasmodium 6-cysteine s48/45 domain.**
795　　　*Proc Natl Acad Sci U S A* 2012, **109:**6692-6697.

796   75.   Taechalertpaisarn T, Crosnier C, Bartholdson SJ, Hodder AN, Thompson J,
797         Bustamante LY, Wilson DW, Sanders PR, Wright GJ, Rayner JC, et al:
798         **Biochemical and functional analysis of two Plasmodium falciparum blood-**
799         **stage 6-cys proteins: P12 and P41.** *PLoS One* 2012, **7:**e41937.

800   76.   Han JH, Lee SK, Wang B, Muh F, Nyunt MH, Na S, Ha KS, Hong SH, Park WS,
801         Sattabongkot J, et al: **Identification of a reticulocyte-specific binding domain of**
802         **Plasmodium vivax reticulocyte-binding protein 1 that is homologous to the**
803         **PfRh4 erythrocyte-binding domain.** *Sci Rep* 2016, **6:**26993.

804   77.   Prajapati SK, Singh OP: **Insights into the invasion biology of Plasmodium vivax.**
805         *Front Cell Infect Microbiol* 2013, **3:**8.

806   78.   Zuccala ES, Gout AM, Dekiwadia C, Marapana DS, Angrisano F, Turnbull L,
807         Riglar DT, Rogers KL, Whitchurch CB, Ralph SA, et al:
808         **Subcompartmentalisation of proteins in the rhoptries correlates with ordered**
809         **events of erythrocyte invasion by the blood stage malaria parasite.** *PLoS One*
810         2012, **7:**e46160.

811   79.   Ridley RG, Takacs B, Etlinger H, Scaife JG: **A rhoptry antigen of Plasmodium**
812         **falciparum is protective in Saimiri monkeys.** *Parasitology* 1990, **101 Pt 2:**187-
813         192.

814   80.   Moreno-Perez DA, Saldarriaga A, Patarroyo MA: **Characterizing PvARP, a novel**
815         **Plasmodium vivax antigen.** *Malar J* 2013, **12:**165.

816   81.   Moreno-Perez DA, Montenegro M, Patarroyo ME, Patarroyo MA: **Identification,**
817         **characterization and antigenicity of the Plasmodium vivax rhoptry neck**
818         **protein 1 (PvRON1).** *Malar J* 2011, **10:**314.

819   82.   Mongui A, Angel DI, Moreno-Perez DA, Villarreal-Gonzalez S, Almonacid H,
820         Vanegas M, Patarroyo MA: **Identification and characterization of the**
821         **Plasmodium vivax thrombospondin-related apical merozoite protein.** *Malar J*
822         2010, **9:**283.

823   83.   Mehlin C, Boni E, Buckner FS, Engel L, Feist T, Gelb MH, Haji L, Kim D, Liu C,
824         Mueller N, et al: **Heterologous expression of proteins from Plasmodium**
825         **falciparum: results from 1000 genes.** *Mol Biochem Parasitol* 2006, **148:**144-160.

826   84.   Yu X, LaBaer J: **High-throughput identification of proteins with AMPylation using self-assembled human protein (NAPPA) microarrays.** *Nat Protoc* 2015, **10:**756-767.

829   85.   Barry AE, Trieu A, Fowkes FJ, Pablo J, Kalantari-Dehaghi M, Jasinskas A, Tan X, Kayala MA, Tavul L, Siba PM, et al: **The stability and complexity of antibody responses to the major surface antigen of Plasmodium falciparum are associated with age in a malaria endemic area.** *Mol Cell Proteomics* 2011, **10:**M111 008326.

834   86.   Tsuboi T, Takeo S, Iriko H, Jin L, Tsuchimochi M, Matsuda S, Han ET, Otsuki H, Kaneko O, Sattabongkot J, et al: **Wheat germ cell-free system-based production of malaria proteins for discovery of novel vaccine candidates.** *Infect Immun* 2008, **76:**1702-1708.

838   87.   Chen JH, Jung JW, Wang Y, Ha KS, Lu F, Lim CS, Takeo S, Tsuboi T, Han ET: **Immunoproteomics profiling of blood stage Plasmodium vivax infection by high-throughput screening assays.** *J Proteome Res* 2010, **9:**6479-6489.

841   88.   Bartholdson SJ, Crosnier C, Bustamante LY, Rayner JC, Wright GJ: **Identifying novel Plasmodium falciparum erythrocyte invasion receptors using systematic extracellular protein interaction screens.** *Cell Microbiol* 2013, **15:**1304-1312.

844   89.   LaCount DJ, Vignali M, Chettier R, Phansalkar A, Bell R, Hesselberth JR, Schoenfeld LW, Ota I, Sahasrabudhe S, Kurschner C, et al: **A protein interaction network of the malaria parasite Plasmodium falciparum.** *Nature* 2005, **438:**103-107.

848   90.   Templin MF, Stoll D, Schrenk M, Traub PC, Vohringer CF, Joos TO: **Protein microarray technology.** *Trends Biotechnol* 2002, **20:**160-166.

850   91.   Bozdech Z, Mok S, Hu G, Imwong M, Jaidee A, Russell B, Ginsburg H, Nosten F, Day NP, White NJ, et al: **The transcriptome of Plasmodium vivax reveals divergence and diversity of transcriptional regulation in malaria parasites.** *Proc Natl Acad Sci U S A* 2008, **105:**16290-16295.

854

855

**Figure legends**

857 **Figure 1. Outline of NAPPA protocol for detecting PPI in *P. vivax*. Step 1. Cloning:** 35

858 DNA fragments from 20 *P. vivax* genes were amplified, adding attB recombination

859 sequences for each one. Entry vector (pDONR221) recombination involved using BP

860 clonase. **Step 2. Sub-cloning:** A second recombination involved positive clones (pDONR-

861 Pv gene) and destination vectors (pANT7-cGST or pJFT7-nHalo) using LR clonase. **Step**

862 **3. Printing and quality control:** *P. vivax* plasmids were mixed with BSA, a crosslinker

863 and rabbit polyclonal anti-GST antibody, and printed in spots on aminosilane-coated glass

864 slides. After blocking, PicoGreen dye or IVTT (RRL or HCIVT) were used for staining

865 slides. PicoGreen readings were used to calculate intra- and inter-slide correlation for

866 assessing DNA printing quality. IVTT involved detecting captured proteins using mouse

867 monoclonal anti-GST (primary) and HRP-linked anti-mouse IgG (secondary) antibodies,

868 using tyramide as activated substrate. The amount of positive and negative spots was used

869 to estimate expression performance. **Step 4. Prey/bait co-expression:** The IVTT system

870 (RLL) was added together with prey plasmid to the array containing bait plasmid. **Step 5.**

871 **PPI detection:** The PPI were revealed using mouse anti-Halo monoclonal (primary) and

872 HRP-linked anti-mouse IgG (secondary) antibodies, using tyramide as activated substrate.

873 **Step 6. Data analysis:** Fluorescence values were normalised to estimate positive signal

874 values (greater than 1) for DNA printing and protein expression.

875

876 **Figure 2. Analysing printed DNA reproducibility.** (a) Analysis of expression library

877 quality by enzymatic digestion. The BsrGI enzyme was used for digestion; two DNA

878 fragments were produced. The smaller fragment was insert release. MWM: molecular

879 weight marker. At least two fragments were observed in all cases. (b) Scanning images

35

880    showing the spots (i.e. DNA printed onto cell surface before expression). The Figure shows

881    16 sub-arrays (containing 29 clones and negative controls) for each array. Each region is

882    represented by two sub-arrays. (c) Inter-slide reproducibility showing the relationship

883    between normalised PicoGreen signals for clones printed in different arrays. (d) Intra-slide

884    reproducibility showing the relationship between clones printed on different sub-arrays.

885

886    **Figure 3. Analysing *Plasmodium vivax* protein expression using RRL or HCIVT in**

887    **NAPPA arrays and Western blot.** (a) Scanning images showing the spots for three sub-

888    arrays for proteins expressed after incubation with anti-GST. (b) Comparing *P. vivax*

889    antigen expression with rabbit reticulocyte lysate (RRL) and 1-step human coupled IVT

890    (HCIVT). The relationship between normalised cDNA signal and normalised protein signal

891    for each expression system is shown. Values greater than 1 were considered positive.

892

893    **Figure 4. NAPPA functional assessment of *Plasmodium vivax* proteins.** The *Pv*12

894    protein was used as query for evaluating its interaction with 29 *P. vivax* proteins displayed

895    on the array. Query DNA encoding an N-terminal Halo tag was added to reticulocyte lysate

896    for co-expression with bait proteins. The interaction signal was determined with anti-Halo

897    antibodies. Normalised values are shown for 30 clones evaluated on the array. A > 1 value

898    was considered positive interaction.

899

900    **Table S1**

901    List of primers used, amplicon size, expressed products' molecular weight and destination

902    vectors for the genes analysed.

903

904     **Figure S1.** A representative sample of *P. vivax* gene amplicons.

905

906

907

908

909

Table 1. *P. vivax* proteins selected for NAPPA array.

| Annotation | Pv gene ID | Time Transcription[a] | Localisation | Proteome data[c] | Fragments | Regions expressed |
|---|---|---|---|---|---|---|
| **Target *P. vivax* Proteins** | | | | | | |
| **Merozoite Surface protein 1 (*Pv*MSP1)** | PVX_099980 | TP7 | | X | 2 | $^{1350}$D-F$^{1723}$ ; $^{761}$G-E$^{1349}$ |
| **Merozoite Surface protein 4 (*Pv*MSP4)** | PVX_003775 | TP7 | | | 1 | $^{30}$I-S$^{248}$ |
| **Merozoite Surface protein 8 (*Pv*MSP8)** | PVX_097625 | TP2 | | X | 1 | $^{24}$G-Y$^{462}$ |
| **Merozoite Surface protein 10 (*Pv*MSP10)** | PVX_114145 | TP7 | Merozoite Surface | | 1 | $^{30}$L-A$^{459}$ |
| **6-cysteine protein 41 (*Pv*41)** | PVX_000995 | TP7 | | X | 1 | $^{19}$A-Q$^{383}$ |
| **6-cysteine protein 12 (*Pv*12)** | PVX_113775 | TP7 | | X | 1 | $^{27}$T-G$^{336}$ |
| **Asparagine Rich Protein (*Pv*ARP)** | PVX_090210 | TP7 | | X | 1 | $^{16}$C-V$^{284}$ |
| **Thrombospondin-related protein (*Pv*TRAMP)** | PVX_123575 | TP8 | Apical/Merozoite Surface | | 1 | $^{24}$K-I$^{300}$ |
| **Merozoite Surface protein 5 (*Pv*MSP5)** | PVX_003770 | TP8 | | X | 1 | $^{22}$R-I$^{362}$ |
| **Apical Merozoite Antigen 1 (*Pv*AMA1)** | PVX_092275 | TP8 | Micronemes/Apical | X | 2 | $^{43}$P-E$^{343}$; $^{43}$P-$^{L487}$ |
| **Duffy Binding Protein 1 (DBP1)** | PVX_110810 | ↓ transcription[b] | | | 3 | $^{26}$E-C$^{217}$; $^{198}$T-D$^{524}$; $^{521}$T-T$^{1000}$ |
| **Reticulocyte-binding protein 1a (*Pv*RBP1a)** | PVX_098585 | TP8 | | | 4 | $^{582}$E-E$^{1457}$; $^{1549}$F-G$^{1758}$; $^{1880}$S-R$^{2229}$; $^{2245}$S-E$^{2832}$ |
| **Rhoptry Neck Protein 1 (*Pv*RON1)** | PVX_000945 | TP7 | | | 1 | $^{25}$K-R$^{772}$ |
| **Rhoptry Neck Protein 2 (*Pv*RON2)** | PVX_117880 | TP7 | Rhoptry neck protein | X | 2 | $^{735}$G-L$^{1560}$ and $^{1554}$L-V$^{2203}$ |
| **Rhoptry Neck Protein 5** | PVX_089530 | TP7 | | X | 1 | $^{23}$F-W$^{500}$ |

38

| | | | | | | |
|---|---|---|---|---|---|---|
| (*Pv*RON5) | | | | | | |
| **Rhoptry Neck Protein 4 (*Pv*RON4)** | PVX_091434 | TP7 | | | 1 | $^{25}$F-I$^{756}$ |
| **Rhoptry-associated protein 1 (*Pv*RAP1)** | PVX_085930 | TP7 | | | 1 | $^{2}$T-Y$^{633}$ |
| **Rhoptry-associated protein 2 (*Pv*RAP2)** | PVX_097590 | TP7 | Rhoptries | X | 1 | $^{22}$H-H$^{382}$ |
| **High molecular weight rhoptry protein 3 (*Pv*RhopH3)** | PVX_098712 | No data | | | 1 | $^{21}$Q-F$^{599}$ |
| **Rhoptry associated membrane antigen (*Pv*RAMA)** | PVX_087885 | TP7 | Rhoptry body protein | X | 1 | $^{21}$F-G$^{710}$ |
| **Prey *P. vivax* Protein** | | | | | | |
| **6-cysteine protein 12 (*Pv*12)** | PVX_113775 | TP7 | Merozoite surface | X | 1 | $^{27}$T-G$^{336}$ |

[a] Transcription data from time points (TP) 1 to 9 of 3 *vivax* malaria isolates [91].
[b] Low transcriptional levels in all time points measured (TP1-TP9) [91].
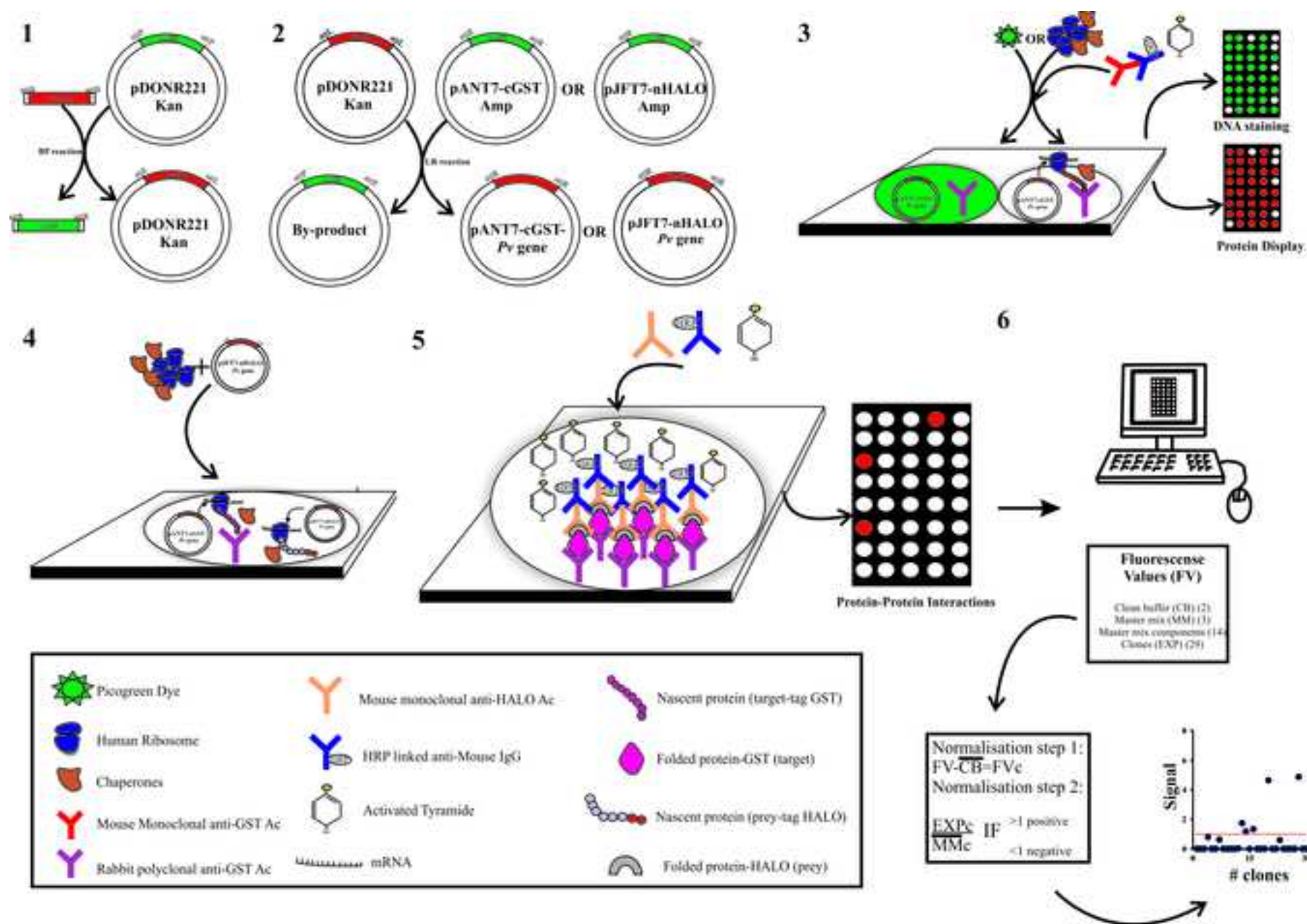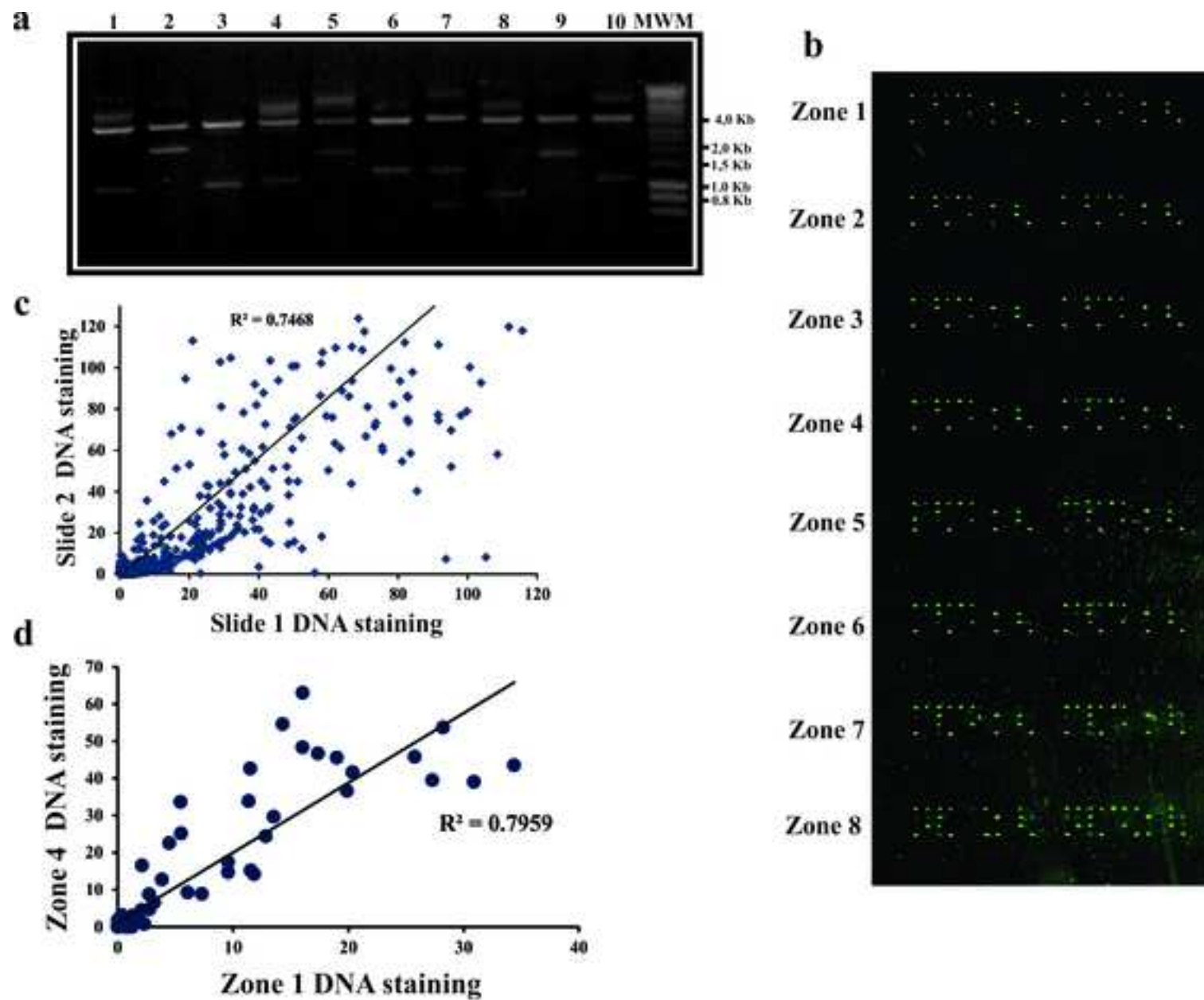[c] Data from proteomic analyses [63, 67].

911

912

913

914
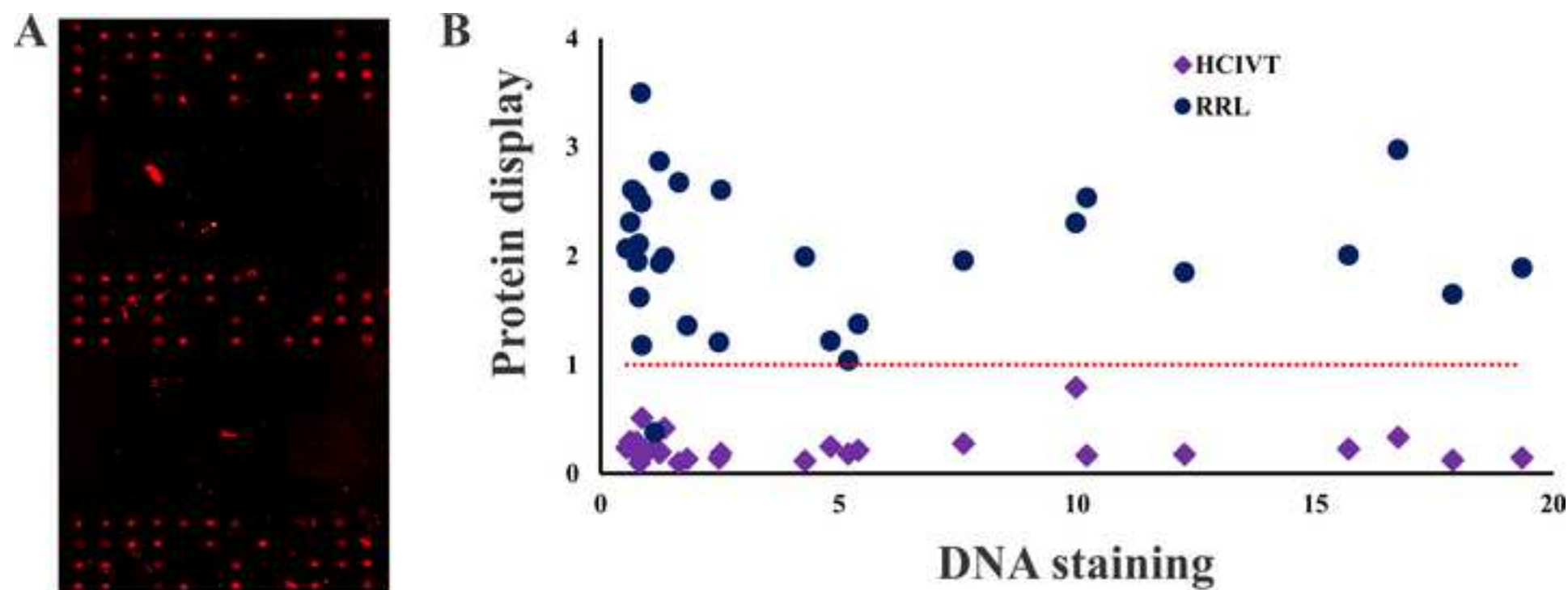
Figure 1

Click here to download Figure Figure 1.tif



**Figure 1**

Figure 2

**Figure 2**

Figure 3

Figure 3

Figure 4

Figure 4